

DOCTORAL THESIS

Long-term Changes of the Eutrophication Indicators of the Baltic Sea

Mariliis Kõuts

TALLINN UNIVERSITY OF TECHNOLOGY
DOCTORAL THESIS
2/2023

Long-term Changes of the Eutrophication Indicators of the Baltic Sea

MARILIIS KÕUTS



TALLINN UNIVERSITY OF TECHNOLOGY

School of Science

Department of Marine Systems

This dissertation was accepted for the defence of the degree 29/11/2022

Supervisors: Prof. Urmas Raudsepp
School of Science
Tallinn University of Technology
Tallinn, Estonia

Dr. Gennadi Lessin
Plymouth Marine Laboratory
Plymouth, United Kingdom

Opponents: Dr. Anda Ikauniece
Latvian Institute of Aquatic Ecology
Riga, Latvia

Dr. Alo Laas
Estonian University of Life Sciences
Tartu, Estonia

Defence of the thesis: 25/01/2023 Tallinn

Declaration: Hereby I declare that this doctoral thesis, my original investigation and achievement, submitted for the doctoral degree at Tallinn University of Technology has not been submitted for doctoral or equivalent academic degree.

Mariliis Kõuts

Signature



European Union
European Regional
Development Fund



Investing
in your future

Copyright: Mariliis Kõuts, 2022

ISSN 2585-6898 (publication)

ISBN 978-9949-83-945-2 (publication)

ISSN 2585-6901 (PDF)

ISBN 978-9949-83-946-9 (PDF)

Printed by Auratrükk

TALLINNA TEHNIKAÜLIKOOL
DOKTORITÖÖ
2/2023

Läänemere eutrofeerumise indikaatorite pikaajalised muutused

MARILIIS KÕUTS



Contents

List of publications	7
Author's contribution to the publications	8
List of abbreviations.....	9
1 Introduction	11
1.1 The Baltic Sea general description.....	12
1.2 Aim and objectives	15
2 Methods	16
2.1 Coupled Nemo-Nordic and SCOBI reanalysis.....	16
2.2 Coupled GETM and ERGOM model system	16
2.3 Nutrient loads from an anthropogenic source	17
2.4 Remote sensing data	18
2.5 Oxygen measurements	19
3 Results	20
3.1 Nutrient pools and phytoplankton blooms	20
3.2 Pools of dissolved oxygen and recent evolution of hypoxia and anoxia in the Baltic Sea.....	25
3.3 Effect of additional nutrients on the ecosystem	27
4 Discussion.....	30
4.1 Changes in nitrogen pools	30
4.2 Changes in phosphorus pools	31
4.3 DIN:DIP ratio	32
4.4 Effect of nutrient pools on phytoplankton blooms	33
4.5 Oxygen	34
4.6 Baltic Sea nutrient reduction and biogeochemistry	36
5 Conclusions	39
References	41
Acknowledgements.....	55
Abstract.....	56
Lühikokkuvõte.....	57

Appendix	59
Paper I.....	59
Paper II.....	79
Paper III.....	101
Paper IV	117
Curriculum vitae.....	139
Elulookirjeldus.....	142

List of publications

- I Kõuts, M., Maljutenko, I., Elken, J., Liu, Y., Hansson, M., Viktorsson, L. and Raudsepp, U., 2021. **Recent regime of persistent hypoxia in the Baltic Sea.** *Environmental Research Communications*, 3(7), p. 075004.
- II Raudsepp, U., Maljutenko, I., Kõuts, M., Granhag, L., Wilewska-Bien, M., Hassellöv, I.M., Eriksson, K.M., Johansson, L., Jalkanen, J.P., Karl, M. and Matthias, V., 2019. **Shipborne nutrient dynamics and impact on the eutrophication in the Baltic Sea.** *Science of the Total Environment*, 671, pp. 189–207.
- III Raudsepp, U., She, J., Brando, V.E, Santoleri, R., Sammartino, M., Kõuts, M., Uiboupin, R., Maljutenko, I., 2019. **Phytoplankton blooms in the Baltic Sea.** In: Copernicus Marine Service Ocean State Report, Issue 3, Journal of Operational Oceanography, 12:sup1, pp. s26–s30; DOI: 10.1080/1755876X.2019.1633075
- IV Kõuts, M., Maljutenko, I., Liu, Y. and Raudsepp, U., 2021. **Nitrate, ammonium and phosphate pools in the Baltic Sea.** In: Copernicus Marine Service Ocean State Report, Issue 5, Journal of Operational Oceanography, 14:sup1, pp. s140–s148; DOI: 10.1080/1755876X.2021.1946240

Author's contribution to the publications

- I** Prepared manuscript, data analysis.
- II** Data analysis, writing and editing.
- III** Prepared manuscript, data analysis.
- IV** Prepared manuscript, data analysis.

List of abbreviations

MBI	Major Baltic Inflow
Chl-a	Chlorophyll-a
DNRA	Dissimilatory nitrate reduction to ammonium
Anammox	Anaerobic ammonium oxidation
SCOB	Swedish Coastal and Ocean Biogeochemical model
NEMO	Nucleus for European Modelling of the Ocean
CMEMS	Copernicus Marine Environment Monitoring Service
OSISAF	Satellite Application Facility on Ocean and Sea Ice
LSEIK	Localized Singular Evolutive Interpolated Kalman
ICES	International Council for the Exploration of the Sea
SST	Sea surface temperature
SHARK	Swedish Ocean Archive database
GETM	General Estuarine Transport Model
ERGOM	Ecological regional ocean model
BSBD	Baltic Sea Digital Database
STEAM	The Ship Traffic Emission Assessment Model
COSMO-CLM/CMAQ	Climate Limited Area Modelling/ Community Multiscale Air Quality model system
SHIP	Modelling scenario with ship-derived nutrient loads
NOSHIP	Modelling scenario without ship-derived nutrient loads
SO_x	sulphur oxide
SO₄	sulphate
H₂S	Hydrogen Sulphide
NO₃	Nitrate
NO₂	Nitrite
NO_x	Nitrogen oxide
N₂O₅	Nitrogen pentoxide
DO	Dissolved oxygen
PM_NO₃	Particulate nitrate
HNO₃	nitric acid
HNO₄	peroxynitric acid
OPAN	oxidised peroxyacetyl nitrate
HONO	nitrous acid
PAN	peroxyacetyl nitrate
PM_NH₄	Particulate ammonium
NH₃	Ammonia
NH₄	Ammonium
SMHI	The Swedish Meteorological and Hydrological Institute
HELCOM	Helsinki Commission
DIN	Dissolved inorganic nitrogen

DIP	Dissolved inorganic phosphorus
AIS	Automatic Identification System
BSAP	Baltic Sea Action Plan
BW	Black water
FW	Food waste
GW	Grey water
SWO	Scrubber water from open loop systems
SWC	Scrubber water from closed loop systems
Rrs	remote sensing reflectance spectra

1 Introduction

Marine eutrophication has accelerated simultaneously with the development of intensive agriculture, which involves vast amounts of fertilisers, most notably nitrogen (N) and phosphorus (P) (Rabalais et al., 2009; Beusen et al., 2016). These macronutrients have been transported into the marine ecosystem, where they have initiated a cascade of changes, the essence of which can be summarised as an imbalance in biogeochemical cycles and the consequent accumulation of organic matter and nutrients in the system (Duarte et al., 2009; Nixon, 2009). Negative effects of marine eutrophication include the occurrence of dead zones, harmful algal blooms, habitat loss, changes in food-web dynamics, decreasing biodiversity and loss of coastal ecosystem services to society (Schindler, 2006; Hietanen and Lukkari, 2007; Reusch et al., 2018; Malone and Newton, 2020). Beyond certain thresholds, eutrophicated systems lose their balance and could shift into a new, stable but ecologically poorer state (Schindler, 2006; Duarte et al., 2009; Chislock et al., 2013). The 20th century brought a dramatic increase in the extent of coastal eutrophication on the global scale (Watson et al., 2017; Malone and Newton, 2020). Well-known examples of eutrophication-degraded ecosystems across the world include the Gulf of Mexico, the East China Sea, the Chesapeake Bay, the Black Sea, the Wadden Sea, the Great Barrier Reef, the North Adriatic Sea and the Baltic Sea (Ménesguen and Lacroix, 2018; Malone and Newton, 2020).

While eutrophication in lakes is mainly triggered by phosphorus inputs, the controlling agent in most marine areas is assumed to be nitrogen, although this can vary in time and space (Carstensen et al., 2011; Ménesguen and Lacroix, 2018). It has been suggested that anthropogenic input of nitrogen (160 Tg N yr^{-1}) exceeds all natural N-fixation in the ocean (140 Tg N yr^{-1}) as well as the proposed planetary boundary (of 62 Tg N yr^{-1}), a threshold beyond which human perturbations are predicted to destabilise the Earth's nitrogen cycle on a global scale (Steffen et al., 2015). This has resulted in systematic changes as nowadays in worldwide oceans a unit of nitrogen in coastal waters produces almost twice the quantity of algal biomass measured as chlorophyll-a (chl-a) concentration than it did 30–40 years ago (Carstensen et al., 2011). The global anthropogenic supply of dissolved inorganic nitrogen (DIN) is projected to continue increasing, and is expected to double by 2050 (Beusen et al., 2016; Lee et al., 2016; Seitzinger et al., 2010). The estimation of global nonpoint inputs of nitrogen ($\sim 200 \text{ Tg N yr}^{-1}$) is multiple times higher than the point source inputs of $\sim 10 \text{ Tg N yr}^{-1}$, which partly explains the difficulties in controlling nitrogen input (Malone and Newton, 2020). River runoff and atmospheric deposition represent the most important pathways for anthropogenic nitrogen to enter coastal ecosystems (Green et al., 2004; Howarth, 2008; Jickells et al., 2017).

Global phosphorus input to coastal areas has also increased alongside nitrogen, although mostly via river runoff and point source input as atmospheric deposition of phosphorus is small, equal to only $\sim 10\%$ of the riverine input (Graham and Duce, 1979). Estimations of total global phosphorus input from rivers vary from 4 to 9 Tg P yr^{-1} (Seitzinger et al., 2010; Beusen et al., 2016). Although efforts to contain the nutrient from urban sewage water effluents have been mostly successful (Aloe et al., 2014; Pulido-Velazquez and Ward, 2017), global increase is still projected in the future (Seitzinger et al., 2010). Dissolved inorganic phosphorus (DIP) is the other essential nutrient for primary production and tends to accumulate in the ecosystem, with the only considerable sink being burial in the sediments (Watson et al., 2017; Kulinski et al., 2021). Areas with large oxygen minimum zones such as the Baltic Sea and the Gulf of Mexico

have well-established mechanisms of phosphorus inner cycling, with continuous release of phosphates from the sediments during anoxic events, which boosts production in the water column and provides bioavailable phosphorus to the system despite input limitations from external sources (Conley et al., 2002; Adhikari et al., 2014).

Phytoplankton (biomass estimated from chl-a) is the first link in the ecosystem to be directly affected by changes in physical or biogeochemical factors and is hence considered a sensitive indicator of eutrophication (Paerl et al., 2003; HELCOM, 2018). Setting aside the physical conditions of the environment, phytoplankton is limited by the availability of nutrients, which can drastically alter phytoplankton growth, biomass and species composition, which in turn has an effect on the functioning of the entire ecosystem (Hecky and Kilham, 1988; Chislock et al., 2013). The likelihood of changes is stronger when the increase in nutrients exceeds the capacity of the system to absorb increased production (Nixon, 2009; Malone and Newton, 2020). In parallel with increasing nutrient input, a rise in phytoplankton biomass is observed globally, along the coastlines with intense anthropogenic activity (Gregg et al., 2005; Rabalais et al., 2009; Malone and Newton, 2020). In five years (1998–2003), surface chl-a concentration increased by 10% in the coastal ocean (Gregg et al., 2005), which is in line with the increase of land-based anthropogenic nitrogen inputs (Schulte-Uebbing and de Vries, 2018). Many marine areas from the Gulf of Mexico and Chesapeake Bay to the Adriatic Sea also experience an unprecedented occurrence or extent of potentially toxic algal blooms, which is yet another unpleasant manifestation of eutrophication (Reece, 2015; Bargu et al., 2016; Corriero et al., 2016).

Oxygen deficient zones develop when excess organic matter sinks below the pycnocline (a layer with a steep density gradient), where it is metabolised by aerobic heterotrophic bacteria (Lehmann et al., 2014; Carstensen and Conley, 2019). As dissolved oxygen gradually runs out, organic matter starts to accumulate and local biogeochemistry switches to an anaerobic regime, which retains the phosphorus in the ecosystem, changes nitrogen transformation pathways and fuels the already intense eutrophication process (Lukkari et al., 2009; Conley et al., 2009a). Expanding dead zones reduce the marine life habitats, especially for benthic macrofauna, which significantly hampers the benthic-pelagic coupling and the efficiency of the coastal filter as nutrient storage and removal (Conley et al., 2009a; Carstensen et al., 2020). The number of coastal ecosystems, which experience oxygen debt, has increased globally from < 5 prior to WWII to ~700 today, and is growing as eutrophication spreads (Díaz and Rosenberg, 2008; Vaquer-Sunyer and Duarte, 2009; Altieri and Diaz, 2019; Diaz et al., 2019). Well-known examples of areas with large oxygen deficient zones include the Gulf of Mexico, the Black Sea and the Baltic Sea. Areas with improved oxygen conditions are rare, despite restrictions of nutrient discharges. A major factor is climate change, which promotes the spread of hypoxia and anoxia with elevated water temperatures, increased freshwater runoff and strengthening stratification, which could potentially offset nutrient reductions in the long run (Meier et al., 2017; Meier et al., 2021).

1.1 The Baltic Sea general description

The Baltic Sea is a brackish semi-enclosed sea in northeastern Europe with a surface area of 422,000 km² and volume of 21,205 km³ (Leppäranta and Myrberg, 2009) (Figure 1). The average depth of the Baltic Sea is only 54 m and the water volume is small relative to the surface area because ⅓ of the sea is shallower than 30 m (Leppäranta and Myrberg, 2009). The maximum depth of 459 m is located in the deep trench of the

Landsort Deep. The Gotland Deep in the central Baltic Proper has a maximum depth of 250 m and is considered a dynamic deep area that is highly significant in shaping hydrographic and biogeochemical fields of the Baltic Sea (Leppäranta and Myrberg, 2009).

The surface salinity of the Baltic Sea varies horizontally from approximately 10 g/kg near the Danish Straits to 2 g/kg at the northernmost and easternmost subbasins (Leppäranta and Myrberg, 2009). The long-term salinity is determined by net precipitation (e.g. Jaagus et al., 2018) and river discharge across the Baltic Sea coast (Hansson et al., 2011) and by the saline water inflows from the North Sea through very narrow and shallow channels in the Danish Straits (Lehmann et al., 2022). The saline and oxygenated water inflows to the Baltic Sea, especially the Major Baltic Inflows (MBI-s), occur only intermittently (e.g. Mohrholz, 2018; Lehmann et al., 2022). The halocline, a vertical layer with a strong gradient of salinity that separates the well-mixed surface layer from the weakly stratified layer below, is located in the depth range 60–80 m (Matthäus, 1984). The bottom layer salinity below the halocline depth varies from 15 g/kg in the south to 3 g/kg in the northern Baltic Sea (Väli et al., 2013). Long-lasting periods (>10 years) of decreased salinity in the deep layers of the central Baltic, accompanied by oxygen depletion and overall weakening of the vertical stratification, are referred to as stagnation periods, which appear approximately once per century (Schimanke and Meier, 2016). The last extensive stagnation period lasted from 1976 until 1992 (Schimanke and Meier, 2016).

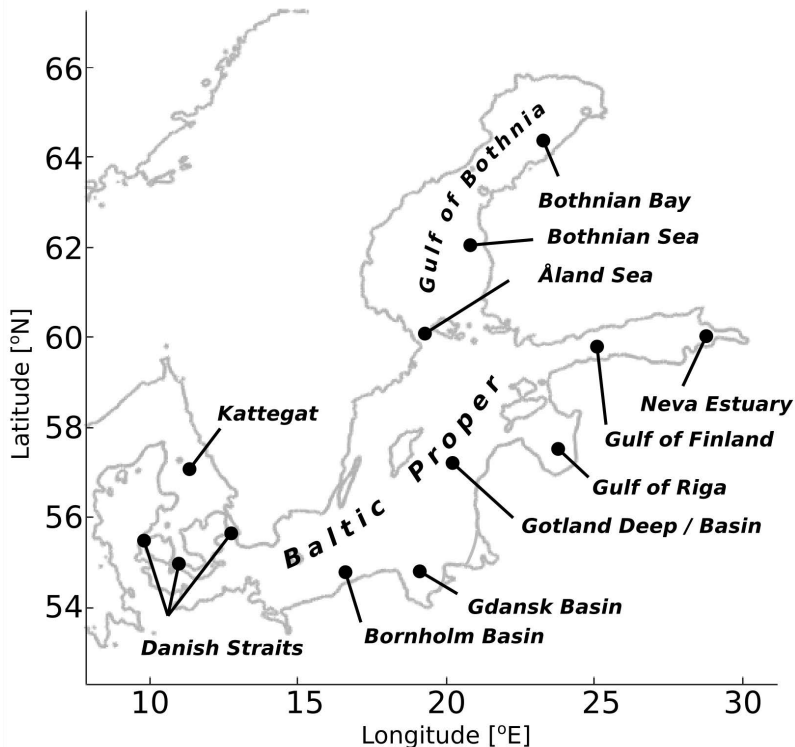


Figure 1. The Baltic Sea and the locations mentioned in the thesis.

The upper mixed layer temperature of the Baltic Sea has a strong seasonal cycle, which is driven by the annual course of solar radiation (Leppäranta and Myrberg, 2009). Maximum water temperatures are reached in July and August and minimums in February, when the Baltic Sea becomes partially frozen (Leppäranta and Myrberg, 2009). The seasonal sea ice coverage has a vital role in the annual course of physical and ecological conditions. In general, ice starts to form in October and may last until June in the northern parts of the Baltic Sea (Leppäranta and Myrberg, 2009). Depending on the year, maximum ice extent could vary in the range of 30,000 km² (e.g. in 2015) to 260,000 km² (e.g. in 2011). In the case of a fully ice-covered Baltic, the maximum ice extent is 422,000 km², which was last observed in the 1940s (Vihma and Haapala, 2009). The seasonal thermocline, a steep vertical temperature gradient which develops at the depth range 10–30 m in spring, is strongest in summer and erodes in autumn, followed by a thermal mixing down to the permanent halocline at the depth 60–80 m (Matthäus, 1984). The 20–50 m thick cold intermediate layer forms below the upper mixed layer in March and is observed until October within the 15–65 m depth (Liblik and Lips, 2011; Chubarenko and Stepanova, 2018).

The large-scale mean horizontal circulation is dominantly cyclonic in the Baltic (Meier, 2007; Jędrasik and Kowalewski, 2019). Deep water circulation consists of dense bottom currents of the inflowing saline water in the southern Baltic Sea, while convection, mixing, entrainment and vertical advection of water masses lead to interactions between upper and lower layers (Leppäranta and Myrberg, 2009). Instantaneous surface circulation patterns are driven by wind in the Baltic Sea (Leppäranta and Myrberg, 2009).

The Baltic Sea is a severely eutrophicated marine area, which has earned it the title “Time-machine for the future state of other coastal marine areas” (Reusch et al., 2018). Of the external sources, rivers contribute most to the Baltic Sea nutrient input (HELCOM, 2018). Rivers with catchments in densely populated agricultural areas, such as Vistula, Nemunas and Oder in the southern part of the Baltic Sea have a bigger nutrient input compared to northern areas, where large parts of river drainage areas are under forest (Andersen et al., 2016; Kulinski et al., 2021).

Recent estimates (year 2017) of the total nutrient input remain around 900,000 tonnes for nitrogen and 30,000 tonnes for phosphorus (HELCOM, 2018). The Baltic Sea Action Plan (BSAP) was adopted by HELCOM in 2007 (and updated in 2021) to coordinate the measures of nutrient reduction for achieving a good environmental status of the Baltic Sea. Significant decrease of the nutrient input into the Baltic Sea has been achieved – the loads have reached the level of the 1960s for nitrogen and the 1950s for phosphorus (-12% and -25%, respectively) (HELCOM, 2018). The ecological status of the Baltic Sea, however, has not improved at the same rate, as stated by HELCOM (2018). 86 % of the coastal waters and 100% of the open sea are not in good status (HELCOM, 2018). Nutrient concentrations in the water have not reached the target value and remain high across the Baltic Sea. Even though total nitrogen concentrations do show a decreasing trend across most of the Baltic Sea, the steady increase in phosphorus levels overrides the possible effects (Savchuk, 2018). This also reflects in primary production estimates as in the vast majority of the Baltic Sea the chl-a concentrations remained essentially unchanged from 1990 onwards, while cyanobacterial blooms increased in frequency after 1998, although interannual variation was high, with hotspots in the Baltic Proper and the Gulf of Finland, and the Bothnian Sea emerging as an area with increasing cyanobacteria blooms (Kahru and Elmgren, 2014; Olofsson et al., 2020; Olofsson et al., 2021).

Oxygen debt has increased since 1990, indicating worsening oxygen conditions in the Baltic Sea. Hypoxia, i.e. low oxygen, with dissolved oxygen concentrations below 2 mg/L, can occur in the open sea as well as coastal areas, lasting from a few days to several years (Vaquer-Sunyer and Duarte, 2008; Lehmann et al., 2014; Virtanen et al., 2019). In the Baltic Sea, permanent hypoxia can occur in areas where a permanent halocline is present (Väli et al., 2013). Permanent hypoxia has been evident in the open central Baltic Sea since the 1950s (Carstensen and Conley, 2019). Seasonal hypoxia may develop in the areas with a well-developed seasonal stratification (Liblik et al., 2018). Episodic events with hypoxia are related to specific local conditions such as secluded location, warm water and oxygen consumption prevailing over oxygen production (Conley et al., 2011; Virtanen et al., 2019). Shallow coastal areas with complex bottom topography are prone to seasonal hypoxia (Conley et al., 2011; Carstensen and Conley, 2019, Virtanen et al., 2019). Anoxia, i.e. total lack of DO, is characteristic of the deep central basins of the Baltic Sea (Hansson et al., 2011). Although the extent of anoxic areas in the Baltic Sea today is unprecedented, intermittent hypoxia has occurred in the region over the Holocene, which has shaped an ecosystem that is at least partly adapted to fluctuating oxygen content (Conley et al., 2009b; Carstensen et al., 2014; Jokinen et al., 2018). MBI-s from the North Sea are the only means to interrupt anoxia in the deep bottom layers of the Baltic Sea (Neumann et al., 2017; Mohrholz, 2018). Interannual variations of the anoxic area mostly coincide with interannual variations of the hypoxic area (Lehmann et al., 2014).

1.2 Aim and objectives

The Baltic Sea is so far relatively resilient to reductions in nutrient input, a measure which was supposed to improve the eutrophication situation in a relatively short time-period. In this thesis we analyse long-term changes of the main eutrophication indicators: nutrients, phytoplankton spatial coverage and oxygen concentrations, and provide insight into the effect of manipulation with nutrient input measures to the eutrophication status of the Baltic Sea. The following scenario has been expected for the Baltic Sea:

- as nutrient inputs have gone through significant decreases, the nutrient pools in the water are expected to decrease as well;
- in the context of decreased nutrient input, phytoplankton blooms should decrease in size;
- in response to nutrient input reductions oxygen conditions should improve – anoxic and hypoxic areas are expected to decrease;
- the probability of anoxia and hypoxia, which is an important indicator of oxygen conditions in a marine system, is also expected to decrease.

To prove the concept, a simulation was conducted with nutrient manipulation and the response trajectories of key ecosystem elements were studied. The expectation is that with nutrient additions to the already eutrophic Baltic Sea, the system would respond with an accelerated change of all the aforementioned eutrophication indicators – phytoplankton biomass increasing, nutrients accumulating in the system and oxygen decreasing.

2 Methods

A set of modelling, observations and remote sensing data was used to analyse the status of three different eutrophication indicators in the Baltic Sea in papers I, III and IV. The impact of increased nutrient load on the Baltic Sea ecosystem was evaluated, based on the example of shipborne nutrient input to the Baltic Sea in Paper II. A model simulation experiment was used to describe the eutrophication indicators' response to additional nutrients in the system during the periods of 1 and 5 years (Paper II).

The models and data used to analyse the state of the Baltic Sea are described in the following sections.

2.1 Coupled Nemo-Nordic and SCOBI reanalysis

For papers I and IV the physics and biogeochemistry reanalysis products of the Copernicus Marine Environment Monitoring Service (CMEMS, www.marine.copernicus.eu) were used, which are based on the Nemo-Nordic hydrodynamic model (Hordoir et al., 2015), coupled with the Swedish Coastal and Ocean Biogeochemical model (SCOBI) (Marmefelt et al., 1999; Eilola et al., 2009). The SCOBI biogeochemical model consists of 9 state variables: nitrate (NO_3), ammonium (NH_4), phosphate (PO_4), three functional species of phytoplankton, zooplankton, detritus and oxygen (Eilola et al., 2009). Oxygen dynamics are governed by air-sea exchange, primary production, respiration of plankton species, decomposition of detritus, denitrification of NO_3 , and oxidation of ammonia by nitrifying bacteria. The surface oxygen flux is calculated using oxygen solubility, temperature and wind-dependent exchange rates. In the current application, the model system uses the Localized Singular Evolutive Interpolated Kalman (LSEIK, Nerger et al., 2005) filter data assimilation method to combine simulation and the SST observations from the Satellite Application Facility on Ocean and Sea Ice (OSISAF) (<https://osi-saf.eumetsat.int/>) and *in situ* profiles of salinity and temperature from the the International Council for the Exploration of the Sea (ICES) database (www.ices.dk), and NO_3 , NH_4 , PO_4 and oxygen state variables from the Swedish Ocean Archive database (SHARK; <http://sharkweb.smhi.se>). The model domain consists of the North Sea and the Baltic Sea with a 2 nautical mile resolution (Hordoir et al., 2019). The numerical model simulation data covers the period 1993–2017.

A more detailed models' description, setup and model validation results are found in Paper I.

2.2 Coupled GETM and ERGOM model system

The impact of shipborne nutrients on the marine ecosystem in Paper II is estimated using the coupled physical and biogeochemical model system: the General Estuarine Transport Model (GETM) and the Ecological Regional Ocean Model (ERGOM) (Burchard and Bolding, 2002; Neumann and Schernewski, 2008; Bruggeman and Bolding, 2014; www.ergom.net).

GETM is a 3D numerical hydrodynamics model which solves sea state by means of salinity, temperature, currents and water level (Burchard and Bolding, 2002). The model domain covers the whole Baltic Sea with a closed boundary in the Kattegat. The bathymetry has been derived from the Baltic Sea Digital Database (BSBD 0.9.3) and interpolated on a 1 nautical mile grid, which is the horizontal resolution of the model. In vertical direction 40 bottom-following and adaptive layers have been defined,

ensuring 5 m vertical resolution in the halocline and near the surface. The timestep for the biogeochemical processes is set to baroclinic timestep, which is 500 s.

A more detailed description of GETM is provided in Paper II.

ERGOM (Neumann, 2000; 2002) is a N-based biogeochemical ecosystem model taking into account processes like N-fixation, phosphorus limitation, denitrification and binding of phosphorus into iron compounds. 12 state variables are used which describe the nitrogen cycle in molar nitrogen units. The inorganic nutrients consumed by primary producers are defined as NO_3 , NH_4 and PO_4 . Primary producers are divided into three functional phytoplankton groups: diatoms, flagellates and N-fixing cyanobacteria. Nitrogen in phytoplankton and detritus is converted into molar carbon-content according to the Redfield ratio (Redfield, 1934). Grazing of phytoplankton is described as the growth of zooplankton. Phyto- and zooplankton are transformed into dead organic matter, which sinks and contributes to the sediment pool as detritus. Under oxic conditions part of the detritus is remineralized back to dissolved nutrients; this process uses oxygen and has a temperature-dependent rate. Under anoxic conditions denitrification reduces NO_3 to molecular N, which leaves the system. When NO_3 is depleted under anoxic conditions, detritus is oxidised with sulphate (SO_4) and hydrogen sulphide (H_2S) is generated, which is considered as negative oxygen. Under oxic conditions reactive PO_4 are bound into iron-phosphates, which sink out of the water-column and accumulate in the sediment layer. In case of anoxia with the presence of sulfuric acid, iron-oxide gets reduced and PO_4 is released back to the system as nutrients available to the primary producers. A fraction of these iron-phosphate compounds is also assumed to be buried permanently, depending on the sediment thickness and sedimentation rate (Neumann and Schernewski, 2008).

Nutrient input from the 36 largest rivers has been derived from the European hydrology model (E-HYPE) hindcast simulation of Donnelly et al. (2016). The diffuse inputs of adjacent regions along the coast have been added to the nearest rivers. Since only total nitrogen (TN) was available from hindcast simulations, we used fractions of 0.70 and 0.05 for NO_3 and NH_4 , respectively. The remaining fraction of 0.25 from TN contributes to the organic nitrogen pool as detritus input. The input of PO_4 and organic phosphorus was assumed to be 0.25 and 0.75 fraction of the total P, respectively. The used fractions were inferred from numerous studies on nutrient loads to the Baltic Sea (e.g. Stålnacke et al., 1999; Vahtera et al., 2007; Savchuk et al., 2012).

More detailed descriptions of the ERGOM model are available in Neumann (2000), Neumann et al. (2002), Neumann and Schernewski (2008), Radtke et al. (2012) and Lessin et al. (2014).

2.3 Nutrient loads from an anthropogenic source

Nutrient loads from shipping in Paper II were obtained from The Ship Traffic Emission Assessment Model (STEAM) (Jalkanen et al., 2009; Jalkanen et al., 2012; Johansson et al., 2013; 2017) and atmospheric chemistry model using the Community Multiscale Air Quality (COSMO-CLM/CMAQ) modelling system (Byun and Schere, 2006; Rockel et al., 2008; Matthias, 2008; Karl et al., 2019).

The STEAM is a ship Automatic Identification System (AIS)-based emission model providing shipping emissions for the CMAQ model system and direct ship discharges to the water. The atmospheric deposition fields from the CMAQ model provide the input of NO_3 , NH_4 , PO_4 and organic matter mass fluxes to the surface layer of the sea. The emission of nitrogen oxides (NO_x) to the atmosphere from shipping has been taken from the

hourly emission dataset of STEAM simulation covering the full calendar year of 2012, which is used as the reference year (SHIP model simulation) because it experienced typical hydrographic and biogeochemical conditions relative to the climatological period 1993–2014. The NOSHIP model simulation is performed excluding the above-mentioned external input of nutrients from shipping activity.

In STEAM, each vessel is considered as a unique case considering vessel specific ship activity and technical description. Daily emissions of NO_x, sulphur oxides (SO_x), carbon monoxide (CO), Elementary Carbon (EC), Organic Carbon (OC), sulphate (SO₄) and Ash were gridded and used as input for atmospheric modelling.

Atmospheric deposition of NO_x species into the sea have been considered from the following wet and dry depositions of: particulate nitrate (NO₃) (PM_NO₃), nitrogen trioxide (NO₃), nitrogen dioxide (NO₂), nitric oxide (NO), nitric acid (HNO₃), nitrous acid (HONO), nitrogen pentoxide (N₂O₅), peroxyacetyl nitrate (PAN), oxidised peroxyacetyl nitrate (OPAN) and peroxyntic acid (HNO₄). Particulate ammonium (PM_NH₄) and NH₃ contribute to reduced nitrogen deposition. These compounds are the source of bioavailable nitrogen in the marine system.

Atmospheric phosphorus deposition has been considered as 3.5% of mineral ash deposition calculated in CMAQ. The hourly atmospheric depositions from a 4 × 4 km² atmospheric deposition grid have been interpolated on the 2 × 2 km² shipping discharge grid used for the direct nutrient inputs.

Direct discharge from ships originates from black water (BW), grey water (GW), food waste (FW), scrubber water from open and closed loop systems (SWO and SWC), which have been calculated from the discharge volumes and measured concentrations in wastewaters (Jönsson et al., 2005; Hufnagl et al., 2005; Furstenberg et al., 2009; Wärtsilä, 2010; McLaughlin et al., 2014; Wilewska-Bien et al., 2016; Wilewska-Bien et al., 2019). The organic nitrogen is considered as dead organic matter input and is recycled to dissolved nutrients in the water by bacteria. The actual numbers of different inputs are given in Table 1 in Paper II.

2.4 Remote sensing data

CMEMS ocean colour remote sensing data was used in Paper III to calculate phytoplankton bloom characteristics. The phytoplankton abundance and succession in the Baltic Sea are characterised by dinoflagellate- and diatom-dominated spring bloom and cyanobacterial summer bloom (Kahru and Nömmann, 1990; Kahru et al., 2018). The spring bloom (spring is from days 31 to 160) is detected using the Siegel (2002) approach (i.e. it is a spring bloom if chl-a > median + 5%) for each pixel in the basin, after which the statistics for the bloom onset are calculated as in Groetsch et al. (2016) and presented as distribution of the start, peak and end days over the whole basin per each year.

The spring and summer bloom spatio-temporal coverage (day km²) are aggregated from daily subsurface and surface bloom following Hansson and Håkansson (2007). Summer blooms are detected by applying the thresholds defined by Hansson et al. (2010) on remote sensing reflectance spectra (Rrs) at the wavelength of 550 nm and Rrs at 676 nm for the subsurface and surface blooms, respectively. Although the method for calculation of the spatio-temporal distribution of the phytoplankton blooms is homogeneous over the time period under consideration, extremely low values of spring bloom for the year 1998–2001 are disputable.

Although 20 years of satellite data are available in the Baltic Sea, it should be noted that the remote sensing indexes computed by SMHI for HELCOM, recorded from 2010 onwards, should not be directly compared with the 1997–2009 values, as an improved detection method is now used (i.e. Hansson et al., 2010). The time series for Rrs and chl-a used in this study are fully homogeneous as they are based on a merged product from different satellites that corrects for inter-sensor differences (Mélin et al., 2017; Sathyendranath et al., 2017).

2.5 Oxygen measurements

Initial oxygen data sources in Paper I consist of the international ICES trawl surveys, national monitoring programmes of each country surrounding the Baltic Sea and different research projects. The hypoxic ($DO < 2$ mg/L) and anoxic ($DO = 0$ mg/L) area and volume were calculated for the autumn period (August–October) of each year (Hansson et al., 2019).

The vertical profiles with at least three data points of oxygen values were used. To obtain a complete oxygen profile the interpolation between the measurements and extrapolation down to the bottom was performed. Then, the shallowest point of the hypoxia and anoxia occurrence was found in the profile. The Delaunay triangulation interpolation method was used to create a spatial depth map of hypoxia and anoxia. The region outside the water points was masked out and hypoxic and anoxic area and volume were calculated from gridded data.

3 Results

3.1 Nutrient pools and phytoplankton blooms

From the coupled NEMO-Nordic and SCOBI reanalysis results the pools of NO_3 , NH_4 , PO_4 and dissolved oxygen have been calculated for 3 layers: surface layer 0–15 m, intermediate layer 15–80 m and deep layer 80 m and below, using the concentrations from the daily mean fields (Paper IV).

The period 1993–2017 marked a decrease in the pelagic NO_3 pool from ~2400 to 1700 kT (Figure 2 a). The decline of the NO_3 pool (up to 60%) was uniform over the Baltic Proper. In the Gulf of Bothnia the subsurface layer NO_3 pool decreased slightly, but turned to a modest increase in the deep layer (Figure 3 a–b). Pelagic NH_4 pools, which contributed about 10–20% (except for the bottom layer) to the DIN pools, decreased in the surface and intermediate layers (Figure 2 b). In the deep layer the NH_4 pool increased, referring to the low concentration of dissolved oxygen there (Figure 3 b–c).

PO_4 had an inverse response to input reduction: the pelagic pool increased from ~600 to 750 kT, predominantly in the surface and intermediate layers (Figure 2 c). The increase of the PO_4 pool (up to 60%) covers the entire Baltic Proper area, most of the Gulf of Finland and the Gulf of Riga (Figure 3 e–f). Interestingly, the pool in the deep layer was more stable, indicating only a slight increasing tendency. In the Gulf of Bothnia, where PO_4 pools are smaller compared to the rest of the Baltic Sea, the decrease of PO_4 in the surface and intermediate layers was confronted by a small increase in the deep layer (Figure 1.5.4 b, d, f in Paper IV).

The changes in the pelagic pools of DIN and DIP across most of the Baltic Sea have resulted in a decreasing nitrogen to phosphorus ratio (Figure 4). The period 1993–1999 is characterised by the DIN:DIP ratio less than 16 in the Baltic Proper and the Gulf of Finland, and more than 16 in the Gulf of Bothnia and the Gulf of Riga (Figure 4 a). By 2000–2017 the area with the low ratio of DIN:DIP increased as nitrogen limitation spread to the Åland Sea and coastal areas across the entire Baltic (Figure 4 b). It should also be noted that the high DIN:DIP ratio in large estuaries indicates that there is no nitrogen limitation due to constant input of nitrogen, regardless of high PO_4 concentrations (Figure 4).

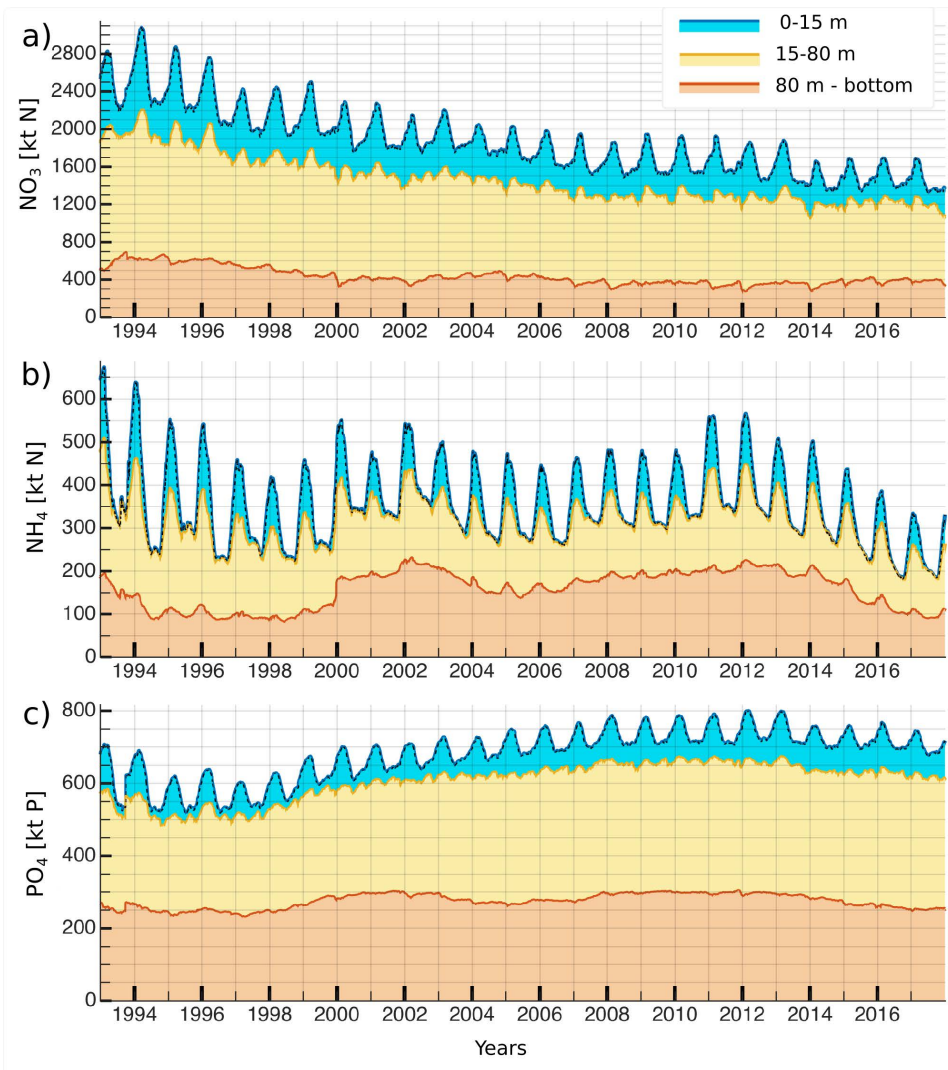


Figure 2. Stacked plot of time series of summarised dissolved nutrient pools: NO_3 on (a), NH_4 on (b), PO_4 on (c) in three different layers (surface layer 0–15 m: blue; Intermediate layer 15–80 m: yellow; and Deep layer starting at 80 m and extending to the bottom: red) across the entire Baltic Sea.

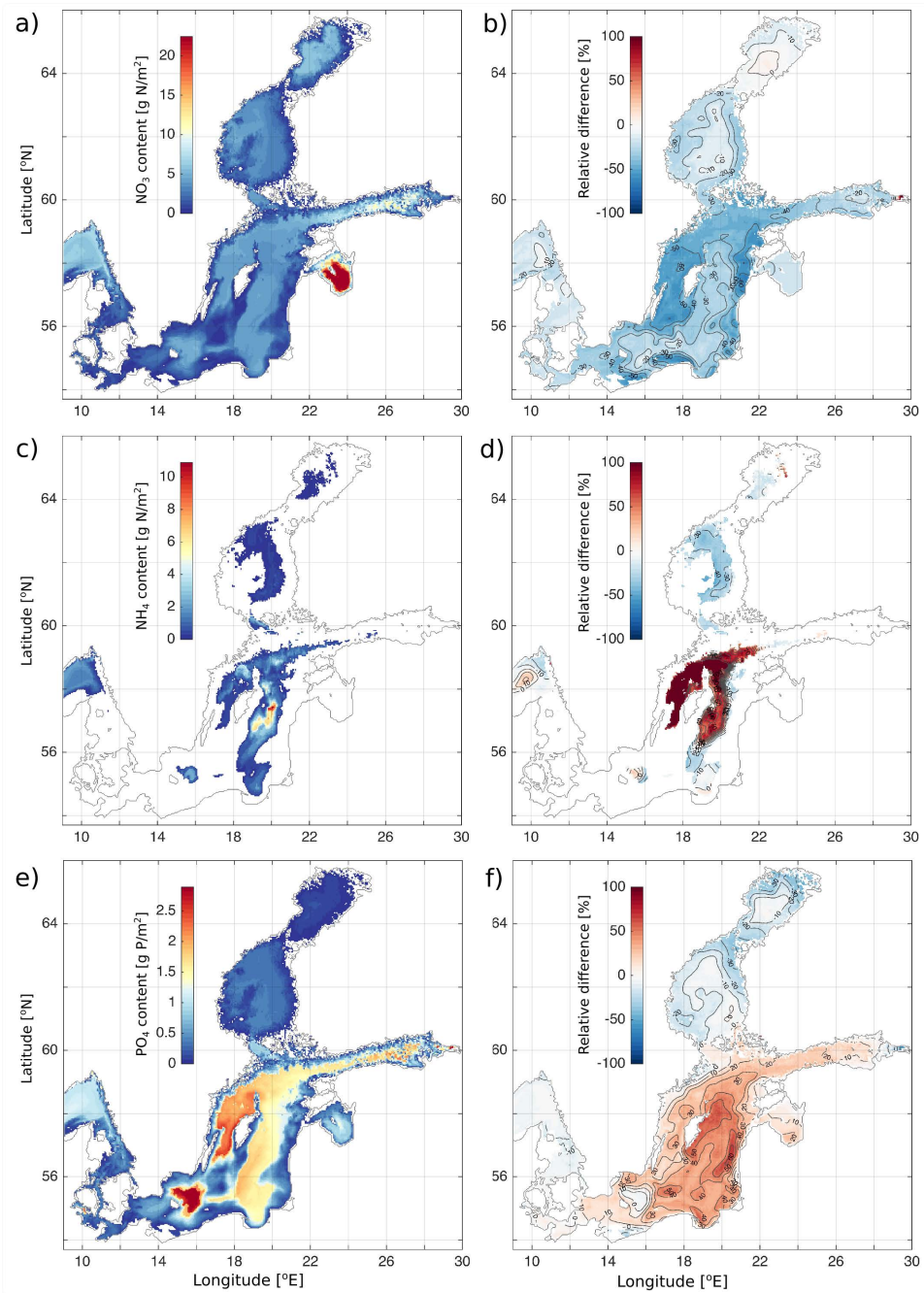


Figure 3. Mean NO_3 (a, b) in the intermediate layer, NH_4 (c, d) in the deep layer and PO_4 (e, f) pools in the intermediate layer in February during the period 1993–1999 in the left panels (a, c, e) and their relative changes $(t - \text{ref}) / \text{ref} * 100$ for the period 2000–2017 in the right panels (b, d, f) in the Baltic Sea. The left plots show nutrient pools as the amount of nutrient per square metre. The layers are depicted as the intermediate layer (15–80 m) and deep layer (80–bottom). The contour lines on (b), (d) and (f) show relative changes with a 10% step.

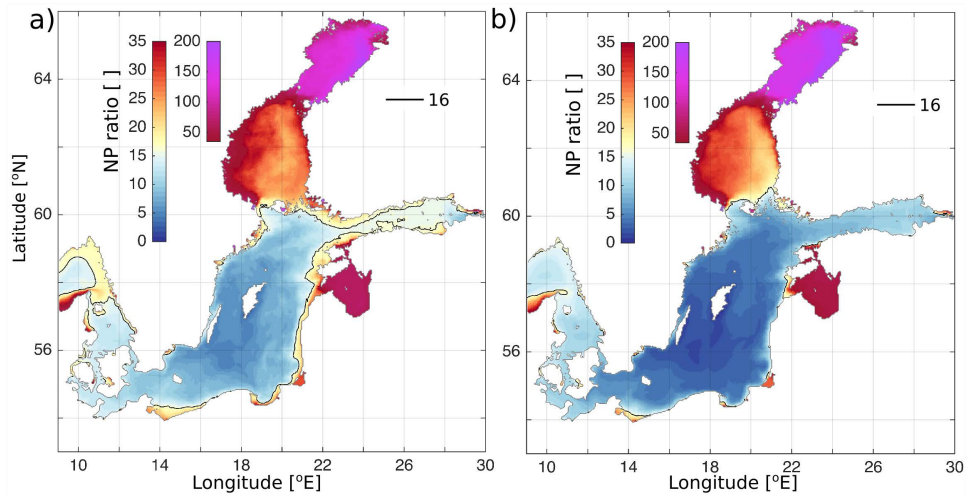


Figure 4. The mean DIN:DIP ratio (NO_3+NH_4/PO_4) in the 0–15 m layer during the period 1993–1999 (a) and during the period 2000–2017 (b). The black contour corresponds to areas with DIN:DIP ratio of ≥ 16 .

The variations in nutrient pools should be reflected in the statistics of spring and summer phytoplankton blooms. Over the study period 1998–2017, the spring bloom spatiotemporal coverage has shown a general tendency to increase from 2002 to 2008–2011, followed by a decrease until 2017 (Figure 5 a). Summer bloom coverage increased from 1998 until 2005, followed by a decreasing tendency until the end of the period, with the subsurface bloom dominating over the surface bloom (Figure 5 b). To attribute this decrease to the decrease of nitrate and phosphate pools (Figure 2) could be premature.

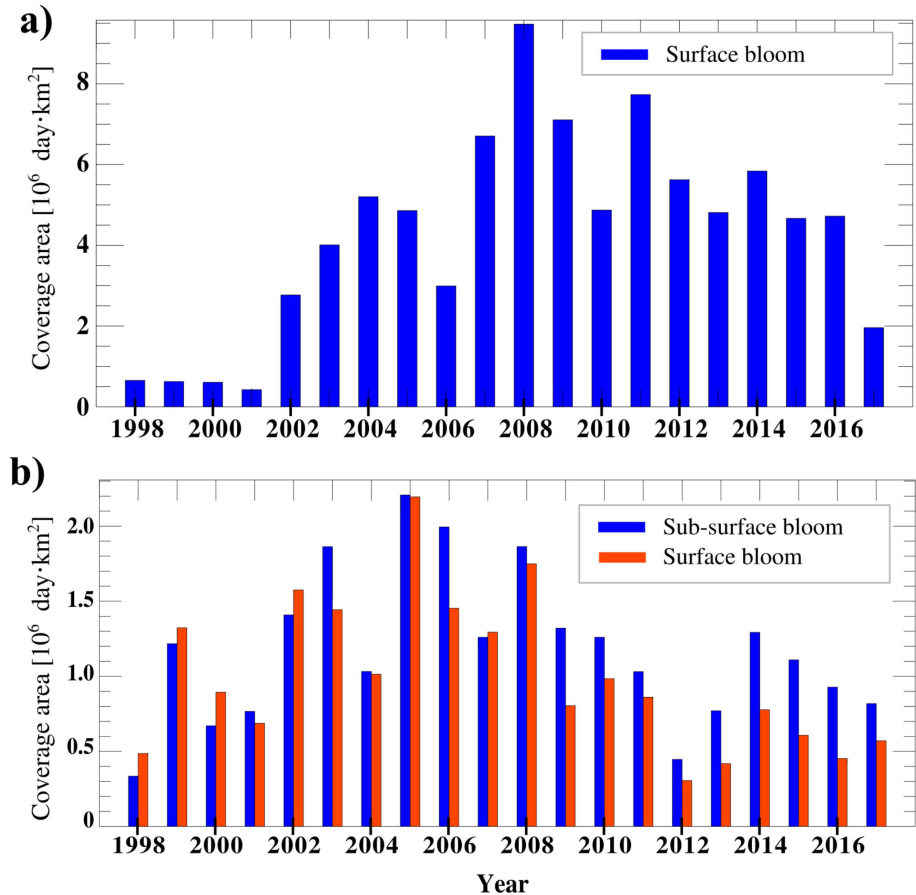


Figure 5. Time series of spring (a) and summer bloom (b) spatiotemporal coverage (day km²) (1998–2017) using the method by Hansson and Håkansson (2007).

Starting with 1998, the mean start day of the spring bloom shifted from day 120 to days 60–80 from 2003 onwards (Figure 2.4.1. In Paper III). According to the start day and spatio-temporal coverage, the spring bloom evolution in the Baltic Sea could be described as follows:

- 1) late onset spring bloom (starting later than day 100) with a small spatio-temporal coverage, characteristic of 1998–2002;
- 2) medium onset spring bloom (starting at around day 80) with a large spatio-temporal coverage, prevalent in 2003–2011;
- 3) early onset spring bloom (starting at around day 60) with a relatively medium spatio-temporal coverage, prevalent in 2012–2016.

The end day of spring bloom as well as peak day has not shown significant shifts over the study period.

3.2 Pools of dissolved oxygen and recent evolution of hypoxia and anoxia in the Baltic Sea

Calculations of the dissolved oxygen pools of the entire Baltic Sea over the period 1993–2017 show only a marginal decrease of oxygen content in the deep layer (Figure 6 a). There are 2 distinctive periods of hypoxia evolution in the Baltic Sea: 1993–1999 and 2000–2017 (Figure 6 b–c). During 1993–1999, hypoxic area and volume increased steadily with the rate of $5000 \text{ km}^2 \text{ yr}^{-1}$ and $200 \text{ km}^3 \text{ yr}^{-1}$, respectively (see Table 4 in Paper I). There are two lines for hypoxia area and volume in Fig. 6 to cover the two definitions of hypoxia ($\text{DO} < 2 \text{ ml/L}$ and $\text{DO} < 2 \text{ mg/L}$). The trends for the anoxic area and volume were smaller, accounting for $1400 \text{ km}^2 \text{ yr}^{-1}$ and $30 \text{ km}^3 \text{ yr}^{-1}$, respectively.

During the second period 2000–2017, variability of the hypoxic area showed a statistically stationary process. The statistical stationarity tests were conducted to detect whether the hypoxic and anoxic areas were at a stable level or going through a change. The hypoxic area varied between $50,000$ and $80,000 \text{ km}^2$ and the anoxic area between $10,000$ and $50,000 \text{ km}^2$. The periodicity of 10 years could be caused by the interplay between MBI-s in 2003 and 2014 (Figure 6 c) and local biogeochemical processes. The area of hypoxic water and the area and volume of anoxic water showed a small negative trend (Figure 6; see table 4 in Paper I), whereas the volumes of hypoxic water had weak positive trends. The mismatch between hypoxic and anoxic area and volume estimated from reanalysis and measurements is mainly due to model deficiencies in simulating physical and biogeochemical processes in the deep layers.

To characterise the spatio-temporal evolution of the hypoxic and anoxic areas, the probabilities of hypoxia and anoxia occurrence were introduced. The probability of anoxia or hypoxia occurrence is defined as the ratio of the number of days when anoxia or hypoxia was present at the grid cell to the total number of days during the period under consideration. The regions with hypoxia and anoxia probability of 0.25 (3 months of the year) could be considered as proxy for seasonal and episodic hypoxia and anoxia. In addition, these areas could be prone to long-term hypoxia or anoxia in the future.

In 1993–1999 permanent hypoxia developed in the areas deeper than 80 m (Figure 7 a,c). From the hypsographic curve of the Baltic Sea (Figure 7 b), we can say that the 80 m isobath represents the characteristic depth of the upper bound of the hypoxic area. However, in the Bornholm Basin, persistent hypoxia with an episodic increase of oxygen concentrations occurs in the areas shallower than 80 m (Figure 7). An opposite pattern with a persistent hypoxia deeper than 80 m is characteristic of the Gdansk Basin (Figure 7). Seasonal or episodic hypoxia occurs in the transition area between Gdansk and Eastern Gotland basins. Among shallow areas, the Neva River estuary is prone to frequent hypoxia and even anoxia (Figure 7). By 2000–2017, the probability of hypoxia increased in the areas deeper than 80 m (Figure 7 b–d). Geographically, the area with increased hypoxia probability spread southward in the Eastern and Western Gotland basins, and increased at the entrance to the Gulf of Finland and in the western part of the gulf.

There were no permanent anoxic regions in the Baltic Sea in 1993–1999, except for the deepest local areas of the Eastern Gotland Basin and Northern Baltic Proper (Figure 7 e). Anoxic area increased geographically and probability-wise from 1993–1999 to 2000–2017 (Figure 7 e–f). In the southern Baltic Sea, the areas with anoxia probability less than 0.25 during 1993–1999 turned into areas with permanent anoxia during 2000–2017. Rather than indicating seasonal and episodic anoxia, the changes in probability from lower

values during the first period to higher values during the second period show gradual development of anoxia. In the Bornholm Basin and Gdansk Basin, the anoxic areas with probability less than 0.25 could indicate seasonal and episodic anoxia.

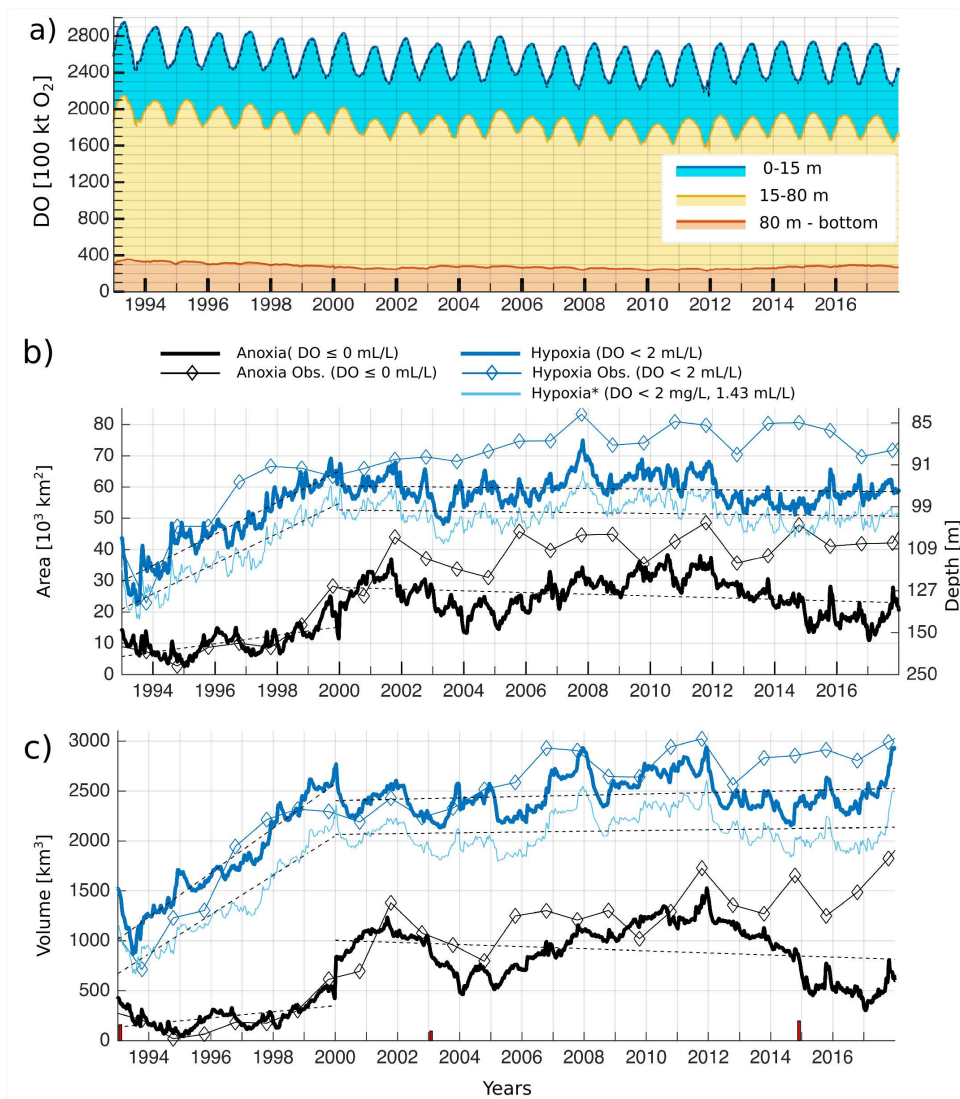


Figure 6. a) Stacked plot of time series of summarised DO in three different layers (surface layer 0–15 m: blue; Intermediate layer 15–80 m: yellow; and Deep layer starting at 80 m and extending to the bottom: red) across the entire Baltic Sea.

The area (b) and volume (c) of anoxic (black line) and hypoxic (blue lines) water masses in the Baltic Sea domain calculated from the model reanalysis (solid lines) and the measurements (diamonds). Dashed lines show linear trends for two periods. The axis on the right side on (a) shows the depths which correspond to the area in the Baltic Proper (including the Gulf of Finland) that lies below the corresponding depth level, as calculated from the hypsographic curve of the Baltic Proper (including the Gulf of Finland). Volume and timing of the Major Baltic Inflows are marked with the bars (b).

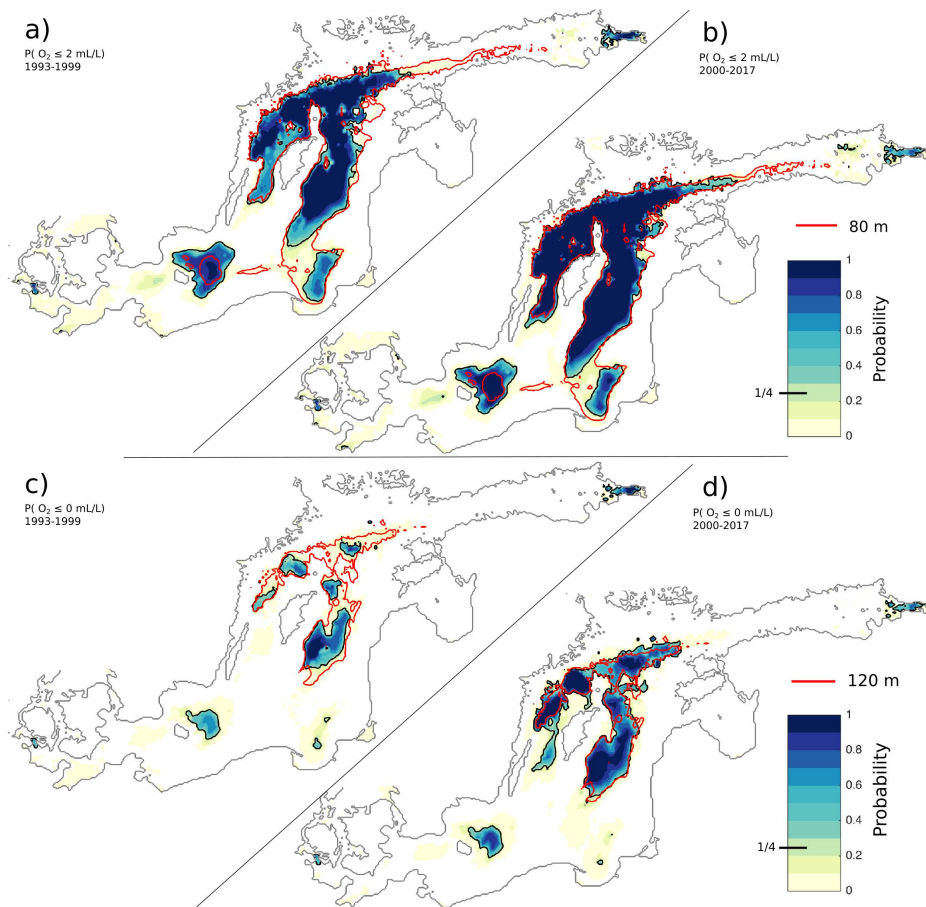


Figure 7. The probability of hypoxic ($DO < 2 \text{ ml l}^{-1}$) on (a)–(b) and anoxic ($DO < 0 \text{ ml l}^{-1}$) on (c)–(d) water masses over the period 1993–1999 on (a),(c) and 2000–2017 on (b),(d) in the Baltic Proper (including the Gulf of Finland). The black isoline corresponds to a 0.25 probability. The red contour shows the 80 m isobath on (a)–(b) and 120 m isobath on (c)–(d).

3.3 Effect of additional nutrients on the ecosystem

In this thesis, the impact of increased nutrient load on the Baltic Sea ecosystem is evaluated, based on the example of shipborne nutrient input to the Baltic Sea (Paper II), calculated from the STEAM and COSMO-CLM/CMAQ model systems (Section 2.3).

The effect of combined nutrient input from shipping-related waste streams and ship emission atmospheric depositions on the overall biogeochemical cycle, primary production, detritus formation and nutrient flows of the Baltic Sea was studied. The impact on the biogeochemical processes was assessed by subtracting the fluxes of nitrogen and phosphorus from two model simulations (SHIP, NOSHIP). Total nitrogen in the marine ecosystem can be divided into NO_3 (the majority), nitrogen in phytoplankton, dissolved molecular nitrogen, i.e. the result of denitrification, and nitrogen bound to detritus (Figure 8). The nitrogen input consists of NO_3 and NH_4 deposition from the emissions to the atmosphere and direct discharge to the water due to shipping activity.

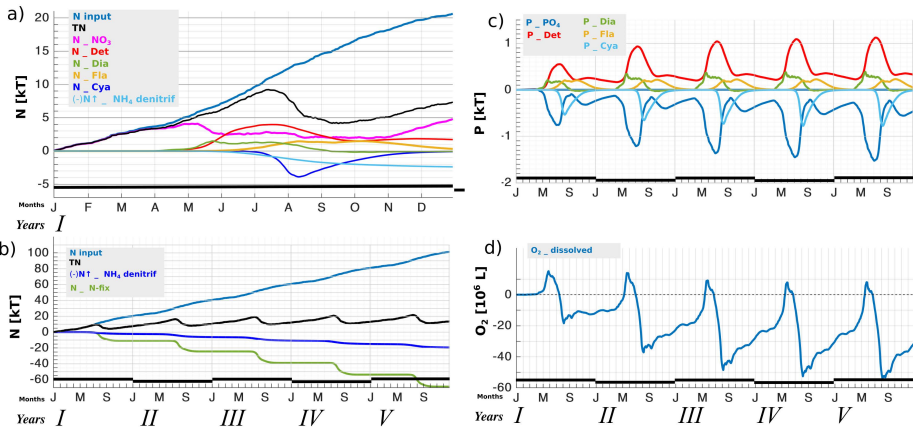


Figure 8. (a) Annual time-series of excess nitrogen pools for the first simulation year between SHIP and NOSHIP simulations. Blue line (N input) stands for nitrogen input, black line (TN) is total nitrogen, pink line (N_NO₃) is nitrate, red line (N_Det) is detritus, green line (N_Dia) is diatoms, yellow line (N_Fla) is dinoflagellates, dark blue line (N_Cya) is cyanobacteria or nitrogen fixation, light blue line ((-)N_NH₄ denitrif) is denitrification.

Five-year time-series of: (b) nitrogen balance between input and total nitrogen pool in the water, where blue line (N input) is nitrogen input, black line (TN) is total nitrogen, dark blue line ((-)N_NH₄ denitrif) is denitrification and light blue line (N_N-fix) is nitrogen fixation. (c) phosphorus budget, where blue line (P_PO₄) is phosphate, red line (P_Det) is phosphorus in detritus, purple line is phosphorus in iron-phosphate, green line (P_Dia) is diatoms, yellow line (P_fla) is dinoflagellates, light blue line (P_cya) is cyanobacteria. (d) oxygen content (SHIP - NOSHIP)

For the first three months of the year nitrogen that enters the ecosystem remains in the water as pelagic NO₃ (Figure 8 a). With the onset of the spring bloom total nitrogen in the water column starts to decrease in relation to the excess nitrogen input due to consumption by diatoms and flagellates. As phytoplankton decomposes, the pool of nitrogen bound to detritus starts to increase. Decomposition also contributes to the NH₄ pool, but this does not reflect in the pool size as NH₄ is rapidly oxidised into NO₃ and molecular N. The nitrogen fluxes during the bioactive period can be summarised as concurrent transformations from phytoplankton-bound nitrogen into detritus, followed by decomposition back to DIN and denitrification to molecular N. As seen in Figure 8 a, the input of additional nitrogen causes cyanobacteria biomass to decrease. With that the amount of dead organic matter (detritus-bound nitrogen) also decreases. The same, although to a lesser extent, applies to nitrogen in diatoms and flagellates, and inorganic nitrogen in the water. From the end of August to November, the pool of inorganic nitrogen remains stable as negative contribution by lessened cyanobacteria bloom decreases, and nitrogen consumption by flagellates balances the decomposition of organic matter. November marks the end of active primary production and with that the consumption of bioavailable nitrogen as detritus nitrogen gains stable positive level and the continuous input enables nitrogen to accumulate in the system. By the end of December the nitrogen added into the system is retained as NO₃ in the water and as organic nitrogen in detritus. The low temperatures and decreased amount of dead organic matter at the end of the year slow the rate of denitrification.

To study the long-term effect of the added nutrients in the Baltic Sea ecosystem we extended the simulation to five years, repeating the same annual input and hydrophysical conditions. The results indicate that the total annual NO_3 in the water and nitrogen in detritus approach a steady state relatively fast (Figure 8 b). The input of excess nitrogen is largely compensated by decreasing nitrogen fixation and increasing nitrogen removal due to denitrification. PO_4 in the water column also decreases, i.e. excess PO_4 is negative, accompanied by the increase of phosphorus pool in the sediments (Figure 8 c). Continuous decomposition of organic material results in higher oxygen consumption and a negative trend of the oxygen content which decelerates in time (Figure 8 d).

4 Discussion

4.1 Changes in nitrogen pools

The internal DIN pools have a decreasing trend across the Baltic Sea (Figure 2 a–b; Paper IV; Vahtera et al., 2007; Bonaglia et al., 2016), which agrees with Lønborg and Markager (2021). The difference from Gustafsson et al. (2012) and Savchuk (2018), where the Baltic Sea nitrogen pools were relatively stable during the last decades, accounts for a different time period and estimation method used. The pelagic nitrogen pools depend on the inputs from land, export and release of organic matter from the sediment and net export of nutrients to downstream areas. The negative tendency in the internal nitrogen pools can be attributed to the significant decrease in nitrogen input and increased removal from the system.

Nitrogen has multiple alternative pathways into the sea, e.g. fixation by diazotrophic organisms, atmospheric deposition, rivers and wet discharge from land and ships. Nitrogen removal from the marine system is an interplay between several processes, which include denitrification, anammox and dissimilatory NO_3 reduction to NH_4 or DNRA. All major nitrogen transformation processes are dependent on oxygen concentrations (Conley et al., 2009b), which is an important feature in Baltic Sea, where oxygen concentrations are extremely variable across time and space.

Denitrification, the main process to remove nitrogen in the Baltic Sea, is carried out by heterotrophic anaerobic bacteria and reduces NO_3 into dinitrogen gas (N_2) (Bonaglia et al., 2016). As the availability of NO_2 and NO_3 is a prerequisite for denitrification, it is assumed to be dependent on nitrification, which in turn is an aerobic process (Dalsgaard et al., 2013). Thus, anaerobic denitrification mostly occurs in transitional conditions: in the sediments at the oxic-anoxic boundary or in the water column, directly below the oxic-anoxic interface (Bonaglia et al., 2016). Active denitrification in the water column explains the notable decrease of the NO_3 pool in the intermediate and deep layers of the Baltic Sea, where the oxic-anoxic interface often lies higher up in the water column (Figure 2 a). The amount of nitrogen denitrified in the water column per year is still debated, but the magnitude can be comparable to sediment denitrification according to the highest estimate by Dalsgaard (2013).

Anammox, the alternative process to remove nitrogen, is predominant in newly anoxic conditions where sulphides have not yet formed, e.g. the Gotland Deep after an inflow event (Hannig et al., 2007; Dalsgaard et al., 2013). Anammox is not as prevailing as denitrification, but can be important periodically and locally – e.g. anammox in the sediments of the seasonally anoxic Gulf of Finland has been measured to contribute 10–15% to the total N_2 production (Hietanen and Lukkari, 2007). Similarly to denitrification, anammox is also dependent on NO_2 and NO_3 which links the process with nitrification and oxygen. This knowledge, however, does not align well with the overall negative correlation which has been observed in a number of studies between the extent of anoxic area and pelagic nitrogen pool, which suggests accelerated nitrogen removal with increased oxygen deficiency (Conley et al., 2009; Kulinski et al., 2021). This could be explained by the effective transport of NO_2 and NO_3 from oxic areas, where they are generated, into deep layers, as well as suggesting the existence of an additional nitrogen removal pathway, chemolithoautotrophic denitrification via e.g. sulphur (or methane), which would enable the process to occur in the deep, permanently anoxic bottom layer (Brettar and Rheinheimer, 1991; Conley et al., 2009a; Hietanen et al., 2012). Nitrogen

removal of chemolithoautotrophic origin in the Baltic Sea is supported by Dalsgaard et al., (2013) and Bonaglia et al. (2016), as they have shown the occurrence of denitrification in the presence of sulphide as an electron donor. Organic carbon and NH_4 have also been suggested as electron donors and important drivers of denitrification in the Baltic Sea (Dalsgaard et al., 2013; Bonaglia et al., 2016).

The accumulation of NH_4 at the bottom of the central deep basins of the Baltic Sea (Paper IV; Figure 3 c–d) can be attributed to prevalent nitrogen retaining processes, represented by DNRA, which is strictly anaerobic and has a larger share due to the expanding anoxic bottoms during the last few decades (Figure 6; Jäntti and Hietanen, 2012; Bonaglia et al., 2016).

The results suggest that the tendency of decreasing water column nitrogen pools in the last decades reflects the reduction of inputs, but also increasing nitrogen removal from the system, which occurs regardless of the negative tendency of oxygen concentrations in the Baltic Sea. Indeed, it has been shown that over time denitrification rates in the Baltic Sea have increased due to the elevated amounts of nitrates and organic material in the water (Gustafsson et al., 2012) as well as due to the effects of the changing climate such as the increase in average temperature and stronger stratification (Lønborg and Markager, 2021). The negative correlation between hypoxic water mass and DIN also suggests increased removal with worsening oxygen concentrations in the last decades, although the exact process behind this phenomenon is still debated, as already discussed (Hietanen and Lukkari, 2007; Vahtera et al., 2007; Hietanen et al., 2012).

4.2 Changes in phosphorus pools

During the last decades, inorganic phosphorus pools have steadily increased across most of the Baltic Sea (Figure 2 c), most notably in the Baltic Proper, the Gulf of Finland and the Gulf of Riga (Paper IV; Gustafsson et al., 2012; Savchuk, 2018).

Phosphorus transformation pathways in a marine system are fundamentally different from nitrogen. Phosphorus enters the sea mostly from rivers and sewage water and remains a part of the marine system indefinitely (HELCOM, 2018). When we exclude advection, the only natural sink for phosphorus is burial in organic form or as authigenic P-bearing minerals (Kulinski et al., 2021). The speed and efficiency of phosphorus burial is heterogeneous in the Baltic Sea, depending on the sedimentation rates, iron availability and oxygen concentrations (Viktorsson et al., 2013; Kulinski et al., 2021). Three groups of minerals have been identified in the Baltic Sea sediments: calcium (Ca)-phosphates (fluorapatite), Mn-Ca carbonates (rhodocrosite) and Fe (II) phosphates (vivianite) (Jilbert and Slomp, 2013; Dijkstra et al., 2016). In addition to burial, sediments also store vast amounts of phosphorus as iron-phosphates (Lehtoranta et al., 2009). Phosphorus cycle in a marine ecosystem is strictly oxygen-dependent (Lukkari et al., 2009; Watson et al., 2017). When the water column turns anoxic, PO_4 is released from the iron-oxides and becomes (bio)available again (Conley et al., 2009a; Viktorsson et al., 2013). The PO_4 that is released into the deep layer can be carried to the euphotic zone by seasonal erosion of the pycnocline and inflows from the North Sea, which transport the deep and intermediate layer PO_4 -laden water masses upstream towards the Gulf of Finland (Stigebrandt, 1985). The increase of phosphorus pools was biggest in the surface and intermediate layers, while the positive tendency at the bottom was modest (Figure 2 c; Paper IV). Indeed, coastal areas bind phosphorus effectively and thereby act as a filter for nutrients deriving from land (Asmala et al., 2017). These areas are especially

vulnerable to hypoxia and anoxia, as inorganic phosphorus is released rapidly when oxygen concentrations fall to zero seasonally and episodically, which is very common in many areas of the Baltic Sea, especially the Gulf of Finland (Figure 7). In coastal areas the water column is usually shallower than the mixing depth, which guarantees the active utilisation of PO_4 by primary producers, activating a positive feedback mechanism with increased sedimentation of organic matter, the consequent seasonal bottom water oxygen depletion and increased sediment phosphorus release back to the water column, also known as the “vicious circle” (Vahtera et al., 2007).

The biogeochemical conditions in the Gulf of Bothnia differ from the rest of the Baltic Sea, which also reflects in the ecological status of the area. The limited exchange with the Baltic Proper, weak stratification and small external load of nutrients explain the year-round sufficient oxygen conditions, although the organic carbon load is high (Kuosa et al., 2017). Consequently, the Gulf of Bothnia is known as the only area in the Baltic Sea that stores phosphorus effectively in the sediments as the presence of oxygen allows phosphorus to be stored in the sediments as iron-phosphates. Still, the Bothnian Sea also experiences a positive winter DIP trend in the deep layer (Paper IV), which possibly reflects the intrusion of oxygen-deficient phosphorus-enriched water mass from the Baltic Proper (Rolff and Elfving, 2015). Simultaneously, the input of phosphorus from the drainage basin could also be increasing (Kuosa et al., 2017).

The effect of the significantly decreased phosphorus input into the Baltic Sea cannot be seen in the pelagic cycling of phosphorus, which is still on an increasing course, with the internal pool now exceeding loads 11 times (Savchuk, 2018). This suggests that the sediments act as an ineffective phosphorus sink due to recurring or permanent anoxia, which effectively maintains the large internal pool, independent of external inputs (Paper I). The increase of phosphorus pools during the last decades across most of the Baltic Sea agrees with previous studies (Paper IV; Gustafsson et al., 2012; Savchuk, 2018).

4.3 DIN:DIP ratio

The decrease of DIN and increase of DIP pools in the Baltic Sea results in a decreasing DIN:DIP ratio, mostly at the expense of coastal areas (Figure 4). Changes in the nutrient ratio play an important role in the eutrophication of a sea and can be a key component in aggravating ecosystem changes (Granéli et al., 1990). Low nitrogen to phosphorus ratio leaves excess phosphorus in the euphotic zone after the spring bloom has terminated (Granéli et al., 1990). The strengthening of nitrogen limitation in the Baltic Sea is driven by the autonomous, self-sustaining “vicious circle”, where nitrogen is removed from the system with increasing rate as oxygen deficient zones increase – which in turn, favours the spread of cyanobacteria, compensating for the “lost” nitrogen (Savchuk, 2018). Simultaneously, phosphorus is released from the sediments in anoxic areas, being the direct result of decreasing dissolved oxygen content in the water (Figure 6–7; Paper IV; Conley et al., 2002; Viktorsson et al., 2013). This cycle is linked with the timing and distribution of phytoplankton blooms: if the spring bloom weakens due to DIN running out, the summer bloom of diazotrophic cyanobacteria is enhanced due to excess DIP in the water (Paper II; Vahtera et al., 2007). The regions of the Baltic Proper with significant changes in the DIN:DIP ratio (Figure 4) overlap with areas of intense cyanobacteria blooms as recorded by Kahru and Elmgren (2014). In the Bothnian Sea, the DIN:DIP ratio has also decreased, and the area is also known for emerging cyanobacteria blooms (Kahru and Elmgren, 2014; Olofsson et al., 2020; Olofsson et al., 2021). Consequently, as poor oxygen conditions prevail, or even expand in the Baltic Sea

(Paper I), nitrogen will continue to be preferentially removed (Paper IV) and the balance with phosphorus, which now strongly relies on the internal release, will be off in the near future, while long-term predictions are yet uncertain based on the knowledge and data we have (Saraiva et al., 2019; Meier et al., 2021). The shift in the DIN:DIP ratio is an integral link in sustaining the state of Baltic Sea ecosystem, which thus far remains quite resilient to external changes and the prevailing trends in nitrogen and phosphorus pools (Figure 2). The lag in the ecosystem's response to nutrient changes effectively demonstrates the exceptionally long time scales of the biogeochemical cycles in the Baltic Sea (Gustafsson et al., 2012).

4.4 Effect of nutrient pools on phytoplankton blooms

Primary production is an integral link in the biogeochemical cycle of nutrients and earlier studies have shown a positive correlation between nutrient concentrations and primary production biomass (Fleming and Kaitala, 2006; Groetsch et al., 2016; Raateoja et al., 2018). The nutrient base of the Baltic Sea sustains a high biomass of phytoplankton, which in turn creates vast amounts of decaying, oxygen-consuming organic matter – a direct reflection of a severely eutrophicated system (HELCOM, 2003). Nutrient reductions and the consequent decreases in the Baltic Sea nutrient pools should result in a decrease of the large and mostly nitrogen-limited spring blooms (Groetsch, 2016). But, as already mentioned, in a nitrogen-limited system, a fraction of the bioavailable phosphorus is left in the water after the spring bloom has terminated. The characteristic features of Baltic Sea – low salinity together with warm water temperatures and strong stratification in summer – enable the growth of cyanobacteria, which will consume the residue phosphorus and can fix nitrogen from the atmosphere, filling the niche void from the other functional groups (Olofsson et al., 2016; Savchuk, 2018; Kahru et al., 2020). Cyanobacteria are linked to eutrophication due to their ability to utilise N₂ from the atmosphere, convert it into bioavailable nitrogen and thereby perform as an additional nutrient source in an already over-fertilized ecosystem (Munkes et al., 2021). Whether this newly imported nitrogen has an effect on the next year's bloom, depends on the system's ability to remove it. The Baltic Sea is relatively effective at eliminating nitrogen, which limits the effect of nitrogen introduced by cyanobacteria to one season (Kulinski et al., 2021). This is supported by our results, which do not indicate a correlation between the spring and summer blooms inter-annually (Figure 5).

The studied time frame (1993–2017) does not reveal a clear pattern for the phytoplankton spatiotemporal coverage in relation to changes in nutrient pools. Both spring and summer bloom have a “broken” trend with an increase until ca. 2005–2008 and a decrease after that (Figure 5). A clear temporal shift of the spring bloom was observed, which indicates that blooms become longer, but less intensive. This can be attributed to nutrients becoming available earlier due to climatic conditions (Groetsch et al., 2016) and the existence of other limiting factors, which restrict the intensity of the bloom. A similar phenomenon has been observed by others (Fleming and Kaitala; 2006; Kahru et al., 2016; Kulinski et al., 2021). If anything, the summer blooms have in fact decreased in the last 8 years of the study period, despite increasing internal phosphorus pools, indicating other causes aside from nutrients. The matter has been more thoroughly discussed in e.g. Kahru et al. (2018) and Olofsson et al. (2020), who concluded that nutrient concentrations in the water are not the only explanation for the inter-annual dynamics of cyanobacteria blooms, which seem to oscillate short-term due to causes yet uncertain. As the controls of cyanobacteria blooms are still not

comprehensively understood, the uncertainty of model-based projections in the Baltic Sea is considerable (Munke et al., 2021; Löptien and Dietze, 2022). Moreover, Carstensen et al. (2011) have discussed the possibility of a shift in the nitrogen – chl-a ratio over time towards a unit of nitrogen supporting a higher yield of phytoplankton biomass, which suggests changes in a variety of other, non system-specific factors which the ratio depends on, e.g. the taxonomic composition of phytoplankton and turnover of nitrogen in the water and sediments. This could also be a part of the explanation why phytoplankton blooms have not changed during the last decades.

Setting aside model discrepancies, it could be assumed that: a) phytoplankton spatio-temporal coverage (day/km^2) does not linearly respond to nutrient pools in the Baltic Sea ecosystem; b) phytoplankton blooms are (co)limited by other factors, which we did not look at; c) the time period is too short to see a clear change.

4.5 Oxygen

Extensive phytoplankton blooms produce vast amounts of detritus, or dead organic matter, most of which sinks to the bottom and is mineralized, as long as oxygen is available. Thus, the extent of hypoxia and anoxia can be used at estimating the eutrophication status of a marine ecosystem (Almroth-Rosell et al., 2021).

Temporal changes of dissolved oxygen concentration in a volume of water are determined by the ratio of cumulative sources and sinks of oxygen (Fennel and Testa, 2019). Atmosphere is the main contributor of oxygen to the sea. Oxygen enters the surface layer via air-sea gas exchange and its penetration depth is determined by the vertical stratification of the water column. Below the active gas exchange layer lateral transport and biogeochemistry control the oxygen concentrations. In the Baltic Sea persistent hypoxia occurs below a permanent halocline, whereas seasonal hypoxia may develop in areas with a seasonal pycnocline (Väli et al., 2013; Liblik et al., 2018). Episodic hypoxia is related to certain circumstances: weak oxygen flux from the air, warm water and oxygen consumption prevailing over oxygen production (Virtanen et al., 2019).

Our results showed a marginal decrease of the calculated oxygen pools in the deep layer of the Baltic Sea (Figure 6 a), which was unexpected, and we assume that it does not reflect the conditions in the problematic areas of the Baltic Sea (BP, GoF). This is due to the pools also taking into account the large volume of deep water (below 80 m) in the well-oxygenated Bothnian Bay, which seemingly reduces the overall poor state of the Baltic Sea.

A clear shift was revealed in the regime of hypoxic and anoxic areas and volumes over the study period 1993–2017. The temporal evolution of anoxic and hypoxic area and volume has two dynamically different periods (Paper I). The first period (1993–1999) was marked by a steady increase of the areas and volumes of hypoxic and anoxic water masses. The second period (2000–2017) showed indications of stabilising anoxic and hypoxic areas and volumes, with periodic fluctuations. We suggest, based on the stationarity tests conducted on the two periods' trends, that in the future the loss of stationarity of the time series of oxygen deficient water masses would indicate a regime change of hypoxia development in the Baltic Sea (Paper I). The switch in regimes of anoxic and hypoxic areas and volumes around the turn of the 20th century was also observed by Almroth-Rosell et al. (2021). The time-series were complemented by anoxia and hypoxia probability maps (Figure 7), which revealed a progressive geographical spreading of permanent hypoxia and anoxia into shallower areas, with the most dramatic expansion occurring in the central Baltic Proper. The distribution of oxygen deficient

zones was mostly limited by the 80 m and 120 m isobaths in the case of hypoxia and anoxia, respectively. The distribution of anoxia and hypoxia confirm the importance of vertical stratification in affecting oxygen concentrations in the Baltic Sea, with some local variations (Meier et al., 2011; Väli et al., 2013). The Baltic Proper has a persistent and strong density stratification with a pycnocline at the depth around 60–80 m, which largely determines the upper limit of the extent of permanent hypoxia, with moderate deviations of the pycnocline being shallower than 80 m in the Bornholm, and deeper than 80 m in the Gdansk Basin. One remarkable exception to this principle is the eastern Gulf of Finland, including the direct vicinity of the Neva River, where seasonal hypoxia and even anoxia are seen in shallow waters of less than 25 m. This is due to seasonal salt wedge dynamics playing a significant role in determining stratification in the Gulf of Finland (Maljutenko and Raudsepp, 2019).

The primary factor to determine deep water stratification in the Baltic Sea are MBI-s, which are known to improve oxygen conditions under the halocline (Leppäranta and Myrberg, 2009). Although this is true, the effect remains temporary, as long-term stratification will instead strengthen, reducing the downward mixing of oxygen (Carstensen and Conley, 2019; Krapf et al., 2022). This is backed up by the positive trend in salinity below 70 m depth since the end of the stagnation period in 1993 (Von Schuckmann et al., 2019), as well as the coincidence between regime shifts in the anoxic area extents in the Gotland Basins and increased frequency of MBI-s (Mohrholz, 2018). Thus, the upsurge of MBI-s is expected to increase hypoxic layer thickness. Recent findings, supported by our results, show that oxygen decline and the restoration of anoxia have been rapid after the 2003 and 2014 inflows, despite the latter being the third strongest salt water inflow into the Baltic Sea since 1880 (Neumann et al., 2017, Paper I). This has happened simultaneously with the decreasing DIN and increasing DIP pools, observed in this thesis as well as by Savchuk (2018). This suggests that local biogeochemistry is the other crucial factor in determining dissolved oxygen content below the halocline. The accelerated worsening of oxygen conditions following the 2014 inflow event was explained by increased amount of organic matter transported into the deep layer, which caused the rapid consumption of available oxygen by decomposers (Meier et al., 2018).

While the occurrence of MBI-s and the consequent water column stratification strength are highly unpredictable and unmanageable, the biogeochemical factors at play in the eutrophication process also determine the outcome of nutrient input reductions. Although nutrient load reductions are significant, there has not yet been an improvement in oxygen conditions of the Baltic Sea. We suggest that the stabilisation of the formerly increasing trend of oxygen deficient zones most likely reflects the maximal extent of the halocline-controlled persistent hypoxia and anoxia, but does not provide a reliable forecast for the future evolution of the oxygen content. By now it has been stated in several studies that the expansion of permanent hypoxia has already reached its maximum extent due to the upper limit resulting from the halocline position and ventilation (Almroth-Rosell et al., 2021; Krapf et al., 2022). The future prospects hold a possible spread of seasonal hypoxia and anoxia in shallow areas due to the decomposition of organic matter, the amount and speed of which is enhanced by climate change, especially elevated water temperatures (Meier et al., 2019). This hampers the efficiency of the coastal filter by altering nutrient removal pathways, as discussed in sections 4.1 and 4.2, and thereby sustaining the “vicious circle” (Asmala et al., 2017; Kulinski et al., 2021). An improvement in the Baltic Sea oxygen conditions is estimated

over the long-term if the current nutrient reduction scheme is continued, as the changing climate will likely not counteract nutrient load reductions, but the time scale of the changes will be measured in decades and will have a high level of uncertainty (Saraiva et al., 2019; Meier et al., 2021).

4.6 Baltic Sea nutrient reduction and biogeochemistry

In the previous sections we looked at the key ecological indicators of the Baltic Sea eutrophication status from 1993 to 2017. The trends and tendencies observed in nutrient, phytoplankton and oxygen concentrations showed indications of a stability within the system despite ongoing changes in major external eutrophication components. As the results provided a mere description of the ecosystem state, it is difficult to say whether this has to do with nutrient reductions, and what could the possible long-term outlook be. Hence, the question still remains: will decreased nutrient inputs bring about an oligotrophication of the Baltic Sea ecosystem, or, in other words, can the eutrophication process be reversed by controlling just one parameter?

In order to analyse the response of the system to manipulation with nutrients' input, a model scenario was simulated, which in its nature is the opposite of the current declining nutrient input situation (Paper II). Three major nutrient loads from ships in 2012 were quantified and the simulation was repeated for 5 years to study possible ecosystem feedback, which was then compared with reference conditions without these nutrient loads. The effect of external nutrient input on the spatial nutrient distribution, as well as sediment pools, and ecosystem in general (phytoplankton, oxygen) was studied. It has to be noted that shipping as a nutrient source, in absolute values ~20 kt of nitrogen per year, is comparable with a big river of the Baltic, e.g. the Neva river (Stålnacke et al., 1999). The advantage of the shipping approach is the possibility to view the effect of nutrients in the nitrogen limited open sea, the scene of major cyanobacteria blooms (Kahru et al., 2007; Kahru and Elmgren, 2014).

As already discussed, the Baltic Sea countries with HELCOM have been successful in significantly decreasing the nutrient loads to the sea (HELCOM, 2018; HELCOM, 2019). According to various sources nutrient reductions from land are known to decrease nitrogen and phosphorus inventories in the adjacent coastal marine areas, but the response can take more than 2 years to have an effect, and even longer in complex natural systems (Neumann et al., 2002; Duarte et al., 2009; Schindler, 2012; Van Beusekom et al., 2019). Some well-known examples of ecosystems improving to a certain level include the Black Sea shelf area, Tampa Bay, Chesapeake Bay and the Wadden Sea, where dissolved oxygen concentrations and water quality improved with nutrient reduction (Langmead et al., 2009; Greening et al., 2014; Lefcheck et al., 2018; Van Beusekom et al., 2019). It has to be taken into account, however, that coastal ecosystems have complex trajectories to changes in nutrient input, as well as a variety of external factors affecting their functioning, which determines that they seldom return to their previous, oligotrophic state, but rather end up in a new balance (Duarte et al., 2009). This reality is illustrated by the many examples, where nutrient reductions have not necessarily hastened recovery from eutrophication, but rather hindered or even worsened the process in some cases (Duarte et al., 2009 and the references within; Friedland et al., 2019). This can be due to additional, weightier limiting factors of phytoplankton growth (Van Beusekom et al., 2019); changes in the stoichiometric nutrient ratio, which bring about unexpected changes in the food web (Kerimoglu et al., 2018); physical factors governing phytoplankton blooms (Cloern et al., 2007); loss in key

species of the ecosystem functioning (Friedland et al., 2019) or the existence of a compensatory mechanism to nutrient reductions, e.g. increased cyanobacteria blooms, which create a self-sustaining cycle, a case also in the Baltic Sea (Schindler, 2012; Savchuk, 2018).

The addition of nutrients into a coastal ecosystem has been studied in parallel with the spread of eutrophication across the world. Although nutrient input is correlated with eutrophication, it is difficult to say what the relative difference with the “default” situation would be. It is known that the addition of nutrients usually increases the biomass of direct consumers, the primary producers, as well as changing the interspecies dynamics of the functional groups of phytoplankton, based on the varying nutrient-acquiring abilities of different species (Stockner and Shortreed, 1988; Heisler et al., 2008). In the Baltic Sea, nitrogen limitation, as discussed earlier, has promoted the growth of cyanobacteria, which is considered an integral part of the self-sustaining “vicious circle” (Savchuk, 2018). In the recent decades, cyanobacteria blooms in the Bothnian Sea have increased to the extent where they introduce more nitrogen into the ecosystem than is imported from external sources (Olofsson et al., 2021; Munkes et al., 2021). Thus, it could be presumed that the addition of the limiting nutrient into the system could potentially turn this relationship around, as is seen in some studies about cyanobacteria blooms being suppressed by additional nitrogen in the ecosystem (Schindler, 2012; Raudsepp et al., 2013). Our results (Paper II) indicate that additional nutrients (mostly nitrogen) in the ecosystem first benefit primary producers that constitute the majority of the spring bloom – the diatoms and flagellates, which are able to increase their biomass. Cyanobacteria biomass in summer, on the other hand, is reduced, with the biggest change in the areas with usually strong cyanobacteria blooms, including southern and central Baltic and the western part of the Gulf of Finland (Kahru et al., 1994, 2007; Kahru and Elmgren, 2014). Phosphorus also plays a role as areas with little to no change in cyanobacteria blooms coincide with phosphorus limitation zones, e.g. the Bothnian Bay and big river estuaries. The explanation why cyanobacteria biomass is reduced lies in the competition for nutrients between the functional groups, where N-fixers lose their advantage over diatoms and dinoflagellates. This assures that nutrients play an important role in controlling the biomass of phytoplankton, but the effect depends on the limiting nutrient in the certain area and season, as also stated by Elmgren and Larsson (2001). Similar results with decreasing nitrogen fixers have been obtained by e.g. Schindler (2012) and the studies within as well as Wang and Wang (2009). The contrasting reactions of the spring and summer bloom to nitrogen addition due to functional differences between the groups are part of the explanation why nutrient reductions have and will not bring about a simultaneous, linear decrease of chl-a in the Baltic Sea.

Inorganic nitrogen concentrations in the water closely followed phytoplankton activity with alternating uptake and decomposition during the bioactive season and accumulation in inorganic form in winter (Paper II). Over the 5-year period total nitrogen first increased, but by the 3rd year reached a stable state, which is reflected in the increased denitrification and decreased nitrogen fixation, compensating for the nitrogen inputs (Figure 8). Organic phosphorus accumulated in the sediments over time, while concentrations in the water column decreased, because there were more consumers present – diatoms and dinoflagellates. Our results demonstrate the volatility of nitrogen in the marine system, indicating that the variety of nitrogen transformation processes are able to adapt to nutrient scenarios in order to maintain a stable state. Phosphorus, on the other hand, is mostly permanent in the marine ecosystem, either in the

consumption-remineralization cycle, or via burial in the sediments. This ensures that phosphorus has a long response time in the marine system and the concentrations lag significantly behind the efforts to decrease the input. The new “balance”, or “vicious circle” is difficult to break due to several parallel factors at play, e.g. the importance of physical factors in the Baltic Sea, which have a major impact on the oxygen conditions; the volatility of nitrogen and the long residence time of phosphorus and the ability of cyanobacteria to grow in the brackish Baltic Sea water. The situation is further complicated by the fact that the Baltic Sea area experiences above-average rates of climate change, which may offset nutrient reduction plans with increased freshwater runoff, enhanced nutrient remineralization with higher temperatures and strengthening water stratification (Duarte et al., 2009; Reusch et al., 2018). Because the Baltic Sea lies in a densely populated and agricultural area, the societal drivers also have to be taken into account as some studies consider them even more influential than climate change itself (Bartosova et al., 2019; Pihlainen et al., 2020).

Similarly to this work, Saraiva et al. (2019) and Meier et al. (2021) have formulated that the Baltic Sea has large natural variability, meaning that factors at play are multiple, and future projections also include a vast uncertainty, which has not been taken into account when proposing and laying out the plans for nutrient mitigation in the past. This is not to say that nutrient reductions have been in vain. As Duarte et al. (2009) have said, reduced nutrient inputs have probably halted further eutrophication in many ecosystems, including the Baltic Sea, and the associated damage and risks related to further eutrophication have hence been avoided, together with improvements in some local ecosystem indicators. Saraiva et al. (2019), Meier et al. (2021) and Friedland et al. (2021) present future projections, where the ecological indicators improved under the BSAP, but also admit that uncertainties and long time scales of the Baltic Sea biogeochemistry challenge the interpretation of the results. The former idea that it is possible to revert ecosystems back into a particular past state is an unlikely outcome in a world of shifting baselines (Duarte et al., 2009; Boesch, 2019). A more realistic target would be to determine and ensure the maintenance of key ecosystem functions which would survive the changing climate and, thereby ensure that the Baltic Sea is a viable ecosystem in the future, and continues to provide valuable services to the society (Choi, 2007; Duarte et al., 2009; Boesch, 2019).

5 Conclusions

The Baltic Sea is a severely eutrophied complex ecosystem. Major factors that shape the biogeochemical functioning and the overall ecological status of the sea are location, topography, specific hydrographic nuances, strong anthropogenic pressure and accelerating climate change. Although recent decades have brought significant decreases in anthropogenic origin nitrogen and phosphorus inputs, improvements in key eutrophication indicators are difficult to see.

In order to study this lack of response, the Baltic Sea ecosystem state was observed long-term, during the post-stagnation period 1993–2017. The results revealed continuous increase of phosphorus pools, which agrees with the tendency of phosphorus to accumulate in the system and be released from the sediments under anoxic conditions. Nitrogen pools decreased, with a few local exceptions, which can be explained by intensifying nitrogen removal processes such as denitrification, and occasionally anammox, under borderline oxygen concentrations prevalent in large areas of the Baltic Sea. This results in the decreasing DIN:DIP ratio, which contributes significantly to the self-sustaining “vicious circle” of the Baltic Sea and makes the system resilient to improvement in terms of eutrophication. Phytoplankton spatial coverage did not change significantly throughout the study, implying that there are other factors at play in addition to nutrients, which determine phytoplankton growth in a eutrophied system, and complicate the response mechanism to changes in nutrient inputs. The earlier start day of the spring bloom and the overall elongation of bloom duration indicate the effect of the changing climate. Anoxic and hypoxic area and volume increased after the stagnation period and reached a stationary state around 2000, which marks the depth of the pycnocline and possibly maximum extent of anoxia in the Baltic Sea, whereas hypoxia can still increase at the expense of seasonally stratified shallow areas.

The dynamics of the Baltic Sea ecosystem were observed in response to nutrient inputs, and compared with reference conditions, which revealed a few principles. Phytoplankton dynamics changed in response to nutrient addition, displaying certain compensation mechanisms. With additional nutrients in the system, N-fixing cyanobacteria were compromised by diatoms and dinoflagellates, which increased their biomass in spring and summer. Phosphorus and dissolved oxygen pools increased, but eventually reached a steady state after 5 years of simulation. The Baltic Sea ecosystem appears to be rather resilient and show various compensation mechanisms to balance change, which could also explain the contradictory situation of nutrient reduction and the lack of immediate, linear response from the system. This falls in line with the theory that ecosystems are not simply reversible to their former oligotrophic states as new steady states emerge and the inertia inside the system is strong. This situation is further complicated by the changing environmental variables and uncertainties in anthropogenic pressure, which shift baselines and thereby the foundations of the entire ecosystem.

We looked at the set of eutrophication indicators and witnessed an unexpected response of the system to nutrient changes, which would deserve a more thorough study with a longer time period. We agree that nutrient reductions, that are already in action, are necessary to curb eutrophication effects in the Baltic Sea ecosystem. However, based on the current ecological status, supported by the results of this thesis, comprehensive knowledge on the mechanism of the Baltic Sea ecosystem is still far from complete. Knowledge gaps include the complexity of the biological interactions between phytoplankton functional groups, the cycling and removal or retaining of nutrients in the

sediments, the factors affecting and the role of the DIN:DIP ratio in the eutrophication of the Baltic Sea.

To understand the functioning of the biogeochemical system of the Baltic Sea, historical data should be revised and the data collection should continue. Complex measurements of the set of variables should be performed simultaneously. Research is required to complement current numerical models or to change the modelling concept. A long-term, integrated approach should be taken, which is where the theoretical or modelling approach in combination with machine learning methods could be of use.

References

- Adhikari, P.L., White, J.R., Maiti, K. and Nguyen, N., 2014, December. Gulf of Mexico Sediment Phosphorus Fractionation: Implication for Hypoxia. In *AGU Fall Meeting Abstracts* (Vol. 2014, pp. GC21A-0515). DOI: <https://doi.org/10.1016/j.ecss.2015.07.016>
- Almroth-Rosell, E., Wåhlstrom, I., Hansson, M., Vali, G., Eilola, K., Andersson, P., Viktorsson, L., Hieronymus, M. and Arneborg, L., 2021. A Regime Shift Toward a More Anoxic Environment in a Eutrophic Sea in Northern Europe. *Frontiers in Marine Science*, 8. DOI: <https://doi.org/10.3389/fmars.2021.799936>
- Altieri, A.H. and Diaz, R.J., 2019. Dead zones: oxygen depletion in coastal ecosystems. In *World seas: An environmental evaluation* (pp. 453-473). Academic Press. DOI: <https://doi.org/10.1016/b978-0-12-805052-1.00021-8>
- Aloe, A.K., Bouraoui, F., Grizzetti, B., Bidoglio, G. and Pistocchi, A., 2014. Managing nitrogen and phosphorus loads to water bodies: characterisation and Solutions. *Towards macro-regional integrated nutrient management. Joint Research Centre, JRC-Ispra* DOI: <https://doi.org/10.2788/14322>
- Andersen, H.E., Blicher-Mathiesen, G., Thodsen, H., Andersen, P.M., Larsen, S.E., Stålnacke, P., Humborg, C., Mörth, C.M. and Smedberg, E., 2016. Identifying hot spots of agricultural nitrogen loss within the Baltic Sea drainage basin. *Water, Air, & Soil Pollution*, 227(1), pp. 1-20. DOI: <https://doi.org/10.1007/s11270-015-2733-7>
- Asmala, E., Carstensen, J., Conley, D.J., Slomp, C.P., Stadmark, J. and Voss, M., 2017. Efficiency of the coastal filter: Nitrogen and phosphorus removal in the Baltic Sea. *Limnology and Oceanography*, 62(S1), pp. S222-S238. DOI: <https://doi.org/10.1002/lno.10644>
- Bargu, S., Baustian, M.M., Rabalais, N.N., Del Rio, R., Von Korff, B. and Turner, R.E., 2016. Influence of the Mississippi River on Pseudo-nitzschia spp. abundance and toxicity in Louisiana coastal waters. *Estuaries and Coasts*, 39(5), pp. 1345-1356. DOI: <https://doi.org/10.1007/s12237-016-0088-y>
- Bartosova, A., Capell, R., Olesen, J.E., Jabloun, M., Refsgaard, J.C., Donnelly, C., Hyytiäinen, K., Pihlainen, S., Zandersen, M. and Arheimer, B., 2019. Future socioeconomic conditions may have a larger impact than climate change on nutrient loads to the Baltic Sea. *Ambio*, 48(11), pp. 1325-1336. DOI: <https://doi.org/10.1007/s13280-019-01243-5>
- Beusen, A.H., Bouwman, A.F., Van Beek, L.P., Mogollón, J.M. and Middelburg, J.J., 2016. Global riverine N and P transport to ocean increased during the 20th century despite increased retention along the aquatic continuum. *Biogeosciences*, 13(8), pp. 2441-2451. DOI: <https://doi.org/10.5194/bg-13-2441-2016>
- Boesch, D.F., 2019. Barriers and bridges in abating coastal eutrophication. *Frontiers in Marine Science*, 6, p. 123. DOI: <https://doi.org/10.3389/fmars.2019.00123>
- Bonaglia, S., Klawonn, I., De Brabandere, L., Deutsch, B., Thamdrup, B. and Brüchert, V., 2016. Denitrification and DNRA at the Baltic Sea oxic–anoxic interface: substrate spectrum and kinetics. *Limnology and Oceanography*, 61(5), pp.1900-1915. DOI: <https://doi.org/10.1002/lno.10343>

- Brettar, I. and Rheinheimer, G., 1991. Denitrification in the Central Baltic: evidence for H₂S-oxidation as motor of denitrification at the oxic-anoxic interface. *Mar. Ecol. Prog. Ser.*, 77(2-3), pp. 157-169. DOI: <https://doi.org/10.3354/meps077157>
- Bruggeman, J. and Bolding, K., 2014. A general framework for aquatic biogeochemical models. *Environmental modelling & software*, 61, pp. 249-265.
- BSBD 0.9.3, Baltic Sea Hydrographic Commission, 2013. Baltic Sea Bathymetry Database Version 0.9.3. Downloaded from <http://data.bshc.pro/> on 2013.11.05.
- Burchard, H. and Bolding, K., 2002. GETM—a general estuarine transport model. *Scientific documentation, no EUR, 20253*.
- Byun, D. and Schere, K.L., 2006. Review of the governing equations, computational algorithms, and other components of the Models-3 Community Multiscale Air Quality (CMAQ) modeling system. DOI: <https://doi.org/10.1115/1.2128636>
- Carstensen, J., Sánchez-Camacho, M., Duarte, C.M., Krause-Jensen, D. and Marbà, N., 2011. Connecting the dots: responses of coastal ecosystems to changing nutrient concentrations. *Environmental Science & Technology*, 45(21), pp. 9122-9132. DOI: <https://doi.org/10.1021/es202351y>
- Carstensen, J., Conley, D.J., Bonsdorff, E., Gustafsson, B.G., Hietanen, S., Janas, U., Jilbert, T., Maximov, A., Norkko, A., Norkko, J. and Reed, D.C., 2014. Hypoxia in the Baltic Sea: Biogeochemical cycles, benthic fauna, and management. *Ambio*, 43(1), pp. 26-36. DOI: <https://doi.org/10.1007/s13280-013-0474-7>
- Carstensen, J. and Conley, D.J., 2019. Baltic Sea hypoxia takes many shapes and sizes. *Limnology and Oceanography Bulletin*, 28(4), pp. 125-129. DOI: <https://doi.org/10.1002/lob.10350>
- Carstensen, J., Conley, D.J., Almroth-Rosell, E., Asmala, E., Bonsdorff, E., Fleming-Lehtinen, V., Gustafsson, B.G., Gustafsson, C., Heiskanen, A.S., Janas, U. and Norkko, A., 2020. Factors regulating the coastal nutrient filter in the Baltic Sea. *Ambio*, 49(6), pp. 1194-1210. DOI: <https://doi.org/10.1007/s13280-019-01282-y>
- Chislock, M.F., Doster, E., Zitomer, R.A. and Wilson, A.E., 2013. Eutrophication: causes, consequences, and controls in aquatic ecosystems. *Nature Education Knowledge*, 4(4), p. 10. DOI: <https://doi.org/10.1007/978-94-007-7814-6>
- Choi, Y.D., 2007. Restoration ecology to the future: a call for new paradigm. *Restoration Ecology*, 15(2), pp. 351-353. DOI: <https://doi.org/10.1111/j.1526-100X.2007.00224.x>
- Chubarenko, I. and Stepanova, N., 2018. Cold intermediate layer of the Baltic Sea: Hypothesis of the formation of its core. *Progress in oceanography*, 167, pp. 1-10. DOI: <https://doi.org/10.1016/j.pocean.2018.06.012>
- Cloern, J.E., Jassby, A.D., Thompson, J.K. and Hieb, K.A., 2007. A cold phase of the East Pacific triggers new phytoplankton blooms in San Francisco Bay. *Proceedings of the National Academy of Sciences*, 104(47), pp. 18561-18565. DOI: <https://doi.org/10.1073/pnas.0706151104>

- Conley, D.J., Humborg, C., Rahm, L., Savchuk, O.P. and Wulff, F., 2002. Hypoxia in the Baltic Sea and basin-scale changes in phosphorus biogeochemistry. *Environmental science & technology*, 36(24), pp. 5315-5320. DOI: <https://doi.org/10.1021/es025763w>
- Conley, D.J., Björck, S., Bonsdorff, E., Carstensen, J., Destouni, G., Gustafsson, B.G., Hietanen, S., Kortekaas, M., Kuosa, H., Markus Meier, H.E. and Müller-Karulis, B., 2009a. Hypoxia-related processes in the Baltic Sea. *Environmental Science & Technology*, 43(10), pp. 3412-3420. DOI: <https://doi.org/10.1021/es802762a>
- Conley, D.J., Paerl, H.W., Howarth, R.W., Boesch, D.F., Seitzinger, S.P., Havens, K.E., Lancelot, C. and Likens, G.E., 2009b. Controlling eutrophication: nitrogen and phosphorus. *Science*, 323(5917), pp. 1014-1015. DOI: <https://doi.org/10.1126/science.116775>
- Conley, D.J., Carstensen, J., Aigars, J., Axe, P., Bonsdorff, E., Eremina, T., Hahti, B.M., Humborg, C., Jonsson, P., Kotta, J. and Lannegren, C., 2011. Hypoxia is increasing in the coastal zone of the Baltic Sea. *Environmental science & technology*, 45(16), pp. 6777-6783. DOI: <https://doi.org/10.1021/es201212r>
- Corriero, G., Pierrri, C., Accoroni, S., Alabiso, G., Bavestrello, G., Barbone, E., Bastianini, M., Bazzoni, A.M., Bernardi Aubry, F., Boero, F. and Buia, M.C., 2016. Ecosystem vulnerability to alien and invasive species: a case study on marine habitats along the Italian coast. *Aquatic Conservation: Marine and Freshwater Ecosystems*, 26(2), pp. 392-409. DOI: <https://doi.org/10.1002/aqc.2550>
- Diaz, R.J. and Rosenberg, R., 2008. Spreading dead zones and consequences for marine ecosystems. *science*, 321(5891), pp. 926-929. DOI: <https://doi.org/10.1126/science.1156401>
- Diaz, R.J., Rosenberg, R. and Sturdivant, K., 2019. Hypoxia in estuaries and semi-enclosed seas. *Ocean deoxygenation: Everyone's problem*, edited by: Laffoley, D. and Baxter, JM, IUCN, Gland, Switzerland.
- Dalsgaard, T., De Brabandere, L. and Hall, P.O., 2013. Denitrification in the water column of the central Baltic Sea. *Geochimica et Cosmochimica Acta*, 106, pp. 247-260. DOI: <https://doi.org/10.1016/j.gca.2012.12.038>
- Dijkstra, N., Slomp, C.P. and Behrends, T., 2016. Vivianite is a key sink for phosphorus in sediments of the Landsort Deep, an intermittently anoxic deep basin in the Baltic Sea. *Chemical Geology*, 438, pp. 58-72. DOI: <https://doi.org/10.1016/j.chemgeo.2016.05.025>
- Donnelly, C., Andersson, J.C. and Arheimer, B., 2016. Using flow signatures and catchment similarities to evaluate the E-HYPE multi-basin model across Europe. *Hydrological Sciences Journal*, 61(2), pp. 255-273. DOI: <https://doi.org/10.1080/02626667.2015.1027710>
- Duarte, C.M., Conley, D.J., Carstensen, J. and Sánchez-Camacho, M., 2009. Return to Neverland: shifting baselines affect eutrophication restoration targets. *Estuaries and Coasts*, 32(1), pp. 29-36. DOI: <https://doi.org/10.1007/s12237-008-9111-2>
- Eilola, K., Meier, H.M. and Almroth, E., 2009. On the dynamics of oxygen, phosphorus and cyanobacteria in the Baltic Sea; A model study. *Journal of Marine Systems*, 75(1-2), pp. 163-184. DOI: <https://doi.org/10.1016/j.jmarsys.2008.08.009>

Elmgren, R. and Larsson, U., 2001. Nitrogen and the Baltic Sea: managing nitrogen in relation to phosphorus. *TheScientificWorldJournal*, 1, pp. 371-377. DOI: <https://doi.org/10.1100/tsw.2001.291>

Fennel, K. and Testa, J.M., 2019. Biogeochemical controls on coastal hypoxia. *Annual Review of Marine Science*, 11, pp. 105-130. DOI: <https://doi.org/10.1146/annurev-marine-010318-095138>

Fleming, V. and Kaitala, S., 2006. Phytoplankton spring bloom intensity index for the Baltic Sea estimated for the years 1992 to 2004. *Hydrobiologia*, 554(1), pp. 57-65. DOI: <https://doi.org/10.1007/s10750-005-1006-7>

Friedland, R., Schernewski, G., Gräwe, U., Greipsland, I., Palazzo, D. and Pastuszak, M., 2019. Managing eutrophication in the Szczecin (Oder) lagoon-development, present state and future perspectives. *Frontiers in Marine Science*, p. 521. DOI: <https://doi.org/10.3389/fmars.2018.00521>

Friedland, R., Macias, D.M., Cossarini, G., Daewel, U., Estournel, C., Garcia-Gorriz, E., Grizzetti, B., Grégoire, M., Gustafson, B., Kalaroni, S. and Kerimoglu, O., 2021. Effects of nutrient management scenarios on marine eutrophication indicators: a Pan-European, multi-model assessment in support of the Marine Strategy Framework Directive. *Frontiers in Marine Science*, 8. DOI: <https://doi.org/10.3389/fmars.2021.596126>

Furstenberg, S., Mohn, H. and Sverud, T., 2009. Study on discharge factors for legal operational discharges to sea from vessels in Norwegian waters. *Det Norske Veritas, Høvik*.

Graham, W.F. and Duce, R.A., 1979. Atmospheric pathways of the phosphorus cycle. *Geochimica et Cosmochimica Acta*, 43(8), pp. 1195-1208. DOI: [https://doi.org/10.1016/0016-7037\(79\)90112-1](https://doi.org/10.1016/0016-7037(79)90112-1)

Granéli, E., Wallström, K., Larsson, U., Granéli, W. and Elmgren, R., 1990. Nutrient limitation of primary production in the Baltic Sea area. *Ambio*, pp. 142-151.

Green, P.A., Vörösmarty, C.J., Meybeck, M., Galloway, J.N., Peterson, B.J. and Boyer, E.W., 2004. Pre-industrial and contemporary fluxes of nitrogen through rivers: a global assessment based on typology. *Biogeochemistry*, 68(1), pp. 71-105. DOI: <https://doi.org/10.1023/B:BI0G.0000025742.82155.92>

Greening, H., Janicki, A., Sherwood, E.T., Pribble, R. and Johansson, J.O.R., 2014. Ecosystem responses to long-term nutrient management in an urban estuary: Tampa Bay, Florida, USA. *Estuarine, Coastal and Shelf Science*, 151, pp. A1-A16. DOI: <https://doi.org/10.1016/j.ecss.2014.10.003>

Gregg, W.W., Casey, N.W. and McClain, C.R., 2005. Recent trends in global ocean chlorophyll. *Geophysical research letters*, 32(3). DOI: <https://doi.org/10.1029/2004GL021808>

Groetsch, P.M., Simis, S.G., Eleveld, M.A. and Peters, S.W., 2016. Spring blooms in the Baltic Sea have weakened but lengthened from 2000 to 2014. *Biogeosciences*, 13(17), pp. 4959-4973. DOI: <https://doi.org/10.5194/bg-13-4959-2016>

- Gustafsson, B.G., Schenk, F., Blenckner, T., Eilola, K., Meier, H.E., Müller-Karulis, B., Neumann, T., Ruoho-Airola, T., Savchuk, O.P. and Zorita, E., 2012. Reconstructing the development of Baltic Sea eutrophication 1850–2006. *Ambio*, 41(6), pp. 534-548. DOI: <https://doi.org/10.1007/s13280-012-0318-x>
- Hannig, M., Lavik, G., Kuypers, M.M.M., Woebken, D., Martens-Habbena, W. and Jürgens, K., 2007. Shift from denitrification to anammox after inflow events in the central Baltic Sea. *Limnology and Oceanography*, 52(4), pp. 1336-1345. DOI: <https://doi.org/10.4319/lo.2007.52.4.1336>
- Hansson, M. and Håkansson, B., 2007. The Baltic Algae Watch System—a remote sensing application for monitoring cyanobacterial blooms in the Baltic Sea. *Journal of Applied Remote Sensing*, 1(1), p. 011507. DOI: <https://doi.org/10.1117/1.2834769>
- Hansson, M., Pamberton, P., Hakansson, B., Reinart, A. and Alikas, K., 2010. Operational nowcasting of algal blooms in the Baltic Sea using MERIS and MODIS. In *ESA Living Planet Symposium* (Vol. 686, p. 337). DOI: <https://doi.org/10.5200/baltica.2016.29.02>
- Hansson, M., Andersson, L., and Axe, P. O., 2011. Areal extent and volume of anoxia and hypoxia in the Baltic Sea, 1960–2011. *Rep. Oceanogr.* 42, pp. 1-63.
- Hansson, M., Viktorsson, L. and Andersson, L., 2019. Oxygen Survey in the Baltic Sea 2019 - Extent of Anoxia and Hypoxia, 1960-2019. *SMHI Report Oceanography* No. 67, 88 pp. ISSN: 0283-1112
- Hecky, R.E. and Kilham, P., 1988. Nutrient limitation of phytoplankton in freshwater and marine environments: a review of recent evidence on the effects of enrichment 1. *Limnology and oceanography*, 33(4part2), pp. 796-822. DOI: <https://doi.org/10.4319/lo.1988.33.4part2.0796>
- Heisler, J., Glibert, P.M., Burkholder, J.M., Anderson, D.M., Cochlan, W., Dennison, W.C., Dortch, Q., Gobler, C.J., Heil, C.A., Humphries, E. and Lewitus, A., 2008. Eutrophication and harmful algal blooms: a scientific consensus. *Harmful algae*, 8(1), pp. 3-13. DOI: <https://doi.org/10.1016/j.hal.2008.08.006>
- HELCOM, 2018. HELCOM Thematic Assessment of Eutrophication 2011–2016. In *Baltic Sea Environ. Proc.* (Vol. 156, pp. 1-102). https://www.helcom.fi/wp-content/uploads/2019/08/HELCOM_Thematic-assessment-of-eutrophication-2011-2016_pre-publication.pdf
- HELCOM, 2019. Inputs of nutrients to the sub-basins. HELCOM core indicator report. Online. Viewed: 16.11.21 https://helcom.fi/media/core%20indicators/HELCOM-core-indicator-on-inputs-of-nutrients-for-period-1995-2017_final.pdf ISSN 2343-2543
- Hietanen, S. and Lukkari, K., 2007. Effects of short-term anoxia on benthic denitrification, nutrient fluxes and phosphorus forms in coastal Baltic sediment. *Aquatic Microbial Ecology*, 49(3), pp. 293-302. DOI: <https://doi.org/10.3354/ame01146>
- Hietanen, S., Jäntti, H., Buizert, C., Jürgens, K., Labrenz, M., Voss, M. and Kuparinen, J., 2012. Hypoxia and nitrogen processing in the Baltic Sea water column. *Limnology and Oceanography*, 57(1), pp. 325-337. DOI: <https://doi.org/10.4319/lo.2012.57.1.0325>

- Hordoir, R., Axell, L., Löptien, U., Dietze, H. and Kuznetsov, I., 2015. Influence of sea level rise on the dynamics of salt inflows in the Baltic Sea. *Journal of Geophysical Research: Oceans*, 120(10), pp. 6653-6668. DOI: <https://doi.org/10.1002/2014JC010642>
- Hordoir, R., Axell, L., Höglund, A., Dieterich, C., Fransner, F., Gröger, M., Liu, Y., Pemberton, P., Schimanke, S., Andersson, H. and Ljungemyr, P., 2019. Nemo-Nordic 1.0: a NEMO-based ocean model for the Baltic and North seas—research and operational applications. *Geoscientific Model Development*, 12(1), pp. 363-386. DOI: <https://doi.org/10.5194/gmd-12-363-2019>
- Howarth, R.W., 2008. Coastal nitrogen pollution: a review of sources and trends globally and regionally. *Harmful algae*, 8(1), pp. 14-20. DOI: <https://doi.org/10.1016/j.hal.2008.08.015>
- Hufnagl, M., Liebezeit, G. and Behrends, B., 2005. Effects of Sea Water Scrubbing, Final Report to BP Marine. *Research Centre Terramare, Wilhelmshaven, Germany and School of Marine Science and Technology, University of Newcastle, Newcastle upon Tyne, UK.*
- Jaagus, J., Briede, A., Rimkus, E. and Sepp, M., 2018. Changes in precipitation regime in the Baltic countries in 1966–2015. *Theoretical and Applied Climatology*, 131(1), pp. 433-443. DOI: <https://doi.org/10.1007/s00704-016-1990-8>
- Jalkanen, J.P., Brink, A., Kalli, J., Pettersson, H., Kukkonen, J. and Stipa, T., 2009. A modelling system for the exhaust emissions of marine traffic and its application in the Baltic Sea area. *Atmospheric Chemistry and Physics*, 9(23), pp. 9209-9223. DOI: <https://doi.org/10.5194/acp-9-9209-2009>
- Jalkanen, J.P., Johansson, L., Kukkonen, J., Brink, A., Kalli, J. and Stipa, T., 2012. Extension of an assessment model of ship traffic exhaust emissions for particulate matter and carbon monoxide. *Atmospheric Chemistry and Physics*, 12(5), pp. 2641-2659. DOI: <https://doi.org/10.5194/acp-12-2641-2012>
- Jędrasik, J. and Kowalewski, M., 2019. Mean annual and seasonal circulation patterns and long-term variability of currents in the Baltic Sea. *Journal of Marine Systems*, 193, pp. 1-26. DOI: <https://doi.org/10.1016/j.jmarsys.2018.12.011>
- Jickells, T.D., Buitenhuis, E., Altieri, K., Baker, A.R., Capone, D., Duce, R.A., Dentener, F., Fennel, K., Kanakidou, M., LaRoche, J. and Lee, K., 2017. A reevaluation of the magnitude and impacts of anthropogenic atmospheric nitrogen inputs on the ocean. *Global Biogeochemical Cycles*, 31(2), pp. 289-305. DOI: <https://doi.org/10.1002/2016GB005586>
- Jilbert, T. and Slomp, C.P., 2013. Iron and manganese shuttles control the formation of authigenic phosphorus minerals in the euxinic basins of the Baltic Sea. *Geochimica et Cosmochimica Acta*, 107, pp. 155-169. DOI: <https://doi.org/10.1016/j.gca.2013.01.005>
- Jokinen, S.A., Virtasalo, J.J., Jilbert, T., Kaiser, J., Dellwig, O., Arz, H.W., Hänninen, J., Arppe, L., Collander, M. and Saarinen, T., 2018. A 1500-year multiproxy record of coastal hypoxia from the northern Baltic Sea indicates unprecedented deoxygenation over the 20th century. *Biogeosciences*, 15(13), pp. 3975-4001. DOI: <https://doi.org/10.5194/bg-15-3975-2018>

- Johansson, L., Jalkanen, J.P., Kalli, J. and Kukkonen, J., 2013. The evolution of shipping emissions and the costs of recent and forthcoming emission regulations in the northern European emission control area. *The Journal Atmospheric Chemistry and Physics Discuss*, 13, pp. 16113-16150. DOI: <https://doi.org/10.5194/acpd-13-16113-2013>
- Johansson, L., Jalkanen, J.P. and Kukkonen, J., 2017. Global assessment of shipping emissions in 2015 on a high spatial and temporal resolution. *Atmospheric Environment*, 167, pp. 403-415. DOI: <https://doi.org/10.1016/j.atmosenv.2017.08.042>
- Jönsson, H., Baky, A., Jeppson, U., Hellström, D., Kärrman, E., 2005. Composition of Urine, Faeces, Greywater and Biowaste for Utilisation in the UWARE Model. Urban Water, Chalmers University of Technology, Gothenburg <http://www.iea.lth.se/publications/Reports/LTH-IEA-7222.pdf>
- Jäntti, H. and Hietanen, S., 2012. The effects of hypoxia on sediment nitrogen cycling in the Baltic Sea. *Ambio*, 41(2), pp. 161-169. DOI: <https://doi.org/10.1007/s13280-011-0233-6>
- Kahru, M. and Nömmann, S., 1990. The phytoplankton spring bloom in the Baltic Sea in 1985, 1986: multitude of spatio-temporal scales. *Continental Shelf Research*, 10(4), pp. 329-354. DOI: [https://doi.org/10.1016/0278-4343\(90\)90055-Q](https://doi.org/10.1016/0278-4343(90)90055-Q)
- Kahru, M., Horstmann, U. and Rud, O., 1994. Satellite detection of increased cyanobacteria blooms in the Baltic Sea: natural fluctuation or ecosystem change? *AMBIO: A journal of the Human Environment*, 23, pp. 469-472.
- Kahru, M., Savchuk, O.P. and Elmgren, R., 2007. Satellite measurements of cyanobacterial bloom frequency in the Baltic Sea: interannual and spatial variability. *Marine ecology progress series*, 343, pp. 15-23. DOI: <https://doi.org/10.3354/meps06943>
- Kahru, M. and Elmgren, R., 2014. Multidecadal time series of satellite-detected accumulations of cyanobacteria in the Baltic Sea. *Biogeosciences*, 11(13), pp. 3619-3633. DOI: <https://doi.org/10.5194/bg-11-3619-2014>
- Kahru, M., Elmgren, R. and Savchuk, O.P., 2016. Changing seasonality of the Baltic Sea. *Biogeosciences*, 13(4), pp. 1009-1018. DOI: <https://doi.org/10.5194/bg-13-1009-2016>
- Kahru, M., Elmgren, R., Di Lorenzo, E. and Savchuk, O., 2018. Unexplained interannual oscillations of cyanobacterial blooms in the Baltic Sea. *Scientific Reports*, 8(1), pp. 1-5. DOI: <https://doi.org/10.1038/s41598-018-24829-7>
- Kahru, M., Elmgren, R., Kaiser, J., Wasmund, N. and Savchuk, O., 2020. Cyanobacterial blooms in the Baltic Sea: Correlations with environmental factors. *Harmful Algae*, 92, p. 101739. DOI: <https://doi.org/10.1016/j.hal.2019.101739>
- Karl, M., Bieser, J., Geyer, B., Matthias, V., Jalkanen, J.P., Johansson, L. and Fridell, E., 2019. Impact of a nitrogen emission control area (NECA) on the future air quality and nitrogen deposition to seawater in the Baltic Sea region. *Atmospheric Chemistry and Physics*, 19(3), pp. 1721-1752. DOI: <https://doi.org/10.5194/acp-19-1721-2019>
- Kerimoglu, O., Große, F., Kreuz, M., Lenhart, H.J. and van Beusekom, J.E., 2018. A model-based projection of historical state of a coastal ecosystem: relevance of phytoplankton stoichiometry. *Science of the Total Environment*, 639, pp. 1311-1323. DOI: <https://doi.org/10.1016/j.scitotenv.2018.05.215>

- Krapf, K., Naumann, M., Dutheil, C. and Meier, M., 2022. Investigating Hypoxic and Euxinic Area Changes Based on Various Datasets From the Baltic Sea. *Frontiers in Marine Science*, 9. DOI: <https://doi.org/10.3389/fmars.2022.823476>
- Kulinski, K., Rehder, G., Asmala, E., Bartosova, A., Carstensen, J., Gustafsson, B., Hall, P.O.J., Humborg, C., Jilbert, T., Jürgens, K. and Meier, M., 2021. Baltic Earth Assessment Report on the biogeochemistry of the Baltic Sea, Earth Syst. Dynam. Discuss. DOI: <https://doi.org/10.5194/esd-2021-33>
- Kuosa, H., Fleming-Lehtinen, V., Lehtinen, S., Lehtiniemi, M., Nygård, H., Raateoja, M., Raitaniemi, J., Tuimala, J., Uusitalo, L. and Suikkanen, S., 2017. A retrospective view of the development of the Gulf of Bothnia ecosystem. *Journal of Marine Systems*, 167, pp. 78-92. DOI: <https://doi.org/10.1016/j.jmarsys.2016.11.020>
- Langmead, O., McQuatters-Gollop, A., Mee, L.D., Friedrich, J., Gilbert, A.J., Gomoiu, M.T., Jackson, E.L., Knudsen, S., Minicheva, G. and Todorova, V., 2009. Recovery or decline of the northwestern Black Sea: a societal choice revealed by socio-ecological modelling. *Ecological modelling*, 220(21), pp. 2927-2939. DOI: <https://doi.org/10.1016/j.ecolmodel.2008.09.011>
- Lee, R.Y., Seitzinger, S. and Mayorga, E., 2016. Land-based nutrient loading to LMEs: A global watershed perspective on magnitudes and sources. *Environmental development*, 17, pp. 220-229. DOI: <https://doi.org/10.1016/j.envdev.2015.09.006>
- Lefcheck, J.S., Orth, R.J., Dennison, W.C., Wilcox, D.J., Murphy, R.R., Keisman, J., Gurbisz, C., Hannam, M., Landry, J.B., Moore, K.A. and Patrick, C.J., 2018. Long-term nutrient reductions lead to the unprecedented recovery of a temperate coastal region. *Proceedings of the National Academy of Sciences*, 115(14), pp. 3658-3662. DOI: <https://doi.org/10.1073/pnas.1715798115>
- Lehmann, A., Hinrichsen, H.H., Getzlaff, K. and Myrberg, K., 2014. Quantifying the heterogeneity of hypoxic and anoxic areas in the Baltic Sea by a simplified coupled hydrodynamic-oxygen consumption model approach. *Journal of Marine Systems*, 134, pp. 20-28. DOI: <https://doi.org/10.1016/j.jmarsys.2014.02.012>
- Lehmann, A., Myrberg, K., Post, P., Chubarenko, I., Dailidiene, I., Hinrichsen, H.H., Hüsey, K., Liblik, T., Meier, H.E., Lips, U. and Bukanova, T., 2022. Salinity dynamics of the Baltic Sea. *Earth System Dynamics*, 13(1), pp. 373-392. DOI: <https://doi.org/10.5194/esd-13-373-2022>
- Lehtoranta, J., Ekholm, P. and Pitkänen, H., 2009. Coastal eutrophication thresholds: a matter of sediment microbial processes. *AMBIO: A Journal of the Human Environment*, 38(6), pp. 303-308. DOI: <https://doi.org/10.1579/09-A-656.1>
- Leppäranta, M. and Myrberg, K., 2009. *Physical oceanography of the Baltic Sea*. Springer Science & Business Media. DOI: https://doi.org/10.1007/978-3-662-04453-7_2
- Lessin, G., Raudsepp, U., Maljutenko, I., Laanemets, J., Passenko, J. and Jaanus, A., 2014. Model study on present and future eutrophication and nitrogen fixation in the Gulf of Finland, Baltic Sea. *Journal of Marine Systems*, 129, pp. 76-85. DOI: <https://doi.org/10.1016/j.jmarsys.2013.08.006>

Liblik, T. and Lips, U., 2011. Characteristics and variability of the vertical thermohaline structure in the Gulf of Finland in summer.

Liblik, T., Naumann, M., Alenius, P., Hansson, M., Lips, U., Nausch, G., Tuomi, L., Wesslander, K., Laanemets, J. and Viktorsson, L., 2018. Propagation of impact of the recent Major Baltic Inflows from the Eastern Gotland Basin to the Gulf of Finland. *Frontiers in Marine Science*, 5, p. 222. DOI: <https://doi.org/10.3389/fmars.2018.00222>

Lønborg, C. and Markager, S., 2021. Nitrogen in the Baltic Sea: Long-term trends, a budget and decadal time lags in responses to declining inputs. *Estuarine, Coastal and Shelf Science*, 261, p. 107529. DOI: <https://doi.org/10.1016/j.ecss.2021.107529>

Lukkari, K., Leivuori, M. and Kotilainen, A., 2009. The chemical character and behaviour of phosphorus in poorly oxygenated sediments from open sea to organic-rich inner bay in the Baltic Sea. *Biogeochemistry*, 96(1), pp. 25-48. DOI: <https://doi.org/10.1007/s10533-009-9343-7>

Löptien, U. and Dietze, H., 2022. Retracing cyanobacteria blooms in the Baltic Sea. *Scientific Reports*, 12(1), pp. 1-8.

Maljutenko, I. and Raudsepp, U., 2019. Long-term mean, interannual and seasonal circulation in the Gulf of Finland—the wide salt wedge estuary or gulf type ROFI. *Journal of Marine Systems*, 195, pp. 1-19. DOI: <https://doi.org/10.1016/j.jmarsys.2019.03.004>

Malone, T.C. and Newton, A., 2020. The globalization of cultural eutrophication in the coastal ocean: causes and consequences. *Frontiers in Marine Science*, 7, p. 670. DOI: <https://doi.org/10.3389/fmars.2020.00670>

Marmefelt, E., Arheimer, B. and Langner, J., 1999. An integrated biogeochemical model system for the Baltic Sea. *Hydrobiologia*, 393, pp. 45-56. DOI: <https://doi.org/10.1023/A:1003541816177>

Matthias, V., 2008. The aerosol distribution in Europe derived with the Community Multiscale Air Quality (CMAQ) model: comparison to near surface in situ and sunphotometer measurements. *Atmospheric Chemistry and Physics*, 8(17), pp. 5077-5097. DOI: <https://doi.org/10.5194/acp-8-5077-2008>

Matthäus, W., 1984. Climatic and seasonal variability of oceanological parameters in the Baltic Sea. *Beiträge zur Meereskunde*, 51, pp. 29-49.

McLaughlin, C., Falatko, D., Danesi, R. and Albert, R., 2014. Characterizing shipboard bilgewater effluent before and after treatment. *Environmental Science and Pollution Research*, 21(8), pp. 5637-5652. DOI: <https://doi.org/10.1007/s11356-013-2443-x>

Meier, H.M., 2007. Modeling the pathways and ages of inflowing salt-and freshwater in the Baltic Sea. *Estuarine, Coastal and Shelf Science*, 74(4), pp. 610-627. DOI: <https://doi.org/10.1016/j.ecss.2007.05.019>

Meier, H.M., Andersson, H.C., Eilola, K., Gustafsson, B.G., Kuznetsov, I., Müller-Karulis, B., Neumann, T. and Savchuk, O.P., 2011. Hypoxia in future climates: A model ensemble study for the Baltic Sea. *Geophysical Research Letters*, 38(24). DOI: <https://doi.org/10.1029/2011GL049929>

- Meier, H.E.M., Höglund, A., Eilola, K. and Almroth-Rosell, E., 2017. Impact of accelerated future global mean sea level rise on hypoxia in the Baltic Sea. *Climate Dynamics*, 49(1), pp. 163-172. DOI: <https://doi.org/10.1007/s00382-016-3333-y>
- Meier, H.M., Väli, G., Naumann, M., Eilola, K. and Frauen, C., 2018. Recently accelerated oxygen consumption rates amplify deoxygenation in the Baltic Sea. *Journal of Geophysical Research: Oceans*, 123(5), pp. 3227-3240. DOI: <https://doi.org/10.1029/2017JC013686>
- Meier, H.E.M., Eilola, K., Almroth-Rosell, E., Schimanke, S., Kniebusch, M., Höglund, A., Pemberton, P., Liu, Y., Väli, G. and Saraiva, S., 2019. Disentangling the impact of nutrient load and climate changes on Baltic Sea hypoxia and eutrophication since 1850. *Climate Dynamics*, 53(1), pp. 1145-1166. DOI: <https://doi.org/10.1007/s00382-018-4296-y>
- Meier, H.E.M., Dieterich, C. and Gröger, M., 2021. Natural variability is a large source of uncertainty in future projections of hypoxia in the Baltic Sea. *Communications Earth & Environment*, 2(1), pp. 1-13. DOI: <https://doi.org/10.1038/s43247-021-00115-9>
- Mélin, F., Vantrepotte, V., Chuprin, A., Grant, M., Jackson, T. and Sathyendranath, S., 2017. Assessing the fitness-for-purpose of satellite multi-mission ocean color climate data records: A protocol applied to OC-CCI chlorophyll-a data. *Remote Sensing of Environment*, 203, pp. 139-151. DOI: <https://doi.org/10.1016/j.rse.2017.03.039>
- Ménesguen, A. and Lacroix, G., 2018. Modelling the marine eutrophication: A review. *Science of the Total Environment*, 636, pp. 339-354. DOI: <https://doi.org/10.1016/j.scitotenv.2018.04.183>
- Mohrholz, V., 2018. Major baltic inflow statistics—revised. *Frontiers in Marine Science*, 5, p. 384. DOI: <https://doi.org/10.3389/fmars.2018.00384>
- Munkes, B., Löptien, U. and Dietze, H., 2021. Cyanobacteria blooms in the Baltic Sea: a review of models and facts. *Biogeosciences*, 18(7), pp. 2347-2378. DOI: <https://doi.org/10.5194/bg-18-2347-2021>
- Nerger, L., Hiller, W. and Schröter, J., 2005. A comparison of error subspace Kalman filters. *Tellus A: Dynamic Meteorology and Oceanography*, 57(5), pp. 715-735. DOI: <https://doi.org/10.3402/tellusa.v57i5.14732>
- Neumann, T., 2000. Towards a 3D-ecosystem model of the Baltic Sea. *Journal of Marine Systems*, 25(3-4), pp. 405-419. DOI: [https://doi.org/10.1016/S0924-7963\(00\)00030-0](https://doi.org/10.1016/S0924-7963(00)00030-0)
- Neumann, T., Fennel, W. and Kremp, C., 2002. Experimental simulations with an ecosystem model of the Baltic Sea: a nutrient load reduction experiment. *Global biogeochemical cycles*, 16(3), pp. 7-1. DOI: <https://doi.org/10.1029/2001GB001450>
- Neumann, T. and Schernewski, G., 2008. Eutrophication in the Baltic Sea and shifts in nitrogen fixation analyzed with a 3D ecosystem model. *Journal of Marine Systems*, 74(1-2), pp. 592-602. DOI: <https://doi.org/10.1016/j.jmarsys.2008.05.003>
- Neumann, T., Radtke, H. and Seifert, T., 2017. On the importance of Major Baltic Inflows for oxygenation of the central Baltic Sea. *Journal of Geophysical Research: Oceans*, 122(2), pp. 1090-1101. DOI: <https://doi.org/10.1002/2016JC012525>

Nixon, S.W., 2009. Eutrophication and the macroscope. In *Eutrophication in Coastal Ecosystems* (pp. 5-19). Springer, Dordrecht. DOI: https://doi.org/10.1007/978-90-481-3385-7_2

Olofsson, M., Egardt, J., Singh, A. and Ploug, H., 2016. Inorganic phosphorus enrichments in Baltic Sea water have large effects on growth, carbon fixation, and N₂ fixation by *Nodularia spumigena*. *Aquatic Microbial Ecology*, 77(2), pp. 111-123. DOI: <https://doi.org/10.3354/ame01795>

Olofsson, M., Suikkanen, S., Kobos, J., Wasmund, N. and Karlson, B., 2020. Basin-specific changes in filamentous cyanobacteria community composition across four decades in the Baltic Sea. *Harmful Algae*, 91, p. 101685. DOI: <https://doi.org/10.1016/j.hal.2019.101685>

Olofsson, M., Klawonn, I. and Karlson, B., 2021. Nitrogen fixation estimates for the Baltic Sea indicate high rates for the previously overlooked Bothnian Sea. *Ambio*, 50(1), pp. 203-214. DOI: <https://doi.org/10.1007/s13280-020-01331-x>

Paerl, H.W., Valdes, L.M., Pinckney, J.L., Piehler, M.F., Dyble, J. and Moisander, P.H., 2003. Phytoplankton photopigments as indicators of estuarine and coastal eutrophication. *BioScience*, 53(10), pp. 953-964. DOI: [https://doi.org/10.1641/0006-3568\(2003\)053\[0953:PPAIOE\]2.0.CO;2](https://doi.org/10.1641/0006-3568(2003)053[0953:PPAIOE]2.0.CO;2)

Pihlainen, S., Zandersen, M., Hyytiäinen, K., Andersen, H.E., Bartosova, A., Gustafsson, B., Jabloun, M., McCrackin, M., Meier, H.M., Olesen, J.E. and Saraiva, S., 2020. Impacts of changing society and climate on nutrient loading to the Baltic Sea. *Science of the Total Environment*, 731, p. 138935. DOI: <https://doi.org/10.1016/j.scitotenv.2020.138935>

Pulido-Velazquez, M. and Ward, F.A., 2017. Comparison of water management institutions and approaches in the United States and Europe—What can we learn from each other? In *Competition for Water Resources* (pp. 423-441). Elsevier. DOI: <https://doi.org/10.1016/B978-0-12-803237-4.00024-0>

Raateoja, M., Hällfors, H. and Kaitala, S., 2018. Vernal phytoplankton bloom in the Baltic Sea: Intensity and relation to nutrient regime. *Journal of Sea Research*, 138, pp. 24-33.

Rabalais, N.N., Turner, R.E., Díaz, R.J. and Justić, D., 2009. Global change and eutrophication of coastal waters. *ICES Journal of Marine Science*, 66(7), pp. 1528-1537. DOI: <https://doi.org/10.1093/icesjms/fsp047>

Radtke, H., Neumann, T., Voss, M. and Fennel, W., 2012. Modeling pathways of riverine nitrogen and phosphorus in the Baltic Sea. *Journal of Geophysical Research: Oceans*, 117(C9). DOI: <https://doi.org/10.1029/2012JC008119>

Raudsepp, U., Laanemets, J., Maljutenko, I., Hongisto, M. and Jalkanen, J.P., 2013. Impact of ship-borne nitrogen deposition on the Gulf of Finland ecosystem: an evaluation. *Oceanologia*, 55(4), pp. 837-857. DOI: <https://doi.org/10.5697/oc.55-4.837>

Raudsepp, U., Uiboupin, R., Laanemäe, K., Maljutenko, I. 2020. Geographical and seasonal coverage of sea ice in the Baltic Sea. In: Copernicus Marine Service Ocean State Report, Issue 4, *Journal of Operational Oceanography*, 13:sup1, pp. s115-s121; DOI: <https://doi.org/10.1080/1755876X.2020.1785097>

- Redfield, A.C., 1934. *On the proportions of organic derivatives in sea water and their relation to the composition of plankton* (Vol. 1). Liverpool: University Press of Liverpool.
- Reece, K.S., 2015. Monitoring for HAB species in VA Waters of Chesapeake Bay during 2009: Emerging HAB species in Chesapeake Bay. *Annual report to the Virginia Department of Health (# VIMSHAB617FY16), (Richmond, VA)*.
- Reusch, T.B., Dierking, J., Andersson, H.C., Bonsdorff, E., Carstensen, J., Casini, M., Czajkowski, M., Hasler, B., Hinsby, K., Hyytiäinen, K. and Johannesson, K., 2018. The Baltic Sea as a time machine for the future coastal ocean. *Science Advances*, 4(5), p. eaar8195. DOI: <https://doi.org/10.1126/sciadv.aar8195>
- Rockel, B., Will, A. and Hense, A., 2008. The regional climate model COSMO-CLM (CCLM). *Meteorologische Zeitschrift*, 17(4), pp. 347-348.
- Rolff, C. and Elfving, T., 2015. Increasing nitrogen limitation in the Bothnian Sea, potentially caused by inflow of phosphate-rich water from the Baltic Proper. *Ambio*, 44(7), pp. 601-611. DOI: <https://doi.org/10.1007/s13280-015-0675-3>
- Saraiva, S., Meier, H.E., Andersson, H., Höglund, A., Dieterich, C., Gröger, M., Hordoir, R. and Eilola, K., 2019. Uncertainties in projections of the Baltic Sea ecosystem driven by an ensemble of global climate models. *Frontiers in Earth Science*, p. 244. DOI: <https://doi.org/10.3389/feart.2018.00244>
- Sathyendranath, S., Brewin, R.J., Jackson, T., Mélin, F. and Platt, T., 2017. Ocean-colour products for climate-change studies: What are their ideal characteristics? *Remote Sensing of Environment*, 203, pp. 125-138. DOI: <https://doi.org/10.1016/j.rse.2017.04.017>
- Savchuk, O.P., Gustafsson, B.G., Medina, M.R., Sokolov, A.V. and Wulff, F.V., 2012. External nutrient loads to the Baltic Sea, 1970-2006. *BNI Techn. Rep*, 22.
- Savchuk, O.P., 2018. Large-scale nutrient dynamics in the Baltic Sea, 1970–2016. *Frontiers in Marine Science*, 5, p. 95. DOI: <https://doi.org/10.3389/fmars.2018.00095>
- Schimanke, S. and Meier, H.M., 2016. Decadal-to-centennial variability of salinity in the Baltic Sea. *Journal of Climate*, 29(20), pp. 7173-7188. DOI: <https://doi.org/10.1175/JCLI-D-15-0443.1>
- Schindler, D.W., 2006. Recent advances in the understanding and management of eutrophication. *Limnology and oceanography*, 51(1part2), pp. 356-363. DOI: https://doi.org/10.4319/lo.2006.51.1_part_2.0356
- Schindler, D.W., 2012. The dilemma of controlling cultural eutrophication of lakes. *Proceedings of the Royal Society B: Biological Sciences*, 279(1746), pp. 4322-4333. DOI: <https://doi.org/10.1098/rspb.2012.1032>
- Schulte-Uebbing, L. and de Vries, W., 2018. Global-scale impacts of nitrogen deposition on tree carbon sequestration in tropical, temperate, and boreal forests: A meta-analysis. *Global Change Biology*, 24(2), pp. e416-e431. DOI: <https://doi.org/10.1111/gcb.13862>
- Seitzinger, S.P., Mayorga, E., Bouwman, A.F., Kroeze, C., Beusen, A.H., Billen, G., Van Drecht, G., Dumont, E., Fekete, B.M., Garnier, J. and Harrison, J.A., 2010. Global river nutrient export: A scenario analysis of past and future trends. *Global Biogeochemical Cycles*, 24(4). DOI: <https://doi.org/10.1029/2009GB003587>

Siegel, D.A., Doney, S.C. and Yoder, J.A., 2002. The North Atlantic spring phytoplankton bloom and Sverdrup's critical depth hypothesis. *Science*, 296(5568), pp. 730-733. DOI: <https://doi.org/10.1126/science.10691>

Stigebrandt, A., 1985. A model for the seasonal pycnocline in rotating systems with application to the Baltic proper. *Journal of Physical Oceanography*, 15(11), pp. 1392-1404. DOI: [https://doi.org/10.1175/1520-0485\(1985\)015<1392:AMFTSP>2.0.CO;2](https://doi.org/10.1175/1520-0485(1985)015<1392:AMFTSP>2.0.CO;2)

Stålnacke, P., Grimvall, A., Sundblad, K. and Tonderski, A., 1999. Estimation of riverine loads of nitrogen and phosphorus to the Baltic Sea, 1970–1993. *Environmental Monitoring and Assessment*, 58(2), pp. 173-200. DOI: <https://doi.org/10.1023/A:1006073015871>

Steffen, W., Richardson, K., Rockström, J., Cornell, S.E., Fetzer, I., Bennett, E.M., Biggs, R., Carpenter, S.R., De Vries, W., De Wit, C.A. and Folke, C., 2015. Planetary boundaries: Guiding human development on a changing planet. *Science*, 347(6223), p. 1259855. DOI: <https://doi.org/10.1126/science.1259855>

Stockner, J.G. and Shortreed, K.S., 1988. Response of Anabaena and Synechococcus to manipulation of nitrogen: phosphorus ratios in a lake fertilization experiment. *Limnology and Oceanography*, 33(6), pp. 1348-1361. DOI: <https://doi.org/10.4319/lo.1988.33.6.1348>

Suter, E.A., Pachiadaki, M.G., Montes, E., Edgcomb, V.P., Scranton, M.I., Taylor, C.D. and Taylor, G.T., 2021. Diverse nitrogen cycling pathways across a marine oxygen gradient indicate nitrogen loss coupled to chemoautotrophic activity. *Environmental microbiology*, 23(6), pp. 2747-2764. DOI: <https://doi.org/10.1111/1462-2920.15187>

Vahtera, E., Conley, D.J., Gustafsson, B.G., Kuosa, H., Pitkänen, H., Savchuk, O.P., Tamminen, T., Viitasalo, M., Voss, M., Wasmund, N. and Wulff, F., 2007. Internal ecosystem feedbacks enhance nitrogen-fixing cyanobacteria blooms and complicate management in the Baltic Sea. *AMBIO: A journal of the Human Environment*, 36(2), pp. 186-194. DOI: [https://doi.org/10.1579/0044-7447\(2007\)36\[186:IEFENC\]2.0.CO;2](https://doi.org/10.1579/0044-7447(2007)36[186:IEFENC]2.0.CO;2)

Van Beusekom, J.E., Carstensen, J., Dolch, T., Grage, A., Hofmeister, R., Lenhart, H., Kerimoglu, O., Kolbe, K., Pätsch, J., Rick, J. and Rönn, L., 2019. Wadden Sea Eutrophication: long-term trends and regional differences. *Frontiers in Marine Science*, p. 370. DOI: <https://doi.org/10.3389/fmars.2019.00370>

Vaquer-Sunyer, R. and Duarte, C.M., 2008. Thresholds of hypoxia for marine biodiversity. *Proceedings of the National Academy of Sciences*, 105(40), pp. 15452-15457. DOI: <https://doi.org/10.1073/pnas.0803833105>

Vihma, T. and Haapala, J., 2009. Geophysics of sea ice in the Baltic Sea: A review. *Progress in Oceanography*, 80(3-4), pp. 129-148. DOI: <https://doi.org/10.1016/j.pocean.2009.02.002>

Viktorsson, L., Ekeröth, N., Nilsson, M., Kononets, M. and Hall, P.O.J., 2013. Phosphorus recycling in sediments of the central Baltic Sea. *Biogeosciences*, 10(6), pp. 3901-3916. DOI: <https://doi.org/10.5194/bg-10-3901-2013>

Virtanen, E.A., Norkko, A., Nyström Sandman, A. and Viitasalo, M., 2019. Identifying areas prone to coastal hypoxia—the role of topography. *Biogeosciences*, 16(16), pp. 3183-3195. DOI: <https://doi.org/10.5194/bg-16-3183-2019>

- Von Schuckmann, K., Le Traon, P.Y., Smith, N., Pascual, A., Djavidnia, S., Gattuso, J.P., Grégoire, M., Nolan, G., Aaboe, S., Aguiar, E. and Álvarez Fanjul, E., 2019. Copernicus marine service ocean state report, issue 3. *Journal of Operational Oceanography*, 12(sup1), pp. S1-S123. DOI: <https://doi.org/10.1080/1755876X.2019.1633075>
- Väli, G., Meier, H.M. and Elken, J., 2013. Simulated halocline variability in the Baltic Sea and its impact on hypoxia during 1961–2007. *Journal of Geophysical Research: Oceans*, 118(12), pp. 6982-7000. DOI: <https://doi.org/10.1002/2013JC009192>
- Wärtsilä, 2010. Exhaust Gas Scrubber Installed Onboard MT Suula, Public Test Report.
- Wang, H. and Wang, H., 2009. Mitigation of lake eutrophication: Loosen nitrogen control and focus on phosphorus abatement. *Progress in Natural Science*, 19(10), pp. 1445-1451. DOI: <https://doi.org/10.1016/j.pnsc.2009.03.009>
- Watson, A.J., Lenton, T.M. and Mills, B.J., 2017. Ocean deoxygenation, the global phosphorus cycle and the possibility of human-caused large-scale ocean anoxia. *Philosophical Transactions of the Royal Society A: Mathematical, Physical and Engineering Sciences*, 375(2102), p. 20160318. DOI: <https://doi.org/10.1098/rsta.2016.0318>
- Wilewska-Bien, M., Granhag, L. and Andersson, K., 2016. The nutrient load from food waste generated onboard ships in the Baltic Sea. *Marine Pollution Bulletin*, 105(1), pp. 359-366. DOI: <https://doi.org/10.1016/j.marpolbul.2016.03.002>
- Wilewska-Bien, M., Granhag, L., Jalkanen, J.P., Johansson, L. and Andersson, K., 2019. Phosphorus flows on ships: case study from the Baltic Sea. *Proceedings of the Institution of Mechanical Engineers, Part M: Journal of Engineering for the Maritime Environment*, 233(2), pp. 528-539. DOI: <https://doi.org/10.1177/1475090218761761>

Acknowledgements

I would like to thank the Institute of Marine Systems and Tallinn University of Technology for being patient with me and my progress. I especially want to thank my supervisor Urmas Raudsepp for providing inspiration, ideas and sometimes also hope that science of the Baltic Sea is worth doing.

My gratitude goes to Ilja Maljutenko for his ever refreshing vision, useful suggestions and many forms of help and support during the years. Many thanks go to my father who has always believed in me and also challenged me to finish my PhD younger than he did – I failed, but a tie is something I'm even more satisfied with.

And last but not least – a big Thank You to my colleagues who have helped me with small but important favours during the preparation and writing of the thesis.

Abstract

Long-term changes of the eutrophication indicators of the Baltic Sea

Eutrophication has become a major problem in coastal marine areas on a global scale, with unpleasant consequences such as massive algal blooms, oxygen deficient zones and loss in biodiversity. The anthropogenically busy Baltic Sea is one of the first areas where large-scale eutrophication was observed and continues to this day, without much improvement despite significant reductions in nutrient inputs since the 1980's. This review determines the state of major eutrophication indicators in the Baltic in 1993–2017, in the context of decreasing nutrient inputs. Decreasing pelagic pools of dissolved inorganic nitrogen (DIN) and increasing dissolved inorganic phosphorus (DIP) reflect the system's response to nutrient reductions, indicating the volatility of nitrogen and the stability of phosphorus in the system, as well as explaining the decreasing DIN:DIP ratio. No clear tendency of spring and summer phytoplankton blooms emerged in the context of declining nutrient input, but a temporal shift in the onset of the spring bloom was observed. A stabilisation of the extent of oxygen deficient zones was observed, implying the importance of physical factors in determining the spread of anoxic and hypoxic waters.

The study is accompanied by a manipulation experiment with an additional load of nitrogen and phosphorus to evaluate the dynamics of the Baltic Sea ecosystem in response to change in nutrients. The results suggest that the Baltic Sea ecosystem is currently in a relatively stable state. The explanation lies in the multi-factor set that determines the ecosystem state and eutrophication course in the Baltic Sea and complicates attempts to change this course with external measures. Physical factors (salt water inflows, stratification), which are unpredictable in their nature, largely determine the extent of the hypoxic zone. Climate change has become the major cause of shifting baselines, which impedes eutrophication improvement and prevents shift to the original state more than a century ago. The Baltic Sea ecosystem's response to nutrient reductions is to a certain extent contrary to what was expected. In that respect, there still remains a gap in our knowledge and understanding of eutrophication and its reversal in a complex marine ecosystem.

Lühikokkuvõte

Läänemere eutrofeerumise indikaatorite pikaajalised muutused

Rannikumere eutrofeerumine on süvenev globaalne probleem, mille väljundiks on intensiivsed vetikaõitsengud, hapnikuvaegus ja pidevalt vähenev liigiline mitmekesisus mereökosüsteemides. Tugevalt inimõjulises Läänemeres on laiaulatuslik eutrofeerumine olnud probleem juba üle 100 aasta. Toitainete sisselasku Läänemerre on edukalt vähendatud alates 1980'ndatest aastatest, kuid sellest hoolimata pole merekeskkonna seisund siiani oluliselt paranenud.

Käesolev töö hindab peamiste eutrofeerumist kirjeldavate indikaatorite seisundit Läänemeres perioodil 1993–2017, mis katab ka olulise osa toitainete vähendamise perioodist, mil positiivne mõju võiks hakata ilmema. Vähenev lahustunud lämmastiku ja kasvav lahustunud fosfori varu vees annavad tunnistust süsteemi reaktsioonist välisele toitainevoo vähendamisele. Meie tulemused kinnitavad seaduspära, et lämmastikuringe on kiire ning lämmastiku püsivus süsteemis väike. Fosfori elemendina on veeökosüsteemis stabiilne, sest looduslike mehhanismide selle ringest välja viimiseks on vähe. Ülaltoodu seletab ka vähenevat lahustunud inorgaanilise lämmastiku ja fosfori suhet Läänemeres. Hoolimata vähendatud toitainete voost ei vähenenud kevadine ega suvine vetikaõitseng oluliselt. Küll aga ilmnes perioodi jooksul ajaline nihe, mis väljendus kevadõitsengu aina varasemas alguses. Hapnikuvaeste tsoonide laienemine stabiliseerus uurimisperioodi teises pooles, viidates füüsikaliste protsesside olulisusele anoksiliste ja hüpoksiliste alade tekkimisel.

Teine osa tööst käsitleb simulatsiooniekspimenti, mille käigus vähendati lämmastiku ja fosfori voogusid Läänemerre ning vaadeldi mere ökosüsteemi oluliste lülide dünaamikat toitainete muutusega seoses. Tulemustest võib järeldada, et Läänemere ökosüsteem on hetkel suhteliselt stabiilses seisus. Seletus peitub asjaolus, et Läänemere ökosüsteemi ja selle eutrofeerumist kujundavad samaaegselt mitmed faktorid, mis raskendab oluliselt looduslike protsesside mõjutamise püüdeid väljastpoolt. Füüsilised faktorid (soolase vee sissevool, kihistumine), mis oma olemuselt on suures osas ennustamatud, mõjutavad otseselt hüpoksia levikut Läänemeres. Kliimamuutus aga nihutab süsteemi baastingimusi, mis omakorda takistab eutrofeerumise vähendamise püüdlusi ning muudab keerukaks kui mitte võimatuks taastada ökosüsteemi seisund sajanditagusel tasemel. Läänemere vastus toitainete vähendamisele on vastupidine oodatule, mis viitab lünkadele meie teadmistes keeruliste ökosüsteemide eutrofeerumisest ja nende hea seisundi taastamisest.

Appendix

Paper I

Kõuts, M., Maljutenko, I., Elken, J., Liu, Y., Hansson, M., Viktorsson, L. and Raudsepp, U., 2021. **Recent regime of persistent hypoxia in the Baltic Sea.** *Environmental Research Communications*, 3(7), p. 075004.



Environmental Research Communications



PAPER

Recent regime of persistent hypoxia in the Baltic Sea

OPEN ACCESS

Mariliis Kõuts¹ , Ilja Maljutenko¹, Jüri Elken¹, Ye Liu², Martin Hansson², Lena Viktorsson² and Urmas Raudsepp^{1,*} RECEIVED
20 February 2021REVISED
15 June 2021ACCEPTED FOR PUBLICATION
18 June 2021PUBLISHED
9 July 2021¹ Department of Marine Systems, Tallinn University of Technology, Akadeemia tee 15a, 12618 Tallinn, Estonia² Swedish Meteorological and Hydrological Institute, SE-601, 76, Norrköping, Sweden

* Author to whom any correspondence should be addressed.

E-mail: urmas.raudsepp@taltech.ee**Keywords:** eutrophication, Baltic Sea, hypoxic area, oxygen concentration, vertical stratification, model reanalysis

Original content from this work may be used under the terms of the [Creative Commons Attribution 4.0 licence](https://creativecommons.org/licenses/by/4.0/).

Any further distribution of this work must maintain attribution to the author(s) and the title of the work, journal citation and DOI.

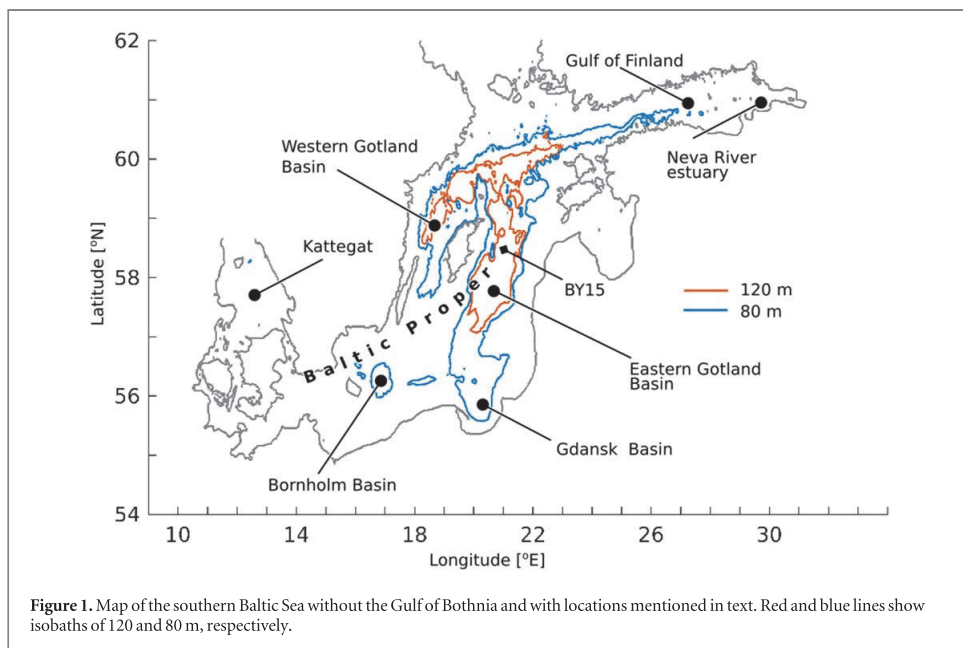
**Abstract**

Oxygen deficiency, in the form of hypoxia and anoxia, is a direct consequence of the eutrophication of the Baltic Sea. There is ongoing debate concerning the increasing extent of hypoxia. We analyse the integral metrics of hypoxia and anoxia: (1) temporal evolution of the hypoxic and anoxic area and volume, (2) the spatial distribution of the probabilities of hypoxia and anoxia occurrence in the Baltic Sea. The results are based on the state-of-the-art coupled physical and biogeochemical numerical model reanalysis data from Copernicus Marine Environment Monitoring Service for the period of 1993–2017. Statistical analysis showed that the variability of hypoxic and anoxic areas since the year 2000 represents stationary processes around their respective mean levels. From 2000 to 2017, the hypoxic area varies between 50000 and 80000 km² and the anoxic area varies between 10000 and 50000 km². Different methods and data sources indicate that the uncertainties of the estimates account for about 10000 km². We suggest that the loss of stationarity of the time series of the hypoxic area would be an indication of the regime change of hypoxia development in the Baltic Sea. Probability distribution maps of hypoxia and anoxia provide detailed information about the persistency of hypoxia and anoxia in different parts of the Baltic Sea. The probability of hypoxia exceeds 0.9 in the eastern and western Gotland basins and in the deep area of the Bornholm basin. The Gulf of Finland and the shallower areas that connect different deep basins of the Baltic Sea exhibit seasonal and episodic hypoxia. The 80 m and 120 m isobaths are the approximate bathymetry limits of hypoxia and anoxia occurrence, respectively. Our study supports previous knowledge that hypoxia development is controlled to a large degree by the depth of the permanent halocline.

1. Introduction

Oxygen concentration is an important indicator of eutrophication and the concurrent ecosystem shift or degradation of natural water bodies (Conley *et al* 2011, Carstensen *et al* 2014a). The Baltic Sea (figure 1) has been the subject of poor oxygen conditions for centuries, with an ecosystem that is mostly adapted to fluctuating oxygen content (Conley *et al* 2009). However, the increase of anthropogenic pressure in the 20th century has escalated the problem and driven the ecosystem to its tolerance limit (Gustafsson *et al* 2012, HELCOM, 2018).

Poor oxygen conditions are most commonly characterized by hypoxia, i.e., oxygen concentration below 2 mg l⁻¹ (e.g. Conley *et al* 2011, Carstensen *et al* 2014a, 2014b, Liblik *et al* 2018, Carstensen and Conley 2019, Sinkko *et al* 2019) or 2 ml l⁻¹ (e.g. Savchuk 2018, Meier *et al* 2019, Stoicescu *et al* 2019), and anoxia, i.e., absolute lack of oxygen, and the occurrence of hydrogen sulfide (Carstensen *et al* 2014b). In the Baltic Sea, hypoxia can occur in the open sea as well as coastal areas, lasting from a few days to several years. The area of hypoxic water at the bottom is the measure of the strength of hypoxia in the Baltic Sea. The geographical extent of the hypoxic area has a major impact on benthic organisms, biogeochemical processes and fisheries. The last period of oxic conditions in Baltic Sea bottoms was in the mid 1930s (Carstensen and Conley 2019). No sufficient measurements were available in the 1940s. Permanent hypoxia has been present in the open central Baltic Sea since the 1950s (Carstensen and Conley 2019). Seasonal hypoxia has been reported in several geographic



locations of the Baltic Sea (Reusch *et al* 2018), with a variable duration from spring to autumn (Conley *et al* 2011, Liblik *et al* 2018, Carstensen and Conley 2019). Episodic hypoxia can occur in shallow coastal areas with complex bottom topography (Conley *et al* 2011, Carstensen and Conley 2019, Virtanen *et al* 2019).

Since 1950, the hypoxic area has increased from 10000–20000 km² to 50000–80000 km² (Savchuk, 2018, Carstensen and Conley, 2019, Hansson *et al* 2019), but this increase has not been steady over the years. Actual values of hypoxic areas depend on whether an oxygen concentration of 2 mg l⁻¹ (Carstensen and Conley 2019) or 2 ml l⁻¹ (Savchuk, 2018, Hansson *et al* 2019) is used for the limit of hypoxia and how the data are processed. All data agree that there was a monotonic increase of hypoxic area from 1950 to 1965. In the period of 1965–1992, the hypoxic area was between 30 000–70 000 km². It is difficult to judge the presence of a distinct temporal pattern in the time series without statistical analysis. There was a clear minimum of the hypoxic area of 20000–25000 km² in 1993 (Savchuk, 2018, Carstensen and Conley 2019, Hansson *et al* 2019). At the end of the 1990s, hypoxic areas were restored to a level of 60000–70000 km² (Savchuk 2018, Carstensen and Conley 2019, Hansson *et al* 2019). Since the end of the 1990s, the hypoxic area has been on a level of 50000–80000 km².

Anoxia is present mainly in the deep central Baltic Sea. Interannual variations of the anoxic area closely follow interannual variations of the hypoxic area and do not exceed 40 000 km² in total during the period of 1970–2010 (Lehmann *et al* 2014). Major Baltic Inflows (Mohrholz 2018), large volume inflows of saline and oxygen rich water from the North Sea to the Baltic, interrupt anoxia in the deep Baltic Sea sub-basins, at least for a limited time period (Neumann *et al* 2017). Saraiva *et al* (2019) concluded that hypoxic and anoxic areas could change significantly, depending on nutrient load and climate change scenarios.

Temporal changes of oxygen concentration in a control volume of water are determined by the difference in cumulative sources and sinks acting on the volume (Fennel and Testa 2019). Atmosphere is the main external source of oxygen for the sea. Oxygen enters the sea via air-sea gas exchange. An excess of oxygen supply results in high oxygen concentration in the upper layer of the water column. The depth of oxygen penetration depends on the vertical stratification of the water column. Beneath the penetration depth of the air-to-sea oxygen flux, hypoxia can be reduced or enhanced by lateral transport of oxygen-rich or oxygen-deficient water and by biogeochemical processes of oxygen consumption and production.

In the Baltic Sea, persistent hypoxia can occur in areas where a permanent halocline is present (Väli *et al* 2013). Seasonal hypoxia may develop in areas with a seasonal pycnocline (Liblik *et al* 2018). Episodic events with hypoxia are related to specific local conditions: weak oxygen flux from the air, warm water and oxygen consumption prevailing over oxygen production (Virtanen *et al* 2019).

The aim of this study is to analyse the development of hypoxic and anoxic area and volume in the Baltic Sea from the end of the stagnation period in 1993 to 2017 using state-of-the-art statistical methods. At the end of the stagnation period, the hypoxic area was at its minimum extent. Since the 1990s, the number of available measurements has increased significantly compared to the preceding period. In addition to the statistical analysis of hypoxic area

development, we introduce the second metric, the hypoxic volume, to gain more confidence in our conclusions. The first objective of this study is to analyse the existence of the trends and statistical stationarity of the hypoxic and anoxic areas and volume development in the Baltic Sea. The second objective is to calculate the spatial distribution of the probabilities of hypoxia and anoxia occurrence in the Baltic proper (including the Gulf of Finland).

2. Materials and methods

2.1. Model description and setup

In this study, we use the physics and biochemistry reanalysis products (BALTICSEA_REANALYSIS_PHY_003_011, BALTICSEA_REANALYSIS_BIO_003_012) (www.marine.copernicus.eu) of the Baltic Monitoring Forecasting Centre of Copernicus Marine Environment Monitoring Service (BALMFC CMEMS). The reanalysis products are based on the Nemo-Nordic general circulation model (Pemberton *et al* 2017, Hordoir *et al* 2019) coupled with the SCOBI (Swedish Coastal and Ocean Biogeochemical) biogeochemistry model (Eilola *et al* 2009, Almroth-Rosell *et al* 2015). The SCOBI model system has been used in many applications, mainly coupled with the Rosby Centre Ocean model (e.g. Meier *et al* 2021).

The SCOBI biogeochemical model consists of 9 state variables: nitrate, ammonium, phosphate, three functional species of phytoplankton, zooplankton, detritus and oxygen (Eilola *et al* 2009). Oxygen dynamics are governed by air-sea exchange, primary production, respiration of plankton species and sediments, decomposition of detritus, denitrification of nitrate, and oxidation of ammonia by nitrifying bacteria. The surface oxygen flux is calculated using oxygen solubility, temperature and wind-dependent exchange rates. The model also takes into account supersaturation caused by injection of bubbles into sea water.

In the current application, the model system uses the Localized Singular Evolutive Interpolated Kalman (LSEIK, Nerger *et al* 2005) filter data assimilation method to combine simulation and the SST observations from OSISAF (<http://www.osi-saf.org/>) and *in situ* profiles of salinity and temperature from the ICES database (www.ices.dk), and nitrate, ammonium, phosphate and oxygen state variables from the Swedish Ocean Archive database (SHARK; <http://sharkweb.smhi.se>). The reanalysis has been produced using 72-hour cycling. This means that every 72 h all available observations were assimilated into the model, and then a 72-hour forecast was made.

The model domain consists of the North Sea and the Baltic Sea (Hordoir *et al* 2019), but we only use the reanalysis data for the Baltic Sea for the period 1993–2017. The horizontal resolution of the model is approximately 2 nautical miles. The thickness of 56 vertical layers varies from 3 m close to the surface, decreasing to 22 m at the bottom of the deepest part of the Norwegian trench. The numerical model simulation data covers the period of 1993–2017. The sea levels at the lateral boundary in the English Channel and northern edge of the North Sea have been derived from the coarse resolution storm-surge model NOAMOD (Dick *et al* 2001). Climatological mean values are prescribed for salinity and temperature at the open boundaries.

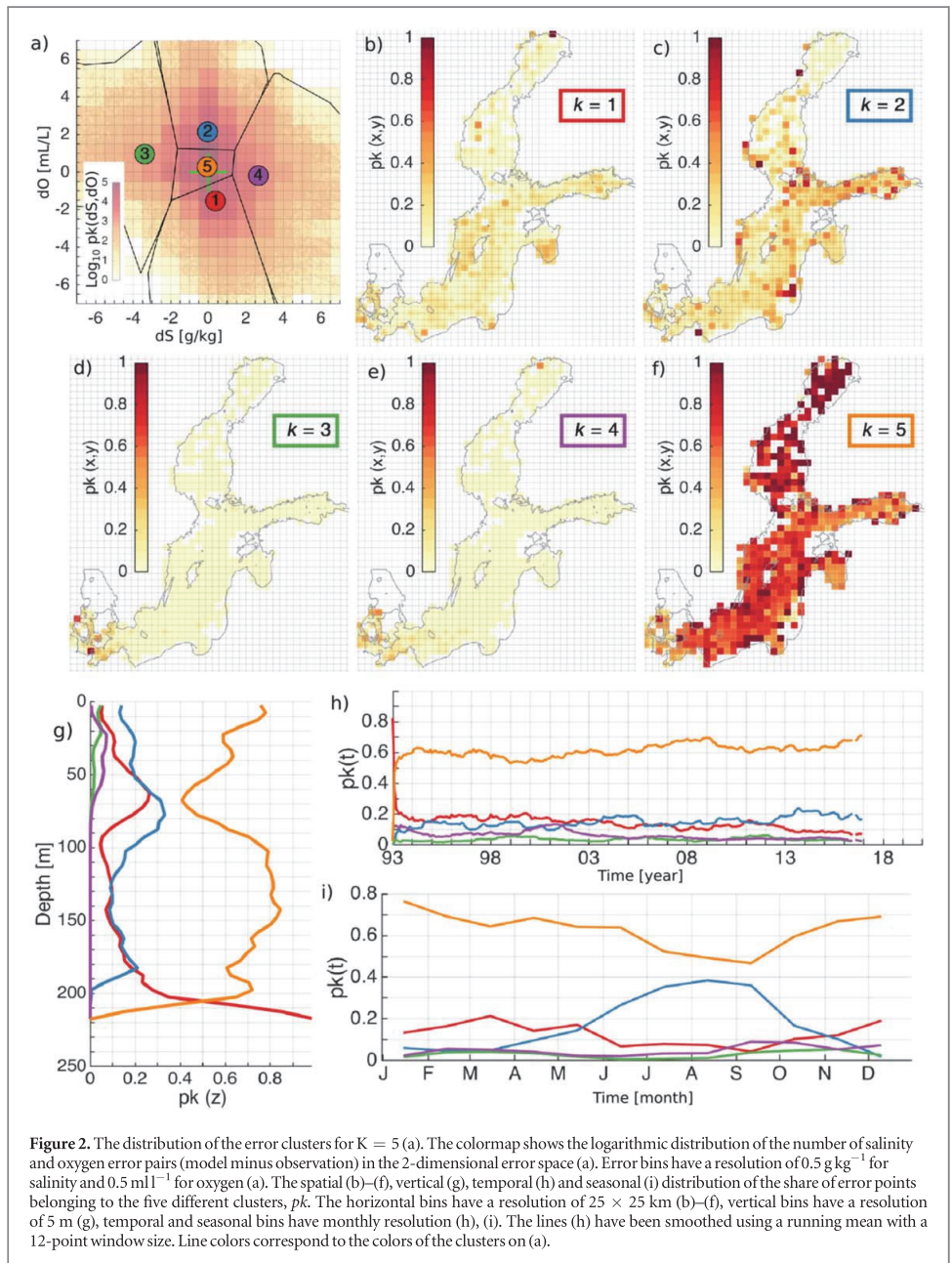
The river runoff is specified as daily means and nutrient loads as monthly means from the output of the HYdrological Predictions for the Environment (HYPE) model (Donnelly *et al* 2016). In total, 250 rivers located in the Baltic Sea are included (Hordoir *et al* 2019).

The meteorological forcing with a 22 km resolution is from HIRLAM (High-Resolution Limited Area Model), from project Euro4M (Dahlgren *et al* 2016, Landelius *et al* 2016), and covers the period 1993–2011. From 2012 to 2017, the meteorological forcing is from the UERRA reanalysis product (European Regional analysis) with an 11 km resolution. The bias correction of 0.8 was implemented for the precipitation from UERRA. Spatial maps of a monthly climatology are used for the atmospheric deposition of biogeochemical substances.

2.2. Model quality assessment using K-means clustering algorithm

We apply a method of clustering of the bivariate model errors that provides information on the accuracy of the model in general. The clustering is done using the K-means algorithm of unsupervised machine learning (Jain 2010). The method is originally described by Raudsepp and Maljutenko (2021). The first step of the method is the formation of a two-dimensional error space of two simultaneously measured parameters. Errors are calculated as the differences between model values and the measurements. The second step is the selection of the number of clusters. The third step is to perform a K-means clustering of the 2-dimensional errors. The clustering is applied to the normalized errors. Normalization is done for each variable separately using corresponding standard deviations of the errors. The fourth step is calculation of statistical metrics of non-normalized clustered errors. The fifth step is the analysis of spatio-temporal distributions of the errors belonging to different clusters.

We form a 2-dimensional error space of salinity and dissolved oxygen (figure 2(a)) as representatives of physical and biogeochemical models of the coupled model system. We use salinity and oxygen measurements



for the Baltic Sea from the EMODnet Chemistry database (Giorgetti *et al* 2020). In total, we have 651 565 simultaneous salinity and oxygen error pairs. Five clusters are selected using the Elbow cluster selection criteria (Yuan and Yang 2019, Bholowalia and Kumar 2014) after testing a different number of clusters. The outcome of the K-means clustering is shown on figure 2 and the metrics are presented in table 1.

2.3. Statistical methods for the validation

In order to assess the uncertainty of the anoxic and hypoxic areas, we have extracted oxygen profiles from the reanalysis and compared them with the *in situ* measurements at the Gotland Deep monitoring station (BY15, figure 1). We have used simulated and measured water temperature and salinity profiles for calculating water density profiles at station BY15. A direct comparison was made for density, as the latter characterizes vertical

Table 1. Statistics of the different error clusters shown in figure 2(a). BIAS is the mean of the errors in each cluster, i.e., coordinates of the centroids in figure 2(a). STD is the standard deviation of the errors in each cluster. RMSD is the root-mean-square deviation of the errors in each cluster. The correlation coefficients are calculated between modeled and measured values of the corresponding cluster.

k	BIAS		STD		RMSD		R	
	S [g kg ⁻¹]	DO [ml l ⁻¹]	S [g kg ⁻¹]	DO [ml l ⁻¹]	S [g kg ⁻¹]	DO [ml l ⁻¹]	S	DO
1	0.37	-1.54	0.61	0.95	0.72	1.81	0.99	0.93
2	-0.03	2.14	0.56	0.95	0.56	2.35	0.99	0.91
3	-3.38	0.95	1.78	1.25	3.82	1.57	0.95	0.76
4	2.67	-0.18	1.19	1.61	2.92	1.62	0.98	0.72
5	-0.06	0.28	0.40	0.47	0.40	0.55	0.99	0.98

stratification rather than temperature and salinity alone. The parameters used in this study are calculated from daily mean oxygen concentration, temperature and salinity fields.

Taylor diagrams (Taylor 2001) were prepared for the depth of selected oxygen isolines and isopycnals. The depths of oxygen and density isolines have been calculated as the first occurrence of the corresponding isoline, starting from the surface. For the Taylor diagram, common statistics, such as the Pearson correlation coefficient (r) and standard deviation (STD), are calculated. To plot multiple standard deviations on a common Taylor diagram, STDs of the simulated isoline depth have been normalized to the corresponding STD of the observed isoline depth. The data are not taken into account if either simulated or measured depth of an isoline is missing. Comparison of the simulated and the measured depths of oxygen isolines enables better assessment of the model performance than comparison of oxygen concentrations at fixed depths, as far as hypoxic and anoxic areas are concerned. Vertical stratification of the water column has a significant role in the development and the geographical extent of hypoxia (Fennel and Testa 2019).

2.4. Statistical methods for the analysis

The grid cell has been defined as anoxic or hypoxic if the concentration of oxygen in the water column is equal to 0 or less than 2 ml l⁻¹, respectively. Total area/volume of hypoxic or anoxic water was calculated as the sum of the area/volume of the grid cells where the anoxic or hypoxic water mass was present. A method for the calculation of hypoxic and anoxia area and volume from the measurements is described by Hansson *et al* (2019). We would like to note that model reanalysis data have daily resolution over the whole modeling period, while the measurements are collected in autumn.

The probability of anoxia or hypoxia occurrence is defined as the ratio of the number of days when anoxia or hypoxia was present at the grid cell to the total number of days during the period under consideration.

The hypsographic curve for the Baltic proper (including the Gulf of Finland) was calculated from the Baltic Sea Bathymetry Database (BSHC 2013) as a function of cumulative area over the given depth.

The temporal dynamics of area and volume below the defined oxygen level have been studied by means of statistical tests. The goal of the statistical tests is to test whether the 0-hypothesis, which is designed to reject the statement, can be rejected with a 95% confidence level, otherwise the statement can be accepted. The Mann-Kendall (MK) test (Mann 1945, Kendall 1975, Wang *et al* 2020) was performed to determine if monotonic increase or decrease exists in the time series of areas and volumes. The calculated Z test statistic of the MK test shows the sign and strength of the trend tendency. Linear trends have been estimated as slope parameters using the least square fit for the straight line, and statistical significance is calculated according to (Drapier and Smith 1998).

The unit root Dickey-Fuller (DF) test has been performed to determine the stationarity of the time series (Dickey and Fuller 1979). For this, we test whether unitroot (stationarity) with a) drift and with b) drift and deterministic trend are present in the time series of oxygen area and volume. Values of the DF test τ statistic below τ_{crit} allow us to reject the 0-hypothesis, meaning that the time series represents a stationary process. Therefore, τ statistic can be interpreted as the strength of the stationarity of the time series.

3. Results

3.1. Overall model quality

62% of comparison points show a good match between the model and measurements (figure 2(a), table 1). The model performs well for the whole Baltic Sea and over the simulation period (figures 2(f), (h)). A somewhat reduced performance is geographically in the Gulf of Finland, Gulf of Riga and at the Danish straits (figures 2(b)–(e)), vertically within the redoxcline and at the bottom of the Gotland Deep (figure 2(g)), and seasonally during summer

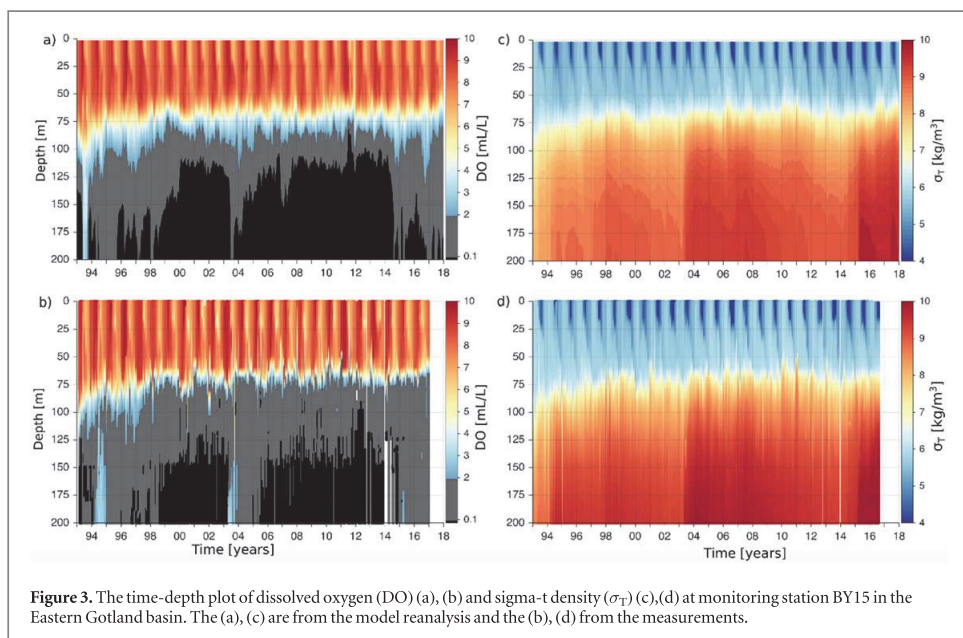


Table 2. The biases of the depth of oxygen and density isolines. The biases are calculated as corresponding model values minus measured values.

DO [mL l^{-1}]	bias [m]	σ_T [kg m^{-3}]	bias [m]
0.1	-13	5	-4
1	9	6	-4
2	11	7	-4
3	4	8	-3
4	3	9	3
5	2		
6	1		
7	0		
8	0		

(figure 2(i)). In the Gulf of Finland, the oxygen concentrations are partly overestimated, while salinity is well reproduced (figure 2(c)). In the Gulf of Riga, oxygen concentrations are underestimated and salinity is well reproduced (figure 2(b)). At the Danish straits, the situation is completely different compared to the rest of the Baltic Sea. The model either underestimates salinity (figure 2(d)), overestimates salinity (figure 2(e)) or reproduces it correctly (figure 2(f)) there. The oxygen concentrations there are well reproduced due to the shallowness of the area. In the redoxcline, i.e., in the depth range of 60–90 m (figure 3), we observe a situation of underestimated oxygen concentration with a peak share of model errors at a depth of 70 meters, and of overestimated oxygen concentration with a peak share of model errors at a depth of 80 meters (figure 2(g)). This type of vertical distribution of errors shows that the redoxcline is wider in the model than in the measurements. Seasonally, a higher share of overestimated oxygen concentration in summer than the rest of the year (figure 2(i)) accounts partly for the errors in the Gulf of Finland (figure 2(c)). The spatial distribution of bottom salinity and oxygen errors for different clusters shows that, although the model and data match is predominantly good, the share of overestimated oxygen concentration errors is still significant (figure A1).

3.2. Model validation in the Gotland Deep

Oxygen and density profiles, measured at the monitoring station BY15 in the eastern Gotland Basin and extracted from the model reanalysis, are compared to assess the model performance in the central Baltic proper (figure 3). Redoxcline and pycnocline are centered at a depth of about 75 m in the measurements and the model

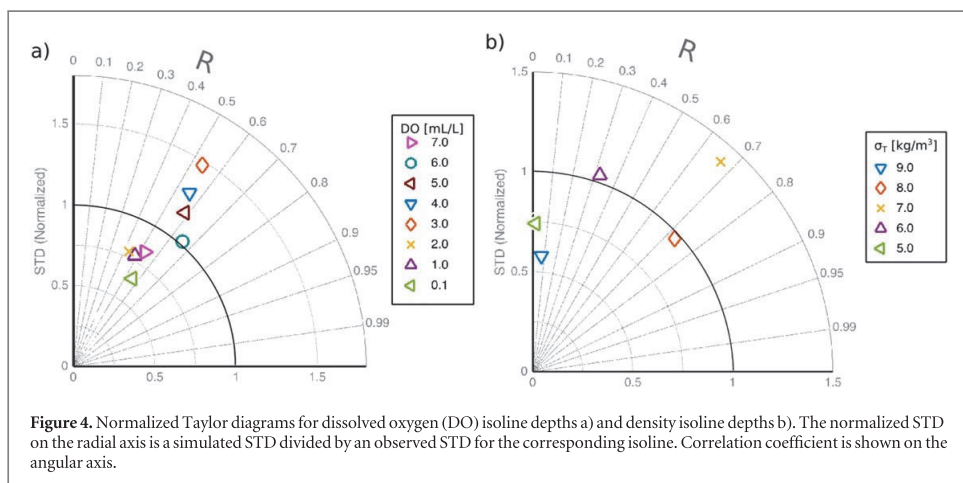


Figure 4. Normalized Taylor diagrams for dissolved oxygen (DO) isoline depths a) and density isoline depths b). The normalized STD on the radial axis is a simulated STD divided by an observed STD for the corresponding isoline. Correlation coefficient is shown on the angular axis.

Table 3. Pearson correlation coefficients between different levels of oxygen volumes (upper triangle, red) and areas (lower triangle, blue).

	Oxy, mL/L	Volume correlation coefficients			
		0	1.43	2	4
Area correlation coefficients	0	1	0.81	0.72	0.53
	1.43	0.82	1	0.99	0.85
	2	0.75	0.98	1	0.91
	4	0.50	0.69	0.76	1

alike. The measured redoxcline is shallower while pycnocline is deeper than in the model, but the mean differences do not exceed 4 meters (table 2) and other metrics are satisfactory (figure 4). The hypoxic water layer extends to about 10 meters shallower in the measurements than in the model, i.e., the model underestimates hypoxic layer thickness. Instead, anoxic water layer thickness is overestimated in the model.

3.3. Temporal evolution of the hypoxic and anoxic area and volume

Time series of anoxic and hypoxic water areas and volumes for the Baltic Sea were calculated for the period of 1993–2017 from the model (figure 5). For comparison, we calculated the hypoxic area and volume corresponding to the hypoxia threshold of 1.43 ml l⁻¹ (stringent hypoxia) and 4 ml l⁻¹ (loose hypoxia). As expected, the area and volume are smaller in the case of stringent hypoxia than in the case of hypoxia, and the area and volume are larger in the case of loose hypoxia than in the case of hypoxia. However, no differences are seen in the temporal dynamics (figure 5, table 3). Seasonal changes in the area and volume of loose hypoxia, with a minimum in early spring and a maximum in early winter, are superimposed to long-term changes. Anoxic water area and volume changes correlate well with the hypoxic water area and volume changes, except in the case of loose hypoxia (table 3). A relatively low correlation coefficient of the oxygen isolines between 4 ml l⁻¹ and 0 ml l⁻¹ shows that the variability of the upper redoxcline and anoxic water below the redoxcline are weakly coupled.

As can be expected from the model and data comparison of the depth of oxygen concentration isoline of 2 ml l⁻¹ (table 2), the hypoxic area calculated from the model is about 10 000 km² smaller than calculated from the measurements (figure 5). The same is true for the anoxic area, although the depth of the anoxia isoline was smaller in the model than in the measurements at the Gotland deep station (figure 5, table 2).

In general, there are two different regimes in the evolution of the hypoxic area and volume in the Baltic Sea (figure 5). The first period, from 1993 to 1999, shows a steady increase of the hypoxic area and volume with a rate of 5000 km²/year and 200 km³/year, respectively (table 4). The trends of anoxic area and volume are smaller, accounting for 1 400 km²/year and 30 km³/year, respectively. From 2000 to 2017, the hypoxic area varies between 50000 and 80000 km². The anoxic area varies between 10000 and 50000 km² with an apparent long-term periodicity of 10 years. The periodicity is related to large volume inflows of North Sea water into the Baltic

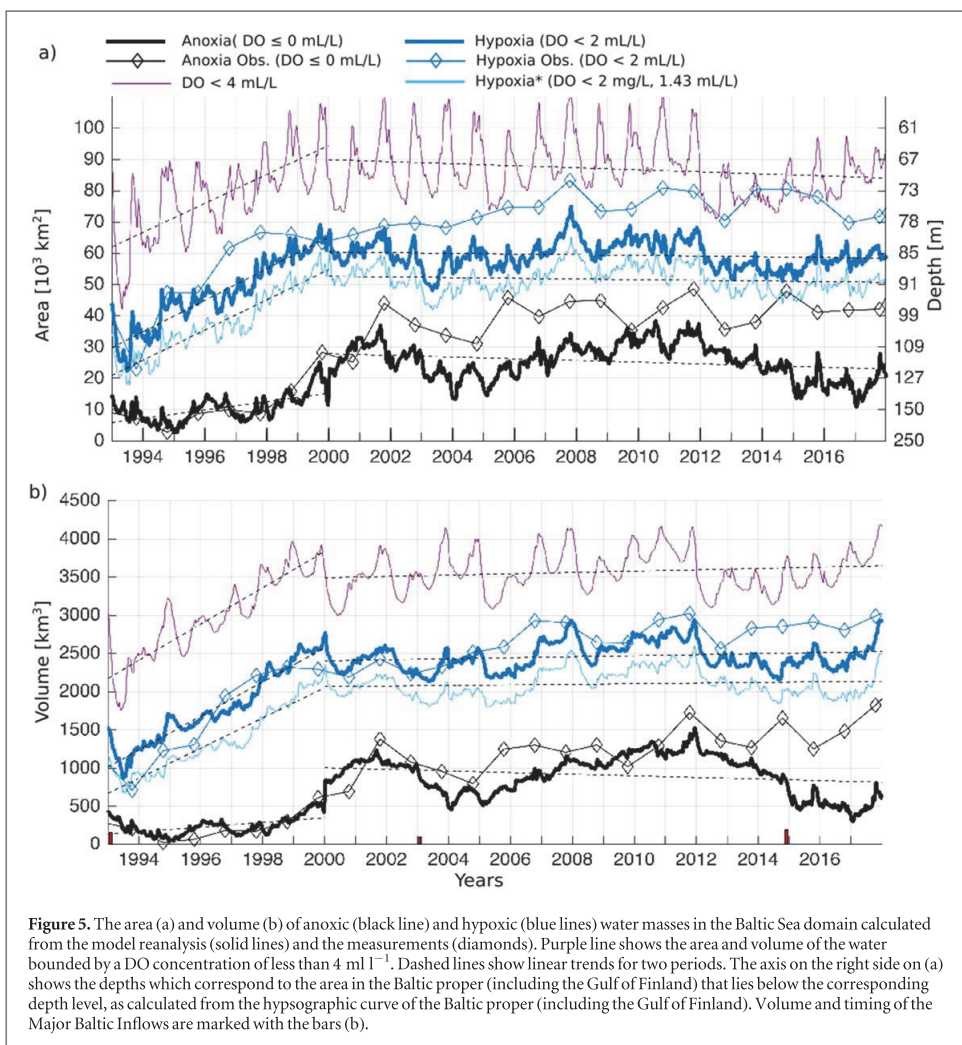


Figure 5. The area (a) and volume (b) of anoxic (black line) and hypoxic (blue lines) water masses in the Baltic Sea domain calculated from the model reanalysis (solid lines) and the measurements (diamonds). Purple line shows the area and volume of the water bounded by a DO concentration of less than 4 ml l⁻¹. Dashed lines show linear trends for two periods. The axis on the right side on (a) shows the depths which correspond to the area in the Baltic proper (including the Gulf of Finland) that lies below the corresponding depth level, as calculated from the hypsographic curve of the Baltic proper (including the Gulf of Finland). Volume and timing of the Major Baltic Inflows are marked with the bars (b).

Table 4. Trend analysis of oxygen volume and area time series. H shows which hypothesis is accepted according to the Mann-Kendall test. p-value shows the probability by which the 0-hypothesis is true with the corresponding Z-statistic.

Area trends [1000 km ² /y]								
Oxy, mL/L	p1 trend	MK H	p-value	MK Z-stat	p2 trend	MK H	p-value	MK Z-stat
0	1.36	1	<10 ⁻⁴	0.41	-0.27	1	<10 ⁻⁴	-0.15
1.43	4.83	1	<10 ⁻⁴	0.79	-0.11	1	<10 ⁻⁴	-0.09
2	5.05	1	<10 ⁻⁴	0.78	-0.11	1	<10 ⁻⁴	-0.08
4	4.64	1	<10 ⁻⁴	0.49	-0.33	1	<10 ⁻⁴	-0.10
Volume trends [km ³ /y]								
Oxy, mL/L	p1 trend	MK H	p-value	MK Z-stat	p2 trend	MK H	p-value	MK Z-stat
0	30.56	1	<10 ⁻⁴	0.34	-10.55	1	<10 ⁻⁴	-0.09
1.43	197.31	1	<10 ⁻⁴	0.84	3.98	1	<10 ⁻⁴	0.06
2	222.97	1	<10 ⁻⁴	0.87	6.72	1	<10 ⁻⁴	0.12
4	237.44	1	<10 ⁻⁴	0.74	8.67	1	<10 ⁻⁴	0.11

Sea, consisting of Major Baltic Inflows in 2003 and 2014 (figure 5(b)). During the second period, 2000–2017, we have a small negative trend in the area and volume of the anoxic water (figure 5; table 4). Somewhat surprisingly, the areas of hypoxic waters have small negative trends, while the volumes have small positive trends (table 4).

The measurements confirm the presence of an increasing trend of hypoxic and anoxic areas and volumes during the period 1993–1999. During the second period, positive trends in the areas and volumes of hypoxic and anoxic water of the Baltic Sea are small.

We performed statistical tests to determine the existence of monotonic trends and stationarity of the time series for two periods. According to the MK test, there are statistically significant trends in all time series during both periods (table 4). The Z statistic of the MK test shows the strength of the trend. Positive trends in the time series of the hypoxic and anoxic area and volume are relatively strong during the first period. Negative trends in the area and positive trends in the volume of hypoxic water are rather weak during the second period (table 4). The DF tests show somewhat scattered results (table 5). The time series of areas of hypoxic and anoxic water show stationarity with a drift in the second period. The DF test with drift and trend shows stationarity of anoxia, stringent hypoxia and hypoxia during both periods. Although the stationarity test fails for loose hypoxia, the p-value is close to the acceptance level, and τ -statistic is relatively low. The DF tests of the volume time series show stationarity only for hypoxia around the trend in the first period, while not showing stationarity for anoxia. In the second period, the test shows no stationarity of hypoxia development (table 5). Although the trends can be calculated, no meaningful statistical test can be performed for measured hypoxia and anoxia area and volume, because there is limited data, only one value per year.

3.4. Probability of hypoxia and anoxia occurrence

For the characterization of hypoxia and anoxia, we use the probability of hypoxia and anoxia occurrence, which enables us to integrate the spatio-temporal variations of hypoxic and anoxic areas in the Baltic Sea (figure 6). The regions with a hypoxia and anoxia probability of 0.25 could be considered as proxy for seasonal hypoxia and anoxia, i.e., 3 months out of 12 could have hypoxia and anoxia. In addition, these areas could potentially be the areas prone to long-term hypoxia or anoxia. The period of 1993–1999 is characterized by the development of permanent hypoxia in the parts of the Baltic Sea that have a greater depth than 80 m (figures 6(a), (c)). Moreover, from the hypsographic curve of the Baltic Sea (figure 5(a)), we can say that the 80 m isobath represents the characteristic depth of the upper bound of the hypoxic area. From a physical point of view, the Baltic proper has a persistent and strong density stratification with a pycnocline at a depth of about 60–80 m (figure 3). Thus, with some concessions, we use the 80 m depth as a robust characteristic depth that binds the depths of hypoxic water and the pycnocline in the central Baltic Sea. However, in the Bornholm Basin, persistent hypoxia with an episodic increase of oxygen concentrations occurs in the areas shallower than 80 m (figure 6). An opposite pattern with a persistent hypoxia deeper than 80 m is characteristic of the Gdansk Basin. Seasonal or episodic hypoxia occurs in the transition area between Gdansk and Eastern Gotland basins. Among shallow areas, the Neva River estuary is prone to frequent hypoxia and even anoxia (figure 6). During the period between 2000–2017, the probability of hypoxia has increased in the areas deeper than 80 m (figure 6). Geographically, the area with increased hypoxia probability has spread southward in the Eastern and Western Gotland basins. In addition, the hypoxic area has increased at the entrance to the Gulf of Finland and in the western part of the gulf.

There were no permanent anoxic regions in the Baltic Sea during the time period of 1993–1999, except in the deepest local areas of the Eastern Gotland Basin and Northern Baltic proper (figure 6(e)). Anoxic area has increased geographically and probability-wise from 1993–1999 to 2000–2017 (figure 6). However, in the southern Baltic Sea, the areas with an anoxia probability of less than 0.25 during 1993–1999 have turned into permanently anoxic areas during 2000–2017. Rather than indicating seasonal and episodic anoxia, the changes in probability from lower values during the first period to higher values during the second period show gradual development of anoxia. In the Bornholm Basin and Gdansk Basin, the anoxic areas with lower probability than 0.25 could point to areas with seasonal and episodic anoxia. A 120 m isobath captures the area with anoxia probability exceeding the value of 0.25 relatively well (figure 6(f)).

Loose hypoxia covers areas with episodic, seasonal and permanent hypoxia. It can be considered as the upper limit of the occurrence of hypoxia and anoxia (figure 6). This statement is justified by comparing the geographical areas where loose hypoxia has a probability that exceeds 0.25. These geographical areas have not spread remarkably from the first to the second period. In the southern Baltic Sea, the area of loose hypoxia with an occurrence probability of less than 0.25 has decreased, yet it has increased in the Gulf of Finland.

In order to summarize the development of hypoxia and anoxia in the Baltic Sea and its relation to vertical stratification, we have drawn mean profiles of oxygen concentration and water density for the first and the second period at the location of the monitoring station BY15 (figure 7). In the upper 50 m layer, water density and oxygen concentration have not changed significantly. The pycnocline and redoxcline have gradually lifted upward, starting at a depth of 60 m. For instance, the depth of the 8 kg m^{-3} density has decreased from 100 to 85 m, and the depth of the 2 ml l^{-1} oxygen concentration has decreased from 110 to 90 m. Below the pycnocline, the water density has increased. Below the redoxcline, the oxygen concentration has decreased. The water has become anoxic below a depth of 120 m.

Table 5. Stationarity test for oxygen area and volume time series. H shows which hypothesis is accepted, p-value shows the probability by which the 0-hypothesis is true with the corresponding τ -statistic.

Area	Drift				Drift + Trend			
	p1	p2	p1	p2	p1	p2	p1	p2
Oxy, mL/L	H	H	H	H	H	H	H	H
	0	1	-2.42	0.004	-3.79	0.015	-3.85	0.009
	1.43	1	-0.76	<10 ⁻³	-4.91	<10 ⁻³	-5.14	<10 ⁻³
	2	1	-0.88	<10 ⁻³	-4.78	<10 ⁻³	-4.94	<10 ⁻³
Volume	H	H	-1.89	0.022	-3.17	0.085	-3.20	0.084
	0	1						
	1.43	0						
	2	0						
Oxy, mL/L	H	H	H	H	H	H	H	H
	0	0	-0.57	0.44	-1.68	0.63	-1.93	0.66
	1.43	0	1.01	0.13	-2.43	0.04	-3.55	0.30
	2	0	0.76	0.15	-2.37	0.01	-3.95	0.25
Volume	H	H	-0.37	0.39	-1.79	0.02	-3.73	0.61
	0	0						
	1.43	0						
	2	0						

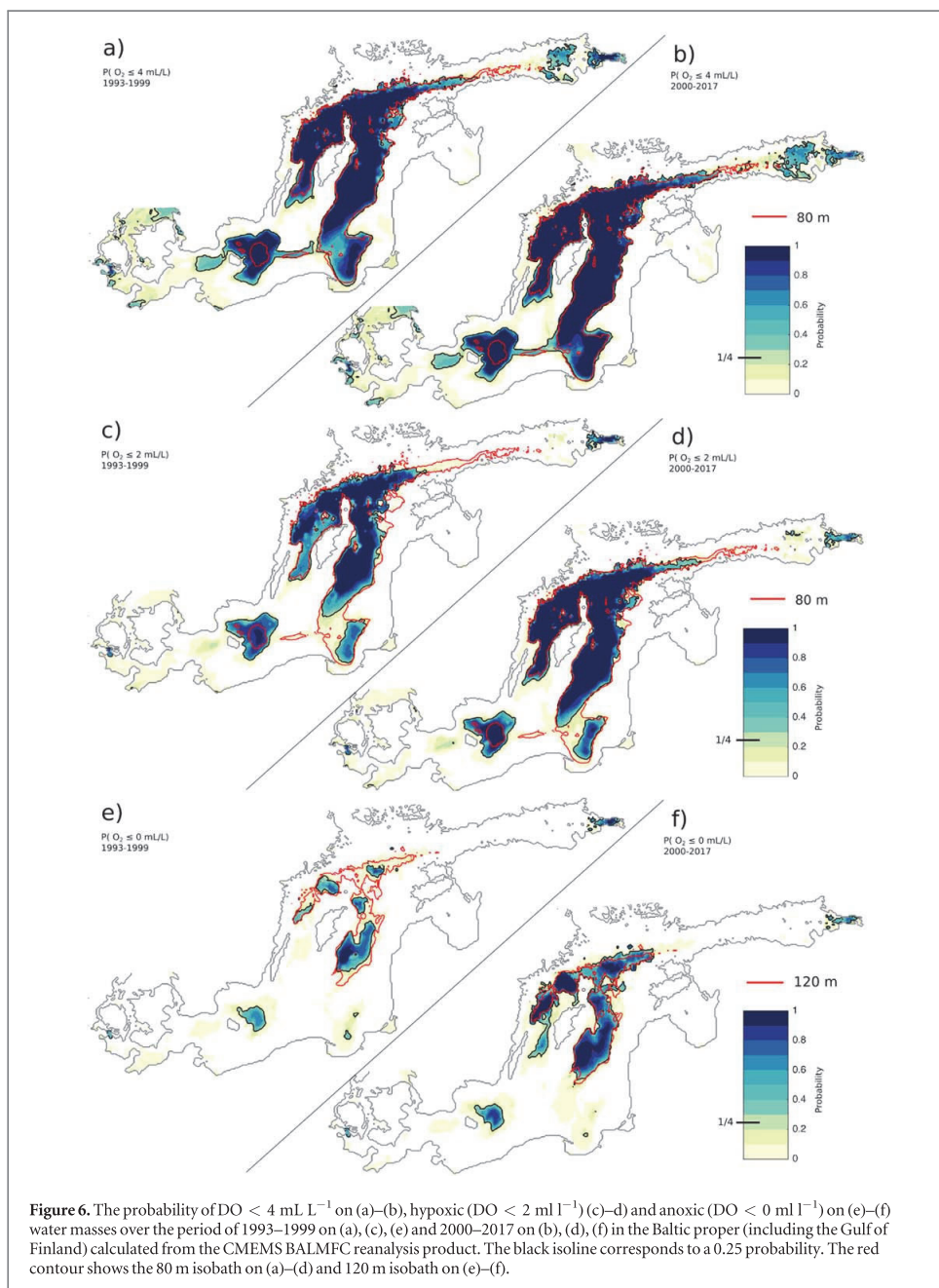
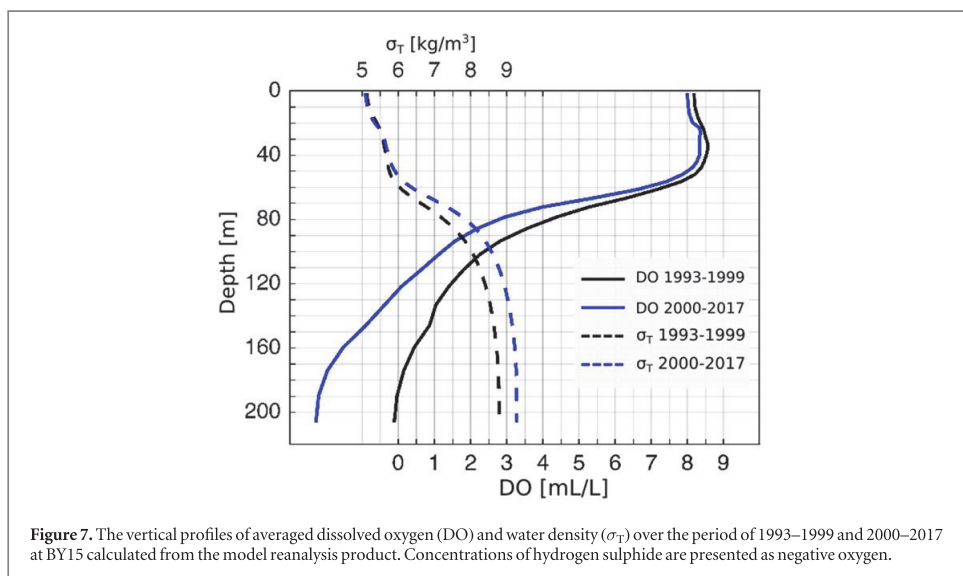


Figure 6. The probability of $\text{DO} < 4 \text{ mL L}^{-1}$ on (a)–(b), hypoxic ($\text{DO} < 2 \text{ mL L}^{-1}$) (c)–(d) and anoxic ($\text{DO} < 0 \text{ mL L}^{-1}$) on (e)–(f) water masses over the period of 1993–1999 on (a), (c), (e) and 2000–2017 on (b), (d), (f) in the Baltic proper (including the Gulf of Finland) calculated from the CMEMS BALMFC reanalysis product. The black isoline corresponds to a 0.25 probability. The red contour shows the 80 m isobath on (a)–(d) and 120 m isobath on (e)–(f).

4. Discussion

In the case of modeling, it can be argued that model-based estimates have large uncertainties due to the deficiencies of the model in describing physical and biogeochemical processes, initial fields, external inputs and forcing. In the case of measurement-based estimates, we once again face the issue of large uncertainties, as measurements lack spatial and temporal resolution and were not made simultaneously, and any kind of interpolation procedure introduces uncertainties in the estimates. Therefore, in this analysis, we use reanalysis fields, which integrate both model simulation ability and existing measurements. In this study, we used an advanced numerical model system which has been proven to provide acceptable results in many applications.



Using the data assimilation technique is definitely an advantage, as it improves the quality of the simulation product. We performed extensive validation of the model oxygen, salinity and density fields to assure the credibility of our results. The discrepancies between reanalysis and observations are mainly due to the imperfect data assimilation method and because the model cannot perfectly resolve the oxygen dynamic at the deeper layers.

Indeed, the current reanalysis data may underestimate the extent of hypoxic area, as indicated by the overestimated depth of the oxygen concentration isoline of 2 ml l^{-1} (table 2) and comparison with the estimates based on measurement data (figure 5). Therefore, we used several thresholds for hypoxia, which enabled us to define the limits of uncertainties and indicate a potential evolution of oxygen deficiency in the Baltic Sea. These thresholds include the range of low oxygen concentrations that have a negative impact on marine life. Animals display a wide tolerance span to oxygen conditions, but the underlying understanding is that lethal and sublethal effects along with stress negatively affect the functionality of marine ecosystems and reduce their resistance to environmental and anthropogenic disturbance (Carstensen *et al* 2014a, Laffoley and Baxter 2019). In the Baltic Sea, fisheries are of high economic importance to the surrounding countries. It has been noted that low oxygen concentrations affect cod reproductive volume, an indicator showing the water volume suitable for cod spawning, which is directly linked to the viability of cod stocks in the Baltic Sea (Carstensen *et al* 2014b, Raudsepp *et al* 2019a). In addition, hypoxia hinders the biogeochemical feedback loops and biomass production carried out by benthic fauna (Carstensen *et al* 2014a). The lack of oxygen at the seabed results in potential dead zones that are uninhabitable by most organisms. With that, the Baltic Sea sediments become an active ammonium and phosphorus source as soon as the sediments turn anoxic (Carstensen *et al* 2014b). These anoxia-related changes counteract nutrient mitigation measures and fuel the eutrophication process (Carstensen *et al* 2014b). The reduction in water quality, in turn, reduces the value of the Baltic Sea for recreation and other uses of marine resources.

In the development of the hypoxic and anoxic areas and volumes of the Baltic Sea from 1993 to 2017, two dynamically different periods are present. The first period, from 1993 to 1999, indicates a continuous increase of the areas and volumes of hypoxic water, no matter which threshold of oxygen concentration we use for the limit of the hypoxic water (figure 5). The MK test showed that increasing trends, which are not necessarily linear, are statistically significant. The DF test confirmed the existence of linear trends in most cases considered. In addition, the test showed that the area and volume changes superimposed to the trends represented the stationary process (tables 4 and 5). Indeed, the time series of hypoxic and anoxic areas and volumes are not perfectly homogenous and the natural variability is quite high.

We obtain from the model and measurements that the hypoxic area increased from 20000 km^2 in 1993 to about 60000 km^2 in 1999 (figure 5(a)). From 2000 until 2017, the area and volume of anoxic and hypoxic waters varied in the range of $10000\text{--}50000 \text{ km}^2$ and $50000\text{--}80000 \text{ km}^2$ and $500\text{--}2000 \text{ km}^3$ and $2000\text{--}3000 \text{ km}^3$, respectively, (figure 5). Independent estimates based on the measurement data have given variations of the

hypoxic area of the Baltic Sea in the range of 50000–80000 km² for the same period (Savchuk 2018, Carstensen and Conley 2019, Hansson *et al* 2019). The seasonal minimum of the loose hypoxic area drops to the value of 80000 km² almost every year (figure 5(a)), which can be assumed as the limit of the area ventilated by seasonal oxygen supply. Hence, we can robustly estimate that the hypoxic area is bounded by the 80 000 km² level during the period of 2000–2017.

The 80 m isobath can be considered as the characteristic depth of the hypoxic area in the Baltic proper (including the Gulf of Finland) (figures 5–7). From a physical point of view, the Baltic proper (including the Gulf of Finland) has a persistent strong density stratification with a halocline at a depth of about 60–80 m (Matthäus 1984, Väli *et al* 2013). The halocline is shallower than 80 m in depth in the Bornholm Basin and deeper in the Gdansk Basin (e.g. Väli *et al* 2013), which explains the hypoxia probability distribution there (figure 6). In the Gulf of Finland, seasonal salt wedge dynamics play a significant role in changing stratification (Maljutenko and Raudsepp 2019). Therefore, the probability of hypoxia occurrence is less than 0.5 there (figure 6).

After the Major Baltic Inflow in 1993, the hypoxic area and volume started to increase in the Baltic Sea (figure 5; Savchuk 2018, Carstensen and Conley 2019, Hansson *et al* 2019). A progressive geographical spreading of hypoxic and anoxic waters in time was described by the decrease of hypoxia probability distribution from deeper to shallower areas during the first period (figures 6(c),(e)). During the second period, the hypoxic and anoxic areas were on a relatively steady level (figure 5(a)). In that instance, high probability corresponds to persistent hypoxia and low probability to episodic hypoxia (figures 6(d),(f)). Visual comparison of our results and annual spatial maps of hypoxia and anoxia by Hansson *et al* (2019) enables us to draw a robust conclusion. The areas with a probability higher than 0.25 represent persistent hypoxia and anoxia. The regions with a hypoxia probability below 0.25 are seasonally or episodically hypoxic.

So far, poor oxygen conditions in the deep basins of the Baltic Sea have been attributed to the absence of the Major Baltic Inflows and additional inflows that do not classify as Major Baltic Inflows due to their small volume (Neumann *et al* 2017). Recent studies have shown a rapid decline of the oxygen concentration and restoration of anoxia in the Gotland Basin after the Major Baltic Inflow in 2014 (Neumann *et al* 2017, Raudsepp *et al* 2018a). Input of total nitrogen and phosphorus has decreased over decades (Savchuk 2018). At the same time, the inorganic nitrogen pool has decreased, but the inorganic phosphorus pool has increased (Savchuk 2018, Kõuts *et al* 2021). Similar tendencies are true for total nitrogen and total phosphorus pools (Savchuk 2018). Therefore, we might need to consider local biogeochemistry as the other important factor directly affecting dissolved oxygen concentrations below the halocline. Meier *et al* (2018) explained the rapidly worsening oxygen conditions after 2015, with higher amounts of organic matter being transported to the deep layers where decomposition consumes the remaining oxygen fast. With worsening oxygen conditions, the role of sediments changes from nitrogen removal to nitrogen release as ammonium (Carstensen *et al* 2014b). Phosphorus, which is buried in the sediment in organic form or bound to iron oxides, is readily released to the water column upon the onset of anoxia (Carstensen *et al* 2014a). This, in turn, can sustain cyanobacterial summer blooms, creating a positive-feedback mechanism that maintains hypoxia (Vahtera *et al* 2007). Neither phytoplankton spring blooms nor cyanobacteria summer blooms have increased in the Baltic Sea since the second half of the 2000s (Raudsepp *et al* 2018b, 2019b).

The halocline depth or vertical stratification in general has an impact on the development of hypoxic areas in the Baltic Sea (Meier *et al* 2011, Väli *et al* 2013) as well as in many other natural water basins (e.g. Fennel and Testa 2019 for review). The coinciding uplift of the pycnocline and redoxcline in the Gotland Basin between the two periods provides evidence of a close relationship between physical and biochemical processes (figure 7). Physical processes affecting vertical stratification in different parts of the Baltic Sea include vertical mixing due to winds and heat exchange between air and sea, wind-driven circulation and spreading of river water on one side, and inflows of the North Sea water into the Baltic Sea and its spreading into the deep sub-basins on the other side (Reissmann *et al* 2009, Väli *et al* 2013). The Major Baltic Inflows bring in oxygenated water, which temporarily improves the conditions under the halocline, but in the long term, this increases stratification and reduces downward mixing of oxygen (Carstensen and Conley 2019). Since 1993, there has been a positive trend in salinity of about 0.025–0.05 g kg⁻¹ per year below the depth of about 70 m, but not in the upper layer of 50 m (von Schuckmann *et al* 2019). This shows the strengthening of vertical stratification. Thus, we might expect a decrease of hypoxic layer thickness from above due to oxygen diffusion in the case of weaker vertical stratification and braking of saline water inflows to the Baltic Sea (Lessin *et al* 2014). In contrast, the hypoxic layer thickness can increase due to frequent transport of saline water from the Kattegat to the deeper layers of the Baltic Sea. The intensity of these processes is highly unpredictable in the future as well as unmanageable by anthropogenic action. Therefore, methods to stop the eutrophication of the Baltic Sea in terms of its poor

oxygen conditions caused by human intervention might not be implemented easily due to the superiority of natural processes.

5. Conclusions

The Baltic Sea is an eutrophic inland sea with multiple stressors, both natural and anthropogenic, affecting its state. The Baltic Sea eutrophication state is evaluated based on dissolved oxygen concentrations over the period of 1993–2017. We have used two metrics, area and volume, for the description of hypoxia and anoxia in the Baltic Sea. Both of these characteristics carry similar but not identical information about the temporal variations of hypoxia and anoxia.

After the stagnation period, which was terminated by the Major Baltic Inflow in 1993, hypoxia development has shown two regimes. The first period, from 1993 to 1999, represents a trend-stationary process of the increase of hypoxic area from 20000 km² to a level of about 60000 km². The second period, from 2000 to 2017, can be characterized as a stationary process with a variable hypoxic area between 50000 and 80000 km². The anoxic area varies between 10 000 and 50000 km². It is recognized that the records of hypoxic and anoxic areas are not perfectly homogenous and can vary due to natural factors. In the Gotland basin, the lower bound of the redoxcline has been uplifted from about a 100 m depth to an 80 m depth calculated as the averages for two periods. Stationarity of the time series means that the statistical properties of a system do not change over time. Therefore, by adding data from the following years, the loss of stationarity of the time series would be an indication of the future change of the hypoxia regime. In addition to natural variability of hypoxic and anoxic areas, about 10 000 km² of uncertainty is caused by different methods, either numerical models or data interpolation procedures, used for the estimation of the areas of hypoxic and anoxic water. We propose using a multi-model ensemble combined with the measurement data for reducing uncertainties in the estimation of the hypoxia area and volume of the Baltic Sea.

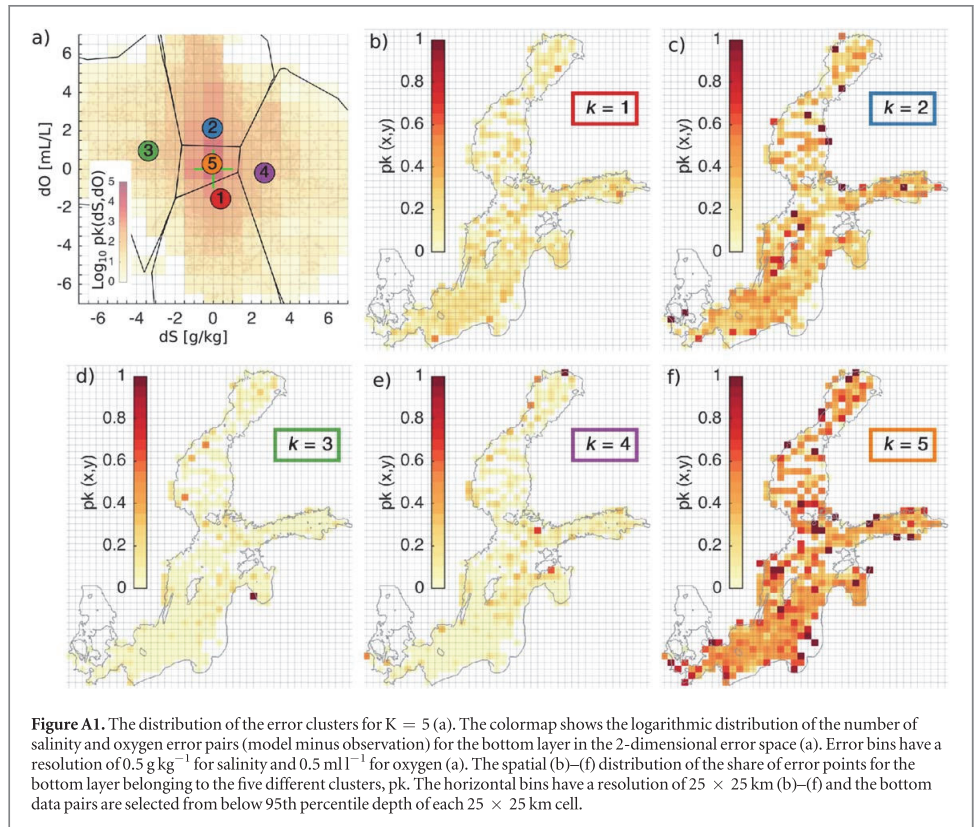
The measurements provide spatial and temporal snapshots of hypoxia coverage. Probability distribution maps of hypoxia occurrence integrate temporal variations of the hypoxia over a certain period into spatial maps. From the period 1993–1999 to 2000–2017 hypoxic and anoxic areas have expanded geographically in the Baltic Sea, but the probability distribution maps show the quantitative measure of this expansion. The southern areas of the eastern and western Gotland basin have become permanently hypoxic. In comparison, the expansion of the hypoxia towards the northeast, i.e., to the Gulf of Finland, has been moderate. The area at the entrance to the Gulf of Finland has turned from seasonal or episodic hypoxia into 50% hypoxic, while the area of seasonal or episodic hypoxia has spread eastward along the thalweg. The eastern Gulf of Finland as well as the connecting shallow area between the Gdansk and eastern Gotland basin are prone to seasonal and episodic hypoxia. Anoxia has become more persistent in the deep basins of the Baltic proper. Probability distribution maps may serve as identification of the areas which can be affected by hypoxia in relation to important ecosystem components, e.g., they allow to explain spatial distribution of marine fauna in response to their tolerance to frequent hypoxia and anoxia.

For following research, we hypothesize that hypoxia development is controlled by vertical stratification, which varies due to highly natural processes and is not prone to human interference. The hypoxic area can decrease with the weakening of stratification due to braking of large volume inflows to the Baltic Sea or increase due to strengthening of the stratification caused by frequent saline water inflows. Taking into consideration the current tendency of the development of hypoxic areas from 1993–1999 to 2000–2017, we suggest that persistent hypoxic areas may increase further in the Gulf of Finland and in the southeastern Baltic Sea where hypoxia is currently seasonal or episodic. The persistent anoxic area could increase to the limits of the hypoxic area in the case of favourable interaction of physical and biogeochemical processes.

Data availability statement

The data generated and/or analysed during the current study are not publicly available for legal/ethical reasons but are available from the corresponding author on reasonable request.

Appendix



ORCID iDs

Mariliis Kõuts  <https://orcid.org/0000-0003-1201-3565>

Urmas Raudsepp  <https://orcid.org/0000-0002-1037-5311>

References

- Almroth-Rosell E, Eilola K, Kuznetsov I, Hall P O and Meier H M 2015 A new approach to model oxygen dependent benthic phosphate fluxes in the Baltic Sea *J. Mar. Syst.* **144** 127–41
- Baltic Sea Hydrographic Commission 2013 Baltic Sea Bathymetry Database version 0.9.3. Downloaded from (<http://www.bshc.pro/>) 2015.10.10)
- Bholowalia P and Kumar A 2014 EBK-means: a clustering technique based on elbow method and K-means in WSN *Int. J. Comput. Appl.* **105** 17–24
- Carstensen J et al 2014a Hypoxia in the Baltic Sea: biogeochemical cycles, benthic fauna, and management *Ambio* **43** 26–36
- Carstensen J, Andersen J H, Gustafsson B G and Conley D J 2014b Deoxygenation of the Baltic Sea during the last century *Proc. Natl Acad. Sci. USA* **111** 5628–33
- Carstensen J and Conley D J 2019 Baltic Sea hypoxia takes many shapes and sizes *Limnol Oceanogr Bull* **28** 125–9
- Conley D J et al 2009 Hypoxia-related processes in the Baltic Sea *Environ. Sci. Technol.* **43** 3412–20
- Conley D J et al 2011 Hypoxia is increasing in the coastal zone of the Baltic Sea *Environ. Sci. Technol.* **45** 6777–83
- Dahlgren P, Landelius T, Kallberg P and Gollvik S 2016 A high resolution regional reanalysis for Europe Part 1: 3-dimensional reanalysis with the regional HIgh Resolution Limited Area Model (HIRLAM) *Q J R Meteorol Soc* **698** 2119–31
- Dick S, Kleine E, Müller-Navarra S H, Klein H and Komo H 2001 The operational circulation model of BSH (BSHcm0d)—model description and validation *Berichte des BSH* **29** 1–48
- Dickey D A and Fuller W A 1979 Distribution of the estimators for autoregressive time series with a unit root *J. Am. Stat. Assoc.* **74** 427–31
- Donnelly C, Andersson J C and Arheimer B 2016 Using flow signatures and catchment similarities to evaluate the E-HYPE multi-basin model across Europe *Hydrol. Sci. J.* **61** 255–73

- Draper N R and Smith H 1998 *Applied regression analysis* 326 (New York, NY: Wiley)
- Eilola K, Meier H M and Almroth E 2009 On the dynamics of oxygen, phosphorus and cyanobacteria in the Baltic Sea; A model study *J. Mar. Syst.* **75** 163–84
- Fennel K and Testa J M 2019 Biogeochemical controls on coastal hypoxia *Ann Rev Mar Sci* **11** 105–30
- Gustafsson B G, Schenk F, Blenckner T, Eilola K, Meier H E M, Müller-Karulis B, Neumann T, Ruoho-Airola T, Savchuk O P and Zorita E 2012 Reconstructing the development of Baltic Sea eutrophication 1850–2006 *Ambio* **41** 534–48
- Giorgetti A et al 2020 *Front Mar Sci.* **7** 583657
- Hansson M, Viktorsson L and Andersson L 2019 Oxygen Survey in the Baltic Sea 2019 - Extent of Anoxia and Hypoxia, 1960–2019 *SMHI Report Oceanography* **67** pp 88
- HELCOM 2018 State of the Baltic Sea—Second HELCOM holistic assessment 2011–2016 *Baltic Sea Environment Proc.* 155ISSN 0357-2994
- Hordoir R et al 2019 Nemo-Nordic 1.0: a NEMO-based ocean model for the Baltic and North seas—research and operational applications *Geosci Model Dev* **12** 363–86
- Jain A K 2010 Data clustering: 50 years beyond K-means *Pattern Recognit. Lett.* **31** 651–66
- Kendall M G 1975 *Rank Correlation Methods*. (London: Griffin, Oxford University Press)
- Kõuts M, Maljutenko I, Liu Y and Raudsepp U 2021 Nitrate, ammonium and phosphate pools in the Baltic Sea *Copernicus Marine Service Ocean State Report J Oper Oceanogr.* (accepted)
- Laffoley D and Baxter J M (ed) 2019 Ocean deoxygenation: Everyone's problem - Causes, impacts, consequences and solutions *Full Report* (Gland, Switzerland: IUCN) 580
- Landelius T, Dahlgren P, Gollvik S, Jansson A and Olsson E 2016 A high resolution regional reanalysis for Europe Part 2: 2D analysis of surface temperature, precipitation and wind *Q J R Meteorol Soc* **142** 2132–42
- Lehmann A, Hinrichsen H H, Getzlaff K and Myrberg K 2014 Quantifying the heterogeneity of hypoxic and anoxic areas in the Baltic Sea by a simplified coupled hydrodynamic-oxygen consumption model approach *J. Mar. Syst.* **134** 20–8
- Lessin G, Raudsepp U and Stips A 2014 Modelling the influence of major baltic inflows on near-bottom conditions at the entrance of the Gulf of Finland *PLoS One* **9** e112881
- Liblik T, Naumann M, Alenius P, Hansson M, Lips U, Nausch G, Tuomi L, Wesslander K, Laanemets J and Viktorsson L 2018 Propagation of impact of the recent major baltic inflows from the Eastern Gotland Basin to the Gulf of Finland *Front Mar Sci* **5** 222
- Maljutenko I and Raudsepp U 2019 Long-term mean, interannual and seasonal circulation in the Gulf of Finland—the wide salt wedge estuary or gulf type ROFI *J. Mar. Syst.* **195** 1–19
- Mann H B 1945 Nonparametric tests against trend *Econometrica* **13** 245–59
- Matthäus W 1984 Climatic and seasonal variability of oceanological parameters in the Baltic Sea *Beiträge zur Meereskunde* **51** 29–49
- Meier H M, Andersson H C, Eilola K, Gustafsson B G, Kuznetsov I, Müller-Karulis B, Neumann T and Savchuk O P 2011 Hypoxia in future climates: A model ensemble study for the Baltic Sea *Geophys. Res. Lett.* **38** L24608
- Meier H M, Väli G, Naumann M, Eilola K and Frauen C 2018 Recently accelerated oxygen consumption rates amplify deoxygenation in the Baltic Sea *J. Geophys. Res. Oceans* **123** 3227–40
- Meier H M, Dieterich C, Eilola K, Gröger M, Höglund A, Radtke H, Saraiva S and Wählström I 2019 Future projections of record-breaking sea surface temperature and cyanobacteria bloom events in the Baltic Sea *Ambio* **48** 1362–76
- Meier H E M, Dieterich C and Gröger M 2021 Natural variability is a large source of uncertainty in future projections of hypoxia in the Baltic Sea *Commun Earth Environ* **2** 50
- Mohrholz V 2018 Major baltic inflow statistics—revised *Front Mar Sci* **5** 384
- Nerger L, Hiller W and Schröter J 2005 A comparison of error subspace Kalman filters *Tellus, Series A: Dynamic Meteorology and Oceanography* **57** 715–35
- Neumann T, Radtke H and Seifert T 2017 On the importance of major Baltic Inflows for oxygenation of the central Baltic Sea *J. Geophys. Res. Oceans* **122** 1090–101
- Pemberton P, Löptien U, Hordoir R, Höglund A, Schimanke S, Axell L and Haapala J 2017 Sea-ice evaluation of NEMO-Nordic 1.0: a NEMO-LIM3.6-based ocean—sea-ice model setup for the North Sea and Baltic Sea *Geosci Model Dev* **10** 3105–23
- Raudsepp U and Maljutenko I 2021 A method for assessment of the general circulation model quality using K-means clustering algorithm *Geosci Model Dev, Discuss.* in review [preprint] (<https://doi.org/10.5194/gmd-2021-68>)
- Raudsepp U, Legeais J-F, She J, Maljutenko I and Jandt S 2018a Baltic inflows. in: copernicus marine service ocean state report, issue 2 *J Oper Oceanogr* **11** s106–10
- Raudsepp U, She J, Brando V E, Kõuts M, Lagema P, Sammartino M and Santoleri R 2018b Eutrophication and hypoxia in the Baltic Sea. In: Copernicus Marine Service Ocean State Report, Issue 2 *J Oper Oceanogr* **11** s110–3
- Raudsepp U, Maljutenko I and Kõuts M 2019a Cod reproductive volume potential in the Baltic Sea. In: Copernicus Marine service ocean state report, issue 3 *J Oper Oceanogr* **12** s26–30
- Raudsepp U, She J, Brando V E, Santoleri R, Sammartino M, Kõuts M, Uiboupin R and Maljutenko I 2019b Phytoplankton blooms in the Baltic Sea. In: Copernicus Marine Service Ocean State Report, Issue 3 *J Oper Oceanogr* **12** s21–6
- Reissmann J H, Burchard H, Feistel R, Hagen E, Lass H U, Mohrholz V, Nausch G, Umlauf U and Wiczorek G 2009 Vertical mixing in the Baltic Sea and consequences for eutrophication—A review *Prog. Oceanogr.* **82** 47–80
- Reusch T B et al 2018 The Baltic Sea as a time machine for the future coastal ocean *Sci. Adv.* **4** eaar8195
- Saraiva S, Meier H E, Andersson H, Höglund A, Dieterich C, Gröger M, Hordoir R and Eilola K 2019 Uncertainties in projections of the Baltic Sea ecosystem driven by an ensemble of global climate models *Front Earth Sci* **6** 244
- Savchuk O P 2018 Large-scale nutrient dynamics in the Baltic Sea, 1970–2016 *Front Mar Sci* **5** 95
- Sinkko H, Hepolehto I, Lyra C, Rinta-Kanto J M, Villnäs A, Norrko J, Norrko A and Timonen S 2019 Increasing oxygen deficiency changes rare and moderately abundant bacterial communities in coastal soft sediments *Sci. Rep.* **9** 16341
- Stoicescu S T, Lips U and Liblik T 2019 Assessment of eutrophication status based on sub-surface oxygen conditions in the Gulf of Finland (Baltic Sea) *Front Mar Sci* **6** 54
- Taylor K E 2001 Summarizing multiple aspects of model performance in a single diagram *J. Geophys. Res. Atmos.* **106** 7183–92
- Vahtera E et al 2007 Internal ecosystem feedbacks enhance nitrogen-fixing cyanobacteria blooms and complicate management in the Baltic Sea *Ambio* **36** 186–94
- Virtanen E A, Norrko A, Nyström Sandman A and Viitasalo M 2019 Identifying areas prone to coastal hypoxia—the role of topography *Biogeosciences* **16** 3183–95
- von Schuckmann K, Le Traon P-Y, Smith N, Pascual A, Djavidnia S, Gattuso J-P, Grégoire M and Nolan G 2019 Copernicus Marine Service Ocean State Report, Issue 3 *J. Oper. Oceanogr* **12** s1–123

- Väli G, Meier H M and Elken J 2013 Simulated halocline variability in the Baltic Sea and its impact on hypoxia during 1961–2007 *J. Geophys. Res. Oceans* **118** 6982–7000
- Wang F, Shao W, Yu H, Kan G, He X, Zhang D, Ren M and Wang G 2020 Re-evaluation of the power of the Mann-Kendall test for detecting monotonic trends in hydrometeorological time Series *Front Earth Sci* **8** 14
- Yuan C and Yang H 2019 Research on K-value selection method of K-means clustering algorithm *J—Multidisciplinary Scientific Journal* **2** 226–35

Paper II

Raudsepp, U., Maljutenko, I., Kõuts, M., Granhag, L., Wilewska-Bien, M., Hassellöv, I.M., Eriksson, K.M., Johansson, L., Jalkanen, J.P., Karl, M. and Matthias, V., 2019. **Shipborne nutrient dynamics and impact on the eutrophication in the Baltic Sea.** *Science of the Total Environment*, 671, pp. 189–207.



Contents lists available at ScienceDirect

Science of the Total Environment

journal homepage: www.elsevier.com/locate/scitotenv

Shipborne nutrient dynamics and impact on the eutrophication in the Baltic Sea

Urmas Raudsepp^{a,*}, Ilja Maljutenko^a, Mariliis Kõuts^a, Lena Granhag^b, Magda Wilewska-Bien^b, Ida-Maja Hassellöv^b, K. Martin Eriksson^b, Lasse Johansson^c, Jukka-Pekka Jalkanen^c, Matthias Karl^d, Volker Matthias^d, Jana Moldanova^e

^a Department of Marine Systems, Tallinn University of Technology, Akadeemia Road 15a, 12618 Tallinn, Estonia

^b Department of Mechanics and Maritime Sciences, Chalmers University of Technology, Hörsehgången 4, 41756 Gothenburg, Sweden

^c Atmospheric Composition Research, Finnish Meteorological Institute, 00560 Helsinki, Finland

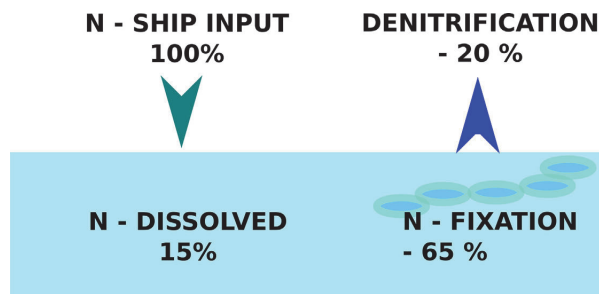
^d Helmholtz-Zentrum Geesthacht, Max-Planck- Straße 1, 21502 Geesthacht, Germany

^e Swedish Environmental Research Institute, Box 530 21, SE-400 14 Gothenburg, Sweden

HIGHLIGHTS

- Relative impact of shipborne nutrients does not exceed 10% locally.
- The North-Eastern and South-Western Baltic Sea are the most impacted.
- Nitrogen fixing cyanobacteria biomass decreases due to the shipborne nitrogen load.

GRAPHICAL ABSTRACT



ARTICLE INFO

Article history:

Received 19 December 2018

Received in revised form 15 March 2019

Accepted 17 March 2019

Available online 21 March 2019

Editor: Damia Barcelo

Keywords:

Nutrients
Modelling
Shipping
Nitrogen cycle
The Baltic Sea

ABSTRACT

The Baltic Sea is a severely eutrophicated sea-area where intense shipping as an additional nutrient source is a potential contributor to changes in the ecosystem. The impact of the two most important shipborne nutrients, nitrogen and phosphorus, on the overall nutrient-phytoplankton-oxygen dynamics in the Baltic Sea was determined by using the coupled physical and biogeochemical model system General Estuarine Transport Model-Ecological Regional Ocean Model (GETM-ERGOM) in a cascade with the Ship Traffic Emission Assessment Model (STEAM) and the Community Multiscale Air Quality (CMAQ) model. We compared two nutrient scenarios in the Baltic Sea: with (SHIP) and without nutrient input from ships (NOSHIP). The model uses the combined nutrient input from shipping-related waste streams and atmospheric depositions originating from the ship emission and calculates the effect of excess nutrients on the overall biogeochemical cycle, primary production, detritus formation and nutrient flows. The shipping contribution is about 0.3% of the total phosphorus and 1.25–3.3% of the total nitrogen input to the Baltic Sea, but their impact on the different biogeochemical variables is up to 10%. Excess nitrogen entering the N-limited system of the Baltic Sea slightly alters certain pathways: cyanobacteria growth is compromised due to extra nitrogen available for other functional groups while the biomass of diatoms and especially flagellates increases due to the excess of the limiting nutrient. In terms of the Baltic Sea ecosystem functioning, continuous input of ship-borne nitrogen is compensated by steady decrease of

* Corresponding author.

E-mail address: urmas.raudsepp@taltech.ee (U. Raudsepp).

nitrogen fixation and increase of denitrification, which results in stationary level of total nitrogen content in the water. Ship-borne phosphorus input results in a decrease of phosphate content in the water and increase of phosphorus binding to sediments. Oxygen content in the water decreases, but reaches stationary state eventually.

© 2019 The Authors. Published by Elsevier B.V. This is an open access article under the CC BY license (<http://creativecommons.org/licenses/by/4.0/>).

1. Introduction

In natural waters, phytoplankton growth is usually limited by physical and biogeochemical factors (Hecky and Kilham, 1988; Chislock et al., 2013). Human-induced change in these limiting factors may have a considerable effect on the entire ecosystem where phytoplankton usually plays the key role (Schelske, 1975; Hecky and Kilham, 1988; Chislock et al., 2013). In coastal waters the limiting element is most often a nutrient; either nitrogen or phosphorus (Hecky and Kilham, 1988; Granéli et al., 1990). Changes in the input of the limiting nutrient into the particular coastal ecosystem may, in turn, alter phytoplankton biomass and cause other ecosystem alterations (Schelske, 1975; Schindler, 2006; Chislock et al., 2013). Since ecosystems are complex and their responses non-linear, secondary changes, which occur as a consequence, are more difficult to assess in advance (Duarte et al., 2009; Savchuk, 2018).

Maritime transport, among other sources, increases nutrient input into the marine ecosystem via emissions to the air and the concurrent deposition, as well as direct discharge (Aulinger et al., 2016; Bartnicki et al., 2011; Herz and Davis, 2002). Emissions from marine transport contribute significantly to air pollution globally, with commercial shipping estimably responsible for around 4–14% of the global nitrogen emissions (Wang et al., 2008; Corbett and Fischbeck, 1997; Corbett and Köhler, 2003; Eyring et al., 2005). Marine pollution from direct sanitary wastewater discharge is an especially pronounced problem with large cruise ships, which represent <1% of the global merchant fleet, while estimably being responsible for 25% of all the waste generated by merchant vessels (Perić et al., 2016; Herz and Davis, 2002). Global maritime transport is experiencing an increasing trend (Eyring et al., 2005; Marmer et al., 2009).

Worldwide, the coastal areas of Western and Southern Europe (North Sea and the Mediterranean), the United States and South-East China have been more thoroughly studied regarding the amount and effect of ship-related emissions on the environment (Viana et al., 2014; Marmer et al., 2009; Aksoyoglu et al., 2016; Chen et al., 2019; Djambazov and Pericleous, 2015).

In Northern Germany and Denmark that are surrounded by numerous shipping lanes, the contribution of shipping emissions to the atmospheric nitrogen dioxide is around 15% in winter and 25% in summer, whereas in the western entrance of the English Channel the ship-derived nitrogen dioxide contribution can be up to 90% (Aulinger et al., 2016). This demonstrates that in the case of lacking additional sources, shipping can be the primary contributor to the atmospheric input of nutrients, providing extra fuel for the already intense eutrophication in the coastal waters of Western Europe. Quantitatively, the contributions from shipping emissions to nitrogen dioxide pollution show a large spatial variability, with maximal contributions in the Mediterranean basin and the North Sea, and the average being 7–24% across Europe (Viana et al., 2014).

A highly industrialized and rapidly transitioning area with dense marine traffic lies in South-East Asia. Modelled annual ship emissions on the most active routes reach up to 10^4 kg N/km²/yr (Chen et al., 2019). The ship-induced increase of nitrogen deposition is not only found along the shipping routes but also spread to wide land regions. The highest simulated total N deposition from ship emissions appeared in the coastal areas, which reached 1000 kg N/km²/yr. In the sea area, the N deposition flux was ranged from 200 kg N/km²/yr to 900 kg N/km²/yr.

The Arctic Ocean is an area of growing global interest, as increasing navigability enables more intense/frequent shipping activity that will bring about higher input of nutrients and pollutants into a formerly pristine environment (Gong et al., 2018).

Multiple studies have implied that additional input of nutrients has an effect on (marine) ecosystems, especially by increasing primary production and decreasing oxygen concentrations due to the increased production of dead organic matter (Herz and Davis, 2002; Perić et al., 2016; Hagy et al., 2004; Spokes and Jickells, 2005; Troost et al., 2013; Djambazov and Pericleous, 2015). In a study by Troost et al. (2013) additional nitrogen from atmospheric deposition lead to increased primary production in the North Sea. There are temporal and spatial differences in the effect of additional nutrient input, which determines ships as effective proxies to areas lacking other nutrient sources. The offshore areas (>30 km off the coast) are, in general, more affected due to absence of land input and the system being nitrogen limited during long periods in summer (Troost et al., 2013). It is thus mainly the nitrogen-limited phytoplankton species that benefit from the atmospheric deposition, that has been estimated to be accountable for 13.8–15% of primary production in several studies (Troost et al., 2013; Spokes and Jickells, 2005). Atmospheric nitrogen input can, hence, support a significant increase in phytoplankton biomass and will, along with other nitrogen sources, enhance long-term eutrophication effects in the intensely shipped coastal waters of Western Europe and England (Spokes and Jickells, 2005; Djambazov and Pericleous, 2015). Similar results have been obtained or are expected to occur in the actively industrializing South-East Asia region and the increasingly shipped Arctic Sea (Zhao et al., 2015; Gong et al., 2018). Through its effects on primary production, addition of nutrients may also influence the rest of the ecosystem via changes in the carbon equilibrium or shifts in the species composition on higher trophic levels of the food chain (Voss et al., 2001; Van de Waal et al., 2010).

The Baltic Sea has been, similarly to other intense shipping areas, under human pressure for a long time, as well as facing natural challenges from being a northerly inland sea with long residual time, limited water exchange and slow degradation processes in a temperate region (Zillén et al., 2008; Reusch et al., 2018). The anthropogenic nutrient input to the Baltic Sea has been the major cause of eutrophication and the consequent extensive cyanobacteria blooms (Elmgren, 1989; Reusch et al., 2018; Jonson et al., 2015; Aksoyoglu et al., 2016; HELCOM, 2014). Contribution of the shipping sector to the total atmospheric deposition of oxidized nitrogen into the Baltic Sea is driven by the source strength as well as by the meteorological conditions which means that the annual contribution does not only vary with changing shipping emissions, but also with inter-annual variability of the meteorology (Bartnicki et al., 2011). Bartnicki et al. (2011) and Jonson et al. (2015) studied atmospheric deposition of nitrogen to the Baltic Sea for the time period between 1995 and 2012 with atmospheric chemistry-transport model EMEP and found contribution from the Baltic Sea and North Sea shipping to the total deposition of oxidized nitrogen to be on average 18 kt N/year which makes a relative contribution of 13–20%. A similar result was obtained by Raudsepp et al. (2013) in the Gulf of Finland, where NO_x deposition to the sea from ship exhaust gases was estimated to be about 12% of the annual atmospheric NO_x deposition. The total atmospheric nitrogen deposition is estimated to be about 220 kt N/year (HELCOM, 2013a, 2013b; Simpson, 2011) and the waterborne nitrogen input ca. 760 kt N/year, which makes the atmospheric contribution of nitrogen around

22%. Therefore, the shipping contribution is about 1.25–3.3% of the total nitrogen to the Baltic Sea.

Phosphorus enters the Baltic Sea mainly as waterborne while the atmospheric contribution is calculated to be approximately 5.5% of the total phosphorus input (HELCOM, 2013b). Shipborne phosphorus enters the sea via waste generated onboard the ships such as sewage (black water), food waste and grey water (Wilewska-Bien et al., 2018). Other possible phosphorus sources of significance are bilge water and atmospheric deposition (Wilewska-Bien et al., 2018; Neumann et al., 2018b, 2018c). The atmospheric contribution of phosphorus from ships is small because marine fuels contain very little (<15 ppm) phosphorus (Wilewska-Bien et al., 2018; ISO 8217, 2012). Compared to the overall phosphorus input to the Baltic Sea, the phosphorus from shipping is estimated to comprise around 0.3% of the total annual input (HELCOM, 2013b; Wilewska-Bien et al., 2018).

Similarly to the North Sea, any additional nutrient deposition in the nitrogen limited offshore areas of the Baltic Sea influences the phytoplankton biomass during spring by changing the interspecies dynamics of different functional groups (Tilman, 1982; Stockner and Shortreed, 1988). Furthermore, increased production of organic matter also increases oxygen demand and may expand the hypoxic areas below the upper mixed layer of the Baltic Sea water column (Zillén et al., 2008; Conley et al., 2002). The share of nutrient input from shipping to the Baltic Sea is small compared to the total input, but its relative importance may become important due to spatio-temporal variance of the different sources and the natural spatio-temporal dynamics. Further, despite being a small share, the shipborne nutrient input contributes to the cumulative nutrient input as one of many small sources.

The objective of this study is to evaluate the response of the Baltic Sea ecosystem to excess nutrients from shipping (SHIP scenario minus NOSHIP scenario). While other studies have either focused on a certain area of the Baltic Sea (Raudsepp et al., 2013; Neumann et al., 2018a, 2018b, 2018c), or a selected discharge or nutrient type (Wilewska-Bien et al., 2016, 2018), the current study takes into account all shipping-related nutrient sources: atmospheric emissions and the concurrent deposition, as well as direct discharges of different categories. We evaluate the impact of shipborne nutrients on the overall nutrient-phytoplankton-oxygen dynamics across the entire Baltic Sea and determine which processes are responsible for a transformation of the nutrients. We compare the situation under current regulation of ship emissions (SHIP) to a zero shipborne nutrient emission scenario (NOSHIP).

2. The Baltic Sea

The Baltic Sea is a brackish semi-enclosed sea in northeastern Europe with a surface area of 422,000 km² and a volume of 21,205 km³ (Leppäranta and Myrberg, 2009). The Baltic Sea is characterized by relative shallowness with an average depth of 54 m, while >1/3 of the sea is shallower than 30 m (Fig. 1), giving it a small total water volume relative to the surface area. The maximum depth of 459 m is located in the deep trench of the Landsort Deep. The Gotland Deep with a maximum depth of 250-m in the central Baltic Proper is considered a dynamic deep area with a high significance in shaping hydrographic and biogeochemical fields of the Baltic Sea. The long-term salinity is determined by net precipitation (e.g. Jaagus et al., 2018) and river discharge across the Baltic Sea coast (Hansson et al., 2011) and by the saline water inflows from the North Sea through very narrow and shallow channels in the Danish Straits (BACCII Author Team, 2015). The saline and oxygenated water inflows to the Baltic Sea, especially the Major Baltic Inflows, occur only intermittently (e.g. Mohrholz, 2018).

The surface salinity varies horizontally from ~10 near the Danish Straits down to ~2 at the northernmost and easternmost subbasins of the Baltic Sea. The halocline, a vertical layer with rapid depth-dependent changes of salinity that separates the well-mixed surface layer from the weakly stratified layer below, is located at the depth

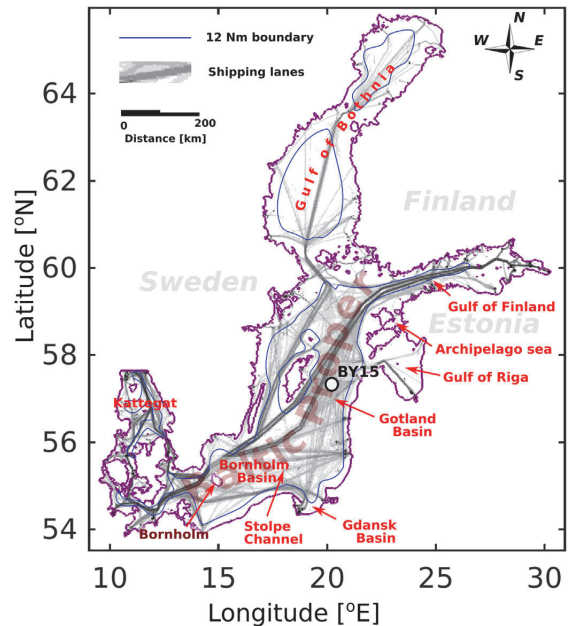


Fig. 1. Map of the Baltic Sea with locations relevant for the article. Blue contour lines show borders of territorial waters. The location of main shipping lanes is shown as grey underlay.

range of 60–80 m (Matthäus, 1984). The bottom layer salinity below the halocline depth varies from 15 in the south down to 3 in the northern Baltic Sea (Väli et al., 2013). Long-lasting periods of oxygen depletion in the deep layers of the central Baltic accompanied by salinity decline and overall weakening of vertical stratification are referred to as stagnation periods. Extensive stagnation periods occurred in the 1920s/1930s, in the 1950s/1960s and in the 1980s/ beginning of 1990s (BACCII Author Team, 2015).

The upper mixed layer temperature of the Baltic Sea is characterized by a strong seasonal cycle driven by the annual course of solar radiation (Leppäranta and Myrberg, 2008). Maximum water temperatures are reached in July and August and minimums during February, when the Baltic Sea becomes partially frozen. The strongly seasonal sea ice coverage has a vital role in the annual course of physical and ecological conditions. In general, sea ice starts to form in October and may last until June. Depending on the year maximum ice extent could vary in the range of 30,000 km² (e.g. in 2015) to 260,000 km² (e.g. in 2011). In case of a fully ice-covered Baltic, the maximum ice extent is 422,000 km², which was last observed during the 1940s (Vihma and Haapala, 2009). Temporal trends of sea ice extent could be a valuable indicator of the climate change signal in the Baltic Sea region. It has been estimated that a 1 °C increase in the average air temperature results in the decline of ice-covered area in the Baltic Sea by about 45,000 km² (Granskog et al., 2006). Seasonal thermocline, developing at the depth range of 10–30 m in spring, is strongest in summer and is eroded in autumn. In autumn and winter the Baltic Sea is thermally mixed down to permanent halocline at the depth of 60–80 m (Matthäus, 1984). The 20–50 m thick cold intermediate layer forms below the upper mixed layer in March and is observed until October within 15–65 m depth (Chubarenko and Stepanova, 2018; Liblik and Lips, 2011). Decrease in maximum ice extent may influence vertical stratification of the Baltic Sea (Hordoir and Meier, 2012). The deep layers of the Baltic Sea are disconnected from the ventilated upper ocean layers, and temperature variations are predominantly driven by mixing processes and horizontal advection.

The large-scale mean horizontal circulation is dominantly cyclonic in the Baltic (Meier, 2007; Jędrasik and Kowalewski, 2019). Deep water circulation consists of dense bottom currents of the inflowing saline water in the southern Baltic Sea, while convection, mixing, entrainment and vertical advection of water masses leads to interactions between upper and lower layers (Leppäranta and Myrberg, 2008). Instantaneous surface circulation pattern is driven by wind in the Baltic Sea.

The Baltic Sea has been suffering from eutrophication for at least half a century already. Out of external sources, rivers contribute most to the Baltic Sea nutrient input (HELCOM, 2018a). Seven biggest rivers – Daugava, Gota, Nemunas, Neva, Oder, Tornio and Vistula – cover 50% of the Baltic drainage area of 1.74 km² (HELCOM, 2018a). The average flow of the largest rivers Neva and Vistula is 2310 m³/s and 1112 m³/s, respectively, whereas smallest contributing rivers have a flow <600 m³/s (HELCOM, 2018a). Rivers with catchments in densely populated agricultural areas, such as Vistula, Nemunas and Oder in the southern part of the Baltic Sea have a bigger nutrient input compared to northern areas, where large parts of river drainage areas are under forest (HELCOM, 2018a). Although, nutrient input from the rivers has decreased by 12% in case of nitrogen and 25% of phosphorus over couple of decades, no improvement of the Baltic Sea state has been detected (HELCOM, 2018b). A warming trend of 0.08 °C/year in the upper 50 m layer and 0.04 °C/year in the deep layers (>60 m) reinforce a cascade of biogeochemical processes which is called the “vicious circle” (Savchuk, 2018; Meier et al., 2012; Vahtera et al., 2007). Due to the “vicious circle” there is enhancement of cyanobacteria blooms, which hampers nitrogen reduction attempts and sustains an elevated trophic state via accelerated oxygen consumption during organic matter oxidation, an increase of denitrification and nitrification rate in sediments and enhanced release of phosphates from the accumulated sediments due to hypoxia and anoxia (Seitzinger, 1988; Vahtera et al., 2007; Savchuk, 2018). On the other hand, the cyanobacteria blooms stimulate summer production in the entire food web, from zooplankton and benthos to fish (Karlson et al., 2015).

3. Methods

The effects of additional shipborne nutrients on the marine primary production is estimated using the coupled physical and biochemical model system GETM-ERGOM (Burchard and Bolding, 2002; Bruggeman and Bolding, 2014) for the Baltic Sea. Combining the simulation results from Automatic Identification System (AIS) based emission modelling using The Ship Traffic Emission Assessment (STEAM) and atmospheric deposition fields from the Community Multiscale Air Quality (COSMO-CLM/CMAQ) model system (Rockel et al., 2008; Matthias, 2008; Byun and Schere, 2006; Karl et al., 2018) using consistent STEAM shipping emissions to the atmosphere, the input of nitrate, ammonium, phosphate and organic matter are applied as mass fluxes to the surface layer of the sea. The year 2012 is considered as the reference year (SHIP model simulation). A NOSHIP model simulation is performed excluding the above-mentioned external input of nutrients from shipping activity. In general, annual mean temperatures were 0.5 °C to 0.7 °C above normal and it was wetter in the Nordic and Baltic regions in 2012 (Achberger et al., 2013). The year 2012 can be considered as typical for hydrographic and biogeochemical conditions relative to the climatological period 1993–2014. Horizontally averaged annual temperature and salinity profiles, as well as sea ice extent and volume were close to the mean (Von Schuckmann, 2019). The year 2012 shows decrease of salinity below the halocline in the Gotland Deep (Von Schuckmann, 2019) and relatively high spatial extent of oxygen depleted water account for the hypoxic area of 60,000 km² in the Baltic Sea (Savchuk, 2018). Previous saline water inflow which signal of the salinity increase was detected in the Gotland Deep took place at the end of 2006. The mean total freshwater discharge into the Baltic Sea for the year 2012 was 14% higher than long-term average in year 2012 (Kronsell and Andersson, 2013).

Spring bloom started relatively early, in March already, with the start date varying little across the entire Baltic Sea area (Raudsepp et al., 2019a). Peak bloom day stretched from the end of March to the end of April. The spring bloom ended at the end of May, similarly to the other years since 2007. The spring bloom's spatiotemporal coverage in 2012 was close to the mean, but the phytoplankton summer bloom was among the smallest (Raudsepp et al., 2018). The latter is consistent with a minimum of the interannual oscillations of cyanobacterial blooms with a period of about 3 years in the Baltic Sea (Kahru et al., 2018).

TN and TP pools were in a stable level of about 6000 ktons and 680 ktons, respectively since 2005, as well as DIN and DIP pools of about 1000 ktons and 480 ktons, respectively (Savchuk, 2018). In general this is consistent with the period of stable nutrient input, within otherwise decreasing trend since 1980 (Savchuk, 2018).

The modelling system consists of the ship emission model, The Ship Traffic Emission Assessment Model (STEAM) (Jalkanen et al., 2009; Jalkanen et al., 2012; Johansson et al., 2013; Johansson et al., 2017), the atmospheric chemistry modelling system, Climate Limited-area Modelling Community (COSMO-CLM) and The Community Multiscale Air Quality (CMAQ) model system (Rockel et al., 2008; Matthias, 2008; Byun and Schere, 2006; Karl et al., 2018), and the coupled marine physical model, General Estuarine Transport Model (GETM) (Burchard and Bolding, 2002; Bruggeman and Bolding, 2014), and the biogeochemical model, the Ecological Regional Ocean Model (ERGOM) (www.ergom.net; Neumann and Schernewski, 2008). The STEAM is ship Automatic Identification System (AIS)-based emission model providing shipping emissions for the CMAQ model system and direct ship discharges to the water. The atmospheric deposition fields from the CMAQ model provide the input of nitrate, ammonium, phosphate and organic matter mass fluxes to the surface layer of the sea. Further on, the GETM-ERGOM system uses the atmospheric deposition fields and direct ship discharges for the estimation of the effects of shipborne nutrients on the Baltic Sea ecosystem.

The model system simulations were carried out for the year 2012. In general, annual mean temperatures were 0.5 °C to 0.7 °C above normal and it was wetter in the Nordic and Baltic regions in 2012 (Achberger et al., 2013). The year 2012 can be considered as typical for hydrographic and biogeochemical conditions relative to the climatological period 1993–2014. Horizontally averaged annual temperature and salinity profiles, as well as sea ice extent and volume were close to the mean (Von Schuckmann, 2019). The year 2012 shows decrease of salinity below the halocline in the Gotland Deep (Von Schuckmann, 2019) and relatively high spatial extent of oxygen depleted water account for the hypoxic area of 60,000 km² in the Baltic Sea (Savchuk, 2018). Previous saline water inflow which signal of the salinity increase was detected in the Gotland Deep took place at the end of 2006. Freshwater discharge. Spring bloom started relatively early, in March already, with the start date varying little across the entire Baltic Sea area (OSR 3). Peak bloom day stretched from the end of March to the end of April. The spring bloom ended at the end of May, similarly to the other years since 2007. The spring bloom's spatiotemporal coverage in 2012 was close to the mean, but the phytoplankton summer bloom was among the smallest (Raudsepp et al., 2018). The latter is consistent with a minimum of the interannual oscillations of cyanobacterial blooms with a period of about 3 years in the Baltic Sea (Kahru et al., 2018). TN and TP pools were in a stable level of about 6000 ktons and 680 ktons, respectively since 2005, as well as DIN and DIP pools of about 1000 ktons and 480 ktons, respectively (Savchuk, 2018). In general this is consistent with the period of stable nutrient input, within otherwise decreasing trend since 1980 (Savchuk, 2018).

3.1. STEAM model description

The STEAM (Jalkanen et al., 2009, 2012; Johansson et al., 2013, 2017) uses Automatic Identification System (AIS) data to describe ship traffic

activity and the detailed technical knowledge of the ships for the calculation of the atmospheric emissions and discharges directly from the ships to the sea. In this work, new capabilities were built into STEAM, which enabled the description of various discharges, like Black Water (BW), Grey Water (GW), Ballast Water (BLW), Bilge Water (BLG), Food Waste (FW), Scrubber water from open and closed loop systems (SWO, SWC), Stern Tube Oil (STO) and several species of antifouling paints (AFP) from ships. These developments of STEAM are described in a separate manuscript (Jalkanen et al., *in preparation*). BW is defined as sewage, wastewater that originates from toilets, medical facilities, premises for living animals or other wastewaters when mixed with those drainages (MARPOL Annex IV). GW is collected from dishwater, shower, laundry, bath and wash-basin drains, and its discharges are not limited by the international law (MARPOL Annex V). BLG is a mixture of different substances from machinery, spills and overflow tanks and gets accumulated in the lowest part of the ship (Klein Wolterink et al., 2004; IMO, 2006). FW generated on-board can be any 'spoiled or unspoiled' foods and food scraps (MARPOL Annex V). GW, BW and FW are functions of people carried onboard, both crew passengers.

Vessel activity for year 2012 was described with AIS data sent by the Baltic Sea fleet and provided to us by the Helsinki Commission (HELCOM), which consists of all Baltic Sea countries. This data consists of over 320 million automatic position reports. In addition, technical description of the fleet was based on data from IHS (IHS Global, 2016). Passenger capacity utilization was modelled based on the quarterly reports of major passenger vessel operators, who together carry over 20 million passengers each year. Based on these reports, passenger capacity utilization was estimated as 50% throughout the year, except for cruise vessels, which have been reported to use close to 90% of their capacity (HELCOM, 2015; Wilewska-Bien et al., 2018). The time spent on-board was separately estimated for the crew and passengers based on AIS data. This resulted to estimates of the discharge amounts. The spatio-temporal releases of accumulated quantities were modelled as defined by the MARPOL convention Annexes I, IV and V, which define what, where and how discharges can be released to the sea. Some of the releases occur randomly, like GW, BW and BLG, which were modelled as continuous discharges in areas defined by current MARPOL rules and national environmental legislation if they are stricter than MARPOL (like oily releases in Finnish waters and SWO discharges in German waters).

The atmospheric emissions were delivered as input for the chemical transport model CMAQ, which was used to calculate the atmospheric transformation and transport of pollutants. The STEAM outputs consisting of gridded daily inventories of nutrients in BW, GW and BLG as well as total volumes of discharges were used as input data for the GETM-ERGOM.

3.2. CMAQ model description

The CMAQ model used for calculation of the deposition fields (Byun and Schere, 2006; Appel et al., 2013, 2017) is an atmospheric Eulerian chemistry transport model. It computes atmospheric concentrations and deposition of numerous trace gas species and aerosol components, depending on emissions and the physical state of the atmosphere. CMAQ was developed by the US EPA about 20 years ago (Byun and Ching, 1999). It is freely available through the CMAS center and permanently updated. In the SHEBA project, the model was run in version 5.0.1.

The model was set up in three nested domains, a grid with $64 \times 64 \text{ km}^2$ for entire Europe, $16 \times 16 \text{ km}^2$ for northwestern Europe and $4 \times 4 \text{ km}^2$ over the Baltic Sea. In the vertical, the model extends up to 100 hPa in a sigma hybrid pressure coordinate system with 30 layers. Twenty of these layers are below approximately 2 km; the lowest layer extends to ca. 36 m above ground. The entire year 2012 was run with a spin-up period of one month for the initialization of the model runs. Meteorological fields were calculated with the COSMO-CLM

model (Rockel et al., 2008) and interpolated to the CMAQ grid with an adapted version of the Meteorology-Chemistry Interface Processor (MCIP) (Otte and Pleim, 2010).

3.3. GETM description

The GETM is a numerical hydrodynamics model which is solving sea state by means of salinity, temperature, currents and water level (Burchard and Bolding, 2002). The modular concept of GETM makes it possible to use various parameterizations and numerical techniques to solve numerically three-dimensional primitive ocean equations. The time split technique allows using shorter timestep for solving free-surface evolution in barotropic mode and longer timestep for internal baroclinic mode solving transports. Spatially the equations are discretized on a staggered Arakawa-C grid using spherical horizontal coordinates and bottom-following adaptive layers discretization in vertical direction. The vertical resolution has been enhanced by reducing layer thicknesses near the boundaries and in the vertical ranges where stratification is strong. Such adaptive coordinate system produces less numerical mixing compare to general sigma-coordinate discretization (Gräwe et al., 2015). The horizontal advection has been solved using third-order TVD scheme with P2-PDM limiter. Directional splitting technique has been applied according to Pietrzak (1998). To minimize known pressure gradient errors internal pressure has been solved using z-interpolation method according to (Scheepetkin and McWilliams, 2003). The vertical subgrid turbulence is solved using k- ϵ model using algebraic turbulence closure for momentum equations has been applied via General Ocean Turbulence Model (GOTM, Umlauf and Burchard, 2005). Background vertical diffusivity has been set to $10^{-6} \text{ m}^2/\text{s}$. Horizontal viscosity coefficient has been set to $10 \text{ m}^2 \text{ s}^{-1}$ according to Wallcraft et al. (2005) considerations. Air-ocean momentum and heat fluxes were calculated using Kondo (1975) bulk parameterizations.

The model domain covers the whole Baltic Sea with closed boundary in the Kattegat. The bathymetry has been derived from the Baltic Sea Digital Database (BSBD 0.9.3) and interpolated on a 1 nautical mile grid, which is the horizontal resolution of the model. In vertical direction 40 bottom-following and adaptive layers have been defined, ensuring <5 m vertical resolution in halocline and near the surface. The timestep for the biogeochemical processes is set to baroclinic timestep, which was 500 s.

3.4. ERGOM description

ERGOM (Neumann, 2000, 2002) is an extended version of the N-based NPZD model taking into account processes like N-fixation, phosphorus limitation, denitrification and phosphorus binding into iron compounds. 12 state variables are used which describe the N cycle in molar N units. The inorganic nutrients, which are consumed by primary producers, are defined as dissolved nitrate, ammonium and phosphate. Primary producers are divided into three functional phytoplankton groups: diatoms, flagellates and N-fixing cyanobacteria. Chlorophyll-a (chl-a): is the sum of all three functional groups of algae and detritus. Nitrogen in phytoplankton and detritus (mol N/kg) is converted into molar carbon-content according to the Redfield ratio (Redfield, 1934). Grazing of phytoplankton is described as the growth of zooplankton. Phyto- and zooplankton are transformed into dead organic matter, which sinks and contributes to the sediment pool as detritus. Under oxic conditions part of the detritus is remineralized back to dissolved nutrients; this process uses oxygen and has a temperature-dependent rate. Under anoxic conditions denitrification reduces nitrate to molecular nitrogen, which leaves the system. If nitrate is depleted under anoxic conditions, detritus is oxidized with sulfate and generates dihydrogen sulfur gas, which is considered as negative oxygen. Under oxic conditions reactive phosphates are bound into iron-phosphates, which sink out of the water-column and accumulate in the sediment layer. In case

of anoxia with the presence of sulfuric acid, iron-oxide gets reduced and phosphates are released back to the system as nutrients available to the primary producers. A fraction of these iron-phosphate complexes is also assumed to be buried permanently, depending on the sediment thickness and sedimentation rate (Neumann and Schernewski, 2008). More detailed descriptions of the ERGOM model are available in Neumann (2000); Neumann et al. (2002); Neumann and Schernewski (2008); Radtke et al. (2012) and Lessin et al. (2014a).

The initial conditions for salinity and temperature have been taken from a hindcast simulation of Maljutenko and Raudsepp (2014) to avoid a long spin-up period and instabilities, which occur during cold starts. Stable density fields from December 2000 were chosen based on similar measured salinity values and stratification conditions in the Gotland Deep in 2012. A short spin-up period of one month was applied to adjust the model with new atmospheric forcing and river inflows. Initial nutrient pools have been adopted from climatic average fields for January from the 40 year long hindcast ERGOM simulation for the Baltic Sea (Köuts et al., 2019). The oxygen profile measured in 2011 December at the Gotland Deep has been assimilated to the initial field of oxygen for the whole Baltic Proper domain to adjust the extent of the anoxic area for the year 2012. The open boundary conditions have been closed to neglect the nutrient fluxes from the North Sea and therefore to study the Baltic Sea as a closed system. This assumption affects the biogeochemistry in the Kattegat and southwestern Baltic but as we deal with one year and one year simulation repeated for five years, we assume the impact to be minor in the context of the entire Baltic Sea.

3.5. Coupled GETM-ERGOM justification

Placke et al. (2018) have compared main hydrographic and circulation fields of the long-term model simulation results performed by GETM, MOM and RCO circulation models in the Baltic Sea. Their assessment remains without general conclusion that all considered fields are reproduced better by one of the model than by the others. Therefore, we do not have solid justification of using one particular circulation model in our study. Although, Gräwe et al. (2015) have argued that the adaptive vertical coordinate system (Burchard and Beckers, 2004; Hofmeister et al., 2010) implemented in GETM has an advantage in comparison to fixed vertical coordinate system implemented in MOM and RCO by having less numerical mixing due to a better resolution of a strong vertical stratification. Our argument of using GETM is that we have successfully validated the model for long-term simulation period of 1996–2006 (Maljutenko and Raudsepp, 2014).

Comprehensive comparison of the Ecological Regional Ocean Model (ERGOM) (www.ergom.net; Neumann and Schernewski, 2008) coupled to the physical Modular Ocean Model (MOM 3.1) (e.g. Pacanowski and Griffies, 2000), the Swedish Coastal and Ocean Biogeochemical (SCOBI) model (Eilola et al., 2009; Almroth-Rosell et al., 2011) coupled to the Rossby Centre Ocean (RCO) circulation model (RCO-SCOBI) and the Baltic sea Long-Term large-Scale Eutrophication Model (BALTSEM) (Gustafsson, 2003) long-term simulation results of nutrient and oxygen dynamics in the Baltic Sea show no advantage of any model (Eilola et al., 2011). The ERGOM and SCOBI models are relatively similar in terms of the set of state variables used and key biogeochemical processes implemented in the models (e.g. Eilola et al., 2011).

The SCOBI model has been mainly used in the coupling with RCO model for climate change studies (e.g. Meier et al., 2018) and recently coupled with NEMO (Raudsepp et al., 2019b). The MOM-ERGOM coupled model system has been widely used for the biogeochemical studies of the Baltic Sea (e.g. Neumann et al., 2017). A coupled GETM-ERGOM model has been used for different studies of the biogeochemistry of the Baltic Sea in multi-year simulations (Lessin et al., 2014a, 2014b) and in particularly for investigating the ship impact to marine biogeochemistry (Raudsepp et al., 2013). Besides, the model system of the 3D ocean circulation Hiromb-BOOS model (HBM) coupled with

the biogeochemical ERGOM model (Maar et al., 2011, 2014; Wan et al., 2012) has been used for studying nutrient loads impact to primary production in the western Baltic Sea (Maar et al., 2016) and for evaluation of atmospheric nitrogen inputs including ship-borne nitrogen to marine ecosystems (Neumann et al., 2018a, 2018b, 2018c).

3.6. Meteorological forcing

Meteorological fields to drive the CMAQ and GETM-ERGOM system were calculated with COSMO CLM version 5.0 (Geyer, 2014). COSMO was driven with ERA-Interim reanalysis fields using the spectral nudging technique to force the model to stay close to the reanalysis. The runs were performed on a $0.11^\circ \times 0.11^\circ$ rotated lat/lon grid with 40 vertical layers up to approx. 20 km altitude. A nested model run on a $0.025^\circ \times 0.025^\circ$ grid with 50 vertical layers was applied to the Baltic Sea region and then interpolated on a $4 \times 4 \text{ km}^2$ grid with a modified version of the MCIP (Otte and Pleim, 2010). We have applied hourly atmospheric forcing for the GETM-ERGOM model system.

3.7. Input of nutrients

Nutrient input from the 36 largest rivers has been derived from the European hydrology model (E-HYPE) hindcast simulation of Donnelly et al. (2015). The diffuse inputs of adjacent regions along the coast have been added to the nearest rivers. Since only total nitrogen (TN) was available from hindcast simulations, we used fractions of 0.70 and 0.05 for nitrate and ammonium, respectively. The remaining fraction of 0.25 from TN contributes to the organic nitrogen pool as detritus input. The input of phosphates and organic phosphorus was assumed 0.25 and 0.75 fraction of the total phosphorus, respectively. The used fractions were inferred from numerous studies on nutrient loads to the Baltic Sea (e.g. Stålnacke et al., 1999; Vahtera et al., 2007; Savchuk et al., 2012).

Nutrient input from shipping to the Baltic Sea has been considered from two main sources: atmospheric depositions and discharge from shipping. The emission of NO_x to the atmosphere from shipping has been taken from hourly emission dataset of STEAM simulation covering the full calendar year of 2012. In STEAM, each vessel is considered as unique case considering vessel specific ship activity and technical description. Daily emissions of NO_x, SO_x, CO, Elementary Carbon (EC), Organic Carbon (OC), SO₄ and Ash were generated as emission grids, which were used as input for atmospheric modelling.

Emissions for all other anthropogenic sources except shipping are based on EMEP emission data for the year 2012. They include NO_x, NH₃, SO₂, CO, NMVOCs and PM₁₀. Biogenic emissions were calculated with BEIS 3.4 (Schwede et al., 2005; Vukovich and Pierce, 2002). Sea salt emissions followed the parametrization of Gong (2003), but excluding surf zone emissions because of overestimation of the emission flux in some regions (Neumann et al., 2016). All emissions were temporally and spatially disaggregated and distributed to the CMAQ model's grids with the SMOKE for Europe emission model (Bieser et al., 2011a). The vertical distribution of the emissions from certain sectors followed the standard profiles given in Bieser et al. (2011b).

Atmospheric deposition of NO_x species into the sea have been considered from the following wet and dry depositions of: particulate NO₃ (PM_NO₃), nitrogen trioxide (NO₃), nitrogen dioxide (NO₂), nitric oxide (NO), nitric acid (HNO₃), nitrous acid (HONO), nitrogen pentoxide (N₂O₅), peroxyacetyl nitrate (PAN), oxidized peroxyacetyl nitrate (OPAN) and peroxyacetic acid (HNO₄). Particulate ammonium (PM_NH₄) and ammonia (NH₃) contribute to reduced nitrogen deposition. The atmospheric phosphorus deposition has been considered as 3.5% of mineral ash deposition calculated in CMAQ. The hourly atmospheric depositions from a $4 \times 4 \text{ km}^2$ atmospheric deposition grid have been interpolated on the $2 \times 2 \text{ km}^2$ shipping discharge grid used for the direct nutrient inputs.

Discharge of nutrients from BW, GW, FW, SWO and SWC have been calculated from the discharge volumes and concentrations in wastewaters (Wilewska-Bien et al., 2018; Jalkanen et al., *in preparation*, Wilewska-Bien et al., 2016, Jönsson et al., 2005, McLaughlin et al., 2014, Furstenberg et al., 2009, Hufnagl et al., 2005, Wartsila, 2010*Ops. comm.*). The organic nitrogen is considered as dead organic matter input and is recycled to dissolved nutrients in the water by bacteria. The actual numbers of different inputs are given in Table 1.

3.8. GETM-ERGOM validation

GETM-ERGOM system validation is performed for the year 2012. We have calculate model and data bias and root mean square error (RMSE) for basic state variables as water temperature, salinity, nitrate, phosphate, oxygen and chlorophyll *a* (Chl-*a*) at the station BY15 of the Gotland Basin. Surface layer temperature is significant abiotic variable that controls the seasonal cycle of the biogeochemical processes and is well reproduced by the model (Fig. 2a, Bias = -0.5 °C, RMSE = 0.8 °C). Bottom temperature (Fig. 2a, Bias = -0.3 °C, RMSE = 0.4 °C) and bottom salinity (Fig. 2b, Bias = 0.7 g/kg, RMSE = 0.7 g/kg) do not vary significantly in time, as their dynamics is mainly related to the Major Baltic Inflows which are absent in 2012 (Raudsepp et al., 2018). Surface salinity (Fig. 2b, Bias = 0.5 g/kg, RMSE = 0.5 g/kg) as well as entire vertical temperature (Fig. 2d) and salinity (Fig. 2e) profiles are well reproduced except that halocline is about 10-m deeper in the model than in the measurements. The latter affects vertical distribution of nitrate (Fig. 2f), phosphate (Fig. 2g) and oxygen (Fig. 2h). Seasonal variations of nitrate (Bias = 1.1 mmol N/m³, RMSE = 1.5 mmol N/m³), phosphate (Bias = -0.1 mmol P/m³, RMSE = 0.2 mmol P/m³) and chl-*a* (Bias = -0.9 mg/m³, RMSE = 1.0 mg/m³) in the surface layer are depicted in Fig. 2c. Their basic seasonal cycle is well reproduced by the model - nutrients concentrations are high in spring before the spring bloom of diatoms, depleted in summer and start to increase in autumn; spring diatom bloom and summer cyanobacteria bloom are present in the model results. Deficiencies of the model are that phosphate concentration is underestimated in spring and spring bloom is delayed in time (Fig. 2c). Large model errors in the nitrate concentration between the depth of 60 and 150 m (Fig. 2f) and in the phosphate concentration from 60 m depth to the bottom (Fig. 2g) originate from the errors in the model initial fields (not shown) indicated by the variability of the model profiles of corresponding variables.

The GETM-ERGOM system consists a number of nonlinear related equations and calibration parameters. To perform mathematically correct uncertainty estimations and model sensitivity analyses is complex task on its own. Besides of the uncertainties of the GETM-ERGOM system, we have uncertainties related to the STEAM model and their treatment of emission and discharge of each particular ship, uncertainties related to COSMO CLM and CMAQ model; uncertainties due to river load of nutrients and uncertainties related to the GETM-ERGOM setup. The provided list of potential sources of uncertainties is far from being complete. In the present application of the GETM-ERGOM we rely on the wide use of this model system for similar research (Schernewski and Neumann, 2005; Neumann and Schernewski, 2008; Radtke et al., 2012; Lessin et al., 2014a; Lessin et al., 2014b; Neumann et al., 2018a,

2018b, 2018c; Kõuts et al., 2019). Therefore, we have kept the set of calibration parameters similar to the previous studies and rely on the validation results of the model. The strong argument for the reliability of the model results and conclusion drawn from the study is that we have performed two identical model simulation, i.e. with and without input of the ship-borne nutrients. Mainly, differences of the spatio-temporal distribution of the biogeochemical variables and their fluxes are analysed, not the absolute values. The calculated RMSE values are considered as proxies for the uncertainties of state variables.

The choice of biogeochemical model parameters and systems dynamics is sensitive to the physical model parameters and external forcing (Burchard et al., 2006; Miladinova and Stips, 2010).

4. Results

4.1. Sources of nutrients from shipping

Annual input of nitrate is two orders of magnitude larger than the input of other nutrient compounds (Fig. 3a). Nitrate deposition consists of atmospheric deposition and direct discharges to the water. Atmospheric deposition of nitrate prevails over the direct discharge, which results in continuous distribution over the Baltic Sea. There is a southwest gradient of the nitrate input distribution due to increase of shipping intensity towards the southern Baltic Sea and Danish Sounds (Sime, 2014) and due to prevailing atmospheric circulation. Prevalent winds are from W/SW, so the area receives shipping emissions from the North Sea as well.

N-NH₄ input also combines atmospheric deposition and ship discharge (Fig. 3b). High input from discharges is observed on the shipping lanes, while more continuous spatial map of the atmospheric input is negative. The negative values increase towards the southwestern Baltic according to the increase of shipping activity. Discharge of N-NH₄ from ships, which originates mainly from BW, are compensated by reduced atmospheric deposition of N-NH₄ in the SHIP case compared to the NOSHIP case along the main shipping routes. Input remains positive on the routes of passenger ferries in the Gulf of Finland and northern Baltic Proper. Same holds for the southwestern Baltic and the Danish Sounds, although reduced deposition of ammonium in the SHIP case compared to the NOSHIP case is high there.

P-PO₄, which enters the sea via direct discharge, has a distribution pattern with elevated concentrations directly on the shipping lanes, where the input takes place (Fig. 3c).

Discharge of organic compounds of nitrogen and phosphorus takes place in the shipping lanes (Fig. 3c,d). BW, GW and FW are discharged to the sea in shipping lanes, but only allowed outside of 12 Nm from the coast. Only not comminuted or disinfected discharges were taken into account because at the time of modelling regulations did not require nutrient reduction in wastewater. The untreated wastewater was modelled beyond 12 Nm from coastline and when ships were en route moving at 4 knots. The wastewater generated within the 12 Nm boundary is collected onboard the ships and released outside the 12 Nm zone with a determined rate. Parameters like kinetics, mixing or transport (advection) were not included in the modelling. In the case of cargo ships, it results in point-discharge at the start of the shipping lanes outside of the 12 Nm coastal zone. The much larger volumes released from passenger ferries are assumed to be continuous, which results in a line discharge. The discharge rates for different type of ships are included in the modelling runs.

4.2. Time series of marine environment response to ship deposition compared to natural processes

The Gotland Basin was selected to study the immediate effect of shipborne nutrient input on the biogeochemistry of the Baltic Sea. Time series of main biogeochemical parameters were selected from the BY15 monitoring station (Fig. 1), which is a HELCOM monitoring

Table 1

Annual total excess nutrient input (SHIP minus NOSHIP), nutrient input in the form of direct discharge from the ships and percentage of contribution from different sources to direct discharge.

Nutrients	Annual nutrient input Inputs (t)	Share of shipping emissions						
		Total (t)	BW (%)	GW (%)	FW (%)	SWO (%)	SWC (%)	BLG (%)
N-NO ₃	20,260.00	14.27	–	63.59	–	1.92	34.49	–
N-NH ₄	–664.20	518.99	94.60	3.52	1.87	0.01	–	–
N-Det	239.20	258.65	33.58	36.40	28.90	–	–	1.12
P-PO ₄	57.50	60.54	62.17	33.09	4.69	0.05	–	–

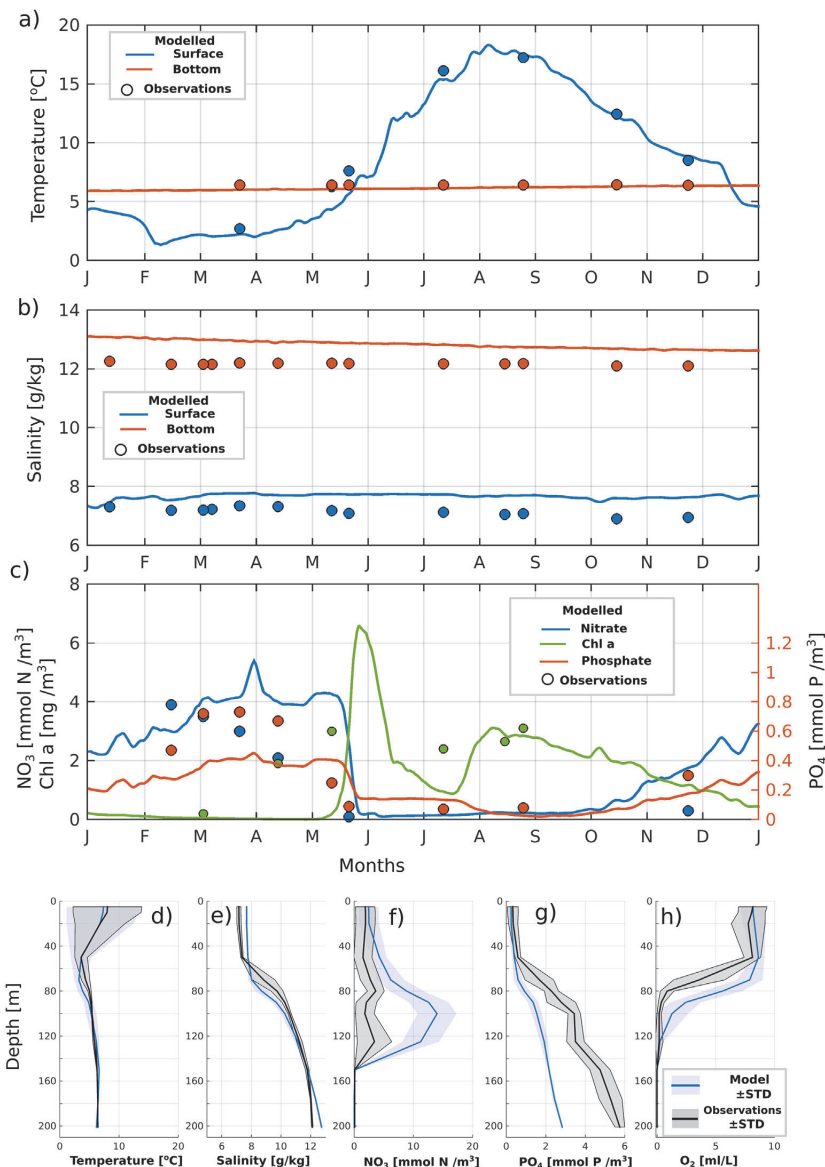


Fig. 2. Timeseries of bottom and surface temperature a) and salinity b) at Gotland station. Timeseries of surface nitrate, Chl a and phosphate is shown on c). Vertical mean profiles and the range of ± 1 STD variability (as shaded area) of d) temperature, e) salinity, f) nitrate, g) phosphorus and h) oxygen at Gotland station. Observations from HELCOM database are shown as black line and modelled profiles as blue line.

station since 1978. BY15 is located in the middle of the Eastern Gotland Basin close to the main shipping lines (Fig. 1). BY15 as a deep station (250 m) represents deep-layer biogeochemical processes, which are detrimental in steering the eutrophication process in the Baltic Sea. A major part of the research on the influence of MBIs on hydrophysical and biogeochemical conditions in the Baltic Sea are based on the measurements there (e.g. Savchuk, 2018; Mohrholz, 2018). It is also considered as a representative area of spring and summer blooms - with medium to high chl-a concentrations (Kahru et al., 2007; Zhang et al., 2018).

Nitrate, phosphate, phytoplankton and zooplankton variations undergo the commonly known annual cycle in the Baltic Sea without visible differences between the SHIP and NOSHIP simulations. In order to estimate the impact of the SHIP scenario on the Baltic Sea ecosystem we calculated the relative changes of the main biogeochemical variables as (SHIP-NOSHIP)/SHIP.

Nitrate and phosphate concentration increases on the surface until April–May and go into steep decline mid-May (Fig. 4a,b). This coincides with the diatom bloom, which peaks at the end of June when nitrate becomes depleted (Fig. 4c). Simultaneously to the steep decline of nitrate

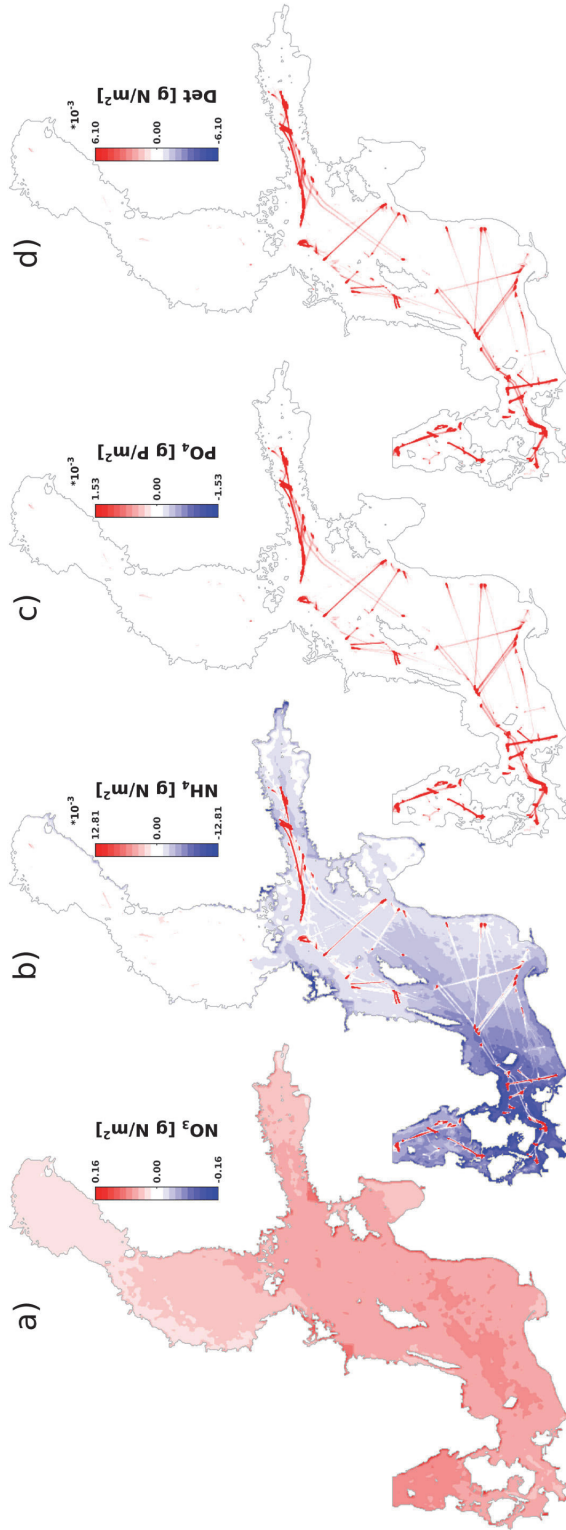


Fig. 3. Spatial distribution of annual shipping related inputs of a) nitrate, b) ammonium, c) organic nitrogen, and d) phosphorus.

and phosphate at the end of May, shipping-derived relative changes in nitrate and phosphate become apparent: more nitrate (max. +10%) and less phosphate (max. -3%) is available on the surface, in SHIP case compared to NOSHIP case (Fig. 4a,b). This lasts from June till the end of July/beginning of August. Relative changes of nitrate and phosphate are then reversed, starting at the end of August, with less than average surface nitrate being available from August to the second half of September and more phosphate from the beginning of August to the end of September. Relative increase (max. +5%) of diatoms is evident mostly after their bloom, whereas flagellates experience a relative increase (+12–13%) before their bloom peak (Fig. 4c,d). Cyanobacteria go through a relative decrease (-10%) from June to October and coincides with the relative shipping-related increase of diatoms and flagellates (Fig. 4e). Zooplankton experiences very little relative change due

to shipping, with a slight increase (+1%) during their bloom in end of May/June and decrease (-4%) from August to October (Fig. 4f), slightly shifted from the cyanobacteria bloom peak (Fig. 4e).

Snapshots of vertical profile of the biogeochemical variables at station BY15 show that the surface layer is representative of the entire upper mixed layer and shipping-related impact does not go below the pycnocline, except for oxygen (Fig. 5). While nutrient concentrations are determined by the depth of the mixed layer (around 75 m) (Fig. 5a,b,c), phytoplankton and zooplankton depend on the euphotic zone in the upper 30 m (Fig. e,f,g,h). Changes in dissolved oxygen are most pronounced at the transition depth from hypoxic to anoxic conditions (concentration of dissolved oxygen between 1 and 2 ml l⁻¹), which is at 150 m depth at the BY15 station (Fig. 5d). Relative changes are most severe where oxygen values are close to zero initially. Absolute decrease in oxygen results in an increase of the anoxic bottom area by 50 km² at the end of the year compared to the total anoxic area of 40,000 km² in NOSHIP scenario.

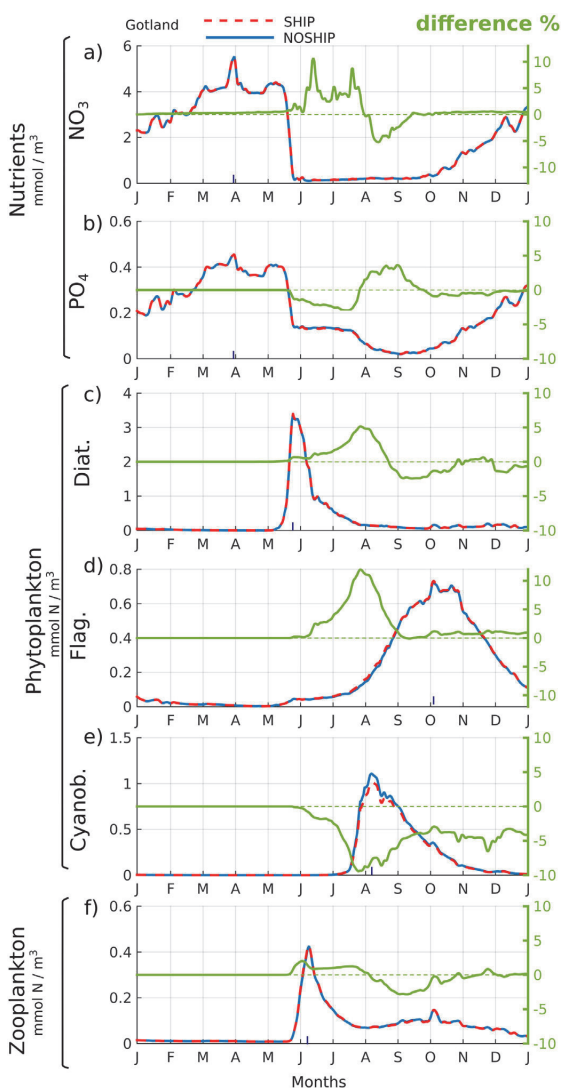


Fig. 4. Time-series of concentrations at the surface layer of the Gotland Deep for the SHIP and the NOSHIP scenario regarding a) nitrate, b) phosphorus, c) diatom, d) flagellate, e) cyanobacteria, and f) zooplankton. Relative difference between the SHIP and the NOSHIP scenario is shown as green line.

4.3. Spatial distribution to complement time series

The exact location of the shipping lanes does not have a substantial effect on the spatial distribution of the surface excess nitrate (Figs. 1, 6a) as NO_x is mainly emitted to the air, where it undergoes atmospheric chemistry transformation and redistribution due to atmospheric circulation. This means that the spatial pattern of atmospheric deposition of nitrate is strongly dispersed compared to the concentrated discharge pattern of e.g. phosphate (Fig. 3c).

Deposited atmospheric nitrate is redistributed in the marine environment due to currents and mixing, so there is no resemblance of excess nitrate (Fig. 6a) to the deposition pattern (Fig. 3a). The Bothnian Bay has the lowest excess nitrate in the surface layer, which corresponds to the low nitrate input in the area. The rest of the Baltic coastal areas have higher surface concentrations of excess nitrate than the open sea areas. This pattern of redistribution is explained by shallower water column near the coast where the water depth is smaller than the mixing depth. For instance, in the case of equal deposition of nitrate to the deep and shallow area relative to mixing depth, the nitrate is equally mixed over the surface mixed layer in the deep area, but equally mixed over the entire water column in the shallow area. As the layer thickness is bigger in the first case than in the second case, the concentration of nitrate is lower in the first case than in the second case. The excess nitrate has highest concentrations on the eastern coast of the Baltic.

The mean distribution of excess phosphate in the water has a fragmented pattern (Fig. 6b). The area of high excess phosphate is clearly seen in the northeastern Baltic Proper due to the continuous line discharge from passenger ships. The other region of elevated excess phosphate concentration is in the southern Baltic around the Danish Sounds, also explained by very heavy ship traffic which is concentrated in a relatively small sea area.

The elevated excess diatom concentrations correspond to the excess nitrate, most notably in the Estonian Archipelago Sea (Fig. 6a,c). Elevated concentrations are also evident in the northern Baltic Proper and the northern part of the Gulf of Finland, in the central part of the Gulf of Bothnia, on the Polish coast and in the Kattegat. No excess diatoms are seen in the phosphorus limited areas, e.g. southern and eastern Gulf of Riga, and the eastern coastal area of the Baltic Proper.

The distribution of excess flagellates, which bloom at the end of summer and in autumn, mostly concentrates into Kattegat and less intensively in the Northern Baltic Proper - Gulf of Finland area (Fig. 6d), which slightly reflects the pattern of excess phosphorus on the surface. The spatial extent of cyanobacteria blooms is reduced in vast areas in the Baltic Proper, the Gulf of Finland and several coastal areas (Fig. 6e). The areas with little to no change in cyanobacteria blooms overlap with the areas with phosphorus limitation - e.g. Bothnian Bay and big river estuaries.

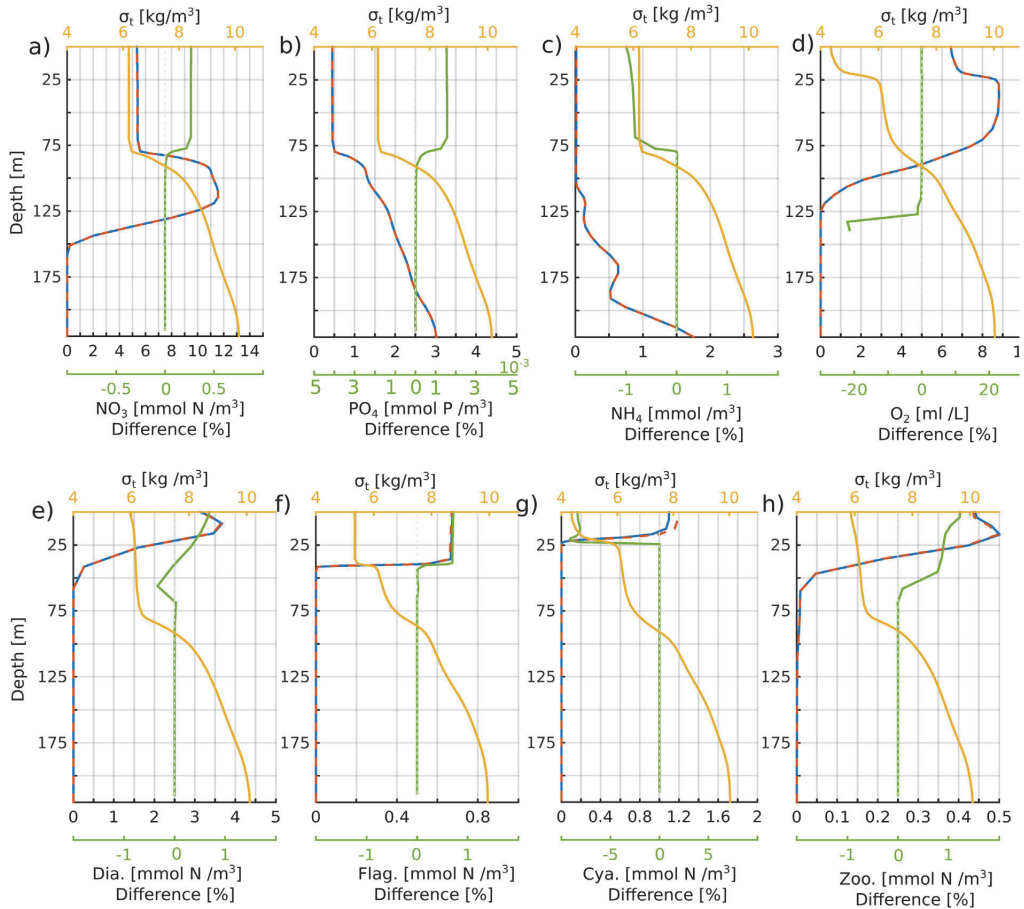


Fig. 5. Vertical profiles of modelled a) nitrate, b) phosphorus, c) ammonium, d) oxygen, e) flagellate, e) cyanobacteria and f) zooplankton concentrations at the Gotland station from SHIP (blue line) and NOSHIP (red dashed line) scenario. The time instances for correspond to peak concentrations in the surface layer (Fig. 3). The time instance for the oxygen profile d) corresponds to cyanobacteria bloom peak. Relative difference between the SHIP and the NOSHIP scenario is shown as green line. Potential density (σ_t) is shown as yellow line.

Deposition of organic matter into the sediment was calculated during two periods: intense phytoplankton bloom period May–June and decomposition period in October–December (Fig. 6f,g). Maximum excess sedimentation in the period of May–June is heaviest in the southern Baltic (south of Gotland), the West-Estonian archipelago, Gulf of Finland and the Aland Sea. The Gulf of Bothnia, the southern part of the Gulf of Riga and areas on the eastern coast of the Baltic Proper are less affected by excess organic matter. The distribution of surplus sediments is spread uniformly over the Baltic Proper and the Gulf of Finland by water circulation. Organic matter accumulation in May–July is spatially more extensive and contains more organic matter due to primary production than in October–December when sediments are already being remineralized and the flux from the surface is declining. In autumn organic matter mostly accumulates in the medium deep and deep areas in the central part of the basins. The period from October to December reflects a more long-term distribution of sediments, shaped by transport. Another distinctive feature of the sediment distributions from both periods (Fig. 6f, g) is the small-scale spatial heterogeneity. This is related to the small-scale topographic irregularities that hinder smooth horizontal transport and favor sedimentation on the slopes of topographic shoals.

The pattern of organic matter accumulation in the two periods is in most parts similar to oxygen distribution, with decreased oxygen areas overlapping with high organic material accumulation spots (Fig. 6h,i). Summer bottom oxygen reduction is mostly seen in shallow, coastal areas in the Archipelago Sea in Estonia, as well as the coasts of southern Finland and Sweden. Large areas are affected by ship-induced oxygen decline west of Bornholm island and in the Danish Straits, where marine traffic is also intensive. Central deep and mostly anoxic areas of the Baltic Proper are not affected by ship-induced oxygen decline. Winter oxygen conditions show a different pattern with minimum concentrations in the areas of medium depth, i.e. 60 m depth. The shallower sea areas are well ventilated by wind and thermal mixing and are not affected. The most severe impact is seen in the Kattegat, southern Baltic, Bornholm Basin, Stolpe Channel and Gdansk Basin (Fig. 6h, i). Winter oxygen conditions reflect the accumulation impact of shipborne nutrients and represent oxygen conditions that remain poor after dead organic matter has decomposed. Longitudinally, the reduction of bottom oxygen is stronger along the eastern bottom slope than along the western slope of the Baltic Proper due to the prevailing cyclonic circulation (Omstedt et al., 2014).

5. Discussion

This study is based on one year of ship traffic data, the corresponding emissions and discharges and the atmospheric and marine conditions of the year 2012. The intensity of ship traffic can vary annually (HELCOM, 2010) and the same holds for atmospheric and marine conditions, which influence the actual deposition of nutrients to the sea and their spreading. A study by Raudsepp et al. (2013) for repeated ship deposition in changing hydrodynamic conditions in the Gulf of Finland

shows interannual variations of different biogeochemical variables in the range of 50%. The ship routes do not change from year to year, hence the general pattern of direct nutrient discharge from ships remains unchanged, which means that main discharge areas are southwestern and northeastern Baltic Proper. Nitrogen discharge is two orders of magnitude lower than atmospheric deposition of nitrogen. Atmospheric nitrogen deposition could be inter-annually more variable in terms of the spatial distribution. However, as the results show a rather smooth and only slightly varying spatial nitrogen deposition pattern,

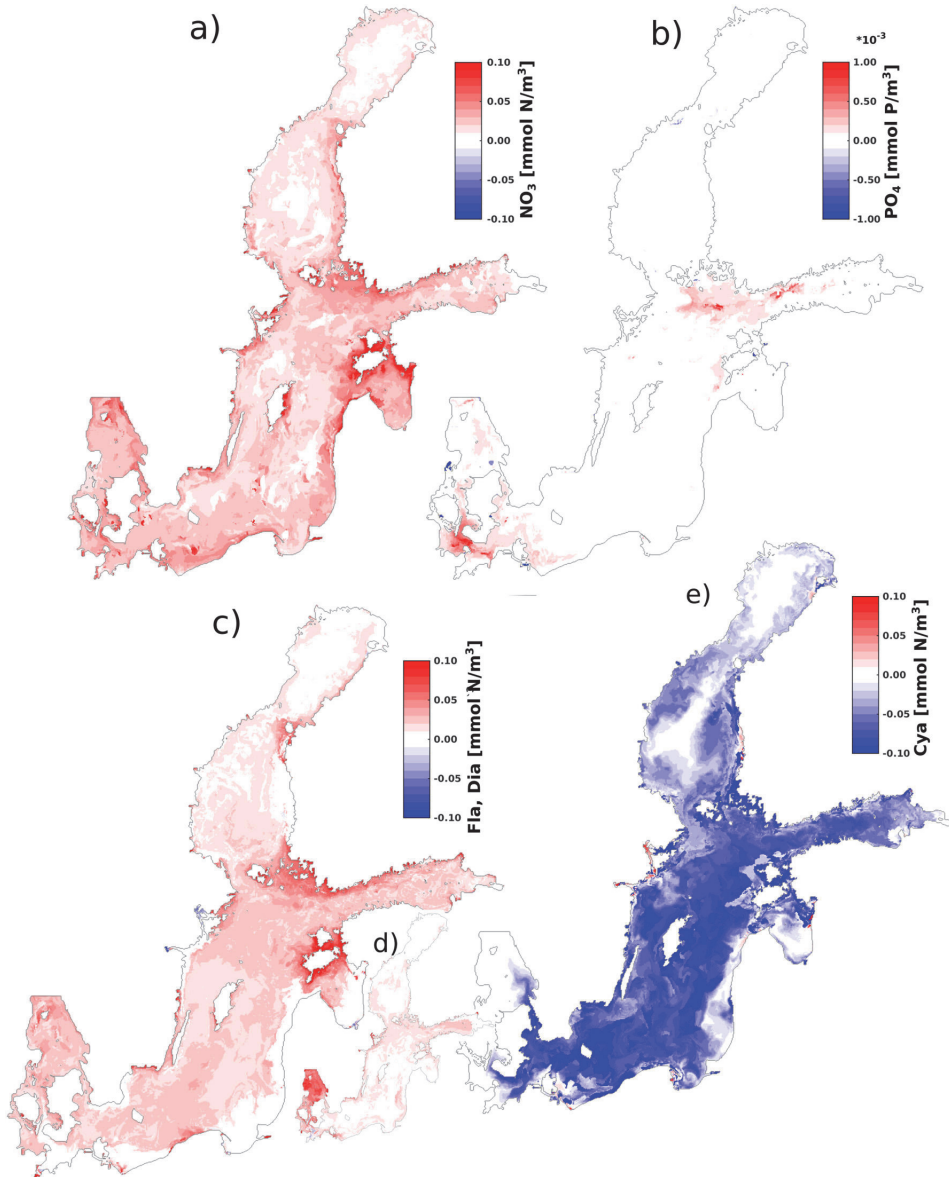


Fig. 6. Spatial distributions of variable differences between the SHIP and the NOSHIP scenario. The difference in surface concentrations at the time of their maxima in the NOSHIP scenario during the period from February to June, for a) nitrate, and b) phosphorus. The difference of c) diatoms, and d) flagellates, during the time of the peak bloom in spring for the NOSHIP scenario. e) Difference of summer bloom (cyanobacteria) during the peak bloom for the NOSHIP scenario. Distribution of the maximum difference of the nitrogen in sediments f) after the spring bloom from May to July, and g) after the bioactive period from October to December. The distribution of maximum differences between the SHIP and the NOSHIP scenario for the near-bottom oxygen concentrations during the summer months from h) July to September, and i) for the period after the bioactive season from October to December.

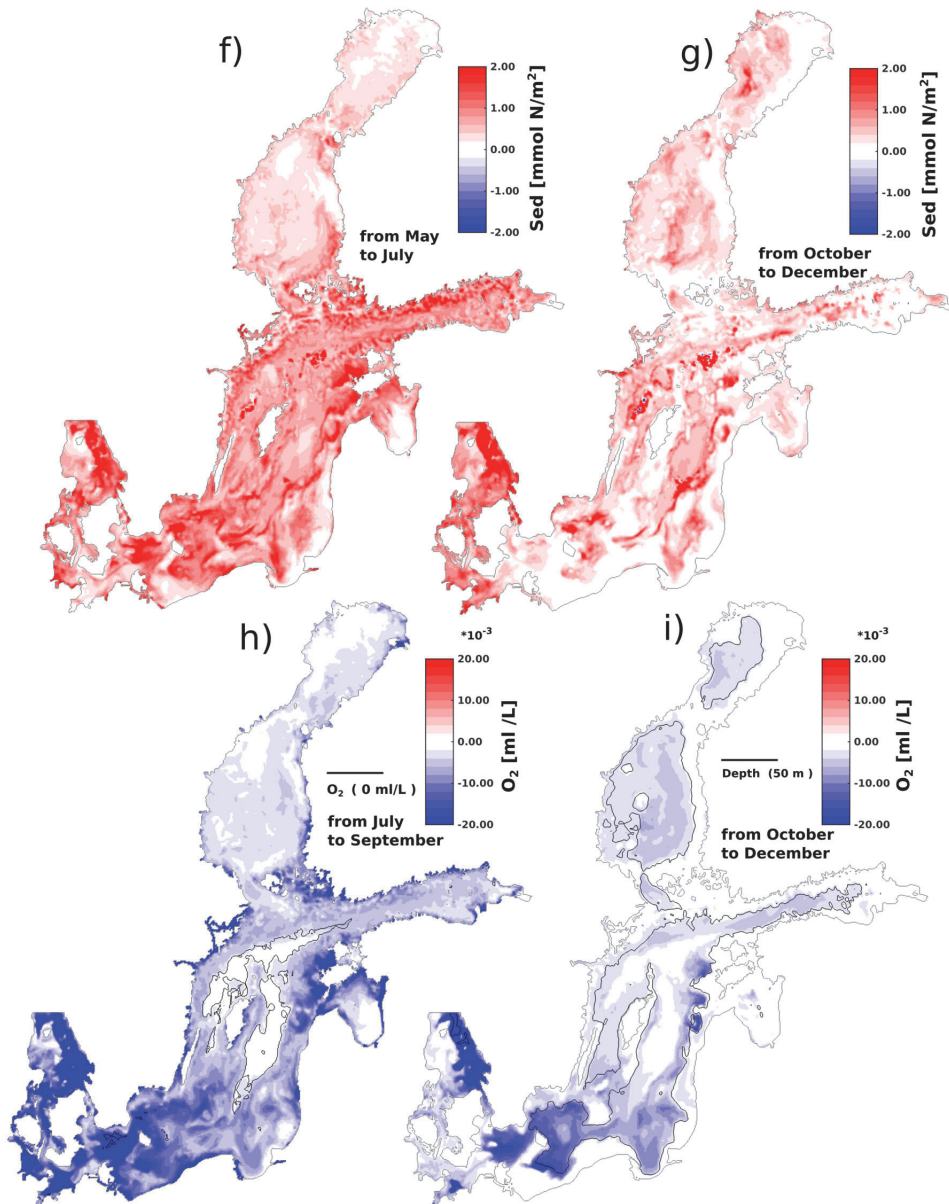


Fig. 6 (continued).

we expect that atmospheric circulation will redistribute NO_x emitted to air rather homogeneously in the other years, as well. The spatial distribution of excess nitrate, phosphate and organic matter from shipping discharge is more heterogeneous than atmospheric deposition of nitrate. The circulation can vary a lot in the Baltic Sea from year to year (Lehmann et al., 2002; Meier and Kauker, 2003; Väli et al., 2013), so the areas of high and low nitrate concentration can vary accordingly between years.

Diatoms and flagellates benefit from the ship-borne nutrients which reflects in the increase of their biomass. The spatial distribution of

excess diatoms and flagellates might depend on the competition for the nitrogen between two groups. Nutrients play an important role in the structure of phytoplankton communities, which can be explained by varying nutrient-acquiring abilities of different species (Lomas and Glibert, 2000). However, it must be taken into consideration that it is difficult to determine exactly how important nutrients are, as there are also many other factors at play (which we do not look at in this study) regarding the competition between diatoms and dinoflagellates - e.g. other nutrients (silica), light conditions, water stratification, ice conditions and specific characteristics of the species, e.g. mixotrophy,

which gives a competitive advantage in some nutrient enrichment situations (Lagus et al., 2004; Granéli et al., 1990; Lomas and Glibert, 2000; Spilling et al., 2014).

Cyanobacteria biomass is reduced the most in the areas with usually strong cyanobacteria blooms, which include southern and central Baltic and the western part of the Gulf of Finland (Kahru et al., 1994, 2007; Kahru and Elmgren, 2014). This result is in accordance with previous studies on the effect of additional nitrogen on cyanobacteria blooms (Elmgren and Larsson, 2001). The areas with little to no change in cyanobacteria blooms overlap with the areas with phosphorus limitation - e.g. Bothnian Bay and big river estuaries (Kõuts et al., 2019). Excess detritus distribution and corresponding oxygen reduction reflect the pattern of excess diatom distribution and possibly water circulation in summer. The same is generally true for autumn except that shallow areas are well ventilated then. Deep areas in the central and northern Baltic Proper are unaffected as they are anoxic already (Fig. 6h).

The biogeochemical cycle in the Baltic Sea is defined by nitrogen being mostly the limiting nutrient. This is due to the system's ability to remove the added biologically available nitrogen through the microbial conversion back to N_2 gas via denitrification, which each year removes nitrogen corresponding to most of the input (Voss et al., 2005; Radtke et al., 2012). This takes place in the sediments as well as in oxygen-deficient deep waters and becomes more effective when oxygen-deficiency is widespread (Voss et al., 2005; Radtke et al., 2012). Therefore, any changes in nitrogen input affect the Baltic Sea ecosystem functioning.

To assess the impact of shipping-related excess nitrogen on the biogeochemical processes in the Baltic Sea we subtract fluxes of nitrogen from two model simulations, i.e. SHIP minus NOSHIP, like we did for the biogeochemical variables. The nitrogen balance in the marine system takes into account nitrogen content in the sea, both in water and sediments, nitrate and ammonium flux from the atmosphere and rivers, nitrogen brought to the system by nitrogen fixation and outflow of nitrogen to the air in the form of molecular nitrogen, i.e. the result of denitrification. River fluxes of nitrogen are the same in both cases giving zero contribution to excess nitrogen.

The results show that since the beginning of January until the end of March, shipborne nitrogen input exists in the form of nitrate in the water column (Fig. 7a). When the spring bloom starts, not all nitrogen load into the water remains there, i.e. total nitrogen in the ecosystems becomes lower than the shipborne nitrogen input. Total nitrogen in the marine system consists of nitrate in the water as the main contributor, nitrogen bound in phytoplankton, dissolved molecular nitrogen and nitrogen in detritus in the water and sediments. The difference of the input and the total nitrogen in the marine system increases slowly until mid-July.

The pool of dissolved inorganic nitrogen decreases due to the spring bloom of diatoms in May. Diatom biomass remains on an elevated level after bloom peak, compared to NOSHIP scenario, due to additional nitrates in the surface layer (Fig. 3a,c). With a short delay, the pool of nitrogen bound to detritus grows as phytoplankton starts to decay. Decomposition of organic matter leads to an increase of the ammonium pool, but as ammonium is rapidly oxidized to nitrate and molecular nitrogen, the concentration of ammonium-bound nitrogen remains low. Until mid-July when cyanobacteria start blooming, the content of inorganic nitrogen stays stable in the water, as well as nitrogen bound to diatoms, while nitrogen content in the sediments increases. In July the share of nitrogen in phytoplankton increases slowly due to the uptake of nitrogen by increasing flagellates. In principle, the nitrogen fluxes during that period could be described as concurrent uptake of inorganic nitrogen by phytoplankton, their death (formation of detritus) and decomposition of organic nitrogen into NH_4 as a short-lived compound, and finally transformation into molecular nitrogen and dissolved inorganic nitrogen again via denitrification.

The Baltic Sea as a nitrogen-limited ecosystem gives an advantage to the phosphorus-limited nitrogen fixing cyanobacteria (Granéli et al.,

1990). Hence, additional nitrogen input due to shipping results in lower cyanobacteria biomass and an overall decrease of total excess nitrogen in the marine system. The decline in cyanobacteria biomass results in a decrease of the amount of dead organic matter and detritus-bound nitrogen as well as a negative contribution to molecular nitrogen. The share of nitrogen in the other functional groups of phytoplankton and inorganic nitrogen in the water is also declining, but less strongly compared to cyanobacteria. Since the end of August until November, the amount of inorganic nitrogen in the water is stable, the negative contribution of cyanobacteria is decreasing, nitrogen in phytoplankton and in detritus varies slowly around stable content, mostly due to the flagellate bloom, but total nitrogen starts to increase slowly. Roughly since November primary production ceases, concentration of inorganic nitrogen increases due to shipborne input, nitrogen in phytoplankton decreases to zero, and nitrogen in detritus gains stable positive level. By the end of the year shipborne nitrogen consists mainly of inorganic nitrogen in the form of nitrate in the water and organic nitrogen in the form of detritus in the water and in the sediments. Smaller amount of dead organic matter results in lower denitrification in the NOSHIP case compared to the SHIP case and negative excess gaseous nitrogen.

Considering all the fluxes as explained above, the 5-year nitrogen balance is depicted in Fig. 5b. The difference in the atmospheric fluxes consists of shipping related deposition of nitrate and ammonium. Nitrogen fixing is lower with SHIP scenario due to smaller amount of cyanobacteria in the system and has negative excess flux. Also, denitrification is higher in the SHIP case due to the internal dynamics of the marine system and the excess flux is negative, which means that more nitrogen is removed from the system in the case of SHIP scenario. The difference in the nitrogen input to the sea and excess nitrogen is more than twofold after one year of shipping activity (Fig. 5a). When we extend our simulation to a five-year period, repeating the same annual ship input and hydrophysical conditions, we obtain that the total annual amount of nitrate, i.e. sum of nitrate in the water and nitrogen in detritus approaches a steady state. The ship input of excess nitrogen is largely compensated by decreasing nitrogen fixation and increasing nitrogen removal due to denitrification compared to the NOSHIP case.

The phosphorus content shows a decrease of the phosphate in the water column, i.e. excess phosphate is negative, but an increase of the phosphorus pool in the sediments (Fig. 5c). The phosphorus input to the Baltic is mainly eliminated by binding them in the sediments. In the Baltic Proper, where much of the sediment is oxygen-deficient, sediments are an inefficient sink, indicating that phosphorus, that is already in the system, is eliminated very slowly (Savchuk and Wulff, 2009). Continuous decomposition of organic material results in higher oxygen consumption and a negative trend of the oxygen content which decelerates in time (Fig. 5d).

In absolute values, an annual nitrogen input of 20 kt from shipping, is comparable with the nitrogen input of a big river of the Baltic, e.g. the Neva river (Stålnacke et al., 1999). Hence, it could also be assumed that ship-nutrient reductions have a similar response in the ecosystem as the reduction of nutrients in rivers, which has been more thoroughly studied in the Baltic Sea. River nutrient reduction has an effect on the ecosystem - nitrogen and phosphorus inventories decrease, but it usually takes more than two years to be significant according to simulations (Neumann et al., 2002) and even longer in natural systems, depending on their complexity (Duarte et al., 2009; Schindler, 2012). Also, a compensatory mechanism often contributes in relation to the N/P ratio - cyanobacteria concentrations are known to increase after nutrient reductions (Higgins et al., 2017).

Coastal ecosystems are complex and respond differently when nutrient input is decreased, as the response trajectories are rather complex. Duarte et al. (2009) has stated that coastal ecosystems seldom return to a previous, oligotrophic level, but rather remain on a new, medium level. In general an oligotrophication process starts when nutrients are reduced - phytoplankton biomass will decrease and so will the oxygen deficient zones, until a new steady state is achieved. Well-known

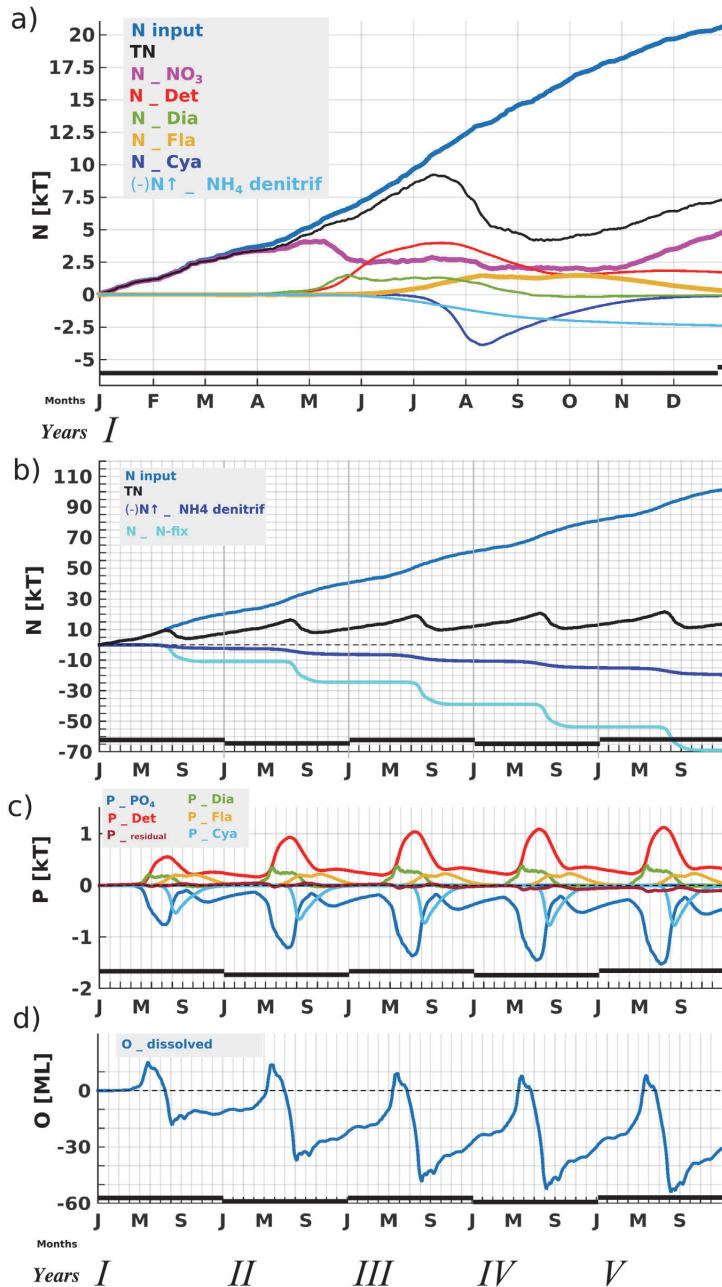


Fig. 7. a) Annual time-series of excess nitrogen pools for the first simulation year. Five-year time-series of b) nitrogen balance between input and total nitrogen pool in the water, c) phosphorus budget, and d) oxygen content.

examples of ecosystems improving to a certain level are the Black Sea shelf area and Chesapeake bay (Kideys, 2002; Langmead et al., 2009; Lefcheck et al., 2018), where dissolved oxygen conditions have improved and phytoplankton blooms have slightly decreased with nutrient reduction and ecological communities have benefitted from that. Several studies suggest that decreasing inputs of nitrogen will not hasten recovery from eutrophication (in lakes) and may even hinder it by

favoring nitrogen fixers or stimulating internal loading of phosphorus. Instead repeated adding of additional nitrogen could suppress cyanobacteria blooms and in the long-term reduce nitrogen import to the system (Schindler, 2012), which was also seen in our study. Similar relative contribution of shipborne dissolved inorganic and particulate organic nitrogen has been estimated for the southern Baltic Sea by Neumann et al. (2018c). Raudsepp et al. (2013) have shown annual

decrease of nitrogen fixation due to ship nitrogen deposition by 2–6% in the Gulf of Finland. Other previous studies have estimated relative ship contribution to be around 10% for different nitrogen compounds into the Baltic Sea (Tsyro and Berge, 1998; Bartnicki and Fagerli, 2008; Bartnicki et al., 2011; HELCOM, 2005).

6. Conclusions

The shipping contributes about 0.3% of the total phosphorus and 1.25–3.3% of the total nitrogen input to the Baltic Sea. The amount of nitrogen directly discharged to the sea from the ships is about two orders of magnitude smaller than atmospheric input of excess nitrogen (SHIP minus NOSHIP). Excess ammonium deposition is negative.

Spatially, the Gulf of Bothnia has almost negligible deposition and discharge of nutrients due to shipping, while the North-Eastern and South-Western Baltic Sea and the Kattegat area are the most impacted. Relative impact of shipborne nutrients on the biogeochemical variables in the surface layer does not exceed 10% locally, but this is already four to eight times larger than the share of the ships in total nitrogen input to the Baltic Sea. Diatoms and flagellates have a marked increase in spatial distribution while the reduction of the spatial extent of cyanobacteria blooms is extensive and covers vast areas in the Baltic Proper as well as the Gulf of Finland and several coastal areas. The relative reduction of cyanobacteria concentration of 10% due to shipping is significant during their blooming period, whereas other phytoplankton functional groups experience notable relative changes during their low concentration period in summer. Some of the additional organic matter produced with the added nitrogen sinks to the bottom, where its decomposition consumes oxygen and increases the areas of oxygen-deficient bottoms by 50 km² in the deep area of the central Baltic Proper within one year of model simulation. This increase in anoxic bottom area decelerates in time.

In general, the nitrogen balance showed that shipborne nitrogen input does not result in equal increase of total excess nitrogen in the water system. In the mostly nitrogen-limited Baltic Sea ecosystem, the excess nitrate is consumed by diatoms and flagellates. The increase of diatoms and flagellates biomass leaves less phosphate in the water for the cyanobacteria that occur later in summer. Their biomass decreases, which results in less atmospheric nitrogen being fixed and brought to the marine environment. Besides, denitrification is higher due to the internal dynamics of the marine system, the excess flux is negative, which means that more nitrogen is removed from the system. Multi-year continuous input of ship-borne nitrogen does not accumulate in the marine environment, but total nitrogen reaches a stationary state. The excess phosphate in the water column is negative, but phosphorus pool in the sediments increases steadily.

In summary, nutrient input from shipping does not have a significant effect on the Baltic Sea ecosystem in terms of the ecosystem functioning as changes remain within 10%. Still, shipping accounts as an important nutrient source in the context of the Baltic Sea, and is comparable in size to a large river.

Acknowledgement

This work resulted from the BONUS SHEBA project and it was supported by BONUS (Art 185), funded jointly by the European Union, the Academy of Finland, Estonian Research Council, Swedish Agency for Marine and Water Management, Swedish Environmental Protection Agency, Forschungszentrum Jülich Beteiligungsgesellschaft mbH (Germany) and FORMAS. We are also grateful to the HELCOM member states for allowing the use of HELCOM AIS data in this research. This study was partly supported by institutional research funding IUT 19-6 from the Estonian Ministry of Education and Research. We are grateful to GETM, FABM and ERGOM community for the code development and maintenance. An allocation of computing time from the High Performance Computing cluster

at the TalTech is gratefully acknowledged. We would like to thank the three anonymous reviewers for their suggestions and comments.

References

- Achberger, C., Mühr, B., Ehmann, C., Bissolli, P., Parker, D., Kennedy, J., 2013. Nordic and Baltic countries [in "state of the climate in 2012"]. Bull. Am. Meteorol. Soc. 94 (8), S121–S123. <https://doi.org/10.1175/2013BAMSStateoftheClimate.1>.
- Aksoyoglu, S., Baltensperger, U., Prévôt, A.S.H., 2016. Contribution of ship emissions to the concentration and deposition of air pollutants in Europe. Atmos. Chem. Phys. 16, 1895–1906. <https://doi.org/10.5194/acp-16-1895-2016>.
- Almroth-Rosell, E., Eilola, K., Hordoir, R., Meier, H.E.M., Hall, P.O.J., 2011. Transport of fresh and resuspended particulate organic matter in the Baltic Sea – a model study. J. Mar. Syst. 87, 1–12. <https://doi.org/10.1016/j.jmarsys.2011.02.005>.
- Appel, K.W., Poulriot, G.A., Simon, H., Sarwar, G., Pye, H.O.T., Napelenok, S.L., Akhtar, F., Roselle, S.J., 2013. Evaluation of dust and trace metal estimates from the Community Multiscale Air Quality (CMAQ) model version 5.0. Geosci. Model Dev. 6, 883–899. <https://doi.org/10.5194/gmd-6-883-2013>.
- Appel, K.W., Napelenok, S., Foley, K., Pye, H., Hogrefe, C., Luecken, D., Bash, J., Roselle, S., Pleim, J., Foroutan, H., Hutzell, B., Poulriot, G., Sarwar, G., Fahey, K., Gantt, B., Gilliam, R.C., Heath, N., Kang, D., Mathur, R., Schwede, D., Spero, T., Wong, D.C., Young, J., 2017. Description and evaluation of the Community Multiscale Air Quality (CMAQ) modeling system version 5.1. Geosci. Model Dev. 10, 1703–1732. <https://doi.org/10.5194/gmd-10-1703-2017>.
- Aulinger, A., Matthias, V., Zeretzke, M., Bieser, J., Quante, M., Backes, A., 2016. The impact of shipping emissions on air pollution in the greater North Sea region – part 1: current emissions and concentrations. Atmos. Chem. Phys. 16, 739–758. <https://doi.org/10.5194/acp-16-739-2016>.
- BACCI Author Team, 2015. Second Assessment of Climate Change for the Baltic Sea Basin. Regional Climate Studies. Berlin: Heidelberg: Springer Verlag, 6, 131–144.
- Bartnicki, J., Fagerli, H., 2008. Airborne load of nitrogen to European seas. Ecol. Chem. Eng. S. 15, 297–313.
- Bartnicki, J., Semeena, V.S., Fagerli, H., 2011. Atmospheric deposition of nitrogen to the Baltic Sea in the period 1995–2006. Atmos. Chem. Phys. 11, 10057–10069. <https://doi.org/10.5194/acp-11-10057-2011>.
- Bieser, J., Aulinger, A., Matthias, V., Quante, M., Bultjes, P., 2011a. SMOKE for Europe – adaptation, modification and evaluation of a comprehensive emission model for Europe. Geosci. Model Dev. 4, 47–68. <https://doi.org/10.5194/gmd-4-47-2011>.
- Bieser, J., Aulinger, A., Matthias, V., Quante, M., Denier van der Gon, H.A.C., 2011b. Vertical emission profiles for Europe based on plume rise calculations. Environ. Pollut. 159, 2935–2946. <https://doi.org/10.1016/j.envpol.2011.04.030>.
- Bruggeman, J., Bolding, K., 2014. A general framework for aquatic biogeochemical models. Environ. Model Softw. 61, 249–265. <https://doi.org/10.1016/j.envsoft.2014.04.002>.
- BSBD 0.9.3, Baltic Sea Hydrographic Commission, 2013. Baltic Sea Bathymetry Database Version 0.9.3. Downloaded from <http://data.bshc.pro/> on 2013.11.05.
- Burchard, H., Beckers, J.-M., 2004. Non-uniform adaptive vertical grids in one-dimensional numerical ocean models. Ocean Model. 6, 51–81. [https://doi.org/10.1016/S1463-5003\(02\)00060-4](https://doi.org/10.1016/S1463-5003(02)00060-4).
- Burchard, H., Bolding, K., 2002. GETM – A General Estuarine Transport Model. Scientific Documentation. Technical Report, EUR 20253 9n.
- Burchard, H., Bolding, K., Kühn, W., Meister, A., Neumann, T., Umlauf, L., 2006. Description of a flexible and extendable physical–biogeochemical model system for the water column. J. Mar. Syst. 61, 180–211. <https://doi.org/10.1016/j.jmarsys.2005.04.011>.
- Byun, D., Ching, J., 1999. Science Algorithms of the EPA Models-3 Community Multiscale Air Quality Modeling System. EPA/600/r-99/030. US Environmental Protection Agency, Office of Research and Development, Washington DC.
- Byun, D., Schere, K., 2006. Review of the governing equations, computational algorithms, and other components of the Models-3 Community Multiscale Air Quality (CMAQ) modeling system. Appl. Mech. Rev. 59, 51–77.
- Chen, D., Tian, X., Lang, J., Zhou, Y., Li, Y., Guo, X., Wang, W., Liu, B., 2019. The impact of ship emissions on PM_{2.5} and the deposition of nitrogen and sulfur in Yangtze River Delta, China. Sci. Total Environ. 649, 1609–1619. <https://doi.org/10.1016/j.scitotenv.2018.08.313>.
- Chislock, M.F., Doster, E., Zitomer, R.A., Wilson, A.E., 2013. Eutrophication: causes, consequences, and controls in aquatic ecosystems. Nature Education Knowledge 4 (4), 10.
- Chubarenko, I., Stepanova, N., 2018. Cold intermediate layer of the Baltic Sea: hypothesis of the formation of its core. Prog. Oceanogr. 167, 1–10. <https://doi.org/10.1016/j.pcean.2018.06.012>.
- Conley, D.J., Humborg, C., Rahm, L., Savchuk, O.P., Wulff, F., 2002. Hypoxia in the Baltic Sea and Basin-scale changes in phosphorus biogeochemistry. Environ. Sci. Technol. 36, 5315–5320. <https://doi.org/10.1021/es025763w>.
- Corbett, J.J., Fischbeck, P., 1997. Emissions from ships. Science 278 (5339), 823–824. <https://doi.org/10.1126/science.278.5339.823>.
- Corbett, J.J., Köhler, H.W., 2003. Updated emissions from ocean shipping. Journal of Geophysical Research: Atmospheres 108, 4650. <https://doi.org/10.1029/2003JD003751>.
- Djambazov, G., Pericleous, K., 2015. Modelled atmospheric contribution to nitrogen eutrophication in the English Channel and the southern North Sea. Atmos. Environ. 102, 191–199. <https://doi.org/10.1016/j.atmosenv.2014.11.071>.
- Donnelly, C., Andersson, J.C.M., Arheimer, B., 2015. Using flow signatures and catchment similarities to evaluate the E-HYPE multi-basin model across Europe. Hydrological Sciences Journal, 61, No. 2, 255–273. <https://doi.org/10.1080/02626667.2015.1027710>.
- Duarte, C.M., Conley, D.J., Carstensen, J., Sánchez-Camacho, M., 2009. Return to Neverland: shifting baselines affect eutrophication restoration targets. Estuar. Coasts 32, 29–36. <https://doi.org/10.1007/s12237-008-9111-2>.

- Eilola, K., Meier, H.E.M., Almqvist, E., 2009. On the dynamics of oxygen, phosphorus and cyanobacteria in the Baltic Sea; a model study. *J. Mar. Syst.* 75, 163–184. <https://doi.org/10.1016/j.jmarsys.2008.08.009>.
- Eilola, K., Gustafsson, B.G., Kuznetsov, I., Meier, H.E.M., Neumann, T., Savchuk, O.P., 2011. Evaluation of biogeochemical cycles in an ensemble of three state-of-the-art numerical models of the Baltic Sea. *J. Mar. Syst.* 88, 267–284. <https://doi.org/10.1016/j.jmarsys.2011.05.004>.
- Elmgren, R., 1989. Man's impact on the ecosystem of the Baltic Sea: energy flows today and at the turn of the century. *Ambio*, 18, 326–332.
- Elmgren, R., Larsson, U., 2001. Nitrogen and the Baltic Sea: managing nitrogen in relation to phosphorus. *The Scientific World*, 1 (S2), 371–377. <https://doi.org/10.1100/tsw.2001.291>.
- Eyring, V., Köhler, H. W., van Aardenne, J., Lauer, A., 2005. Emissions from international shipping: 1. The last 50 years. *Journal of Geophysical Research: Atmospheres*, vol. 110, D17305. doi:<https://doi.org/10.1029/2004JD005619>
- Furstenberg, S., Mohn, H., Sverdrup, T., 2009. Study on Discharge Factors for Legal Operational Discharges to Sea From Vessels in Norwegian Waters. Det Norske Veritas, Høevik.
- Geyer, B., 2014. High-resolution atmospheric reconstruction for Europe 1948–2012: coastDat2. *Earth System Science Data* 6, 147–164. <https://doi.org/10.5194/essd-6-147-2014>.
- Gong, S.L., 2003. A parameterization of sea-salt aerosol source function for sub- and super-micron particles. *Glob. Biogeochem. Cycles* 17, 1097. <https://doi.org/10.1029/2003GB002079>.
- Gong, W., Beagle, S.R., Cousineau, S., Sassi, M., Munoz-Alpizar, R., Ménard, S., Racine, J., Zhang, J., Chen, J., Morrison, H., Sharma, S., Huang, L., Bellavance, P., Ly, J., Izdebski, P., Lyons, L., Holt, R., 2018. Assessing the impact of shipping emissions on air pollution in the Canadian Arctic and northern regions: current and future modelled scenarios. *Atmos. Chem. Phys.* 18, 16653–16687. <https://doi.org/10.5194/acp-18-16653-2018>.
- Granéli, E., Wallström, K., Larsson, U., Granéli, W., Elmgren, R., 1990. Nutrient limitation of primary production in the Baltic Sea area. *Ambio*, 19, 142–151.
- Granskog, M.A., Vihma, T., Pirazzini, R., Cheng, B., 2006. Superimposed ice formation and surface energy fluxes on sea ice during the spring melt-freeze period in the Baltic Sea. *J. Glaciol.* 52 (176), 119–127.
- Gräve, U., Holtermann, P., Klingbeil, K., Burchard, H., 2015. Advantages of vertically adaptive coordinates in numerical models of stratified shelf seas. *Ocean Model.* 92, 56–68. <https://doi.org/10.1016/j.ocemod.2015.05.008>.
- Gustafsson, B.G., 2003. A Time-dependent Coupled-basin Model of the Baltic Sea. C47. Earth Sciences Centre. Göteborg University, Göteborg, p. 61 <https://doi.org/10.2307/1352831>.
- Hagy, J.D., Boynton, W.R., Keefe, C.W., Wood, K.V., 2004. Hypoxia in Chesapeake Bay, 1950–2001: long-term change in relation to nutrient loading and river flow. *Estuaries* 27 (4), 634–658. <https://doi.org/10.1007/BF02907650>.
- Hansson, D., Eriksson, C., Omstedt, A., Chen, D., 2011. Reconstruction of river runoff to the Baltic Sea, AD 1500–1995. *Int. J. Climatol.* 31 (5), 696–703. <https://doi.org/10.1002/joc.2097>.
- Hecky, R.E., Kilham, P., 1988. Nutrient limitation of phytoplankton in freshwater and marine environments: a review of recent evidence on the effects of enrichment. *Limnology and Oceanography*, 33 (4, p 2), 196–822. doi:<https://doi.org/10.4319/lo.1988.33.4part2.0796>.
- HELCOM, 2005. Airborne nitrogen loads to the Baltic Sea. Tech. rep., Helsinki Commission, Baltic Marine Environment Protection Commission. <http://www.helcom.fi/Lists/Publications/AirbornenitrogenloadstotheBalticSea.pdf>.
- HELCOM, 2010. Maritime Activities in the Baltic Sea – an integrated thematic assessment on maritime activities and response to pollution at sea in the Baltic Sea Region. *Baltic Sea Environment Proceedings* No. 123.
- HELCOM, 2013a. Approaches and methods for eutrophication target setting in the Baltic Sea region. *Baltic Sea Environment Proceedings* No. 133.
- HELCOM, 2013b. Review of the Fifth Baltic Sea Pollution Load Compilation for the 2013 HELCOM Ministerial Meeting, Baltic Sea Environment Proceedings No. 141. <http://www.helcom.fi/Lists/Publications/BSEP141.pdf>
- HELCOM, 2014. Report on shipping accidents in the Baltic Sea area during 2013. <http://www.helcom.fi/Lists/Publications/Annual%20report%20on%20shipping%20accidents%20in%20the%20Baltic%20Sea%20area%20during%202013.pdf>
- HELCOM, 2015. HELCOM Baltic Sea Sewage Port Reception Facilities: Overview 2014. 2nd ed. Baltic Marine Environment Protection Commission, Helsinki <http://www.helcom.fi/Lists/Publications/Baltic%20Sea%20Sewage%20Port%20Reception%20Facilities.%20HELCOM%20Overview%202014.pdf>.
- HELCOM, 2018a. Input of nutrients by the seven biggest rivers in the Baltic Sea region. *Baltic Sea Environment Proceedings* No. 161.
- HELCOM, 2018b. HELCOM Thematic Assessment of Eutrophication 2011–2016.
- Herz, M., Davis, J., 2002. Cruise control A Report on How Cruise Ships Affect the Marine Environment. On behalf of The Ocean Conservancy.
- Higgins, S.N., Paterson, M.J., Hecky, R.E., Schindler, D.W., Jason, J.V., Findlay, D.L., 2017. Biological nitrogen fixation prevents the response of a eutrophic lake to reduced loading of nitrogen: evidence from a 46-year whole-lake experiment. *Ecosystems* 21 (6), 1088–1100. <https://doi.org/10.1007/s10021-017-0204-2>.
- Hofmeister, R., Burchard, H., Beckers, J.-M., 2010. Non-uniform adaptive vertical grids for 3d numerical ocean models. *Ocean Model.* 33, 70–86.
- Hordoir, R., Meier, H.E.M., 2012. Effect of climate change on the thermal stratification of the Baltic Sea: a sensitivity experiment. *Clim. Dyn.* 38, 1703–1713. <https://doi.org/10.1007/s00382-011-1036-y>.
- Hufnagel, M., Liebezeit, G., Behrends, B., 2005. Effects of Sea Water Scrubbing. Final Report. Retrieved from Martin's Marine Engineering Page -. <http://www.dieseldirect.net>.
- IHS Global: SeaWeb Database of the Global Ship Fleet, 2016.
- International Maritime Organization, 2006. MARPOL Consolidation 2006: Annex I-Regulations for the Prevention of Pollution by Oil. [Online] Available at: http://www.marpoltraining.com/MMSKOREAN/MARPOL/Annex_I/index.htm
- International Maritime Organization, MARPOL Annex IV, Regulation 1, 1978 Annex IV of the 1978 Protocol Relating to the 1973 International Convention for the Prevention of Pollution From Ships: Regulations for the Prevention of Pollution by Sewage From Ships (Revised Version as of 2011). In: IMO, London, 17 February 1978.
- International Maritime Organization, 2011. Resolution MEPC.201(62). Revised MARPOL Annex V, Regulations on the Prevention of Pollution by Garbage From Ships. London: International Maritime Organization, 15 July 2011.
- International Maritime Organization, 2012. Resolution MEPC.219(63)2012. Guidelines for the Implementation of MARPOL Annex V. London: International Maritime Organization, 2 March 2012.
- ISO 8217, 2012. Petroleum Products – Fuels (Class F) – Specifications of Marine Fuels.
- Jaagus, J., Briede, A., Rimkus, E., Sepp, M., 2018. Changes in precipitation regime in the Baltic countries in 1966–2015. *Theor. Appl. Climatol.* 131, 433–443. <https://doi.org/10.1007/s00704-016-1990-8>.
- Jalkanen, J.-P., Brink, A., Kalli, J., Pettersson, H., Kukkonen, J., Stipa, T., 2009. A modelling system for the exhaust emissions of marine traffic and its application in the Baltic Sea area. *Atmos. Chem. Phys.* 9, 9209–9223. <https://doi.org/10.5194/acp-9-9209-2009>.
- Jalkanen, J.-P., Johansson, L., Brink, A., Kalli, J., Kukkonen, J., Stipa, T., 2012. Extension of an assessment model of ship traffic exhaust emissions for particulate matter and carbon monoxide. *Atmos. Chem. Phys.* 12, 2641–2659. <https://doi.org/10.5194/acp-12-2641-2012>.
- Jalkanen, J.-P., Johansson, L., Wilewska-Bien, M., Granhag, L., Ytreberg, E., Eriksson, K.M., Yngsøll, D., Hasselöv, I.-M., Magnusson, K., Raudsepp, U., Maljutenko, I., Styhre, L., Winnes, H., Moldanova, J., 2019. Modeling of Water Emissions From Baltic Sea shipping (in preparation).
- Jedrasik, J., Kowalewski, M., 2019. Mean annual and seasonal circulation patterns and long-term variability of currents in the Baltic Sea. *J. Mar. Syst.* 193 (November 2018), 1–26. <https://doi.org/10.1016/j.jmarsys.2018.12.011>.
- Johansson, L., Jalkanen, J.-P., Kalli, J., Kukkonen, J., 2013. The evolution of shipping emissions and the costs of recent and forthcoming emission regulations in the northern European emission control area. *Atmos. Chem. Phys.* 13, 11375–11389. <https://doi.org/10.5194/acp-13-11375-2013>.
- Johansson, L., Jalkanen, J.-P., Kukkonen, J., 2017. Global assessment of shipping emissions in 2015 on a high spatial and temporal resolution. *Atmos. Environ.* 167, 403–415. <https://doi.org/10.1016/j.atmosenv.2017.08.042>.
- Jonson, J.E., Jalkanen, J.-P., Johansson, L., Gauss, M., Van der Gon, H.A.C.D., 2015. Model calculations of the effects of present and future emissions of air pollutants from shipping in the Baltic Sea and the North Sea. *Atmos. Chem. Phys.* 15, 783–798. <https://doi.org/10.5194/acp-15-783-2015>.
- Jönsson, H., Baký, A., Jeppsson, U., Hellström, D., Kärrman, E., 2005. Composition of Urine, Faeces, Greywater and Biowaste for Utilisation in the UWARE Model. Urban Water, Chalmers University of Technology, Gothenburg <http://www.iea.lth.se/publications/Reports/LTH-IEA-7222.pdf>.
- Kahru, M., Elmgren, R., 2014. Multidecadal time series of satellite-detected accumulations of cyanobacteria in the Baltic Sea. *Biogeosciences* 11, 3619–3633. <https://doi.org/10.5194/bg-11-3619-2014>.
- Kahru, M., Horstmann, U., Rud, O., 1994. Satellite detection of increased cyanobacteria blooms in the Baltic Sea: natural fluctuation or ecosystem change? *Ambio*, 23, 469–472.
- Kahru, M., Savchuk, O.P., Elmgren, R., 2007. Satellite measurements of cyanobacterial bloom frequency in the Baltic Sea: interannual and spatial variability. *Mar. Ecol. Prog. Ser.* 343, 15–23. <https://doi.org/10.3354/meps06943>.
- Kahru, M., Elmgren, R., Di Lorenzo, E., Savchuk, O.P., 2018. Unexplained interannual oscillations of cyanobacterial blooms in the Baltic Sea. *Scientific Reports*, 8 <https://doi.org/10.1038/s41598-018-24829-7>.
- Karl, M., Bieser, J., Geyer, B., Matthias, V., Jalkanen, J.-P., Johansson, L., Fridell, E., 2018. Impact of a nitrogen emission control area (NECA) on the future air quality and nitrogen deposition to seawater in the Baltic Sea region. *Atmos. Chem. Phys. Discuss.* acp-2018-2017, in review. doi:<https://doi.org/10.5194/acp-2018-1107>.
- Karlson, A.M., Duberg, J., Motwani, N.H., Hogfors, H., Klawonn, I., Ploug, H., Barthel Svedén, J., Garbaras, A., Sundelin, B., Hajdu, S., Larsson, U., Elmgren, R., Gorokhova, E., 2015. Nitrogen fixation by cyanobacteria stimulates production in Baltic food webs. *Ambio*, Suppl. 3, 413–426. <https://doi.org/10.1007/s13280-015-0660-x>.
- Kideys, A.E., 2002. Fall and rise of the Black Sea ecosystem. *Science* 297 (5586), 1482–1484. <https://doi.org/10.1126/science.1073002>.
- Klein Wolterink, J.W., Hess, M., Schoof, L.A.A., Wijnen, J.W., 2004. Port reception facilities for collecting ship-generated garbage, bilge waters and oily wastes. Activity B. Optimum solutions for collecting, treatment and disposal of relevant ship-generated solid and liquid wastes. REMPEC.
- Kondo, J., 1975. Air-sea bulk transfer coefficients in diabatic conditions. *Bound.-Layer Meteorol.* 9 (1), 91–112.
- Köuts, M., Raudsepp, U., Maljutenko, I., Treimann, M.L., 2019. Eutrophication in the Gulf of Finland – oxygen and nutrient dynamics. *Journal of Marine Systems*, Submitted.
- Kronsell, J., Andersson, P., 2013. Total and regional Runoff to the Baltic Sea. HELCOM Baltic Sea Environment Fact Sheets. Online, 2019.03.15. <http://www.helcom.fi/baltic-sea-trends/environment-fact-sheets/>.
- Lagus, A., Suomela, J., Weithoff, G., Heikkilä, K., Helminen, H., Sipura, J., 2004. Species specific differences in phytoplankton responses to N and P enrichments and the N:P ratio in the Archipelago Sea, northern Baltic Sea. *J. Plankton Res.* 26 (7), 779–798. <https://doi.org/10.1093/plankt/fbh070>.
- Langmead, O., McQuatters-Gollop, A., Mee, L.D., Friedrich, J., Gilbert, A.J., Gomoïu, M.-T., Jackson, E.L., Knudsen, S., Minicheva, G., Todorova, V., 2009. Recovery or decline of the northwestern Black Sea: a societal choice revealed by socio-ecological modelling. *Ecol. Model.* 220 (21), 2927–2939. <https://doi.org/10.1016/j.ecolmodel.2008.09.011>.

- Lefcheck, J.S., Orth, R.J., Dennison, W.C., Wilcox, D.J., Murphy, R.R., Keisman, J., Gurbisz, C., Hannam, M., Landry, J.B., Moore, K.A., Patrick, C.J., Testa, J., Weller, D.E., Batiuk, R.A., 2018. Long-term nutrient reductions lead to the unprecedented recovery of a temperate coastal region. *PNAS* 115 (14), 3658–3662; published ahead of print March 5, 2018 doi:<https://doi.org/10.1073/pnas.1715798115>.
- Lehmann, A., Krauss, W., Hinrichsen, H.H., 2002. Effects of remote and local atmospheric forcing on circulation and upwelling in the Baltic Sea. *Tellus, Series A: Dynamic Meteorology and Oceanogr.* 54 (3), 299–316. <https://doi.org/10.1034/j.1600-0870.2002.00289.x>.
- Leppäranta, M., Myrberg, K., 2008. *Physical Oceanography of the Baltic Sea*. Springer, Praxis Publishing, Chichester, UK, p. 370.
- Leppäranta, M., Myrberg, K., 2009. *Physical Oceanography of the Baltic Sea*. Springer Berlin Heidelberg, Berlin, Heidelberg. <https://doi.org/10.1007/978-3-540-79703-6>.
- Lessin, G., Raudsepp, U., Maljutenko, I., Laanemets, J., Passenko, J., Jaanus, A., 2014a. Model study on present and future eutrophication and nitrogen fixation in the Gulf of Finland. *Baltic Sea. Journal of Marine Systems*, 129, 76–85. <https://doi.org/10.1016/j.jmarsys.2013.08.006>.
- Lessin, G., Raudsepp, U., Stips, A., 2014b. Modelling the influence of Major Baltic Inflows on near-bottom conditions at the entrance of the Gulf of Finland. *PLoS One* 9, e112881. <https://doi.org/10.1371/journal.pone.0112881>.
- Liblik, T., Lips, U., 2011. Characteristics and variability of the vertical thermohaline structure in the Gulf of Finland in summer. *Boreal Environ. Res.* 16, 73–83.
- Lomas, M.W., Glibert, P.M., 2000. Comparisons of nitrate uptake, storage, and reduction in marine diatoms and flagellates. *J. Phycol.* 36 (5), 903–913. <https://doi.org/10.1046/j.1529-8817.2000.99029.x>.
- Maar, M., Möller, E.F., Larsen, J., Madsen, K.S., Wan, Z.W., She, J., Jonasson, L., Neumann, T., 2011. Ecosystem modelling across a salinity gradient from the North Sea to the Baltic Sea. *Ecol. Model.* 222, 1696–1711. <https://doi.org/10.1016/j.ecolmodel.2011.03.006>.
- Maar, M., Rindorf, A., Möller, E.F., Christensen, A., Madsen, K.S., van Deurs, M., 2014. Zooplankton mortality in 3D ecosystem modelling considering variable spatial-temporal fish consumptions in the North Sea. *Prog. Oceanogr.* 124, 78–91. <https://doi.org/10.1016/j.pocean.2014.03.002>.
- Maar, M., Markager, S., Madsen, K.S., Windolf, J., Lyngsgaard, M.M., Andersen, H.E., Möller, E.F., 2016. The importance of local versus external nutrient loads for Chl a and primary production in the Western Baltic Sea. *Ecol. Model.* 320, 258–272. <https://doi.org/10.1016/j.ecolmodel.2015.09.023>.
- Maljutenko, I., Raudsepp, U., 2014. Validation of GETM model simulated long-term salinity fields in the pathway of saltwater transport in response to the Major Baltic Inflows in the Baltic Sea. 2014 IEEE/OES Baltic International Symposium (BALTIC 2014): 2014 IEEE/OES Baltic International Symposium, Tallinn, 24–27.04.2014. Institute of Electrical and Electronics Engineers (IEEE), 23–31. <https://doi.org/10.1109/BALTIC.2014.6887830>.
- Marmar, E., Dentener, F., van Aardenne, J., Cavalli, F., Vignati, E., Velchev, K., Hjorth, J., Boersma, F., Vinken, G., Mihalopoulos, N., Raes, F., 2009. What can we learn about ship emission inventories from measurements of air pollutants over the Mediterranean Sea? *Atmos. Chem. Phys.* 9, 6815–6831. <https://doi.org/10.5194/acp-9-6815-2009>.
- Matthäus, W., 1984. Climatic and seasonal variability of oceanological parameters in the Baltic Sea. *Beiträge zur Meereskunde* 51, 29–49.
- Matthias, V., 2008. The aerosol distribution in Europe derived with the Community Multiscale Air Quality (CMAQ) model: comparison to near surface in situ and sunphotometer measurements. *Atmos. Chem. Phys.* 8, 5077–5097. <https://doi.org/10.5194/acp-8-5077-2008>.
- McLaughlin, C., Falatko, D., Danesi, R., 2014. Characterizing shipboard bilge water effluent before and after treatment. *Environ. Sci. Pollut. Res.* 21, 5637–5652. <https://doi.org/10.1007/s11356-013-2443-x>.
- Meier, H.E.M., 2007. Modeling the pathways and ages of inflowing salt- and freshwater in the Baltic Sea. *Estuar. Coast. Shelf Sci.* 74 (4), 717–734. <https://doi.org/10.1016/j.ecss.2007.05.019>.
- Meier, H.E.M., Kauker, F., 2003. Modeling decadal variability of the Baltic Sea: 2. Role of freshwater inflow and large-scale atmospheric circulation for salinity. *Journal of Geophysical Research: Oceans*, 108(C11, 3368), 1–16. doi:<https://doi.org/10.1029/2003JC001799>
- Meier, H.E.M., Müller-Karulis, B., Andersson, H.C., Dieterich, C., Eilola, K., Gustafsson, B.G., Schimanke, S., 2012. Impact of climate change on ecological quality indicators and biogeochemical fluxes in the Baltic Sea: a multi-model ensemble study. *Ambio* 41 (6), 558–573. <https://doi.org/10.1007/s13280-012-0320-3>.
- Meier, H.E.M., Eilola, K., Almqvist-Rosell, E., Schimanke, S., Kniebusch, M., Höglund, A., Pemberton, P., Liu, Y., Väli, G., Saraiva, S., 2018. Disentangling the impact of nutrient load and climate changes on Baltic Sea hypoxia and eutrophication since 1850. *Climate Dynamics*, 1–22. doi:<https://doi.org/10.1007/s00382-018-4296-y> (in press).
- Miladinova, S., Stips, A., 2010. Sensitivity of oxygen dynamics in the water column of the Baltic Sea to external forcing. *Ocean Sci.* 6, 461–474. <https://doi.org/10.5194/os-6-461-2010>.
- Mohrholz, V., 2018. Major Baltic Inflow statistics – revised. *Front. Mar. Sci.* 5, 384. <https://doi.org/10.3389/fmars.2018.00384>.
- Neumann, T., 2000. Towards a 3D-ecosystem model of the Baltic Sea. *J. Mar. Syst.* 25, 405–419. [https://doi.org/10.1016/S0924-7963\(00\)00030-0](https://doi.org/10.1016/S0924-7963(00)00030-0).
- Neumann, T., Schernewski, G., 2008. Eutrophication in the Baltic Sea and shifts in nitrogen fixation analyzed with a 3D ecosystem model. *J. Mar. Syst.* 74, 592–602. <https://doi.org/10.1016/j.jmarsys.2008.05.003>.
- Neumann, T., Fennel, W., Kremp, C., 2002. Experimental simulations with an ecosystem model of the Baltic Sea: a nutrient load reduction experiment. *Glob. Biogeochem. Cycles* 16 (3), 1033. <https://doi.org/10.1029/2001GB001450>.
- Neumann, D., Matthias, V., Bieser, J., Aulinger, A., Quante, M., 2016. Sensitivity of modeled atmospheric nitrogen species and nitrogen deposition to variations in sea salt emissions in the North Sea and Baltic Sea regions. *Atmos. Chem. Phys.* 16, 2921–2942. <https://doi.org/10.5194/acp-16-2921-2016>.
- Neumann, T., Radtke, H., Seifert, T., 2017. On the importance of Major Baltic Inflows for oxygenation of the central Baltic Sea. *Journal of Geophysical Research: Oceans* 122 (2), 1090–1101. <https://doi.org/10.1002/2016JC012525>.
- Neumann, D., Friedland, R., Karl, M., Radtke, H., Matthias, V., Neumann, T., 2018a. Importance of high resolution nitrogen deposition data for biogeochemical modeling in the western Baltic Sea and the contribution of the shipping sector. *Ocean Science Discussions* <https://doi.org/10.5194/os-2018-71>.
- Neumann, D., Karl, M., Radtke, H., Neumann, T., 2018b. Evaluation of atmospheric nitrogen inputs into marine ecosystems of the North Sea and Baltic Sea—part a: validation and time scales of nutrient accumulation. *Biogeosci. Discuss.* <https://doi.org/10.5194/bg-2018-364>.
- Neumann, D., Radtke, H., Karl, M., Neumann, T., 2018c. Evaluation of atmospheric nitrogen inputs into marine ecosystems of the North Sea and Baltic Sea—part B: contribution by shipping and agricultural emissions. *Biogeosci. Discuss.* <https://doi.org/10.5194/bg-2018-365>.
- Omstedt, A., Elken, J., Lehmann, A., Leppäranta, M., Meier, H.E.M., Myrberg, K., Rutgersson, A., 2014. Progress in physical oceanography of the Baltic Sea during the 2003–2014 period. *Prog. Oceanogr.* 128, 139–171. <https://doi.org/10.1016/j.pocean.2014.08.010>.
- Otte, T.L., Pleim, J.E., 2010. The Meteorology-Chemistry Interface Processor (MCIP) for the CMAQ modeling system: updates through MCIPv3.4.1. *Geosci. Model Dev.* 3, 243–256. <https://doi.org/10.5194/gmd-3-243-2010>.
- Pacanowski, R.C., Griffies, S.M., 2000. *Model 3.0 Manual*. Technical Report. Geophysical Fluid Dynamics Laboratory, 4 (708 pages).
- Perić, T., Komadina, P., Račić, N., 2016. Wastewater pollution from cruise ships in the Adriatic Sea. *Traffic & Transportation* 28 (4), 425–433. <https://doi.org/10.7307/ptt.v28i4.2087>.
- Pietrzak, J., 1998. The use of TVD limiters for forward-in-time upstream-biased advection schemes in ocean modeling. *Mon. Weather Rev.* 126, 812–830. [https://doi.org/10.1175/1520-0493\(1998\)126<0812:TUOTLF>2.0.CO;2](https://doi.org/10.1175/1520-0493(1998)126<0812:TUOTLF>2.0.CO;2).
- Placke, M., Meier, H.E.M., Gräwe, U., Neumann, T., Frauen, C., Liu, Y., 2018. Long-term mean circulation of the Baltic Sea as represented by various ocean circulation models. *Frontiers in Marine Science*. <https://doi.org/10.3389/fmars.2018.00287>.
- Radtke, H., Neumann, T., Voss, M., Fennel, W., 2012. Modeling pathways of riverine nitrogen and phosphorus in the Baltic Sea. *Journal of Geophysical Research: Oceans* 117, C09024. <https://doi.org/10.1029/2012JC008119>.
- Raudsepp, U., Laanemets, J., Maljutenko, I., Hongisto, M., Jalkanen, J.-P., 2013. Impact of ship-borne nitrogen deposition on the Gulf of Finland ecosystem: an evaluation. *Oceanologia* 55 (4), 837–857. <https://doi.org/10.5697/oc.55-4-837>.
- Raudsepp, U., Legeais, J.-F., She, J., Maljutenko, I., Jandt, S., 2018. Baltic inflows. In: *Copernicus Marine Service Ocean State Report, Issue 2, Journal of Operational Oceanography*, 11(sup1), s13–s16. doi:<https://doi.org/10.1080/1755876X.2018.1489208>.
- Raudsepp, U., She, J., Brando, V.E., Santoleri, R., Sarmartino, M., Köuts, M., Uiboupin, R., Maljutenko, I., 2019a. Phytoplankton blooms in the Baltic Sea. In: *Copernicus Marine Service Ocean State Report, Issue 3, Journal of Operational Oceanography*, submitted.
- Raudsepp, U., Maljutenko, I., Köuts, M., 2019b. Cod reproductive volume potential in the Baltic Sea. In: *Copernicus Marine Service Ocean State Report, Issue 3, Journal of Operational Oceanography*, submitted.
- Redfield, A.C., 1934. On the proportions of organic derivations in sea water and their relation to the composition of plankton. *James Johnstone Memorial Volume* (ed. R.J. Daniel). Univ. Press of Liverpool, 176–192.
- Reusch, T.B.H., Dierking, J., Andersson, H.C., Bonsdorff, E., Carstensen, J., Casini, M., Czajkowski, M., Hasler, B., Hinsby, K., Hyytiäinen, K., Johannesson, K., Jomaa, S., Jormalainen, V., Kuosa, H., Kurland, S., Laikre, L., MacKenzie, B.R., Margonski, P., Melzner, F., Oesterwind, D., Ojaveer, H., Refsgaard, J.C., Sandström, A., Schwarz, G., Tonderski, K., Winder, M., Zandersen, M., 2018. The Baltic Sea as a time machine for the future coastal ocean. *Science Advances*, 4(5), eaar8195. doi:<https://doi.org/10.1126/sciadv.aar8195>.
- Rockel, B., Will, A., Hense, A., 2008. The regional climate model COSMO-CLM (CCLM). *Meteorol. Z.* 17 (4), 347–348. <https://doi.org/10.1127/0941-2948/2008/0309>.
- Savchuk, O.P., 2018. Large-scale nutrient dynamics in the Baltic Sea, 1970–2016. *Front. Mar. Sci.* 5, 95. <https://doi.org/10.3389/fmars.2018.00095>.
- Savchuk, O.P., Wulff, F., 2009. Long-term modeling of large-scale nutrient cycles in the entire Baltic Sea. In *Eutrophication in Coastal Ecosystems* (pp. 209–224). Springer, Dordrecht. doi:https://doi.org/10.1007/978-90-481-3385-7_18.
- Savchuk, O.P., Gustafsson, B.G., Medina, R.R., Alexander, S., Wulff, F., 2012. External nutrient loads to the Baltic Sea, 1970–2006. *Baltic Nest Institute Technical Report*. 5.
- Schelske, C.L., 1975. Silica and nitrate depletion as related to rate of eutrophication in Lakes Michigan, Huron and Superior. *Coupling of Land and Water Systems*, p. 277–298.
- Schernewski, G., Neumann, T., 2005. The trophic state of the Baltic Sea a century ago: a model simulation study. *J. Mar. Syst.* 53, 109–124. <https://doi.org/10.1016/j.jmarsys.2004.03.007>.
- Schindler, D.W., 2006. Recent advances in the understanding and management of eutrophication. *Limnology and Oceanography*, 51(1part2), pp. 356–363. doi:https://doi.org/10.4319/lo.2006.51.1_part_2.0356.
- Schindler, D.W., 2012. The dilemma of controlling cultural eutrophication of lakes. *Proc. R. Soc. B Biol. Sci.* 279 (1746), 4322–4333. <https://doi.org/10.1098/rspb.2012.1032>.
- Schwede, D., Pouliot, G., Pierce, T., 2005. Changes to the Biogenic Emissions Inventory System Version 3 (BEIS3). Proceedings of the 4th CMAS Models-3 Users' Conference 26–28 September 2005, Chapel Hill, NC. www.cmascenter.org/conference/2005/abstracts/2_7.pdf.
- Seitzinger, S.P., 1988. Denitrification in freshwater and coastal marine ecosystems: ecological and geochemical significance. *Limnology and Oceanography*, 33(4part2), pp. 702–724. doi:<https://doi.org/10.4319/lo.1988.33.4part2.0702>
- Shecheptkin, A.F., McWilliams, J.C., 2003. A method for computing horizontal pressure-gradient force in an oceanic model with a nonaligned vertical coordinate. *Journal of Geophysical Research: Oceans* 108, 1–34. <https://doi.org/10.1029/2001JC001047>.

- Simpson, D., 2011. The European Nitrogen Assessment, Chap. 14: Atmospheric Transport and Deposition of Reactive Nitrogen in Europe, 298–316, in: Sutton et al. (2011). <http://www.nine-esf.org>, 2011.
- Spilling, K., Kremp, A., Klais, R., Olli, K., Tamminen, T., 2014. Spring bloom community change modifies carbon pathways and C:N:P:Chl a stoichiometry of coastal material fluxes. *Biogeosciences* 11, 7275–7289. <https://doi.org/10.5194/bg-11-7275-2014>.
- Spokes, L.J., Jickells, T.D., 2005. Is the atmosphere really an important source of reactive nitrogen to coastal waters? *Cont. Shelf Res.* 25 (16), 2022–2035. <https://doi.org/10.1016/j.csr.2005.07.004>.
- Stålnacke, P., Grimvall, A., Sundblad, K., Tonderski, A., 1999. Estimation of riverine loads of nitrogen and phosphorus to the Baltic Sea, 1970–1993. *Environ. Monit. Assess.* 58 (2), 173–200. <https://doi.org/10.1023/A:1006073015871>.
- Stockner, J.G., Shortreed, K.S., 1988. Response of *Anabaena* and *Synechococcus* to manipulation of nitrogen: phosphorus ratios in a lake fertilization experiment. *Limnol. Oceanogr.* 33 (6), 1348–1361. <https://doi.org/10.4319/lo.1988.33.6.1348>.
- Swedish Institute for the Marine Environment (SIMM), 2014. Mapping Shipping Intensity and Routes in the Baltic Sea. Report 2014, 5.
- Tilman, D., 1982. *Resource Competition and Community Structure*. Princeton University Press, Princeton, NJ (296 pp.).
- Troost, T.A., Blaas, M., Los, F.J., 2013. The role of atmospheric deposition in the eutrophication of the North Sea: a model analysis. *J. Mar. Syst.* 125, 101–112. <https://doi.org/10.1016/j.jmarsys.2012.10.005>.
- Tsyro, S.G., Berge, E., 1998. Estimation of acidifying deposition in Europe due to international shipping emissions in the North Sea and the North East Atlantic Ocean. *WIT Transactions on Ecology and the Environment*, 25. doi:<https://doi.org/10.2495/CENV980171>.
- Umlauf, L., Burchard, H., 2005. Second-order turbulence closure models for geophysical boundary layers. A review of recent work. *Cont. Shelf Res.* 25 (7–8), 795–827. <https://doi.org/10.1016/j.csr.2004.08.004>.
- Vahtera, E., Conley, D.J., Gustafsson, B.G., Kuosa, H., Pitkänen, H., Savchuk, O.P., Tamminen, T., Viitasalo, M., Voss, M., Wasmund, N., Wulff, F., 2007. Internal ecosystem feedbacks enhance nitrogen-fixing cyanobacteria blooms and complicate management in the Baltic Sea. *Ambio*, pp. 186–194 [https://doi.org/10.1579/0044-7447\(2007\)36\[186:IEFENC\]2.0.CO;2](https://doi.org/10.1579/0044-7447(2007)36[186:IEFENC]2.0.CO;2).
- Väli, G., Meier, H.E.M., Elken, J., 2013. Simulated halocline variability in the Baltic Sea and its impact on hypoxia during 1961–2007. *Journal of Geophysical Research: Oceans* 118 (12), 6982–7000. <https://doi.org/10.1002/2013JC009192>.
- Van de Waal, D.B., Verschoor, A.M., Verspagen, J.M.H., Van Donk, E., Huisman, J., 2010. Climate-driven changes in the ecological stoichiometry of aquatic ecosystems. *Front. Ecol. Environ.* 8 (3), 145–152. <https://doi.org/10.1890/080178>.
- Viana, M., Hammingh, P., Colette, A., Querol, X., Degraeuwe, B., de Vlieger, I., van Aardenne, J., 2014. Impact of maritime transport emissions on coastal air quality in Europe. *Atmos. Environ.* 90, 96–105. <https://doi.org/10.1016/j.atmosenv.2014.03.046>.
- Vihma, T., Haapala, J., 2009. Geophysics of sea ice in the Baltic Sea: a review. *Prog. Oceanogr.* 80 (3–4), 129–148. <https://doi.org/10.1016/j.pocean.2009.02.002>.
- Von Schuckmann, K., 2019. Copernicus marine service ocean state report, Issue 3, *Journal of Oceanography*, submitted.
- Voss, M., Baker, A., Bange, H.W., Conley, D., Cornell, S., Deutsch, B., Engel, A., Ganeshram, R., Garnier, J., Heiskanen, A., Jickells, T., Lancelot, C., McQuatters-Gollop, A., Middelburg, J., Schiedek, D., Slomp, C.P., Conley, D.P., 2001. Chapter 8: Nitrogen Processes in Coastal and Marine Ecosystems.
- Voss, M., Emeis, K.C., Hille, S., Neumann, T., Dippner, J.W., 2005. Nitrogen cycle of the Baltic Sea from an isotopic perspective. *Glob. Biogeochem. Cycles* 19 (3). <https://doi.org/10.1029/2004GB002338>.
- Vukovich, J., Pierce, T., 2002. The Implementation of BEIS3 within the SMOKE Modeling Framework, in: Proceedings of the 11th International Emissions Inventory Conference, Atlanta, Georgia, 15–18 April 2002. www.epa.gov/ttn/chieff/conf/ei11/modeling/vukovich.pdf.
- Wallcraft, A.J., Kara, A.B., Hurlburt, H.E., 2005. Convergence of Laplacian diffusion versus resolution of an ocean model. *Geophys. Res. Lett.* 32 (7). <https://doi.org/10.1029/2005GL022514>.
- Wan, She, J., Maar, M., Jonasson, L., Baasch-Larsen, J., 2012. Assessment of a physical–biogeochemical coupled model system for operational service in the Baltic Sea. *Ocean Science Discussions*, 9(2). doi:<https://doi.org/10.5194/os-8-683-2012>.
- Wang, C., Corbett, J.J., Firestone, J., 2008. Improving spatial representation of global ship emissions inventories. *Environmental Science & Technology* 42 (1), 193–199. <https://doi.org/10.1021/es0700799>.
- Wartsila, 2010. Exhaust Gas Scrubber Installed Onboard MT Suula, Public Test Report.
- Wilewska-Bien, M., Granhag, L., Andersson, K., 2016. The nutrient load from food waste generated on-board ships in the Baltic Sea. *Mar. Pollut. Bull.* 105 (1), 359–366. <https://doi.org/10.1016/j.marpolbul.2016.03.002>.
- Wilewska-Bien, M., Granhag, L., Jalkanen, J.-P., Johansson, L., Andersson, K., 2018. Phosphorus flows on ships: case study from the Baltic Sea. Proceedings of the Institution of Mechanical Engineers. Part M: *J. Eng. Marit. Environ.*, 1475090218761761 <https://doi.org/10.1177/1475090218761761>.
- Zhang, D., Lavender, S., Muller, J.-P., Walton, D., Zou, X., Shi, F., 2018. MERIS observations of phytoplankton phenology in the Baltic Sea. *Sci. Total Environ.* 642, 447–462. <https://doi.org/10.1016/j.scitotenv.2018.06.019>.
- Zhao, Y., Zhang, L., Pan, Y., Wang, Y., Paulot, F., Henze, D.K., 2015. Atmospheric nitrogen deposition to the northwestern Pacific: seasonal variation and source attribution. *Atmos. Chem. Phys.* 15, 10905–10924. <https://doi.org/10.5194/acp-15-10905-2015>.
- Zillén, L., Conley, D.J., Andrén, T., Andrén, E., Björck, S., 2008. Past occurrences of hypoxia in the Baltic Sea and the role of climate variability, environmental change and human impact. *Earth Sci. Rev.* 91 (1–4), 77–92. <https://doi.org/10.1016/j.earscirev.2008.10.001>.

Paper III

Raudsepp, U., She, J., Brando, V.E, Santoleri, R., Sammartino, M., Kõuts, M., Uiboupin, R., Maljutenko, I., 2019. **Phytoplankton blooms in the Baltic Sea**. In: Copernicus Marine Service Ocean State Report, Issue 3, Journal of Operational Oceanography, 12:sup1, pp. s26–s30; DOI: 10.1080/1755876X.2019.1633075



Copernicus Marine Service Ocean State Report, Issue 3

Karina von Schuckmann ((Editor)), Pierre-Yves Le Traon ((Editor)), Neville Smith (Chair) ((Review Editor)), Ananda Pascual ((Review Editor)), Samuel Djavidnia ((Review Editor)), Jean-Pierre Gattuso ((Review Editor)), Marilaure Grégoire ((Review Editor)), Glenn Nolan ((Review Editor)), Signe Aaboe, Eva Aguiar, Enrique Álvarez Fanjul, Aida Alvera-Azcárate, Lotfi Aouf, Rosa Barciela, Arno Behrens, Maria Belmonte Rivas, Sana Ben Ismail, Abderrahim Bentamy, Mireno Borgini, Vittorio E. Brando, Nathaniel Bensoussan, Anouk Blauw, Philippe Bryère, Bruno Buongiorno Nardelli, Ainhoa Caballero, Veli Çağlar Yumruktepe, Emma Cebrian, Jacopo Chiggiato, Emanuela Clementi, Lorenzo Corgnati, Marta de Alfonso, Álvaro de Pascual Collar, Julie Deshayes, Emanuele Di Lorenzo, Jean-Marie Dominici, Cécile Dupouy, Marie Dréviron, Vincent Echevin, Marieke Eleveld, Lisette Enserink, Marcos García Sotillo, Philippe Garnesson, Joaquim Garrabou, Gilles Garric, Florent Gasparin, Gerhard Gayer, Francis Gohin, Alessandro Grandi, Annalisa Griffo, Jérôme Gourrion, Stefan Hendricks, Céline Heuzé, Elisabeth Holland, Doroteaciro Iovino, Mélanie Juza, Diego Kurt Kersting, Silvija Kipson, Zafer Kizilkaya, Gerasimos Korres, Mariliis Kõuts, Priidik Lagema, Thomas Lavergne, Heloise Lavigne, Jean-Baptiste Ledoux, Jean-François Legeais, Patrick Lehodey, Cristina Linares, Ye Liu, Julien Mader, Ilja Maljutenko, Antoine Mangin, Ivan Manso-Narvarte, Carlo Mantovani, Stiig Markager, Evan Mason, Alexandre Mignot, Milena Menna, Maeva Monier, Baptiste Mourre, Malte Müller, Jacob Woge Nielsen, Giulio Notarstefano, Oscar Ocaña, Ananda Pascual, Bernardo Patti, Mark R. Payne, Marion Peirache, Silvia Pardo, Begoña Pérez Gómez, Andrea Pisano, Coralie Perruche, K. Andrew Peterson, Marie-Isabelle Pujol, Urmas Raudsepp, Michalis Ravdas, Roshin P. Raj, Richard Renshaw, Emma Reyes, Robert Ricker, Anna Rubio, Michela Sammartino, Rosalia Santoleri, Shubha Sathyendranath, Katrin Schroeder, Jun She, Stefania Sparnocchia, Joanna Staneva, Ad Stoffelen, Tanguy Szekely, Gavin H. Tilstone, Jonathan Tinker, Joaquín Tintoré, Benoît Tranchant, Rivo Uiboupin, Dimitry Van der Zande, Karina von Schuckmann, Richard Wood, Jacob Woge Nielsen, Mikel Zabala, Anna Zacharioudaki, Frédéric Zuberer & Hao Zuo

To cite this article: Karina von Schuckmann ((Editor)), Pierre-Yves Le Traon ((Editor)), Neville Smith (Chair) ((Review Editor)), Ananda Pascual ((Review Editor)), Samuel Djavidnia ((Review Editor)), Jean-Pierre Gattuso ((Review Editor)), Marilaure Grégoire ((Review Editor)), Glenn Nolan ((Review Editor)), Signe Aaboe, Eva Aguiar, Enrique Álvarez Fanjul, Aida Alvera-Azcárate, Lotfi Aouf, Rosa Barciela, Arno Behrens, Maria Belmonte Rivas, Sana Ben Ismail, Abderrahim Bentamy, Mireno Borgini, Vittorio E. Brando, Nathaniel Bensoussan, Anouk Blauw, Philippe Bryère, Bruno Buongiorno Nardelli, Ainhoa Caballero, Veli Çağlar Yumruktepe, Emma Cebrian, Jacopo Chiggiato, Emanuela Clementi, Lorenzo Corgnati, Marta de Alfonso, Álvaro de Pascual Collar,

Julie Deshayes, Emanuele Di Lorenzo, Jean-Marie Dominici, Cécile Dupouy, Marie Drévilion, Vincent Echevin, Marieke Eleveld, Lisette Enserink, Marcos García Sotillo, Philippe Garnesson, Joaquim Garrabou, Gilles Garric, Florent Gasparin, Gerhard Gayer, Francis Gohin, Alessandro Grandi, Annalisa Griffa, Jérôme Gourrion, Stefan Hendricks, Céline Heuzé, Elisabeth Holland, Doroteaciro Iovino, Mélanie Juza, Diego Kurt Kersting, Silvija Kipson, Zafer Kizilkaya, Gerasimos Korres, Mariliis Kõuts, Priidik Lagemaa, Thomas Lavergne, Heloise Lavigne, Jean-Baptiste Ledoux, Jean-François Legeais, Patrick Lehodey, Cristina Linares, Ye Liu, Julien Mader, Ilya Maljutenko, Antoine Mangin, Ivan Manso-Narvarte, Carlo Mantovani, Stiig Markager, Evan Mason, Alexandre Mignot, Milena Menna, Maeva Monier, Baptiste Mourre, Malte Müller, Jacob Woge Nielsen, Giulio Notarstefano, Oscar Ocaña, Ananda Pascual, Bernardo Patti, Mark R. Payne, Marion Peirache, Silvia Pardo, Begoña Pérez Gómez, Andrea Pisano, Coralie Perruche, K. Andrew Peterson, Marie-Isabelle Pujol, Urmas Raudsepp, Michalis Ravdas, Roshin P. Raj, Richard Renshaw, Emma Reyes, Robert Ricker, Anna Rubio, Michela Sammartino, Rosalia Santoleri, Shubha Sathyendranath, Katrin Schroeder, Jun She, Stefania Sparnocchia, Joanna Staneva, Ad Stoffelen, Tanguy Szekely, Gavin H. Tilstone, Jonathan Tinker, Joaquín Tintoré, Benoît Tranchant, Rivo Uiboupin, Dimitry Van der Zande, Karina von Schuckmann, Richard Wood, Jacob Woge Nielsen, Mikel Zabala, Anna Zacharioudaki, Frédéric Zuberer & Hao Zuo (2019) Copernicus Marine Service Ocean State Report, Issue 3, Journal of Operational Oceanography, 12:sup1, S1-S123, DOI: [10.1080/1755876X.2019.1633075](https://doi.org/10.1080/1755876X.2019.1633075)

To link to this article: <https://doi.org/10.1080/1755876X.2019.1633075>



© 2019 The Author(s). Published by Informa UK Limited, trading as Taylor & Francis Group



Published online: 13 Sep 2019.



Submit your article to this journal [↗](#)



Article views: 7008



View related articles [↗](#)



View Crossmark data [↗](#)



Citing articles: 1 View citing articles [↗](#)

COPERNICUS MARINE SERVICE OCEAN STATE REPORT, ISSUE 3

Editors

Karina von Schuckmann

Pierre-Yves Le Traon

Review Editors

Neville Smith (Chair)

Ananda Pascual

Samuel Djavidnia

Jean-Pierre Gattuso

Marilaure Grégoire

Glenn Nolan

To cite the entire report

How to cite the entire report: von Schuckmann, K., P.-Y. Le Traon, N. Smith, A. Pascual, S. Djavidnia, J.-P. Gattuso, M. Grégoire, G. Nolan (2019) Copernicus Marine Service Ocean State Report, Issue 3, Journal of Operational Oceanography, 12:sup1, s1–s123; DOI: 10.1080/1755876X.2019.1633075

To cite a specific section in the report (example)

Raudsepp, U., I. Maljutenko, M. Kõuts (2019). Cod reproductive volume potential in the Baltic Sea. In: Copernicus Marine Service Ocean State Report, Issue 3, Journal of Operational Oceanography, 12:sup1, s26–s30; DOI: 10.1080/1755876X.2019.1633075

AUTHOR AFFILIATIONS (ALPHABETICAL BY NAME)

Signe Aaboe, MET, Tromsø, Norway
Eva Aguiar, SOCIB, Illes Balears, Spain
Enrique Álvarez Fanjul, Puertos del Estado, Madrid, Spain
Aida Alvera-Azcárate, Université de Liège, Liege, Belgium
Lotfi Aouf, Météo-France, Toulouse, France
Rosa Barciela, Met Office, Exeter, United Kingdom
Arno Behrens, Helmholtz-Zentrum Geesthacht (HZG), Geesthacht, Germany
Maria Belmonte Rivas, KNMI, GA De Bilt, Netherlands
Sana Ben Ismail, INSTM, Tunis, Tunisia
Abderrahim Bentamy, IFREMER, Plouzané, France
Mireno Borgini, Consiglio Nazionale delle Ricerche, Istituto di Scienze Marine (CNR-ISMAR), Pozzuolo di Leri (SP), Italy
Vittorio E. Brando, Institute of Marine Sciences (ISMAR) – National Research Council (CNR), Rome, Italy
Nathaniel Bensoussan, Institute of Marine Sciences-CSIC, Barcelona, Spain
Anouk Blauw, Deltares, Delft, Netherlands
Philippe Bryère, Argans, Brest, France
Bruno Buongiorno Nardelli, Institute of Marine Sciences – CNR, Napoli, Italy
Ainhoa Caballero, AZTI, Pasaia – GIPUZKOA (Spain)
Veli Çağlar Yumruktepe, NERSC, Bergen, Norway
Emma Cebrian, Universitat de Girona, Girona, Spain
Jacopo Chiggiato, Consiglio Nazionale delle Ricerche, Istituto di Scienze Marine (CNR-ISMAR), Venezia, Italy
Emanuela Clementi, CMCC, Bologna, Italy
Lorenzo Corgnati, Institute of Marine Sciences – National Research Council ISMAR-CNR, La Spezia, Italy
Marta de Alfonso, Puertos del Estado, Madrid, Spain
Álvaro de Pascual Collar, Puertos del Estado, Madrid, Spain
Julie Deshayes, LOCEAN/CNRS, Paris, France
Emanuele Di Lorenzo, Georgia Institute of Technology, États-Unis, USA
Jean-Marie Dominici, Parc Naturel Régional de Corse, Galeria, France
Cécile Dupouy, MIO, IRD, Marseille, France
Marie Drévilion, Mercator Ocean International, Ramonville St-Agne, France
Vincent Echevin, LOCEAN/IRD, PARIS, France
Marieke Eleveld, Deltares, Delft, Netherlands
Lisette Enserink, Rijkswaterstaat, Delft, Netherlands
Marcos García Sotillo, Puertos del Estado, Madrid, Spain
Philippe Garnesson, ACRI-ST, Sophia-Antipolis, France
Joaquim Garrabou, ICM/CSIC, Barcelona, Spain
Gilles Garric, Mercator Ocean, Ramonville Saint-Agne, France
Florent Gasparin, Mercator Ocean International, Ramonville Saint-Agne, France
Gerhard Gayer, Helmholtz-Zentrum Geesthacht (HZG), Geesthacht, Germany
Francis Gohin, IFREMER, Plouzané, France
Alessandro Grandi, CMCC, Bologna, Italy
Annalisa Griffa, CNR-ISMAR, La Spezia, Italy
Jérôme Gourrion, Oceanscope, Incheon, South Korea
Stefan Hendricks, Alfred-Wegener-Institut, Bremerhaven, Germany
Céline Heuzé, University of Gothenburg, Gothenburg, Sweden
Elisabeth Holland, University of South Pacific, Fiji, Australia
Doroteaciro Iovino, CMCC, Bologna, Italy
Mélanie Juza, SOCIB, Illes Balears, Spain
Diego Kurt Kersting, Freie Universität, Berlin, Germany
Silvija Kipson, PMF, Zagreb, Croatia
Zafer Kizilkaya, Mediterranean Conservation Society, Bornova/Izmir, Turkey
Gerasimos Korres, HCMR, Attica, Greece
Mariliis Kõuts, Marine Systems Institute at Tallinn University of Technology, Tallinn, Estonia
Priidik Lagemaa, Marine Systems Institute at Tallinn University of Technology, Tallinn, Estonia
Thomas Lavergne, MET, Tromsø, Norway
Heloise Lavigne, RBINS, Brussels, Belgium
Jean-Baptiste Ledoux, ICM/CSIC, Barcelona, Spain
Jean-François Legeais, Collecte Localisation Satellite (CLS), Ramonville-Saint-Agne, France
Patrick Lehodey, Collecte Localisation Satellite (CLS), Ramonville-Saint-Agne, France
Cristina Linares, University of Barcelona, Barcelona, Spain
Ye Liu, Swedish Meteorological and Hydrological Institute, Norrköping, Sweden

(Continued from previous page)

Julien Mader, AZTI, Pasaia – GIPUZKOA (Spain)
Ilija Maljutenko, Marine Systems Institute at Tallinn University of Technology, Tallinn, Estonie
Antoine Mangin, ACRI-ST, Sophia-Antipolis, France
Ivan Manso-Narvarte, AZTI, Pasaia – GIPUZKOA (Spain)
Carlo Mantovani, CNR-ISMAR, La Spezia, Italy
Stiig Markager, Aarhus University, Roskilde, Denmark
Evan Mason, IMEDEA (CSIC-UIB), Illes Balears, Spain
Alexandre Mignot, Mercator Ocean International, Ramonville Saint-Agne, France
Milena Menna, Istituto Nazionale di Oceanografia e di Geofisica Sperimentale (OGS), Sgonico (TS), Italy
Maeva Monier, CELAD/Mercator Ocean International, Ramonville St-Agne, France
Baptiste Mourre, SOCIB, Illes Balears, Spain
Malte Müller, MET, Tromso, Norway
Jacob Woge Nielsen, Danish Meteorological Institute, Copenhagen, Denmark
Giulio Notarstefano, Istituto Nazionale di Oceanografia e di Geofisica Sperimentale (OGS), Sgonico (TS), Italy
Oscar Ocaña, Fundación Museo del Mar de Ceuta, Ceuta, Spain
Ananda Pascual, IMEDEA (CSIC-UIB), Illes Balears, Spain
Bernardo Patti, CNR-IAS, Campobello di Mazara, Italy
Mark R. Payne, Technical University of Denmark (DTU-Aqua), Denmark
Marion Peirache, Parc National de Port-Cros, Hyeres cedex, France
Silvia Pardo, PML, UK
Begoña Pérez Gómez, Puertos del Estado, Madrid, Spain
Andrea Pisano, CNR-ISMAR, Roma, Italy
Coralie Perruche, Mercator Ocean International, Ramonville Saint-Agne, France
K. Andrew Peterson, ECCO, Québec, Canada
Marie-Isabelle Pujol, Collecte Localisation Satellites (CLS), Ramonville St-Agne, France
Urmas Raudsepp, Marine Systems Institute at Tallinn University of Technology, Tallinn, Estonie
Michalis Ravdas, HCMR, Attica, Greece
Roshin P. Raj, Nansen Environmental and Remote Sensing Center, Bergen, Norway
Richard Renshaw, Met Office, Exeter, United Kingdom
Emma Reyes, SOCIB, Palma, Spain
Robert Ricker, Alfred-Wegener-Institut, Bremerhaven, Germany
Anna Rubio, AZTI, Pasaia – GIPUZKOA (Spain)
Michela Sammartino, CNR-ISMAR, Rome, Italy
Rosalia Santoleri, CNR-ISMAR, Rome, Italy
Shubha Sathyendranath, PML, United Kingdom
Katrin Schroeder, CNR-ISMAR, Venezia, Italy
Jun She, Danish Meteorological Institute (DMI), Copenhagen, Denmark
Stefania Sparnocchia, CNR-ISMAR, Trieste, Italy
Joanna Staneva, Helmholtz-Zentrum Geesthacht (HZG), Geesthacht, Germany
Ad Stoffelen, KNMI, GA De Bilt, Netherlands
Tanguy Szekely, Oceanscope, Incheon, South Korea
Gavin H. Tilstone, Plymouth Marine Laboratory, Plymouth, UK
Jonathan Tinker, Met Office, Exeter, United Kingdom
Joaquín Tintoré, SOCIB/IMEDEA (CSIC-UIB), Balears, Spain
Benoît Tranchant, Collecte Localisation Satellites (CLS), Ramonville St-Agne, France
Rivo Uiboupin, TalTech, Tallinn, Estonia
Dimitry Van der Zande, RBINS, Brussels, Belgium
Karina von Schuckmann, Mercator Ocean International, Ramonville St-Agne, France
Richard Wood, Met Office, Exeter, United Kingdom
Jacob Woge Nielsen, Danish Meteorological Institute, Copenhagen, Denmark
Mikel Zabala, UB/IRBIO, Barcelona, Spain
Anna Zacharioudaki, HCMR, Attica, Greece
Frédéric Zuberer, OSU PYTHEAS, Cedex, France
Hao Zuo, ECMWF, United Kingdom

(belonging to the CIESM Hydrochanges network, see Schroeder et al. 2013) monitors the overflowing dense waters in detail since 2003. While until 2005 only the ‘classical’ old deep water was found at the sill, the new denser ones started to cross it since then (Figure 2.3.2 lower panels), being uplifted by even denser new deep waters that were produced in the following winters (Figure 2.3.1). By 2014 the whole layer below 500 m, i.e. the halocline/thermocline and the deep water, has densified to values of 29.11–29.12 kg m⁻³, becoming denser than the ‘classical’ resident water found at <3000 m in the Tyrrhenian Sea (Schroeder et al. 2016).

Given that all processes of dense water formation involve Atlantic and Intermediate Water to some extent, the latter being the main contributor to the heat and salt contents of the newly formed waters, all Mediterranean water masses are intimately related to each other, so that significant modifications to one will also affect the others sooner or later. Indeed, recent studies have also focused on the long-term strong warming and salinification of intermediate water: since the mid-1990s its temperature and salinity have increased by 0.28°C/decade and 0.08/decade in the Sicily Channel (respectively Figure 2.3.3(A–B)), a key site where the intermediate water flowing from east to west may be intercepted. Such trends are at least one order of magnitude higher than the average values reported for the global ocean intermediate layer at mid-latitudes (Schroeder et al. 2017). These outcomes are also of great benefit for intercomparisons with numerical model results (as those in von Schuckmann et al. 2018, their Figure 3.4.3).

Warmer and drier regional climatic conditions over the eastern basin are favouring the formation of increasingly warmer and saltier intermediate water: indeed, the Levantine region in particular is undergoing a dramatic drought since the late 1990s (Cook et al. 2016), the driest period in the past 500 years. As a result, also the upper part of the Eastern Mediterranean deep waters is experiencing a warming (not shown) and a salinification (Figure 2.3.3(C)), as is evident from repeated CTD casts in the central Sicily Channel (between the islands of Pantelleria and Malta) that reach depths below 1700 m, where the upper part of the eastern deep water is found. The thermohaline evolution at this location has already been discussed in Gasparini et al. (2005), Ben Ismail et al. (2014) and Gačić et al. (2013). At any moment, the salinity profile shows a maximum at around 300 m depth, associated with the Levantine Intermediate Water. The temporal evolution reveals two maxima before the very recent period (until

2011), around 1992 and 2008, while since 2011 the layer is warming and becoming saltier at a much higher rate than before, each year reaching higher peak values within the water mass core. Since 2010–2011 this pattern is involving the whole water column down to 1700 m, where the deep water is now as warm and salty as it was the intermediate water during the peak in 2008.

2.4. Phytoplankton blooms in the Baltic Sea

Authors: Urmaz Raudsepp, Jun She, Vittorio E. Brandò, Rosalia Santoleri, Michela Sammartino, Mariliis Kõuts, Rivo Uiboupin, Ilja Maljutenko

Statement of outcome: The Baltic Sea phytoplankton bloom characteristics are evaluated based on spring and summer bloom statistics, summer chlorophyll-a and attenuation coefficient (Kd). Over the past 20 years, the mean start day of the spring bloom changed from day 120 in 1998 to around days 80–60 from the year 2003 onward. The intensity and spatial coverage of summer blooms decreased since 2009, and they tend to be more intensified in the subsurface layer. Low attenuation coefficient and chlorophyll-a anomaly, a late start date and early end date of the spring bloom, as well as low spatiotemporal coverage of the bloom show that the spring bloom in 2017 was exceptionally weak. Summer phytoplankton bloom was strong in the Gulf of Bothnia and dominated by subsurface bloom in 2016, but shifted to the northern Baltic Proper in 2017.

Products used:

Ref. No.	Product name and type	Documentation
2.4.1	OCEANCOLOUR_BAL_OPTICS_L3_REP_OBSERVATIONS_009_097 Remote sensing	PUM: http://marine.copernicus.eu/documents/PUM/CMEMS-OC-PUM-009-ALL.pdf QUID: http://marine.copernicus.eu/documents/QUID/CMEMS-OC-QUID-009-080-097.pdf
2.4.2	OCEANCOLOUR_BAL_CHL_L3_REP_OBSERVATIONS_009_080 Remote sensing	PUM: http://marine.copernicus.eu/documents/PUM/CMEMS-OC-PUM-009-ALL.pdf QUID: http://marine.copernicus.eu/documents/QUID/CMEMS-OC-QUID-009-080-097.pdf

Recently comprehensive classifications of eutrophication status of the Baltic Sea were made using the third version of the HELCOM Eutrophication Assessment Tool (HEAT 3.0), applying indicators with commonly agreed targets of good environmental status (HELCOM

2015). The indicators were grouped under three ‘criteria’: (1) nutrient levels (i.e. winter dissolved inorganic phosphate and nitrogen in the upper 10 m of the water column), (2) direct effects (summer chlorophyll-a in the upper 10 m and secchi depth) and (3) indirect effects (annual oxygen debt below the halocline and benthic invertebrates). Spring bloom has been less considered for the assessment of the Baltic Sea eutrophication. Here we propose that spring and summer bloom statistics, summer chlorophyll-a and attenuation coefficient (Kd) from the products 2.4.1 and 2.4.2 of the product table could be successfully used as one of the relevant indicators in evaluating the Baltic Sea eutrophication status. Annual oxygen content and nutrient conditions in the Baltic Sea will be subject of the forthcoming studies to complete the set of eutrophication status indicators of the Baltic Sea.

CMEMS ocean colour product references 2.4.1 and 2.4.2 provide a good spatiotemporal coverage of the surface bio-optical features in the Baltic Sea, although their uncertainties are still high ($r^2 = 0.4$, for chlorophyll-a, see Pitarch et al. 2016). The phytoplankton abundance and succession in the Baltic Sea are characterised by dinoflagellate- and diatom-dominated spring bloom and cyanobacterial summer bloom (Kahru and Nömmann 1990; Kahru et al. 2018). The spring bloom (spring is from days 31 to 160) is detected using the Siegel (2002) approach (i.e. it is a spring bloom if chlorophyll-a > median + 5%) for each pixel in the basin, after which the statistics for the bloom onset are calculated as in Groetsch et al. (2016) and presented as distribution of the start, peak and end days over the whole basin per each year. The spring and summer bloom spatiotemporal coverage (day km²) is aggregated from daily subsurface and surface bloom following Hansson and Håkansson (2007). Summer blooms are detected by applying the thresholds defined by Hansson et al. (2010) on remote sensing reflectance spectra (Rrs) at the wavelength of 550 nm and Rrs at 676 nm for the subsurface and surface blooms, respectively. Although 20 years of satellite data are available in the Baltic Sea, it should be noted that the remote sensing indexes computed by SMHI for HELCOM, recorded from 2010 onwards, should not be directly compared with the 1997–2009 values, as an improved detection method is now used (i.e. Hansson et al. 2010). The time series for Rrs, chlorophyll-a and attenuation coefficient (Kd490) used in this study are fully homogeneous as they are based on a merged product from different satellites that corrects for inter-sensor differences (Mélin et al. 2017; Sathyendranath et al. 2017). Attenuation coefficient values are proxies for Secchi depth, accounting for water transparency.

During 1998–2001, only SeaWiFS (O’Reilly et al. 1998) was available; while from the year 2002 onwards there are two or three sensors available (Brewin et al. 2015).

We observed the start, peak and end day of the spring bloom during the period of 1998–2017 from product reference 2.4.2 (Figure 2.4.1). In most years, the spring bloom starts first in the western and southern Baltic Sea, then in the central Baltic, and the latest in the Bothnian Sea and Bothnian Bay (Fennel 1999; Wan et al. 2013). This gives significant spatial variability to the starting date of the spring bloom in the Baltic Sea. However, there are also years when the spring bloom starts early, e.g. in 1985 and 1986 as shown by Kahru and Nömmann (1990). The mean start day of the spring bloom shifted earlier during the observation period (from day 120 in 1998 to day 50 in 2015). According to the start day and spatial variability, most of the spring bloom can be divided into three types:

- late onset spring bloom (later than day 100) that shows small spatial variability in the Baltic Sea, evident in 1998–2002;
- medium onset spring bloom (around day 80) that has large spatial variability, mostly found in 2003–2011;
- early onset spring bloom (around day 60) with rather small spatial variability, mostly found in 2012–2016 (Figure 2.4.1(a)).

The year 2017 deviates from this trend of declining start day by a late onset spring bloom (days 80–120). It also differs from the previously mentioned three types of spring blooms due to its high spatial variability that can be inferred by the interquartile range (Figure 2.4.1(a)). There is a good consistency between the start day and spatiotemporal coverage of spring bloom (Figure 2.4.2(a)) – in general, later start day results in smaller spatiotemporal coverage. The seven late onset spring bloom years, 1998–2002, 2006 and 2017 (Figure 2.4.1(a)) also represent the lowest spatiotemporal coverage (Figure 2.4.2(a)). Although the top two years with the largest spatiotemporal coverage (2008 and 2011) are marked with earlier start day (day 55 and day 65), earlier start day does not always result in large spatiotemporal coverage, as found in the years 2012–2016. These years also have quite small spatial variability of the start day in the Baltic Sea. The end day of spring bloom has shifted slightly later, from days 145–148 to day 150 from 2002 onwards. The peak day of spring bloom has fluctuated with no clear trend.

Since 2002 the spring bloom spatiotemporal coverage has shown general tendency to increase until

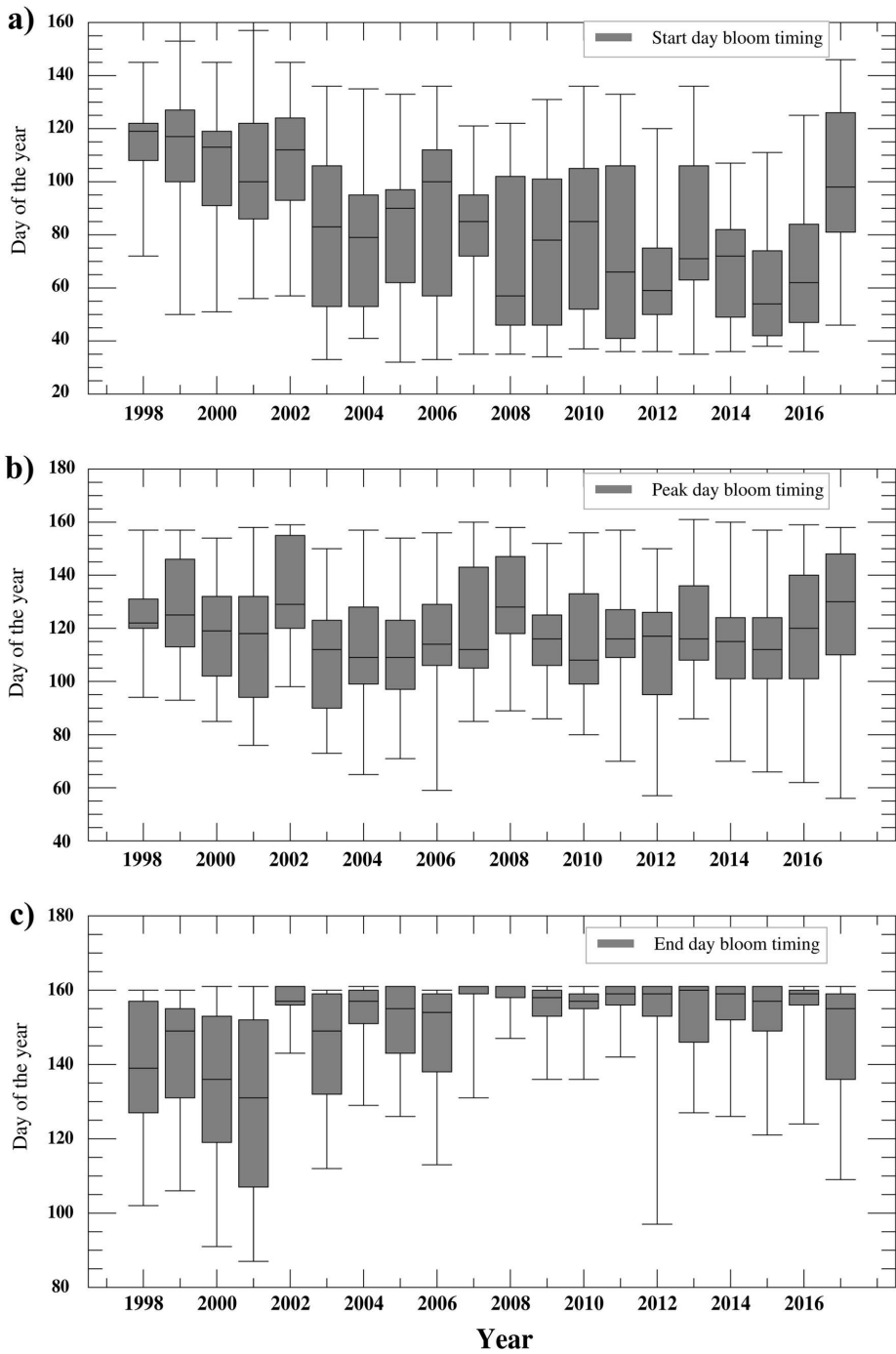


Figure 2.4.1. Time series of the spring bloom statistics (Siegel 2002; Groetsch et al. 2016) for start day (a), peak day (b), end day (c) for the period of 1998–2017 of the Baltic Sea from product reference 2.4.2. The bar refers to first quartile, median (black line) and third quartile, while the whiskers are the 5th and 95th percentiles respectively for start, peak and end days over the basin.

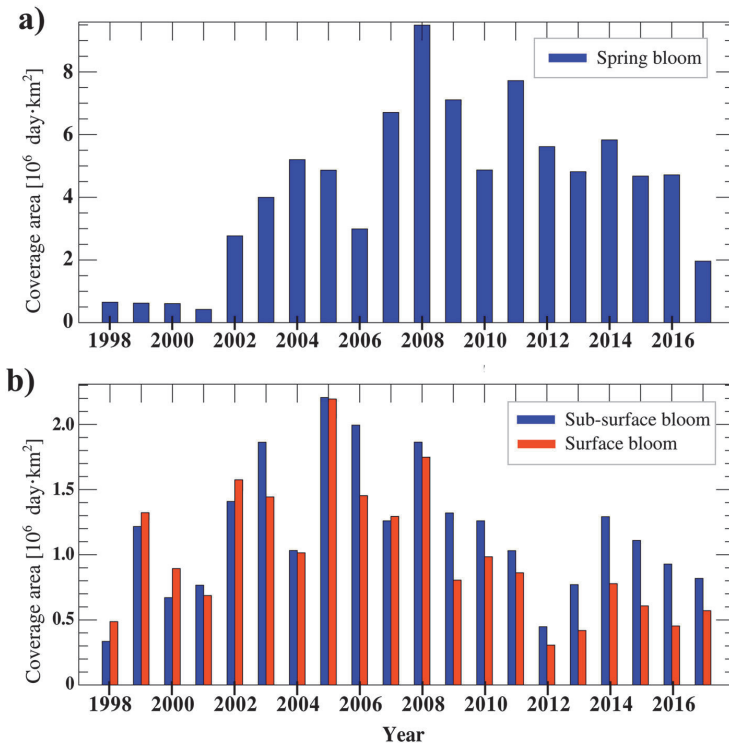


Figure 2.4.2. Time series of spring (a) and summer bloom (b) spatiotemporal coverage (day km^2) (1998–2017) using method by Hansson and Håkansson (2007). Results are based on CMEMS product reference 2.4.2 and 2.4.1 respectively.

2008–2011, followed by a decrease afterwards (Figure 2.4.2(a)). Spring blooms have been reported to weaken in intensity but lengthen during the period of 2000–2014 (Groetsch et al. 2016). Summer bloom coverage, however, increased from 1998 until 2005, and then decreased practically until present with a local minimum in 2012 (Figure 2.4.2(b)). Thus, high spatiotemporal coverage of the spring bloom is detected in 2007, 2008, 2009 and 2011, but peak years of the summer bloom spatiotemporal coverage are 2002, 2003, 2005 and 2008. There are several sub-periods of co-changes of the spatiotemporal coverage of the spring and summer blooms. For instance, the spring and summer blooms have a positive correlation in the period of 2013–2017. There is a slight positive trend in the spring bloom spatiotemporal coverage for the period of 2002–2011, whereas summer bloom shows a decreasing trend during the partially overlapping period of 2005–2012. Over the longer period of 1979–2017, the summer (cyanobacteria) blooms are reported to

be oscillating without a clear, significant trend (Kahru et al. 2018).

Since 2009, the summer bloom has been on a relatively low level, featured by more subsurface than surface bloom. The previous years (1998–2008) were dominated by the opposite feature (Figure 2.4.2(b)). The subsurface bloom declined continuously from 2014 to 2017, whereas the surface bloom increased in 2017, compared to the previous year.

One of the indicators of the eutrophication status of the Baltic Sea is secchi depth (HELCOM 2015) for which we use light attenuation coefficient (K_d) as proxy in this study. Summer mean attenuation coefficient (K_d) values in the Baltic Sea from the period of 1998–2017 derived from product reference 2.4.1. In open water light attenuation is mainly caused by phytoplankton species, while coloured dissolved organic matter (CDOM) and resuspended particulate matter are the main optically active substances in the coastal zone. Summer mean attenuation coefficient values derived from satellite remote sensing reflectance

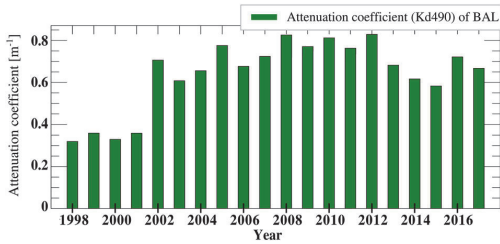


Figure 2.4.3. Time series of the attenuation coefficient (Kd490) averaged over the Baltic Sea in summer of 1998–2017 (product reference 2.4.1).

(Figure 2.4.3) stand for high values in the coastal zones, as reflected on the chlorophyll-a anomaly also (Figure 2.4.5).

In general, low attenuation coefficient values are observed in 1998–2001, followed by an increasing trend until 2010 and a decline until present. Last two years, i.e. 2016 and 2017, indicate an increase in summer mean attenuation coefficient values again. The attenuation coefficient anomaly in the summer of 2016 is positive over the entire sea area except for the eastern part of the Gulf of Finland (Figure 2.4.4(b)). Especially high values are observed in the Bay of Bothnia. In summer 2017, the area with positive attenuation coefficient anomaly has been reduced to the northern and eastern Baltic Proper and southern Gulf of Riga (Figure 2.4.4 (d)). The attenuation coefficient anomaly in the springs of 2016 and 2017 shows strong inter-annual changes (Figure 2.4.4(a,c)). Excluding the coastal areas close to the major river inlets, where coloured dissolved organic

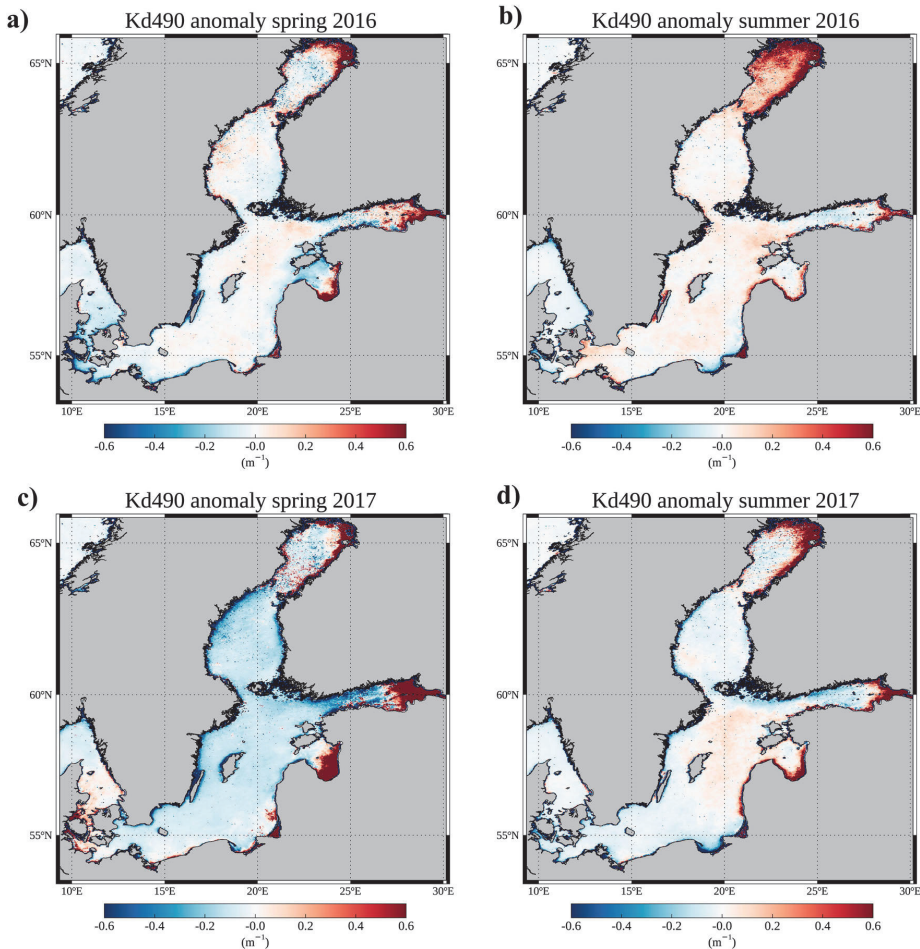


Figure 2.4.4. Attenuation coefficient (Kd) anomaly fields in spring 2016 (a) and 2017 (c) relative to the 1998–2014 spring mean field, and in summer 2016 (b) and 2017 (d) relative to the 1998–2014 summer mean field in the Baltic Sea. Data from product reference 2.4.1.

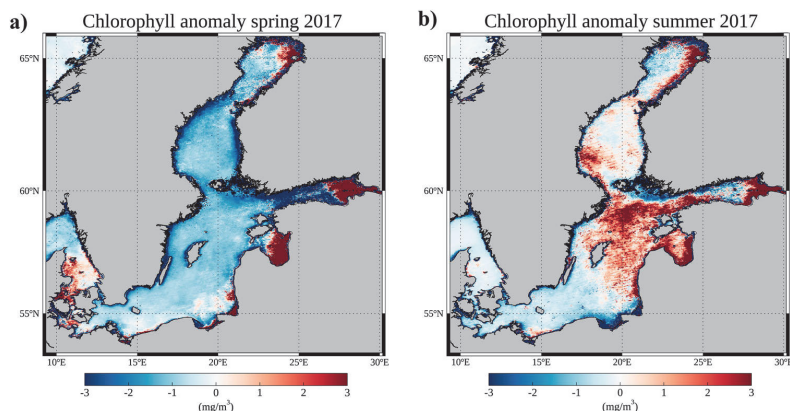


Figure 2.4.5. Chlorophyll-a anomaly fields in the Baltic Sea in spring 2017 relative to the 1998–2014 spring mean field (a) and in summer 2017 relative to the 1998–2014 summer mean field (b). Data from product reference 2.4.2.

matter could be a major contributor to the high attenuation coefficient values, elevated attenuation coefficient values are seen in the entire Baltic Proper and the Bothnian Sea. In spring 2017, attenuation coefficient anomaly is negative all over the Baltic Sea (Figure 2.4.4(c)). A very high positive attenuation coefficient anomaly in the southeastern Gulf of Riga and eastern Gulf of Finland could include contamination of attenuation coefficient values from ice coverage. The differences in the attenuation coefficient anomaly in the springs of 2016 and 2017 are well reflected in the spatiotemporal coverage of the spring bloom, with the 2017 spring bloom being less than half of the spring bloom in 2016 (Figure 2.4.2(a)). The attenuation coefficient anomaly in summer 2016 is higher than in 2017 (Figure 2.4.4(b,d)), which is reflected also in the summer mean attenuation coefficient values (Figure 2.4.3) and in the spatiotemporal coverage of subsurface bloom, but not in the surface bloom (Figure 2.4.2(b)). Measured phytoplankton wet weight during spring bloom has been substantially higher in 2016 than in 2017, but comparable in the summers of 2016 and 2017 (Wasmund et al. 2017, 2018). In general, by comparing time series of summer mean attenuation coefficient values and summer bloom spatiotemporal coverage (Figures 2.4.2(b) and 2.4.3), we conclude no obvious match of these two parameters.

Chlorophyll-a spring anomaly in 2017 showed high values in the Gulf of Riga and the eastern part of the Gulf of Finland. High values with a smaller extent were visible in the northern coastal area of the Bothnian Bay and coastal areas of the Gulf of Gdansk and the Curonian Lagoon. To a larger extent, lower values are evident in the western part of the Gulf of Finland. The spatial

distributions of measured chlorophyll-a are versatile in the spring of 2017 (Wasmund et al. 2018). In March, chlorophyll-a concentrations show higher values near the Danish Straits, with decreasing gradient towards the Gotland Basin. In May, the spatial gradient of chlorophyll-a was reversed – chlorophyll-a concentrations were significantly higher in the eastern and southern Gotland basin and lower near the Danish Straits.

Chlorophyll-a summer anomaly in 2017 has highest values in the eastern part of the Gulf of Finland and the Gulf of Riga, which extend further in space, compared to same areas in 2016 (Raudsepp et al. 2018). Extensive high chlorophyll-a values in the northern Baltic Proper in 2017 are not visible in 2016. At the same time, high chlorophyll-a values, which are seen across the Bothnian Bay in 2016, are only limited to the eastern coast in 2017. Both years share similarly low summer chlorophyll-a anomaly values in the Gulf of Gdansk and on the coasts of Lithuania and Kaliningrad, except for the outflow area from Curonian lagoon. In summer 2017, spatial differences in measured chlorophyll-a concentrations were relatively uniform in the southern Baltic, but much higher in the Eastern Gotland basin (Wasmund et al. 2018).

2.5. Cod reproductive volume potential in the Baltic Sea

Authors: Urmas Raudsepp, Ilja Maljutenko, Mariliis Kõuts

Statement of outcome: Cod (*Gadus morhua*) is a characteristic fish species in the Baltic Sea with major economic importance. The Baltic cod stocks have

- Le Cann B, Serpette A. 2009. Intense warm and saline upper ocean inflow in the southern Bay of Biscay in autumn-winter 2006–2007. *Cont Shelf Res.* 29(8):1014–1025.
- Pingree RD, Le Cann B. 1992. Three anticyclonic Slope Water Oceanic eDDIES (SWODDIES) in the southern Bay of Biscay in 1990. *Deep-Sea Res.* 39(7/8):1147–1175.
- Rubio A, Caballero A, Orfila A, Hernández-Carrasco I, Ferrer L, González M, Solabarrieta L, Mader J. 2018. Eddy-induced cross-shelf export of high Chl-a coastal waters in the SE Bay of Biscay. *Remote Sens Environ.* 205. doi:10.1016/j.rse.2017.10.037.
- Rubio A, Fontán A, Lazure P, González M, Valencia V, Ferrer L, Mader J, Hernández C. 2013. Seasonal to tidal variability of currents and temperature in waters of the continental slope, SE Bay of Biscay. *J Mar Syst.* 109–110:S121–S133.
- Rubio A, Reverdin G, Fontán A, González M, Mader J. 2011. Mapping near-inertial variability in the SE Bay of Biscay from HF radar data and two offshore moored buoys. *Geophys Res Lett.* 38(19):L19607.
- Solabarrieta L, Frolov S, Cook M, Paduan J, Rubio A, González M, Mader J, Charria G. 2016. Skill assessment of HF radar-derived products for Lagrangian simulations in the Bay of Biscay. *J Atmos Ocean Technol.* 33:2585–2597. doi:10.1175/TECH-D-16-0045.1.
- Solabarrieta L, Rubio A, Cárdenas M, Castanedo S, Esnaola G, Méndez FJ, Medina R, Ferrer L. 2015. Probabilistic relationships between wind and Surface water circulation patterns in the SE Bay of Biscay. *Ocean Dyn.* 65(9):1289–1303.
- Solabarrieta L, Rubio A, Castanedo S, Medina R, Fontán A, González M, Fernández V, Charria G, Hernández C. 2014. Surface water circulation patterns in the southeastern Bay of Biscay: new evidences from HF radar data. *Cont Shelf Res.* 74:60–76.
- Teles-Machado A, Peliz A, McWilliams J, Dubert J, Le Cann B. 2016. Circulation on the northwestern Iberian margin: swoddies. *Prog Oceanogr.* 140:116–133. doi:10.1016/j.poc.2015.09.011.
- Josey SA, Somot S, Tsimplis M. 2011. Impacts of atmospheric modes of variability on Mediterranean Sea surface heat exchange. *J Geophys Res.* 116:C02032.
- Naranjo C, García-Lafuente J, Sannarino S, Sánchez-Garrido JC, Sánchez-Leal R, Jesús Bellanco M. 2017. Recent changes (2004–2016) of temperature and salinity in the Mediterranean outflow. *Geophys Res Lett.* 44:5665–5672.
- Rixen M, Beckers JM, Levitus S, Antonov J, Boyer T, Maillard C, Fichaut M, Balopoulos E, Iona S, Dooley H, et al. 2005. The western Mediterranean deep water: a proxy for climate change. *Geophys Res Lett.* 32:L12608.
- von Schuckmann K, Le Traon P, Alvarez-Fanjul E, Axell L, Balmaseda M, Breivik L-A, Brewin RJW, Bricaud C, Drevillon M, Drillet Y, et al. 2018. The Copernicus marine service ocean state report issue 2. *J Oper Oceanogr.* 11 (sup1): s1–S142. doi:10.1080/1755876X.2018.14892808.
- Schroeder K, Chiggiato J, Bryden HL, Borghini M, Ben Ismail S. 2016. Abrupt climate shift in the western Mediterranean Sea. *Sci Rep.* 6:23009.
- Schroeder K, Chiggiato J, Josey SA, Borghini M, Aracri S, Sparnocchia S. 2017. Rapid response to climate change in a marginal sea. *Sci Rep.* 7:4065.
- Schroeder K, Millot C, Bengara L, Ben Ismail S, Bensi M, Borghini M, Budillon G, Cardin V, Coppola L, Curtil C, et al. 2013. Long-term monitoring programme of the hydrological variability in the Mediterranean Sea: a first overview of the hydrochanges network. *Ocean Sci.* 9:1–24.
- Vargas-Yáñez M, García-Martínez MC, Moya F, Balbín R, López-Jurado JL, Serra M, Zunino P, Pascual J, Salat J. 2017. Updating temperature and salinity mean values and trends in the western Mediterranean: THE RADMED project. *Prog Ocean.* 157:27–46.

Section 2.3. Mediterranean deep and intermediate water mass properties

- Ben Ismail S, Schroeder K, Sammari C, Gasparini GP, Aleya L. 2014. Interannual variability of water mass properties in the Tunisia–Sicily channel. *J Mar Syst.* 135:14–28.
- Bethoux JP, Gentili B. 1999. Functioning of the Mediterranean Sea: past and present changes related to fresh water input and climatic changes. *J Mar Syst.* 20:33–47.
- Cook BI, Anchukaitis KJ, Touchan R, Meko DM, Cook ER. 2016. Spatiotemporal drought variability in the Mediterranean over the last 900 years. *J Geophys Res Atmos.* 121:2060–2074.
- Gačić M, Schroeder K, Civitarese G, Cosoli S, Vetrano A, Eusebi Borzelli GL. 2013. Salinity in the Sicily channel corroborates the role of the Adriatic–Ionian Bimodal Oscillating System (BiOS) in shaping the decadal variability of the Mediterranean overturning circulation. *Ocean Sci.* 9:83–90.
- Gasparini GP, Ortona A, Budillon G, Astraldi M, Sansone E. 2005. The effect of the eastern Mediterranean transient on the hydrographic characteristics in the Strait of Sicily and in the Tyrrhenian Sea. *Deep-Sea Res.* 52:915–935.
- Giorgi F. 2006. Climate change Hot-spots. *Geophys Res Lett.* 33:L08707.
- Brewin RJW, Sathyendranath S, Müller D, Brockmann C, Deschamps P-Y, Devred E, Doerffer R, Fomferra N, Franz B, Grant M, et al. 2015. The ocean colour climate change initiative: III. A round-robin comparison on in-water bio-optical algorithms. *Remote Sens Environ.* 162:271–294. doi:10.1016/j.rse.2013.09.016.
- Fennel K. 1999. Convection and the timing of phytoplankton spring blooms in the western Baltic Sea. *Estuar Coast Shelf Sci.* 49(1):113–128. doi:10.1006/ecss.1999.0487.
- Groetsch PMM, Simis SGH, Eleveld MA, Peters SWM. 2016. Spring blooms in the Baltic Sea have weakened but lengthened from 2000 to 2014. *Biogeosciences.* 13(17):4959–4973. doi:10.5194/bg-13-4959-2016.
- Hansson M, Håkansson B. 2007. The Baltic algae watch system – a remote sensing application for monitoring cyanobacterial blooms in the Baltic Sea. *J Appl Remote Sens.* 1. doi:10.1117/1.2834769.
- Hansson M, Pamberton P, Håkansson B, Reinart A, Alikas K. 2010. Operational nowcasting of algal blooms in the Baltic Sea using MERIS and MODIS. *ESA Living Planet Symposium*; Bergen, Norway. Vol. 686.
- HELCOM. 2015. HELCOM eutrophication assessment manual. [accessed 2018 Jul 22]. [http://www.helcom.fi/Documents/Eutrophication assessment manual.pdf](http://www.helcom.fi/Documents/Eutrophication%20assessment%20manual.pdf).
- Kahru M, Elmgren R, Di Lorenzo E, Savchuk O. 2018. Unexplained interannual oscillations of cyanobacterial

Section 2.4. Phytoplankton blooms in the Baltic Sea

- blooms in the Baltic Sea. *Sci Rep.* 8(1):6365. doi:10.1038/s41598-018-24829-7.
- Kahru M, Nömmann S. 1990. The phytoplankton spring bloom in the Baltic Sea in 1985, 1986: multitude of spatio-temporal scales. *Cont Shelf Res.* 10(4):329–354. doi:10.1016/0278-4343(90)90055-Q.
- Mélin F, Vantrepotte V, Chuprin A, Grant M, Jackson T, Sathyendranath S. 2017. Assessing the fitness-for-purpose of satellite multi-mission ocean color climate data records: a protocol applied to OC-CCI chlorophyll-a data. *Remote Sens Environ.* 203:139–151. doi:10.1016/j.rse.2017.03.039.
- O'Reilly JE, Maritorena S, Mitchell BG, Siegel DA, Carder KL, Garver SA, Kahru M, McClain C. 1998. Ocean color chlorophyll algorithms for SeaWiFS. *J Geophys Res Ocean.* 103 (C11):24937–24953. doi:10.1029/98JC02160.
- Pitarch J, Volpe G, Colella S, Krasemann H, Santoleri R. 2016. Remote sensing of chlorophyll in the Baltic Sea at basin scale from 1997 to 2012 using merged multi-sensor data. *Ocean Sci.* 12(2):379–389. doi:10.5194/os-12-379-2016.
- Raudsepp U, She J, Brando VE, Kõuts M, Lagema P, Sammartino M, Santoleri R. 2018. Baltic inflows. In: von Schuckmann K, Le Traon P-Y, Smith N, Pascual A, Brasseur P, Fennel K, Djavidnia S, editors. Copernicus marine service ocean state report, issue 2. *J Oper Oceanogr.* 11 (sup1):s13–s16. doi:10.1080/1755876X.2018.1489208.
- Sathyendranath S, Brewin RJW, Jackson T, Mélin F, Platt T. 2017. Ocean-colour products for climate-change studies: what are their ideal characteristics? *Remote Sens Environ.* 203:125–138. doi:10.1016/j.rse.2017.04.017.
- Siegel DA. 2002. The north Atlantic spring phytoplankton bloom and Sverdrup's critical depth hypothesis. *Science.* 296(5568):730–733. doi:10.1126/science.1069174.
- Wan Z, Bi H, She J. 2013. Comparison of two light attenuation parameterization focusing on timing of spring bloom and primary production in the Baltic Sea. *Ecol Modell.* 259:40–49. doi:10.1016/j.ecolmodel.2013.03.010.
- Wasmund N, Dutz J, Pollehne F, Siegel H, Zettler ML. 2017. Biological assessment of the Baltic Sea 2016. Warnemünde: Leibniz Institute for Baltic Sea Research. *Mar Sci Rep.* 105. doi:10.12754/msr-2017-0105.
- Wasmund N, Dutz J, Pollehne F, Siegel H, Zettler ML. 2018. Biological assessment of the Baltic Sea 2017. Warnemünde: Leibniz Institute for Baltic Sea Research. *Mar Sci Rep.* 108. doi:10.12754/msr-2018-0108.
- Section 2.5. Cod reproductive volume potential in the Baltic Sea**
- Cardinale M, Arrhenius F. 2000. The influence of stock structure and environmental conditions on the recruitment process of Baltic cod estimated using a generalized additive model. *Can J Fish Aquat Sci.* 57(12):2402–2409. doi:10.1139/f00-221.
- Cardinale M, Modin J. 1999. Changes in size-at-maturity of Baltic cod (*Gadus morhua*) during a period of large variations in stock size and environmental conditions. *Fish Res.* 41(3):285–295. doi:10.1016/S0165-7836(99)00021-1.
- EFSA Publication, Nielsen R. 1998. Mechanisms influencing long term trends in reproductive success and recruitment of Baltic cod: implication for fisheries management: CORE program final report. EU Commission DGXIV, I-III. [s.l.]: European Commission. EU AIR2. CT94-1226.
- Heikinheimo O. 2008. Average salinity as an index for environmental forcing on cod recruitment in the Baltic Sea. *Boreal Environ Res.* 13:457–464.
- Hinrichsen H-H, von Dewitz B, Lehmann A, Bergström U, Hüsey K. 2017. Spatio-temporal dynamics of cod nursery areas in the Baltic Sea. *Prog Oceanogr.* 155:28–40. doi:10.1016/j.pocean.2017.05.007.
- ICES. 2005. Report of the study group on multispecies assessment in the Baltic (SGMAB); Jun 13–17; Riga, Latvia. *ICES CM 2005/H:06.*
- ICES. 2016. Report of the Baltic fisheries assessment working group (WGBFAS); Apr 12–19; Copenhagen, Denmark. *ICES HQ. ICES CM 2016/ACOM:11.*
- ICES. 2018. ICES advice on fishing opportunities, catch, and effort. <https://doi.org/10.17895/ices.pub.4378>.
- Karaseva EM, Zezera AS. 2016. Causes of different impact of major Baltic inflows on cod reproduction in the Gotland basin of the Baltic Sea. *Oceanology.* 56(5):643–654. doi:10.1134/S0001437016040068.
- Karasiova EM. 2011. Assessment of production of eggs of eastern Baltic cod (*Gadus morhua callarias* L.) on the basis of long-term ichthyoplankton data. *Russ J Dev Biol.* 42 (3):168–172. doi:10.1134/S1062360411030076.
- Karasiova EM, Voss R, Eero M. 2008. Long-term dynamics in eastern Baltic cod spawning time: from small scale reversible changes to a recent drastic shift. *ICES CM 2008/J:03.*
- Köster FW, Möllmann C, Hinrichsen H-H, Wieland K, Tomkiewicz J, Kraus G, Voss R, Makarchouk A, MacKenzie BR, St John MA, et al. 2005. Baltic cod recruitment – the impact of climate variability on key processes. *ICES J Mar Sci.* 62(7):1408–1425. doi:10.1016/j.icesjms.2005.05.004.
- MacKenzie B, St John M, Wieland K. 1996. Eastern Baltic cod: perspectives from existing data on processes affecting growth and survival of eggs and larvae. *Mar Ecol Prog Ser.* 134:265–281. doi:10.3354/meps134265.
- Plikshs M, Hinrichsen H-H, Elferts D, Sics I, Kornilovs G, Köster FW. 2015. Reproduction of Baltic cod, *Gadus morhua* (Actinopterygii: Gadiformes: Gadidae), in the Gotland basin: causes of annual variability. *Acta Ichthyol Piscat.* 45 (3):247–258. doi:10.3750/AIP2015.45.3.04.
- Raudsepp U, Legeais J-F, She J, Maljutenko I, Jandt S. 2018. Baltic inflows. In: von Schuckmann K, Le Traon P-Y, Smith N, Pascual A, Brasseur P, Fennel K, Djavidnia S, editors. Copernicus marine service ocean state report, issue 2. *J Oper Oceanogr.* 11(sup1):s13–s16. doi:10.1080/1755876X.2018.1489208.
- Section 2.6. The North Pacific Gyre Oscillation**
- Di Lorenzo E, Schneider N, Cobb KM, Chhak K, Franks PJS, Miller AJ, McWilliams JC, Bograd SJ, Arango H, Curchister E, et al. 2008. North Pacific gyre oscillation links ocean climate and ecosystem change. *Geophysical Research Letters.* 35:L08607.
- Kalnay E, Kanamitsu M, Kistler R, Collins W, Deaven D, Gandin L, Iredell M, Saha S, White G, Woollen J, et al. 1996. The NCEP/NCAR 40-year reanalysis project. *Bull Am Meteor Soc.* 77:437–471.

Paper IV

Kõuts, M., Maljutenko, I., Liu, Y. and Raudsepp, U., 2021. **Nitrate, ammonium and phosphate pools in the Baltic Sea.** In: Copernicus Marine Service Ocean State Report, Issue 5, Journal of Operational Oceanography, 14:sup1, pp. s140–s148; DOI: 10.1080/1755876X.2021.1946240



Copernicus Marine Service Ocean State Report, Issue 5

Karina von Schuckmann ((Editor)), Pierre-Yves Le Traon ((Editor)), Neville Smith (Chair) ((Review Editor)), Ananda Pascual ((Review Editor)), Samuel Djavidnia ((Review Editor)), Jean-Pierre Gattuso ((Review Editor)), Marilaure Grégoire ((Review Editor)), Signe Aaboe, Victor Alari, Brittany E. Alexander, Andrés Alonso-Martirena, Ali Aydogdu, Joel Azzopardi, Marco Bajo, Francesco Barbariol, Mirna Batistić, Arno Behrens, Sana Ben Ismail, Alvis Benetazzo, Isabella Bitetto, Mireno Borghini, Laura Bray, Arthur Capet, Roberto Carlucci, Sourav Chatterjee, Jacopo Chiggiato, Stefania Ciliberti, Giulia Cipriano, Emanuela Clementi, Paul Cochrane, Gianpiero Cossarini, Lorenzo D'Andrea, Silvio Davison, Emily Down, Aldo Drago, Jean-Noël Druon, Georg Engelhard, Ivan Federico, Rade Garić, Adam Gauci, Riccardo Gerin, Gerhard Geyer, Rianne Giesen, Simon Good, Richard Graham, Marilaure Grégoire, Eric Greiner, Kjell Gundersen, Pierre Hélaouët, Stefan Hendricks, Johanna J. Heymans, Jason Holt, Marijana Hure, Mélanie Juza, Dimitris Kassis, Paula Kellett, Maaïke Knol-Kauffman, Panagiotis Kountouris, Marilii Kõuts, Priidik Lagemaa, Thomas Lavergne, Jean-François Legeais, Pierre-Yves Le Traon, Simone Libralato, Vidar S. Lien, Leonardo Lima, Sigrid Lind, Ye Liu, Diego Macías, Ilja Maljutenko, Antoine Mangin, Arne Männik, Veselka Marinova, Riccardo Martellucci, Francesco Masnadi, Elena Mauri, Michael Mayer, Milena Menna, Catherine Meulders, Jane S. Møgster, Maeva Monier, Kjell Arne Mork, Malte Müller, Jan Even Øie Nilsen, Giulio Notarstefano, José L. Oviedo, Cyril Palerme, Andreas Pali Alexis, Diego Panzeri, Silvia Pardo, Elisaveta Peneva, Paolo Pezzutto, Annunziata Pirro, Trevor Platt, Pierre-Marie Poulain, Laura Prieto, Stefano Querin, Lasse Rabenstein, Roshin P. Raj, Urmas Raudsepp, Marco Reale, Richard Renshaw, Antonio Ricchi, Robert Ricker, Sander Rikka, Javier Ruiz, Tommaso Russo, Jorge Sanchez, Rosalia Santoleri, Shubha Sathyendranath, Giuseppe Scarcella, Katrin Schroeder, Stefania Sparnocchia, Maria Teresa Spedicato, Emil Stanev, Joanna Staneva, Alexandra Stocker, Ad Stoffelen, Anna Teruzzi, Bryony Townhill, Rivo Uiboupin, Nadejda Valcheva, Luc Vandenbulcke, Håvard Vindenes, Karina von Schuckmann, Nedo Vrgoč, Sarah Wakelin & Walter Zupa

To cite this article: Karina von Schuckmann ((Editor)), Pierre-Yves Le Traon ((Editor)), Neville Smith (Chair) ((Review Editor)), Ananda Pascual ((Review Editor)), Samuel Djavidnia ((Review Editor)), Jean-Pierre Gattuso ((Review Editor)), Marilaure Grégoire ((Review Editor)), Signe Aaboe, Victor Alari, Brittany E. Alexander, Andrés Alonso-Martirena, Ali Aydogdu, Joel Azzopardi, Marco Bajo, Francesco Barbariol, Mirna Batistić, Arno Behrens, Sana Ben Ismail, Alvis Benetazzo, Isabella Bitetto, Mireno Borghini, Laura Bray, Arthur Capet, Roberto Carlucci, Sourav Chatterjee, Jacopo Chiggiato, Stefania Ciliberti, Giulia Cipriano, Emanuela Clementi, Paul Cochrane, Gianpiero Cossarini, Lorenzo D'Andrea, Silvio Davison, Emily Down, Aldo Drago, Jean-Noël Druon, Georg Engelhard, Ivan Federico, Rade Garić, Adam Gauci, Riccardo Gerin, Gerhard Geyer, Rianne

Giesen, Simon Good, Richard Graham, Marilaure Grégoire, Eric Greiner, Kjell Gundersen, Pierre Hélaouët, Stefan Hendricks, Johanna J. Heymans, Jason Holt, Marijana Hure, Mélanie Juza, Dimitris Kassis, Paula Kellett, Maaïke Knol-Kauffman, Panagiotis Kountouris, Marilii Kouts, Priidik Lagemaa, Thomas Lavergne, Jean-François Legeais, Pierre-Yves Le Traon, Simone Libralato, Vidar S. Lien, Leonardo Lima, Sigrid Lind, Ye Liu, Diego Macías, Ilja Maljutenko, Antoine Mangin, Arne Männik, Veselka Marinova, Riccardo Martellucci, Francesco Masnadi, Elena Mauri, Michael Mayer, Milena Menna, Catherine Meulders, Jane S. Møgster, Maeva Monier, Kjell Arne Mork, Malte Müller, Jan Even Øie Nilsen, Giulio Notarstefano, José L. Oviedo, Cyril Palerme, Andreas Palialexis, Diego Panzeri, Silvia Pardo, Elisaveta Peneva, Paolo Pezzutto, Annunziata Pirro, Trevor Platt, Pierre-Marie Poulain, Laura Prieto, Stefano Querin, Lasse Rabenstein, Roshin P. Raj, Urmas Raudsepp, Marco Reale, Richard Renshaw, Antonio Ricchi, Robert Ricker, Sander Rikka, Javier Ruiz, Tommaso Russo, Jorge Sanchez, Rosalia Santoleri, Shubha Sathyendranath, Giuseppe Scarcella, Katrin Schroeder, Stefania Sparnocchia, Maria Teresa Spedicato, Emil Stanev, Joanna Staneva, Alexandra Stocker, Ad Stoffelen, Anna Teruzzi, Bryony Townhill, Rivo Uiboupin, Nadejda Valcheva, Luc Vandenbulcke, Håvard Vindenes, Karina von Schuckmann, Nedo Vrgoč, Sarah Wakelin & Walter Zupa (2021) Copernicus Marine Service Ocean State Report, Issue 5, Journal of Operational Oceanography, 14:sup1, 1-185, DOI: [10.1080/1755876X.2021.1946240](https://doi.org/10.1080/1755876X.2021.1946240)

To link to this article: <https://doi.org/10.1080/1755876X.2021.1946240>



© 2021 The Author(s). Published by Informa UK Limited, trading as Taylor & Francis Group



View supplementary material [↗](#)



Published online: 22 Sep 2021.



Submit your article to this journal [↗](#)



Article views: 15182



View related articles [↗](#)



View Crossmark data [↗](#)



Citing articles: 1 View citing articles [↗](#)

COPERNICUS MARINE SERVICE OCEAN STATE REPORT, ISSUE 5

Editors

Karina von Schuckmann

Pierre-Yves Le Traon

Review Editors

Neville Smith (Chair)

Ananda Pascual

Samuel Djavidnia

Jean-Pierre Gattuso

Marilaure Grégoire

To cite the entire report

How to cite the entire report: von Schuckmann, K., P.-Y. Le Traon, N. Smith, A. Pascual, S. Djavidnia, J.-P. Gattuso, M. Grégoire (Eds.) (2021) Copernicus Marine Service Ocean State Report, Issue 5, Journal of Operational Oceanography, 14:sup1, s1–s185; DOI: 10.1080/1755876X.2021.1946240

To cite a specific section in the report (example)

S. Aaboe, S. Lind, S. Hendricks, E. Down, T. Lavergne and R. Ricker (2021). Sea-ice and ocean conditions surprisingly normal in the Svalbard-Barents Sea region after large sea-ice inflows in 2019. In: Copernicus Marine Service Ocean State Report, Issue 5, Journal of Operational Oceanography, 14:sup1, s140–s148; DOI: 10.1080/1755876X.2021.1946240

AUTHOR AFFILIATIONS (ALPHABETICAL BY NAME)

Signe Aaboe, MET Norway, Norway
Victor Alari, Tallinn University of Technology (TalTech), Estonia
Brittany E. Alexander, European Marine Board, Belgium
Andrés Alonso-Martirena, Qualitas Instruments S.A., Spain
Ali Aydogdu, Fondazione Centro Euro-Mediterraneo sui Cambiamenti Climatici, Italy
Joel Azzopardi, University of Malta, Malta
Marco Bajo, Institute of Marine Sciences (CNR-ISMAR), Italy
Francesco Barbariol, Consiglio Nazionale delle Ricerche, Istituto di Scienze Marine (CNR-ISMAR), Italy
Mirna Batistić, University of Dubrovnik, Institute for Marine and Coastal Research, Croatia
Arno Behrens, Helmholtz-Zentrum Geesthacht, Zentrum für Material- und Küstenforschung GmbH, Germany
Sana Ben Ismail, Institut National des Sciences et Technologies de la Mer (INSTM), Tunisia
Alvise Benetazzo, Consiglio Nazionale delle Ricerche, Istituto di Scienze Marine (CNR-ISMAR), Italy
Isabella Bitetto, COISPA Tecnologia & Ricerca, Italy
Mireno Borghini, Consiglio Nazionale delle Ricerche, Istituto di Scienze Marine (CNR-ISMAR), Italy
Laura Bray, Hellenic Centre of Marine Research, Greece
Arthur Capet, University of Liège, MAST, Department of Astrophysics, Geophysics and Oceanography, Belgium
Roberto Carlucci, Department of Biology, University of Bari; CoNISMa, Italy
Sourav Chatterjee, National Center for Polar Ocean Research (NCPOR), Ministry of Earth Sciences, India
Jacopo Chiggiato, Consiglio Nazionale delle Ricerche, Istituto di Scienze Marine (CNR-ISMAR), Italy
Stefania Ciliberti, Fondazione Centro Euro-Mediterraneo sui Cambiamenti Climatici, Italy
Giulia Cipriano, Department of Biology, University of Bari; CoNISMa, Italy
Emanuela Clementi, Euro-Mediterranean Center on Climate Change (CMCC), Italy
Paul Cochrane, Drift+Noise, Germany
Gianpiero Cossarini, National Institute of Oceanography and Applied Geophysics (OGS), Italy
Lorenzo D'Andrea, Laboratory of Experimental Ecology and Aquaculture, Dept. of Biology, University of Rome, Italy
Silvio Davison, Consiglio Nazionale delle Ricerche, Istituto di Scienze Marine (CNR-ISMAR), Italy
Emily Down, MET Norway, Norway
Aldo Drago, University of Malta, Malta
Jean-Noël Druon, Joint Research Centre, European Commission, Italy
Georg Engelhard, Centre for Environment, Fisheries and Aquaculture Science (Cefas), UK
Ivan Federico, Euro-Mediterranean Center on Climate Change (CMCC), Italy
Rade Garić, University of Dubrovnik, Institute for Marine and Coastal Research, Croatia
Adam Gauci, University of Malta, Malta
Riccardo Gerin, National Institute of Oceanography and Applied Geophysics (OGS), Italy
Gerhard Geyer, Helmholtz-Zentrum Geesthacht, Zentrum für Material- und Küstenforschung GmbH, Germany
Rianne Giesen, Royal Netherlands Meteorological Institute (KNMI), Netherlands
Simon Good, Met Office, UK
Richard Graham, Met Office, UK
Marilaure Grégoire, University of Liège, MAST, Department of Astrophysics, Geophysics and Oceanography, Belgium
Eric Greiner, Collect Localisation Satellites (CLS), France
Kjell Gundersen, Institute of Marine Research (IMR), Norway
Pierre Hélaouët, Marine Biological Association of the United Kingdom, UK
Stefan Hendricks, Alfred Wegener Institute Helmholtz Center for Polar and Marine Research, Germany
Johanna J. Heymans, European Marine Board, Belgium
Jason Holt, NOC, UK
Marijana Hure, University of Dubrovnik, Institute for Marine and Coastal Research, Croatia
Mélanie Juza, Balearic Islands Coastal Observing and forecasting System (SOCIB), Spain
Dimitris Kassis, Hellenic Centre of Marine Research, Greece
Paula Kellett, European Marine Board, Belgium
Maaike Knol-Kauffman, Norwegian College of Fishery Science, University of Tromsø - The Arctic University of Norway, Norway
Panagiotis Kountouris, Drift+Noise, Germany
Mariiii Kõuts, Tallinn University of Technology (TalTech), Estonia
Priidik Lagemaa, Tallinn University of Technology (TalTech), Estonia
Thomas Lavergne, MET Norway, Norway
Jean-François Legeais, Collect Localisation Satellites (CLS), France
Pierre-Yves Le Traon, Mercator Ocean International, France
Simone Libralato, National Institute of Oceanography and Applied Geophysics (OGS), Italy
Vidar S. Lien, Institute of Marine Research (IMR), Norway
Leonardo Lima, Fondazione Centro Euro-Mediterraneo sui Cambiamenti Climatici, Italy
Sigrud Lind, Norwegian Polar Institute, Norway
Ye Liu, Swedish Meteorological and Hydrological institute (SMHI), Estonia

(Continued from previous page)

Diego Macías, European Commission, Joint Research Centre (JRC), Italy
Ilija Maljutenko, Tallinn University of Technology (TalTech), Estonia
Antoine Mangin, ACRI-ST, France
Aarne Männik, Tallinn University of Technology (TalTech), Estonia
Veselka Marinova, Institute of Oceanology, Bulgarian Academy of Science, Bulgaria
Riccardo Martellucci, National Institute of Oceanography and Applied Geophysics (OGS), Italy
Francesco Masnadi, Università di Bologna, Dipartimento di Scienze Biologiche, Geologiche e Ambientali (UNIBO-Bigea); Consiglio Nazionale delle Ricerche, Istituto per le Risorse Biologiche e le Biotecnologie Marine sede di Ancona (CNR-IRBIM), Italy
Elena Mauri, National Institute of Oceanography and Applied Geophysics (OGS), Italy
Michael Mayer, Department of Meteorology and Geophysics, University of Vienna, Austria and European Centre for Medium-Range Weather Forecasts, UK
Milena Menna, National Institute of Oceanography and Applied Geophysics (OGS), Italy
Catherine Meulders, University of Liège, MAST, Department of Astrophysics, Geophysics and Oceanography, Belgium
Jane S. Møgster, Institute of Marine Research (IMR), Norway
Maeva Monier, CLAD, Mercator Océan International, France
Kjell Arne Mork, Institute of Marine Research (IMR), Norway
Malte Müller, Development Centre for Weather Forecasting, Norwegian Meteorological Institute, Norway
Jan Even Øie Nilsen, Institute of Marine Research (IMR), Norway
Giulio Notarstefano, National Institute of Oceanography and Applied Geophysics (OGS), Italy
José L. Oviedo, Instituto de Ciencias Marinas de Andalucía, Consejo Superior de Investigaciones Científicas (ICMAN-CSIC), Spain
Cyril Palerme, Development Centre for Weather Forecasting, Norwegian Meteorological Institute, Norway
Andreas Palialexis, Joint Research Centre, European Commission, Italy
Diego Panzeri, National Institute of Oceanography and Applied Geophysics (OGS); Università degli Studi di Trieste, Italy
Silvia Pardo, Plymouth Marine Laboratory, UK
Elisaveta Peneva, Sofia University St. Kliment Ohridski, Bulgaria
Paolo Pezzutto, Consiglio Nazionale delle Ricerche, Istituto di Scienze Marine (CNR-ISMAR), Italy
Annunziata Pirro, National Institute of Oceanography and Applied Geophysics (OGS), Italy
Trevor Platt, Plymouth Marine Laboratory, UK
Pierre-Marie Poulain, National Institute of Oceanography and Applied Geophysics (OGS), Italy
Laura Prieto, Instituto de Ciencias Marinas de Andalucía, Consejo Superior de Investigaciones Científicas (ICMAN-CSIC), Spain
Stefano Querin, National Institute of Oceanography and Applied Geophysics (OGS), Italy
Lasse Rabenstein, Drift+Noise, Germany
Roshin P. Raj, Nansen Environmental and Remote Sensing Center (NERSC), Norway
Urmas Raudsepp, Tallinn University of Technology (TalTech), Estonia
Marco Reale, National Institute of Oceanography and Applied Geophysics (OGS); Abdus Salam, ICTP, Italy
Richard Renshaw, Met Office, UK
Antonio Ricchi, Department of Physical and Chemical Sciences/ CETEMPS, University of L'Aquila, Italy
Robert Ricker, Alfred Wegener Institute Helmholtz Center for Polar and Marine Research, Germany
Sander Rikka, Tallinn University of Technology (TalTech), Estonia
Javier Ruiz, Instituto Español de Oceanografía (IEO), Spain
Tommaso Russo, Laboratory of Experimental Ecology and Aquaculture, Dept. of Biology, University of Rome; CONISMA, Italy
Jorge Sanchez, Qualitas Instruments S.A., Spain
Rosalía Santoleri, Institute of Marine Sciences (CNR-ISMAR), Italy
Shubha Sathyendranath, Plymouth Marine Laboratory, UK
Giuseppe Scarcella, Consiglio Nazionale delle Ricerche, Istituto per le Risorse Biologiche e le Biotecnologie Marine sede di Ancona (CNR-IRBIM), Italy
Katrin Schroeder, Consiglio Nazionale delle Ricerche, Istituto di Scienze Marine (CNR-ISMAR), Italy
Stefania Sparnocchia, Consiglio Nazionale delle Ricerche, Istituto di Scienze Marine (CNR-ISMAR), Italy
Maria Teresa Spedicato, COISPA Tecnologia & Ricerca, Italy
Emil Stanev, Helmholtz-Zentrum Geesthacht, Zentrum für Material- und Küstenforschung GmbH, Germany
Joanna Staneva, Helmholtz-Zentrum Geesthacht. Zentrum für Material- und Küstenforschung GmbH, Germany
Alexandra Stocker, Department of Geography, Sweden
Ad Stoffelen, Royal Netherlands Meteorological Institute (KNMI), Netherlands
Anna Teruzzi, National Institute of Oceanography and Applied Geophysics (OGS), Italy
Bryony Townhill, Centre for Environment, Fisheries and Aquaculture Science (Cefas), UK
Rivo Uiboupin, Tallinn University of Technology (TalTech), Estonia
Nadejda Valcheva, Institute of Oceanology, Bulgarian Academy of Science, Bulgaria
Luc Vandenbulcke, University of Liège, MAST, Department of Astrophysics, Geophysics and Oceanography, Belgium
Håvard Vindenes, Institute of Marine Research (IMR), Norway
Karina von Schuckmann, Mercator Ocean International, France
Nedo Vrgoč, Institute of Oceanography and Fisheries, Croatia
Sarah Wakelin, NOC, UK
Walter Zupa, COISPA Tecnologia & Ricerca, Italy

status across offshore and outer coastal waters of the Greater North Sea, with a decrease in the size of coastal problem areas in Denmark, France, Germany, Ireland, Norway and the United Kingdom. The absence of active eutrophic flags in the North Sea coastal regions might reflect these trends and a low occurrence of eutrophic episodes during 2019.

2.4.4. Conclusions

The indicators developed here provide a tool to monitor spatial and temporal variations in chlorophyll concentration. While various regions have been flagged as eutrophic/oligotrophic in the 2019 indicator map (Figure 2.4.4), we can only talk about eutrophication/oligotrophication when this state is sustained and showcases a significant trend across a longer period of time. Following studies will only benefit from progressive temporal extensions of the dataset (improving the significance of the climatologies) and from the incorporation of high-resolution satellite ocean colour datasets – such as Sentinel3 OLCI – into the CMEMS OC-CCI REP dataset.

From the results obtained in Figure 2.4.4, we can conclude that the occurrence of eutrophic episodes (chlorophyll concentration higher than the P90 climatological value for more than 25% valid observations) was very low during 2019. Nonetheless, the eutrophic indicator provided in Figure 2.4.2 included some significant P90 anomalies in the 15% to 25% range, and lowering the threshold from 25% to 15% would result in an increase in the areas flagged as eutrophic in Figure 2.4.4. This implies that the 2019 eutrophic episodes in those regions were shorter in duration than their typical phytoplankton growth season. While most regional studies identify the growth season as the standard period for heightened eutrophication risk, and employ it to compute P90 climatologies (Gohin et al. 2008), this paper employed whole-year datasets for the calculation of the P90 and P10 climatologies. This approach was motivated by the need to report on the broad CMEMS North Atlantic region, which includes both coastal and open waters characterised by different productive periods.

It is worth noting that the absence of flags in the top left quarter of Figure 2.4.4 was due to the low significance of the P90/P10 indicators. The impact of satellite data quality and availability in the accuracy of eutrophication indicators has been highlighted for various ocean colour datasets (Gohin et al. 2008; Ha et al. 2014), with Van der Zande et al. (2011) demonstrating that the mean relative error in the estimation of the P90 values can reach 25.4% for MERIS. While the use of the climate-grade CMEMS OC-CCI REP dataset ameliorates these issues by merging various bias-corrected ocean

colour streams (increasing the coverage and sampling frequency), some well-known eutrophication problem areas seem to be below our threshold of detection using the percentile climatology method presented here. This is the case for the coastal waters of the Skagerrak and Kattegat straits, where the significance of the percentile climatologies was too small to confirm previous trends reported for these problem areas (Andersen et al. 2016).

Section 2.5. Nitrate, ammonium and phosphate pools in the Baltic Sea

Authors: Mariliis Kõuts, Ilja Maljutenko, Ye Liu, Urmas Raudsepp

Statement of outcome: Eutrophication is a challenge in the Baltic Sea, with estimates of annual total input of about 830 kT of nitrogen and 31 kT of phosphorus in 2014. Nutrient and oxygen pools were estimated using model reanalysis data. During the period of 1993–2017, the pelagic nitrate pool decreased from ~2400 to 1700 kT in the Baltic Sea. The reduction of the nitrate pool was uniform over the Baltic Sea, with the exception of the Gulf of Bothnia, where decrease in the intermediate layer was small or even turned into an increase in the deep layer. Pelagic ammonium pools increased in the deep layer of the Baltic Proper due to decreasing oxygen concentrations there. The pelagic phosphate pool increased from ~600 to 750 kT, with most of the increase taking place in the surface and intermediate layers. The pool in the deep layer remained on a more stable level, with only a slight increasing trend. The increase of the phosphate pool covers the Baltic Proper area. In the Gulf of Bothnia, a decrease of phosphate has occurred in the upper layers and a slight increase in the deep layer. Only slight changes in the oxygen pool can bring about significant changes in the nutrient pools. Decreasing dissolved inorganic nitrogen pools and increasing phosphorus pools in the water column across the entire Baltic Sea, with the exception of the Bothnian Bay, results in a decreasing nitrogen to phosphorus ratio.

Ref. No.	Product name & type	Documentation
2.5.1	BALTICSEA_REANALYSIS_BIO_003_012 Model reanalysis	PUM: https://marine.copernicus.eu/documents/PUM/CMEMS-BAL-PUM-003-012.pdf QUID: https://marine.copernicus.eu/documents/QUID/CMEMS-BAL-QUID-003-012.pdf

2.5.1. Introduction

Eutrophication is a major challenge in the Baltic Sea, with at least 97% of the region assessed as eutrophied in 2011–2016 according to the HELCOM thematic assessment of eutrophication (HELCOM 2018a). However, the validity of this statement is questionable, as the least eutrophied basin – the Gulf of Bothnia – constitutes as much as 25.16% of the Baltic Sea volume. The HELCOM Eutrophication Assessment (HELCOM 2018a) featured nutrient levels, specifically winter dissolved inorganic phosphate and nitrogen, in the upper 10 m of the water column. According to the assessment, dissolved inorganic nitrogen varied from 3–5 $\mu\text{mol l}^{-1}$ in the Bothnian Bay to $\sim 10 \mu\text{mol l}^{-1}$ in the Gulf of Riga. A similar pattern occurred with dissolved inorganic phosphorus levels, which varied from 0.04 $\mu\text{mol l}^{-1}$ in the Bothnian Bay to $\sim 1.3 \mu\text{mol l}^{-1}$ in the Gulf of Riga. The hypotheses about the Gulf of Bothnia showing a tendency to become eutrophied are currently emerging (Lundberg et al. 2009; Fleming-Lehtinen et al. 2015; Andersen et al. 2017).

Eutrophication is caused by the addition of nutrients from land that accumulate in the marine system. In 2014, the Baltic Sea received an annual total input of about 826,000 tons of nitrogen and 30,900 tons of phosphorus (HELCOM 2018a). Atmospheric inputs account for about 30% of total nitrogen inputs (HELCOM 2018a). The input has decreased since the 1980s to the level of the 1960s for nitrogen and to the level of the 1950s for phosphorus by 2014 (HELCOM 2018a). The importance of nutrients is illustrated by different trophic states the ecosystem can evolve into, depending on the scale of nutrient inputs (Meier et al. 2012; Saraiva et al. 2019; Murray et al. 2019). History has shown that a massive input of nutrients into any lake or sea, including the Baltic, results in a disrupted ecosystem that eventually brings about eutrophication (Gustafsson et al. 2012; Murray et al. 2019). The aforementioned reductions in nutrient inputs are expected to be reflected in the time series of the pools.

The aim of this study is to assess the nutrient status of the Baltic Sea using model reanalysis data for the period 1993–2017. Based on our results, we can evaluate the possible problem areas as well as the success of mitigation measures so far. We can evaluate the state-of-the-art quality of the reanalysis in the Baltic Sea. We do not claim that our analyses are unique, but rather, we intend to provide another set of estimates of total nutrient pools to the family of already existing estimates. Having an ‘ensemble’ of estimates obtained with different tools narrows the interval of uncertainties around the ‘true’ value.

2.5.2. Materials and methods

The BALMFC CMEMS biochemistry reanalysis product (product reference 2.5.1) is calculated using the Nemo-Nordic physical model (Hordoir et al. 2019; Pemberton et al. 2017) coupled with the Swedish Coastal and Ocean Biogeochemical model (SCOBIM) (Eilola et al. 2009; Almroth-Rosell et al. 2015). The model system uses the Localised Singular Evolutive Interpolated Kalman filter data assimilation method (LSEIK, Nerger et al. 2005).

The model domain consists of the North Sea and the Baltic Sea (Hordoir et al. 2019). The horizontal resolution of the Nemo-Nordic model is approximately 2 nautical miles, and there are 56 vertical levels. Vertical resolution varies from 3 m at the surface up to 10 m below the depth of 100 m. The numerical model simulation data for this research covers the period 1993–2017 (product reference 2.5.1). At the lateral boundaries in the western English Channel and along the Scotland-Norway boundary, the sea levels are prescribed using 24 nautical mile resolution storm-surge North Atlantic Model. Climatological monthly mean values of temperature, salinity and biogeochemical variables are used at the open boundary. Atmospheric deposition of biogeochemical substances is supplied as spatial maps of a monthly climatology.

The river runoff is specified as daily means for the whole reanalysis period, 1993–2017, from the output of the Hydrological Predictions for the Environment (HYPER) model (Donnelly et al. 2016). The nutrient loads are specified as monthly mean values. River runoff as well as nutrient load are spread over more than 250 rivers located in the Baltic Sea (Hordoir et al. 2019).

The meteorological forcing is from HIRLAM (High-Resolution Limited Area Model) with a 22 km resolution, from project Euro4M (Dahlgren et al. 2016; Landelius et al. 2016), and covers most of the reanalysis period, 1993–2011. From 2012 onwards, the meteorological forcing is from the UERRA reanalysis product (European Regional analysis) with an 11 km resolution.

The sea surface temperature from the Swedish Ice Service and in-situ measured temperature and salinity profiles from the ICES database (www.ices.dk) are assimilated into the physical model. In-situ profiles of nitrate, ammonium, phosphate and dissolved oxygen from the Swedish Ocean Archive database (SHARK; <https://sharkweb.smhi.se>) are assimilated into the biogeochemical model. In total, 3200 nitrate, 3500 ammonium, 4000 phosphate and 7500 dissolved oxygen profiles were assimilated into the model. Spatial data coverage was strongly inhomogeneous, with high density data at the Swedish coast and in the western Baltic

Sea, less so in the eastern Baltic sea, and in the Gulf of Riga and Gulf of Finland there were only a few profiles. The reanalysis has been produced using 72-hour cycling, which implies that every 72 h all available observations are assimilated into the model before a 72-hour forecast is made. When there was more than one observation per model layer, an average value of the observations in the same layer was used.

In addition to model reanalysis data validation provided in the QUID, we have compared model reanalysis data with the observation data at the central Gotland basin and in the Gulf of Riga for the period 1993–2017. The nutrients concentrations have been extracted at central Gotland basin (BMPJ1 / BY15) and from the Gulf of Riga (BMPG1/ G1) from the model simulation and compared with observational data extracted from two different databases. The observational data has been extracted from The Marine distributed databases in the NEST system (Wulff et al. 2013), which provides monthly mean aggregate data at reference depths, and from the EMODnet database (Buga et al. 2018), which provides data at measured time and depth levels.

Main statistics of the comparison at BY15 for surface and bottom nutrients are summarised in Table 2.5.1. We have used the data from the EMODnet database. The differences in the statistics for the NEST database and the model reanalysis were marginal compared to the EmodNet data. Cost function (CF) was formulated as $CF = |(M-D)/SD|$, where the bias (M-D) of the model mean (M) relative to the mean of observations (D) is normalised to the standard deviation (SD) of the observations (Eilola et al. 2009). Cost function values 0–1 indicate a good match between the model results and measurements, values 1–2 indicate a reasonable match and values above 2 indicate a poor match. Cost function shows that model reanalysis data are good (Table 2.5.1). In general, the model underestimates all nutrients except phosphates at the surface.

In order to assess the nutrient status of the Baltic Sea, we use the combination of time-series analyses of nitrogen and phosphorus pools in three different layers of the water column and spatial maps of vertically integrated

mean concentrations for two periods: 1993–1999 and 2000–2017. The selection of these two periods is motivated by the temporal variations of the hypoxic area of the Baltic Sea. After the stagnation period, which was terminated by the Major Baltic Inflow in 1993 (e.g. Mohrholz 2018), hypoxia development has shown two regimes. The first period, from 1993 to 1999, represents an increase of hypoxic area from 20,000 km² to a level of about 60,000 km² (Savchuk 2018; Meier et al. 2019; Carstensen and Conley 2019; Carstensen et al. 2014). The second period, from 2000 to 2017, can be characterised as variations of hypoxic area around a mean level between 60,000 and 80,000 km² (Savchuk 2018).

The pools of nitrate, ammonium, phosphate and oxygen have been calculated from the biochemistry reanalysis product (product reference 2.5.1). We have separated the water column into 3 layers: upper layer 0–15 m, intermediate layer 15–80 m and deep layer 80 m and below. The time-series of winter (February) nitrate and phosphate in the 0–15 m layer of the upper water column integrated over the Baltic Sea is an estimate of nutrient availability for phytoplankton and the concurrent transformation into biomass during the productive seasons. The upper layer, down to 15 m, characterises the summer mixed layer depth where the nutrients are depleted by plankton production. The intermediate layer characterises nutrient pools down to the average wintertime mixed layer depth, i.e. the depth to which the water column is seasonally mixed. The deep layer characterises the nutrient pool which is within or below the permanent halocline and, therefore, not easily mixed into the euphotic layer and accessible to phytoplankton production. Time-series of nitrate and phosphate pools under the halocline indicate the intensity of removal processes and storage of nutrients in the deep parts of the Baltic Sea.

Time series of pelagic pools are calculated as spatial integrals of nitrate, ammonium, phosphate and oxygen concentrations from the daily mean fields of product reference 2.5.1 for the whole Baltic Sea and for the three different layers separately. The dissolved inorganic nitrogen pool is taken as the sum of nitrate and

Table 2.5.1. Mean and standard deviation (SD) of the model reanalysis data and measurements, model bias (model minus observations), root mean square difference (RMSD) and cost function (CF) at the central Gotland basin (station BY15). Units are mmol/m³.

		MEAN obs	SD obs	MEAN mod	SD mod	BIAS	RMSD	CF
NH4	surf	0.19	0.16	0.14	0.18	-0.06	0.21	0.36
	bot	14.30	10.40	12.84	6.22	-1.46	7.69	0.14
NO3	surf	1.29	1.49	1.09	1.35	-0.20	0.69	0.13
	bot	2.07	4.17	1.24	2.57	-0.84	3.40	0.20
PO4	surf	0.29	0.23	0.44	0.19	0.15	0.22	0.68
	bot	4.64	1.45	3.90	0.76	-0.73	1.34	0.50

ammonia. The spatial distributions of nutrient pools (g/m²) are calculated as vertical integrals over different layers: 0–15 m, 15–80 m, 80 m to the bottom.

The sediment processes are included in the model (Almroth-Rosell et al. 2015), but the nutrient pools in the sediments are not included in the product reference 2.5.1 output list. Thus, the dynamics of benthic pools of nutrients is not analysed in this study.

2.5.3. Results

Over the period of 1993–2017, the nitrate pool decreased monotonically from about 2500 kT to 1400 kT in the Baltic Sea (Figure 2.5.1a). In the upper layer, peak values in winter fell from 800 kT to 400 kT. In the intermediate layer, which constitutes the largest part of the nitrate reserve in the water column, the drop was from ~1600 to 800 kT. The nitrate pool in the deep layer decreased from ~600 to ~400 kT.

The average ammonium pool was 350 kT (Figure 2.5.1b). The most notable changes have been taking place in the upper and intermediate layers since 2012. These have been followed by the decrease of the ammonium pool in the deep layer since 2014. We would like to note the seasonal variability of ammonium in the upper layer and partly in the intermediate layer. Our study shows the presence of ammonium in the upper layer in January. The phosphate pool has increased from 620 kT to 700 kT from 1993 to 2017 (Figure 2.5.1c). Changes in the phosphate pools in the upper layer were seasonal, but there was also a long-term increasing trend. Winter peak values increased from below 100 kT to slightly above, indicating increased availability of phosphate for the phytoplankton blooms in spring and summer. The biggest storage of phosphate pools lies in the intermediate layer, which increased from ~300 kT to a new more or less stable level of ~380 kT from 2005 onwards. Phosphate pools in the deep layer remained on a similar level throughout the study period (250–300 kT).

We complement the time series of nutrient pools with the total amount of oxygen in different layers (Figure 2.5.1d). In total, oxygen content decreased by 20 MT from 1993 to 2017. The most notable decrease of dissolved oxygen of about 13 MT occurred in the intermediate layer, while a 6 MT reduction took place in the deep layer. Over the time period of 1993–2017, oxygen pools decreased by 14 MT from 1993 to 1999 and by 6 MT from 2000 to 2017. The latter decrease took place in the intermediate layer.

Spatial distribution of vertically integrated and temporally averaged nitrate, ammonium, phosphate and bottom oxygen were calculated for two consecutive

periods: 1993–1999 and 2000–2017. The spatial distribution of nutrient pools in February indicates a potential for spring bloom and the following cyanobacteria summer bloom (Laanemets et al. 2006). Nitrate pools are distributed homogeneously over the Baltic Sea sub-basins, with the exception of the Gulf of Riga during the period of 1993–1999 (and also during the following period) (Figure 2.5.2). In the Gulf of Riga, surface nitrate concentrations are overestimated about 10 times. From the data, mean nitrate concentration calculated over the period of 1993–2017 was 5.3 mmol N/m³ but 54 mmol N/m³ in the reanalysis. Bottom values at the depth of 44 m were 11 and 62 mmol N/m³, respectively. The following reduction (up to 60%) has been relatively uniform over the Baltic Sea, with the exception of the Gulf of Bothnia where decrease in the intermediate layer has been small or even turned into an increase. Also, reduction of nitrate has been moderate in the Gulf of Riga. We would like to note that all nutrient pools are high in the Gulf of Riga (Figures 2.5.2–2.5.4). Model reanalysis has significantly overestimated ammonium and phosphate concentrations in the Gulf of Riga. Root mean square error between reanalysis and measurements in the surface of the Gulf of Riga are 2.7 mmol N/m³ and 0.6 mmol P/m³ for ammonium and phosphate, respectively. For the bottom, corresponding values are 4.0 mmol N/m³ and 0.8 mmol P/m³, respectively.

Ammonium contribution to dissolved inorganic nitrogen is in the range of 10–20%, as mentioned earlier in the time series analysis, with the exception of the bottom layer (Figure 2.5.3). In addition, while the ammonium pool has decreased in the upper and intermediate layers with a few exceptions, an increase in the deep layer has been significant, mostly in the Baltic Proper.

The phosphate pools are lower in the Gulf of Bothnia than elsewhere in the Baltic Sea (Figure 2.5.4). The distinction can be made between the Bothnian Sea with a moderate phosphate pool and the Bothnian Bay with low phosphate pool. Areas that stand out with high phosphate pools in the upper layer include the Gulf of Riga, the eastern part of the Gulf of Finland and river estuaries (Figure 2.5.4a). An overall increase of the phosphate pools (up to 60%) has occurred in the Baltic Proper, while a decrease has taken place in the Gulf of Bothnia, especially in the upper and intermediate layers (Figure 2.5.4).

Decrease of dissolved inorganic nitrogen pools and increase of phosphate pools in the upper layer of the Baltic Sea (except the Gulf of Bothnia) has resulted in the decrease of DIN:DIP ratio between two periods (Figure 2.5.5a,b). The DIN:DIP ratio decreased also in

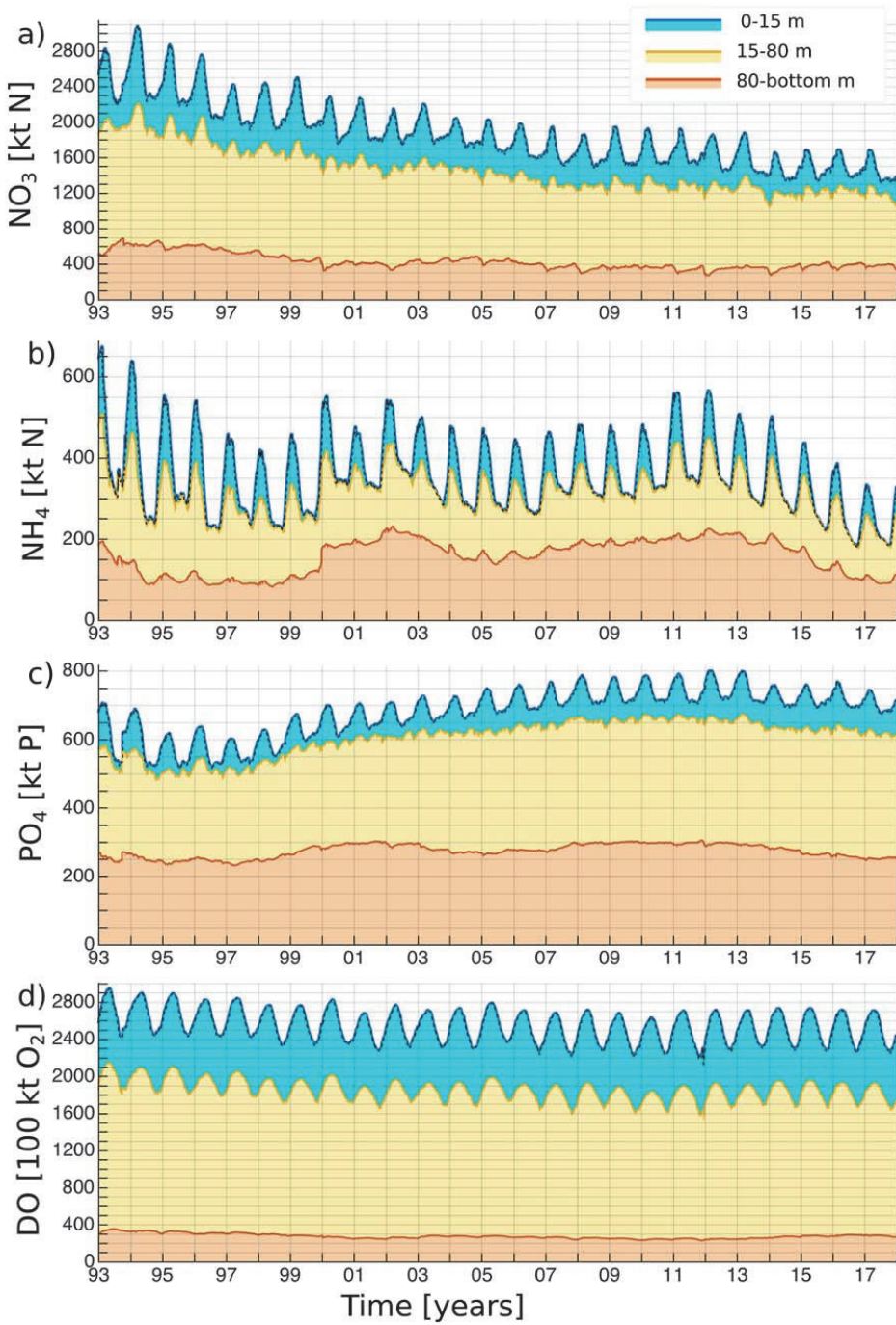


Figure 2.5.1. Stacked plot of time series of summarised dissolved nutrient pools: nitrate on (a), ammonium on (b), phosphate on (c) and dissolved oxygen on (d) in three different layers (Upper layer 0–15 m: blue; Intermediate layer 15–80 m: yellow; and Deep layer starting at 80 m and extending to the bottom: red) across the entire Baltic Sea. Time period is 1993–2017 (Product reference 2.5.1).

Table 2.5.2. Mean and standard deviation of different nutrient pools over the total period, first and last year.

Period	NH ₄ MEAN	[kt] STD	NO ₂ MEAN	[kt] STD	PO ₄ MEAN	[kt] STD	O ₂ MEAN	[100kt] STD
1993–2017	350	90	1850	360	680	70	2530	170
1993	440	120	2490	200	620	60	2690	170
2017	240	50	1430	120	700	20	2490	160

the Bothnian Sea but remained nearly unchanged in the Bothnian Bay, although both the inorganic nitrogen as well as phosphorus pools decreased in the surface layer there (Figures 2.5.2–2.5.4). On average, for the period of 1993–1999, the DIN:DIP ratio was less than 16 in the Baltic Proper and the Gulf of Finland but higher in the Gulf of Bothnia and the Gulf of Riga. Very high values of DIN:DIP ratio in the Bothnian Bay should be taken with caution. In the Bothnian Bay and partly in the Bothnian Sea, inorganic nitrogen and phosphorus concentrations are very small, which means that calculating the ratio of two small variables may result in an artificially high value. In the Gulf of Riga, inorganic nitrogen is unrealistically high but inorganic phosphorus moderately overestimated, which results in a high DIN:DIP ratio. We would like to note that the DIN:DIP ratio exceeds 16 in large river estuaries (Figure 2.5.5a,b), which indicates that there was no nitrogen limitation there, although a high phosphate content was present (Figure 2.5.4).

Spatial map of bottom dissolved oxygen concentration averaged over the period of 1993–1999 shows presence of hypoxia in the Baltic Proper (Figure 2.5.5c). That period was characterised by a significant decrease of oxygen content in the intermediate and deep layers of the Baltic Sea (Figure 2.5.5d). The latter is supported by the decrease of a dissolved oxygen pool from 2000 to 2017 in the intermediate layer (Table 2.5.3).

2.5.4. Discussion

The nutrient pools were estimated for the whole Baltic Sea from the model reanalysis. All things considered, getting estimations of total nutrient pools is a complicated task. In the case of modelling, it can be argued, and rightly so, that model-based estimates have large uncertainties due to deficiencies of the model in describing physical and biogeochemical processes, initial fields, external inputs and forcing. Furthermore, in the case of measurement based estimates, we again face the issue of large uncertainties, as measurements lack spatial and temporal resolution, are not made simultaneously and any kind of interpolation procedure introduces uncertainties in the estimates. Therefore, in this analysis we used reanalysis fields, which integrate both model

simulation results and available measurements. Using the data assimilation technique is definitely an advantage, as it enables the improvement of the validity of the simulation product (e.g. Liu et al. 2014, 2017).

Long-term variations of the nutrient pools in the Baltic Sea (Gustafsson et al. 2017; Savchuk 2018) indicate that the time period for which the estimates of the pools are given should be explicitly stated when comparing the estimates from different sources. In this study, the analysis period was from 1993 to 2017. Over that period, the nitrate pool decreased monotonically from 2500 kT to 1400 kT (Figure 2.5.1a). The ammonium pool showed multi-year oscillatory variations superimposed to an overall decrease from 440 kT in 1993–240 kT in 2017 (Figure 2.5.1b, Figure 2.5.1c). Liu et al. (2014) have estimated a nitrate pool of 800 - 1100 kT and a phosphate pool of 500–600 kT for the period of 1970–1979. Their estimates varied almost two-fold depending on whether the model simulation was without data assimilation, with assimilation of physical data or with assimilation of physical and biogeochemical data. Savchuk (2018) has estimated that the dissolved inorganic nitrogen pool has decreased from ~1250 kT in 1990 to ~1100 kT in 2016. Dissolved inorganic phosphorus has increased from ~300 kT in 1993 to ~420 kT in 2000, and then almost monotonically to 500 kT in 2016. Gustafsson et al. (2017) estimates show a decrease of the dissolved inorganic nitrogen pool from 1500 kT in 1990 to 1150 kT in 2014 using the observations but variations around the mean level of 1200 kT without decreasing tendency over the same period using the simulation results. The dissolved inorganic phosphorus pool increased from about 400 kT in 1993 to about 600 kT in 2014 based on both the observations and simulation, but the temporal course within this time period was different (Gustafsson et al. 2017).

To summarise, temporal dynamics of dissolved inorganic nitrogen and phosphorus pools were similar to the other studies (Gustafsson et al. 2017; Savchuk 2018) but quantitatively overestimated. Here we suggest three explanations. Firstly, model reanalysis data validation for the Gulf of Riga showed that nitrate and ammonium concentrations have been significantly overestimated there. Only a few measured nutrient profiles were assimilated into the model. In general, the number of

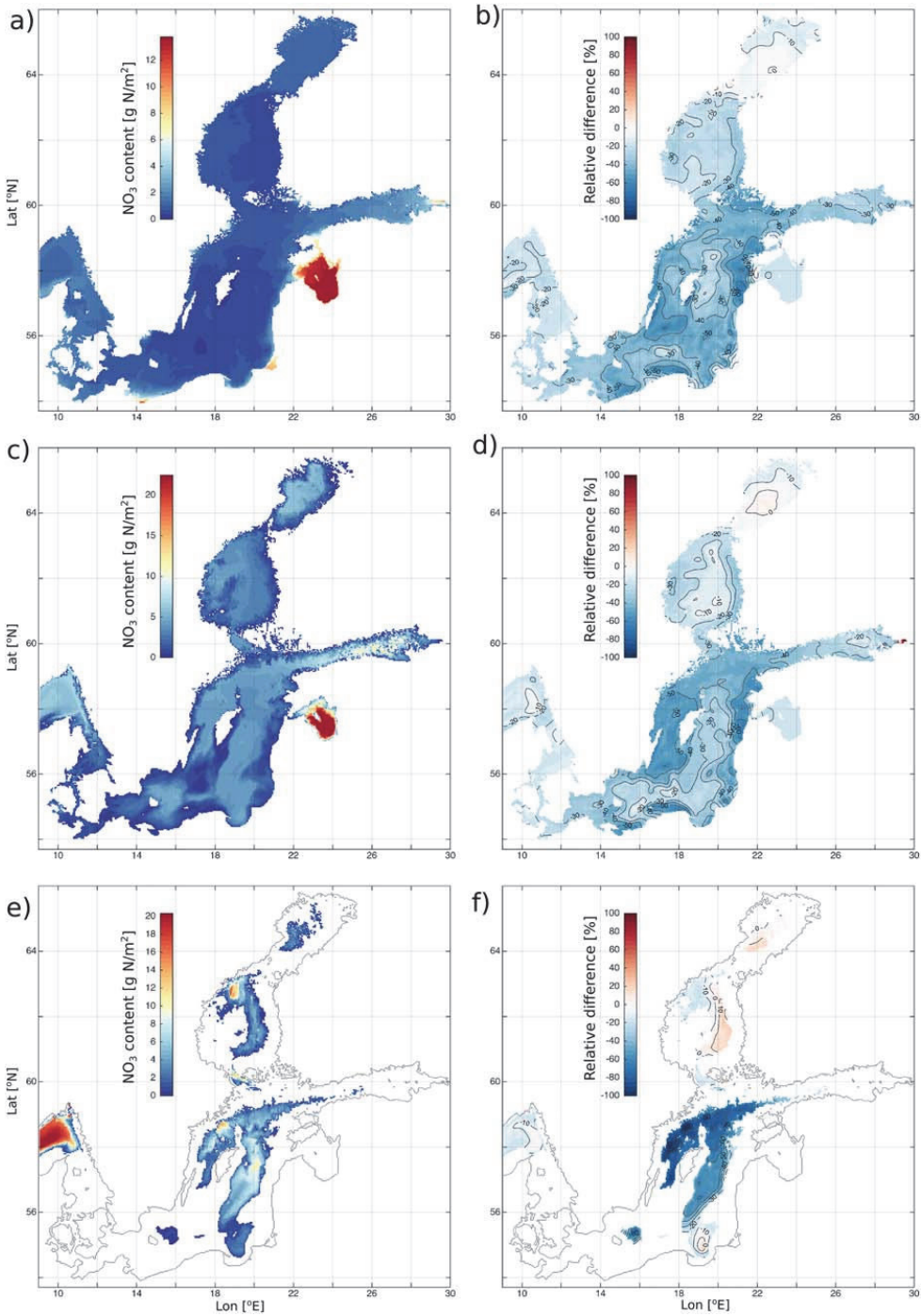


Figure 2.5.2. The mean nitrate pools in the different layers in February during the period of 1993–1999 in the left panels (a, c, e) and their relative changes $((t - \text{ref}) / \text{ref}) * 100$ for the period of 2000–2017 in the right panels (b, d, f) in the Baltic Sea. The left plots show nitrate pools as the amount of nitrogen per square meter. Different layers are depicted as 0–15 m on (a–b), 15–80 on (c–d) and 80–bottom on (e–f). The contour lines on (b), (d) and (f) show relative changes with a 10% step. The grey line on (c) and (d) shows the location of the coastline (Product reference 2.5.1).

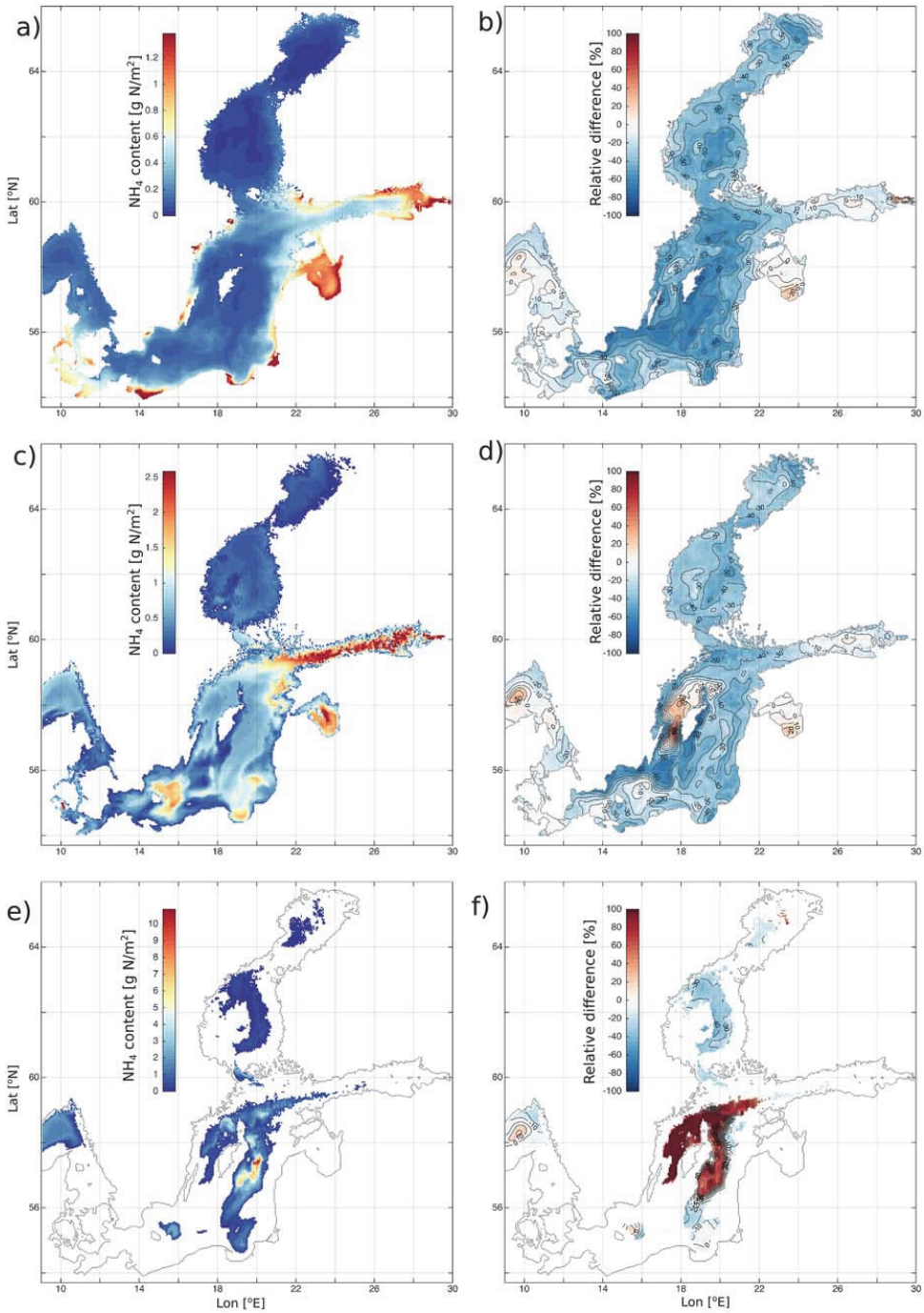


Figure 2.5.3. The mean ammonium pools in the different layers in February during the period of 1993–1999 in the left panels (a, c, e) and their relative changes $((t - \text{ref})/\text{ref}) \cdot 100$ for the period of 2000–2017 in the right panels (b, d, f) in the Baltic Sea. The left plots show ammonium pools as the amount of nitrogen per square meter. Different layers are depicted as 0–15 m on (a–b), 15–80 on (c–d) and 80–bottom on (e–f). The contour lines on (b), (d) and (f) show relative changes with a 10% step. The grey line on (c) and (d) shows the location of the coastline (Product reference 2.5.1).

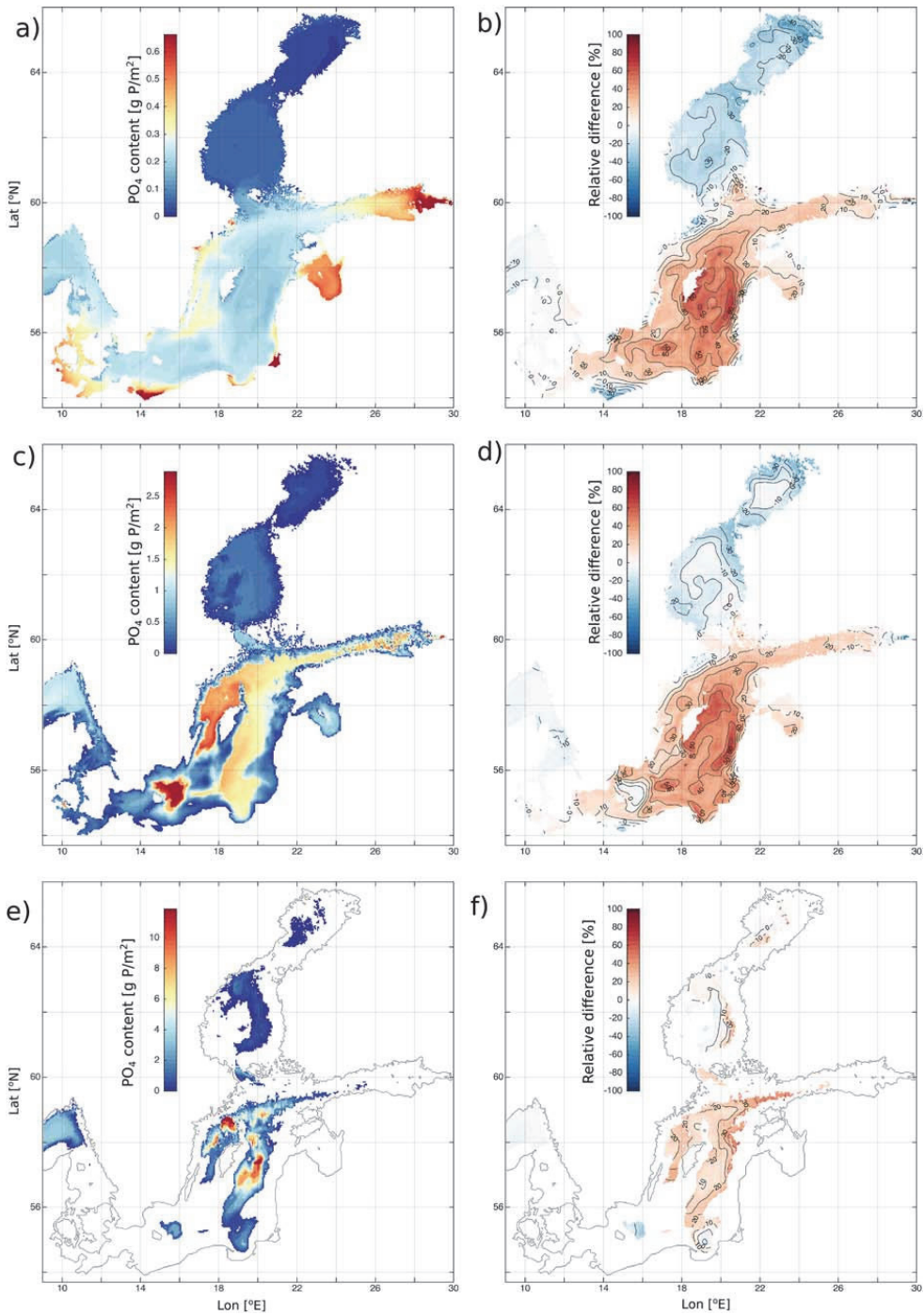


Figure 2.5.4. The mean phosphate pools in the different layers in February during the period of 1993–1999 in the left panels (a, c, e) and their relative changes $((t - \text{ref}) / \text{ref}) * 100$ for the period of 2000–2017 in the right panels (b, d, f) in the Baltic Sea. The left plots show phosphate pools as the amount of phosphorus per square meter. Different layers are depicted as 0–15 m on (a–b), 15–80 on (c–d) and 80–bottom on (e–f). The contour lines on (b), (d) and (f) show relative changes with a 10% step. The grey line on (c) and (d) shows the location of the coastline (Product reference 2.5.1).

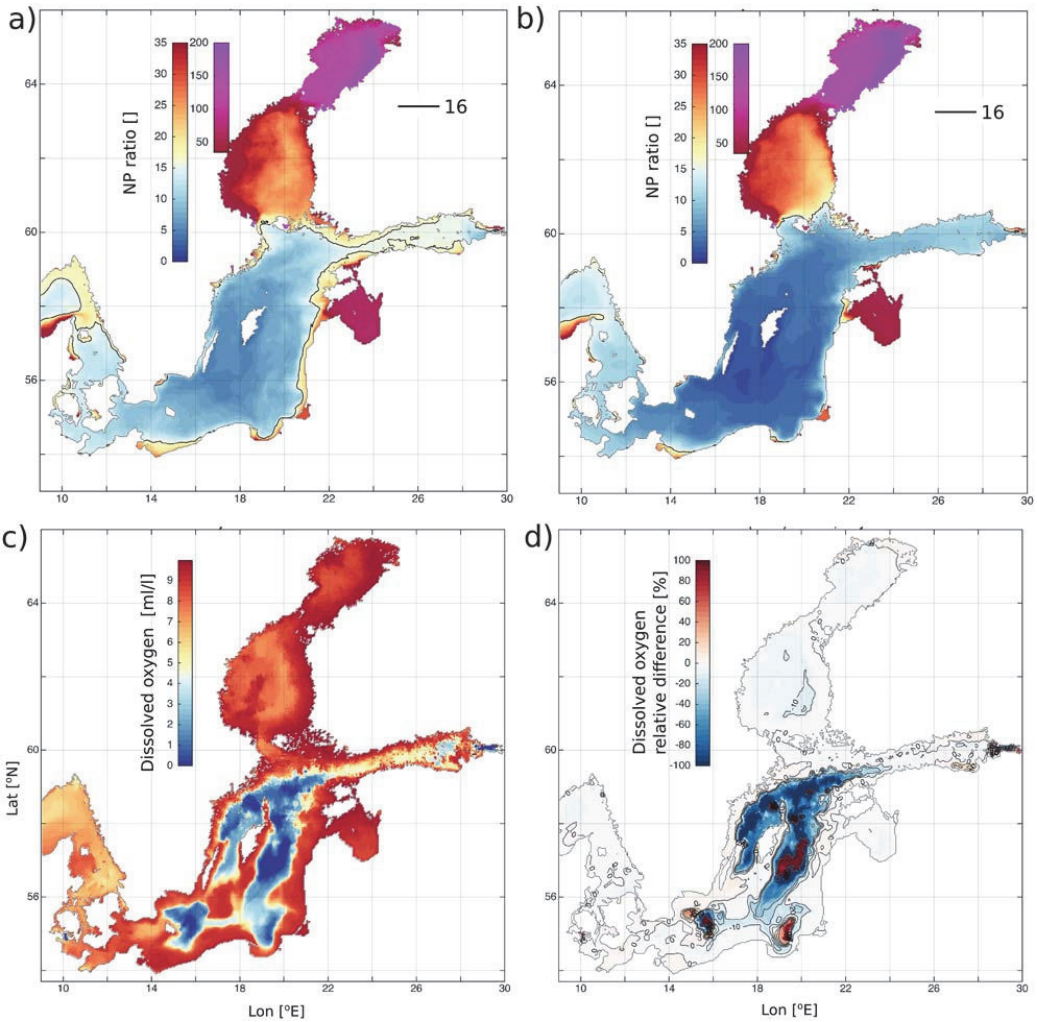


Figure 2.5.5. The mean DIN:DIP ratio (DIN/PO₄) in the 0–15 m layer during the period of 1993–1999 (a) and during the period of 2000–2017 (b). The black contour corresponds to a DIN:DIP ratio of 16. The mean bottom dissolved oxygen concentration (ml/l) in February during the period of 1993–1999 (c) and the relative changes $((t - \text{ref})/\text{ref}) * 100$ for the period of 2000–2017 (d). The contour lines on (d) show relative changes with a 30% step. The grey line on (d) shows the location of the coastline. Product reference 2.5.1.

Table 2.5.3. Mean and standard deviations (STD) of oxygen pools in different layers (TL – total layer, UL – upper layer, ML – middle layer, BL – bottom layer).

Period	TL O ₂ MEAN	[100kt] STD	UL O ₂ MEAN	[100kt] STD	ML O ₂ MEAN	[100kt] STD	BL O ₂ MEAN	[100kt] STD
1993–2017	2530	170	700	70	1560	100	270	27
1993	2690	170	710	70	1650	110	330	13
1999	2550	150	710	70	1580	80	270	4
2017	2490	160	700	70	1520	90	270	7

profiles assimilated into the model decreases significantly from the western part of the Baltic Sea towards east, which might influence the model values and provide an overestimation of nitrogen. Our comparison of the model data with measurements for the central Gotland basin showed good agreement. Secondly, during winter there was ammonium present in the upper layer and upper part of the intermediate layer (Figure 2.5.1b), which are well oxygenated and subject to intense nitrification. Geographically, the high content of ammonium was seen in the Gulf of Riga, the eastern part of the Gulf of Finland and in river estuaries (Figure 2.5.3a). There is almost no ammonium data assimilated in the model in the Gulf of Riga and eastern part of the Gulf of Finland. Comparison of model reanalysis data and independent measurements in the Gulf of Riga showed that at the surface ammonium concentrations were 0.4 and 2.0 mmol/m³ in the measurements and model, respectively. Corresponding values at the depth of 44 m were 1.3 and 4.7 mmol/m³, respectively. The coinciding of model and data was much better for the central Gotland basin (Figure 2.5.2), while the other study areas extend only to the Kattegat. We have kept the area within the limits of the biochemistry reanalysis product (product reference 2.5.1).

The general decrease of dissolved inorganic nitrogen is a reflection of several factors: decrease of dissolved inorganic nitrogen inputs, which have indeed been recorded (HELCOM 2018a, 2018b), and increased nitrogen removal from the system, which could be accelerated by the expanding hypoxic and anoxic areas, and the increasing amount of organic matter (Dalsgaard et al. 2013; Bonaglia et al. 2016). Nitrogen balance in the marine system is an interplay between several processes, including denitrification (in the hypoxic layer), anammox (newly anoxic conditions where sulphides have not yet formed) and dissimilatory nitrate reduction to ammonium (permanently anoxic conditions). Of these, denitrification plays the main role in the Baltic Sea, taking nitrogen out of the system (Gustafsson et al. 2012; Savchuk 2018). A correlation between hypoxic/anoxic area and denitrification has been recorded (Vahtera et al. 2007), indicating an intensification of this specific process as the area with favourable conditions expands (Savchuk 2018). However, nitrogen balance in marine areas and the relative contribution of different processes is still under debate (Dalsgaard et al. 2013; Savchuk 2018; Bonaglia et al. 2016, 2017).

Phosphorus pools have increased in the Baltic Sea. In the Baltic Proper, the increased water column phosphorus concentrations probably indicate that the sediments act as an ineffective phosphorus sink during anoxic periods (Meier et al. 2012). The positive winter

dissolved phosphorus trend in the Bothnian Sea possibly reflects both the intrusion of and oxygen-deficient phosphorus-enriched water mass from the Baltic Proper (Rolff and Elfving 2015) as well as the increasing input from the drainage basin (Kuosa et al. 2017). Phosphorus release from the sediments in the Bothnian Sea is unlikely, as oxygen conditions are relatively good at all times and the area is known for its phosphorus-binding ability (Asmala et al. 2017). The Gulf of Bothnia stands out as an area that performs differently from the rest of the Baltic Sea due to the differing biogeochemical conditions there – small to nonexistent stratification, sufficient oxygen conditions all year round, limited water exchange with the Baltic Proper, small external input of nutrients but high organic carbon load (Kuosa et al. 2017; Carstensen et al. 2020).

Decrease of DIN and increase of DIP results in the decrease of DIN:DIP ratio (Figure 2.5.5b). With some exceptions, inorganic nitrogen is the limiting nutrient for the spring bloom in the Baltic Sea (Granéli et al. 1990). Even in the formerly phosphorus limited Bothnian Sea the ecosystem has shifted towards nitrogen limitation (Rolff and Elfving 2015; Kuosa et al. 2017). Our results still show a DIN:DIP ratio higher than 16 in the Bothnian Sea but are consistent with the results by Liu et al. (2017).

Changes in nutrient ratio play an important role in the eutrophication of a sea (or a lake) (Granéli et al. 1990). In the Baltic Sea, the relatively low nitrogen to phosphorus ratio means that excess phosphorus remains in the euphotic zone after the spring bloom has finished (Figure 2.5.1; Savchuk 2018). This limitation strengthens in the Baltic Sea as nitrogen is removed from the system even more rapidly, while phosphorus starts to be released from the sediments when the water turns anoxic (Conley et al. 2009; Viktorsson et al. 2013).

Decrease in the nitrogen to phosphorus ratio results in a change of the timing and distribution of phytoplankton blooms, as the spring bloom can weaken due to less nitrogen available in the euphotic zone (Raudsepp et al. 2019; Groetsch et al. 2016). However, the fate of the summer bloom is less clear (Raudsepp et al. 2018, 2019). Nitrogen limitation is known to be among the factors that enhance nitrogen-fixing cyanobacteria growth, which in turn leads to increased decomposition of organic matter and the consequent oxygen deficiency in the system (Vahtera et al. 2007; Savchuk 2018). In addition to the changes in dissolved inorganic nitrogen, increased dissolved inorganic phosphorus pools in the Baltic Sea, driven by perennial and seasonal anoxia, enable eutrophication to endure, as phosphorus is not removed from the system as effectively and continues

to cycle through the trophic levels as long as there are consumers available (Viktorsson et al. 2013). In addition to changes in the nutrient ratio, cyanobacteria blooms are also facilitated by elevated water temperature (Kahru and Elmgren 2014), which is granted by climate change (Meier et al. 2012; Meier 2015). Based on this information, it is very likely that we will continue to experience frequent cyanobacterial blooms in the future. Nevertheless, the extent and trend of these blooms is difficult to predict based solely on (winter) nutrient levels, as there are several other factors in play, which obscure the trend and cause regular interannual oscillations of cyanobacterial blooms (Kahru et al. 2018), the mechanism of which is yet to be explained (Kahru and Elmgren 2014; Kahru et al. 2018). Still, we would like to note that the areas of the Baltic Proper where dissolved inorganic nitrogen decreases and phosphorus increases overlap with an intense cyanobacteria bloom area (Kahru and Elmgren 2014). Also, the area in the eastern Bothnian Sea where both nitrogen and phosphorus pools slightly increase in the deep layer coincides with the area with occasional cyanobacteria blooms (Kahru and Elmgren 2014).

It is well known that hypoxic and anoxic areas have increased over the past two decades in the Baltic Sea (Carstensen et al. 2014; Reusch et al. 2018; Hansson et al. 2020). Therefore, it is somewhat surprising that oxygen content in the deep layer has decreased only marginally (Figure 2.5.1d). This counterintuitive looking result is readily explained by the hypsographic curve of the Baltic Sea and its sub-basins (Jakobsson et al. 2019). The area of the Baltic Sea bottom has been the main subject for the investigations of increasing hypoxia and anoxia (Carstensen et al. 2014; Reusch et al. 2018; Meier et al. 2019). The volume prone to low oxygen concentration (≤ 2 ml/l) envelopes ~ 2500 km³ of water (Köuts et al. 2021). The Gulf of Bothnia, which has well-oxygenated water due to weak vertical stratification, consists of a large water volume of 2865 km³ below the depth of 80 m. Therefore, taking into consideration the total volume of the Baltic Sea, the decrease of the oxygen pool is seemingly moderate. The relatively good environmental state of the Gulf of Bothnia assuages the overall 'poor state of the Baltic Sea'.

In the context of different sub basins of the Baltic Sea with their specific physico-biogeochemical conditions, eutrophication is a severe problem in the Baltic Proper, the Gulf of Finland and the Gulf of Riga. Recently, the Major Baltic Inflows, which are known to disrupt the formation of dissolved inorganic nitrogen and phosphorus pools, do not oxygenate the bottoms for long (Neumann et al. 2017). The study by Meier et al. (2019) suggests an increase in the amount of organic matter that is

transported to the deep layers of the Baltic Sea, where intense decomposition accelerates deoxygenation at the bottom and water column alike, rapidly restoring hypoxic/anoxic conditions present pre-Major Baltic Inflow. Reducing oxygen conditions, in turn, facilitates the release of ammonium (Conley et al. 2009) and phosphate from the sediments, which act as fertilisers for the oncoming blooms, creating a positive-feedback loop that maintains hypoxia (Vahtera et al. 2007; Savchuk 2018). The correlation between nutrient pools and oxygen conditions in the Baltic Sea has been shown earlier (Eilola et al. 2009; Savchuk 2018) and in our results and can be explained by the accelerating of the so-called 'vicious circle' (Vahtera et al. 2007).

Section 2.6. Long term changes monitored in two Mediterranean Channels

Authors: Sana Ben Ismail, Katrin Schroeder, Jacopo Chiggiato, Stefania Sparnocchia, Mireno Borghini

Statement of main outcomes: The Mediterranean Sea is a mid-latitude marginal sea which has been recognised to be a climatic hotspot. During the past decade, its water masses have experienced strong and fast increases in temperature and salinity, evidencing the tendency of this area to respond very rapidly to global warming and to changes in the regional freshwater budget. Based on in situ data here it is shown where and how fast these changes occur, with a particular focus on the Western Mediterranean Deep Water and the Intermediate Water. Such trends are at least one order of magnitude higher than the global mid-latitude average trends. Indicator-type curves, routinely updated, for subsurface temperature and salinity evolution represent an outcome that is envisaged to be important for climate science, environmental agencies, concerned citizens as well as regional policy-makers.

CMEMS Products used:

Ref. No.	Product name & type	Documentation
2.6.1	INSITU_MED_NRT_OBSERVATIONS_01_035/MO_TS_MO_SardiniaChannel ftp://nrt.cmems-du.eu/Core/INSITU_MED_NRT_OBSERVATIONS_013_035/med_multiparameter_nrt/history/MO/MO_TS_MO_SardiniaChannel.nc (daily mooring data from 2003 to 2019)	QUID: https://cmems-resources.cls.fr/documents/QUID/CMEMS-INS-QUID-013-030-036.pdf PUM: https://cmems-resources.cls.fr/documents/PUM/CMEMS-INS-PUM-013.pdf

(Continued)

- Novoa S, Chust G, Sagarmínaga Y, Revilla M, Borja A, Franco J. 2012. Water quality assessment using satellite-derived chlorophyll – a within the European directives, in the southeastern Bay of Biscay. *Mar Pollut Bull.* 65:739–750. doi:10.1016/j.marpolbul.2012.01.020.
- NOWPAP CEARAC – Northwest Pacific Action Plan Special Monitoring and Coastal Environmental Assessment Regional Activity Centre. 2007. Eutrophication monitoring guidelines by Remote Sensing for the NOWPAP region. Toyama City, Japan. Available from: https://www.cearac-project.org/wg4/publications/Eutrophication_GL_RS.pdf.
- OSPAR ICG-EUT. Axe, P., Clausen, U., Leujak, W., Malcolm, S., Rüter, H., Prins, T., Harvey, E.T. (2017). Eutrophication Status of the OSPAR Maritime Area. Third Integrated Report on the Eutrophication Status of the OSPAR Maritime Area.
- Papathanasopoulou E, Simis S, Alikas K, Ansper A, Anttila S, Attila J, Barillé AL, Barillé L, Brando V, Bresciani M, et al. 2019. Satellite-assisted monitoring of water quality to support the implementation of the water framework directive. EOMORES White Paper. 28. doi:10.5281/zenodo.3463051.
- Park Y, Ruddick K, Lacroix G. 2010. Detection of algal blooms in European waters based on satellite chlorophyll data from MERIS and MODIS. *Int J Remote Sens.* 31:6567–6583.
- Sathyendranath S, Pardo S, Benincasa M, Brando VE, Brewin RJW, Mélin F, Santoleri R. 2018. 1.5. Essential variables: Ocean colour in Copernicus Marine service Ocean state report – issue 2. *J Operat Oceanogr.* 11(Suppl. 1)):1–142. doi:10.1080/1755876X.2018.1489208.
- Schindler DW. 2006. Recent advances in the understanding and management of eutrophication. *Limnol Oceanogr.* 51:356–363.
- Smith VH. 2003. Eutrophication of freshwater and coastal marine ecosystems a global problem. *Environ Sci Poll Res.* 10:126–139. doi:10.1065/espr2002.12.142.
- Van der Zande D, Lacroix G, Desmit X, Ruddick K. 2011. Impact of irregular sampling by MERIS on eutrophication monitoring products for WFD and MSFD applications. Proceedings of the 6th 683 EuroGOOS Conference, Sopot, Poland; p. 348–357.
- Van der Zande D, Lavigne H, Blauw A, Prins T, Desmit X, Eleveld M, Gohin F, Pardo S, Tilstone G, Cardoso Dos Santos J. 2019. Enhance coherence in eutrophication assessments based on chlorophyll, using satellite data as part of the EU project 'Joint monitoring programme of the eutrophication of the North Sea with satellite data' (Ref: DG ENV/MSFD Second Cycle/2016). Activity 2 Report.
- Van der Zande D, Ruescas A, Storm T, Embacher S, Stelzer K, Ruddick K. 2013. Monitoring eutrophication in the North Sea: an operational CHL-P90 tool. Proceedings of IOCS2013 conference held in Darmstadt, Germany, 6–8 May 2013.
- Van Meerseeke E, Pinckney JL. 2019. Nutrient loading impacts on Estuarine phytoplankton size and community composition: community-based indicators of eutrophication. *Estuaries Coasts.* 42:504–512. doi:10.1007/s12237-018-0470-z.
- Wallace RB, Baumann H, Grear JS, Aller RB, Gobler CJ. 2014. Coastal ocean acidification: The other eutrophication problem. *Estuarine Coastal Shelf Sci.* 148:1–13. doi:10.1016/j.ecss.2014.05.027.

Section 2.5. Nitrate, ammonium and phosphate pools in the Baltic Sea

- Almroth-Rosell E, Eilola K, Kuznetsov I, Hall PO, Meier HM. 2015. A new approach to model oxygen dependent benthic phosphate fluxes in the Baltic Sea. *J Mar Sys.* 144:127–141. doi:10.1016/j.jmarsys.2014.11.007.
- Andersen JH, Carstensen J, Conley DJ, Dromph K, Fleming-Lehtinen V, Gustafsson BG, Josefson AB, Norkko A, Villnäs A, Murray C. 2017. Long-term temporal and spatial trends in eutrophication status of the Baltic Sea. *Biol Rev.* 92(1):135–149. doi:10.1111/brv.12221.
- Asmala E, Carstensen J, Conley DJ, Slomp CP, Stadmark J, Voss M. 2017. Efficiency of the coastal filter: nitrogen and phosphorus removal in the Baltic Sea. *Limnol Oceanogr.* 62:S222–S238. doi:10.1002/lno.10644.
- Bonaglia S, Hylén A, Rattray JE, Kononets MY, Ekeröth N, Roos P, Thamdrup B, Brüchert V, Hall PO. 2017. The fate of fixed nitrogen in marine sediments with low organic loading: an in situ study. *Biogeosciences.* 14(2):285–300. doi:10.5194/bg-14-285-2017.
- Bonaglia S, Klawonn I, De Brabandere L, Deutsch B, Thamdrup B, Brüchert V. 2016. Denitrification and DNRA at the Baltic Sea oxic–anoxic interface: substrate spectrum and kinetics. *Limnol Oceanogr.* 61(5):1900–1915. doi:10.1002/lno.10343.
- Buga L, Sarbu G, Fryberg L, Magnus W, Wesslander K, Gatti J, Leroy D, Iona S, Larsen M, Koefoed Rømer J, et al. 2018. EMODnet Thematic Lot n° 4/S12.749773 EMODnet Chemistry Eutrophication and Acidity aggregated datasets v2018, doi: 10.6092/EC8207EF-ED81-4EE5-BF48-E26FF16BF02E.
- Carstensen J, Andersen JH, Gustafsson BG, Conley DJ. 2014. Deoxygenation of the Baltic Sea during the last century. *Proc Natl Acad Sci USA.* 111(15):5628–5633. doi:10.1073/pnas.1323156111.
- Carstensen J, Conley DJ. 2019. Baltic Sea hypoxia takes many shapes and sizes. *Limnol Oceanogr.* 64(4):125–129. doi:10.1002/lno.10350.
- Carstensen J, Conley DJ, Almroth-Rosell E, Asmala E, Bonsdorff E, Fleming-Lehtinen V, Gustafsson BG, Gustafsson C, Heiskanen AS, Janas U, Norkko A. 2020. Factors regulating the coastal nutrient filter in the Baltic Sea. *Ambio.* 49(6):1194–1210. doi:10.1007/s13280-019-01282-y.
- Conley DJ, Björck S, Bonsdorff E, Carstensen J, Destouni G, Gustafsson BG, Hietanen S, Kortekaas M, Kuosa H, Markus Meier HE, Müller-Karulis B. 2009. Hypoxia-related processes in the Baltic Sea. *Environ Sci Technol.* 43(10):3412–3420. doi:10.1021/es802762a.
- Dahlgren P, Landelius T, Kallberg P, Gollvik S. 2016. A high resolution regional reanalysis for Europe Part 1: 3-dimensional reanalysis with the regional high resolution limited area model (HIRLAM). *Q J Roy Meteor Soc.* 698:2119–2131. doi:10.1002/qj.2807.
- Dalsgaard T, De Brabandere L, Hall PO. 2013. Denitrification in the water column of the central Baltic Sea. *Geochim Cosmochim Acta.* 106:247–260. doi:10.1016/j.gca.2012.12.038.
- Donnelly C, Andersson JC, Arheimer B. 2016. Using flow signatures and catchment similarities to evaluate the E-HYPE multibasin model across Europe. *Hydrolog. Sci J.* 61:255–273. doi:10.1080/02626667.2015.1027710.

- Eilola K, Meier HM, Almroth E. 2009. On the dynamics of oxygen, phosphorus and cyanobacteria in the Baltic Sea; a model study. *J Mar Sys.* 75(1-2):163–184. doi:10.1016/j.jmarsys.2008.08.009.
- Fleming-Lehtinen V, Andersen JH, Carstensen J, Lysiak-Pastuszek E, Murray C, Pyhälä M, Laamanen M. 2015. Recent developments in assessment methodology reveal that the Baltic Sea eutrophication problem is expanding. *Ecol Indic.* 48:380–388. doi:10.1016/j.ecolind.2014.08.022.
- Granéli E, Wallström K, Larsson U, Granéli W, Elmgren R. 1990. Nutrient limitation of primary production in the Baltic Sea area. *Ambio.* 19(3):142–151.
- Groetsch PM, Simis SG, Eleveld MA, Peters SW. 2016. Spring blooms in the Baltic Sea have weakened but lengthened from 2000 to 2014. *Biogeosciences.* 13(17):4959–4973. doi:10.5194/bg-13-4959-2016.
- Gustafsson BG, Schenk F, Blenckner T, Eilola K, Meier HM, Müller-Karulis B, Neumann T, Ruoho-Airola T, Savchuk OP, Zorita E. 2012. Reconstructing the development of Baltic Sea eutrophication 1850–2006. *Ambio.* 41(6):534–548. doi:10.1007/s13280-012-0318-x.
- Gustafsson E, Savchuk OP, Gustafsson BG, Müller-Karulis B. 2017. Key processes in the coupled carbon, nitrogen, and phosphorus cycling of the Baltic Sea. *Biogeochemistry.* 134:301–317. doi:10.1007/s10533-017-0361-6.
- Hansson M, Viktorsson L, Andersson L. 2020. Oxygen Survey in the Baltic Sea 2019–Extent of Anoxia and Hypoxia, 1960–2019. SMHI, Report Oceanography No. 67.
- HELCOM. 2018a. HELCOM Thematic assessment of eutrophication 2011–2016. Baltic Sea Environment Proceedings No. 156.
- HELCOM. 2018b. Sources and pathways of nutrients to the Baltic Sea. Baltic Sea Environment Proceedings No. 153.
- Hordoir R, Axell L, Höglund A, Dieterich C, Fransner F, Gröger M, Liu Y, Pemberton P, Schimanke S, Andersson H, et al. 2019. Nemo-Nordic 1.0: a NEMO-based ocean model for the Baltic and North seas – research and operational applications. *Geosci Model Dev.* 12:363–386. doi:10.5194/gmd-12-363-2019.
- Jakobsson M, Stranne C, O’Regan M, Greenwood SL, Gustafsson B, Humborg C, Weidner E. 2019. Bathymetric properties of the Baltic Sea. *Ocean Science.* 15(4):905–924. doi:10.5194/os-15-905-2019.
- Kahru M, Elmgren R. 2014. Multidecadal time series of satellite-detected accumulations of cyanobacteria in the Baltic Sea. *Biogeosciences.* 11(13):3619–3633. doi:10.5194/bg-11-3619-2014.
- Kahru M, Elmgren R, Di Lorenzo E, Savchuk O. 2018. Unexplained interannual oscillations of cyanobacterial blooms in the Baltic Sea. *Sci Rep.* 8(1):Article number 6365. doi:10.1038/s41598-018-24829-7.
- Köuts M, Maljutenko I, Elken J, Liu Y, Hansson M, Viktorsson L, Raudsepp U. 2021. Recent regime of persistent hypoxia in the Baltic Sea. *Environ Res Comm.* DOI:10.1088/2515-7620/ac0cc4.
- Kuosa H, Fleming-Lehtinen V, Lehtinen S, Lehtiniemi M, Nygård H, Raateoja M, Raitaniemi J, Tuimala J, Uusitalo L, Suikkanen S. 2017. A retrospective view of the development of the Gulf of Bothnia ecosystem. *J Mar Sys.* 167:78–92. doi:10.1016/j.jmarsys.2016.11.020.
- Laanemets J, Lilover MJ, Raudsepp U, Autio R, Vahtera E, Lips I, Lips U. 2006. A fuzzy logic model to describe the cyanobacteria *Nodularia spumigena* blooms in the Gulf of Finland, Baltic Sea. *Hydrobiologia.* 554(1):31–45. doi:10.1007/s10750-005-1004-x.
- Landelius T, Dahlgren P, Gollvik S, Jansson A, Olsson E. 2016. A high resolution regional reanalysis for Europe Part 2: 2D analysis of surface temperature, precipitation and wind. *Q J Roy Meteor Soc.* 142:2132–2142. doi:10.1002/qj.2813.
- Liu Y, Meier HEM, Eilola K. 2014. Improving the multiannual, high-resolution modelling of biogeochemical cycles in the Baltic Sea by using data assimilation. *Tellus A: Dyn Meteorol Oceanogr.* 66(1):24908. doi:10.3402/tellusa.v66.24908.
- Liu Y, Meier HEM, Eilola K. 2017. Nutrient transports in the Baltic Sea – results from a 30-year physical–biogeochemical reanalysis. *Biogeosciences.* 14:2113–2131. doi:10.5194/bg-14-2113-2017.
- Lundberg C, Jakobsson BM, Bonsdorff E. 2009. The spreading of eutrophication in the eastern coast of the Gulf of Bothnia, northern Baltic Sea—An analysis in time and space. *Estuarine Coastal Shelf Sci.* 82(1):152–160. doi:10.1016/j.ecss.2009.01.005.
- Meier HEM. 2015. Projected change – marine physics. In: Second assessment of climate change for the Baltic Sea basin. BACC II author team, 2015. Cham: Springer International Publishing; p. 243–252.
- Meier HEM, Andersson HC, Arheimer B, Blenckner T, Chubarenko B, Donnelly C, Eilola K, Gustafsson BG, Hansson A, Havenhand J, et al. 2012. Comparing reconstructed past variations and future projections of the Baltic Sea ecosystem – first results from multi-model ensemble simulations. *Environ Res Lett.* 7(3):034005. doi:10.1088/1748-9326/7/3/034005.
- Meier HEM, Eilola K, Almroth-Rosell E, Schimanke S, Kniebusch M, Höglund A, Pemberton P, Liu Y, Väli G, Saraiva S. 2019. Disentangling the impact of nutrient load and climate changes on Baltic Sea hypoxia and eutrophication since 1850. *Clim Dyn.* 53(1-2):1145–1166. doi:10.1007/s00382-018-4296-y.
- Mohrholz V. 2018. Major baltic inflow statistics—revised. *Front Mar Sci.* 5:384. doi:10.3389/fmars.2018.00384.
- Murray CJ, Muller-Karulis B, Carstensen J, Conley DJ, Gustafsson B, Andersen JH. 2019. Past, present and future eutrophication status of the Baltic Sea. *Front Mar Sci.* 6:2. doi:10.3389/fmars.2019.00002.
- Nerger L, Hiller W, Schröter J. 2005. A comparison of error subspace Kalman filters. *Tellus A: Dyn Meteorol Oceanogr.* 57(5):715–735. doi:10.1111/j.1600-0870.2005.00141.x.
- Neumann T, Radtke H, Seifert T. 2017. On the importance of Major Baltic Inflows for oxygenation of the central Baltic Sea. *J Geophys Res Ocean.* 122(2):1090–1101. doi:10.1002/2016JC012525.
- Pemberton P, Löptien U, Hordoir R, Höglund A, Schimanke S, Axell L, Haapala J. 2017. Sea-ice evaluation of NEMONordic 1.0: a NEMO–LIM3.6-based ocean–sea-ice model setup for the North Sea and Baltic Sea. *Geosci Model Dev.* 10:3105–3123. doi:10.5194/gmd-10-3105-2017.
- Raudsepp U, She J, Brando VE, Köuts M, Lagema P, Sammartino M, Santoleri R. 2018. Eutrophication and hypoxia in the Baltic Sea. In: Copernicus Marine Service Ocean State Report, Issue 2. *J Operat Oceanogr.* 11 (Supp. 1):s13–s16. doi:10.1080/1755876X.2018.1489208.

- Raudsepp U, She J, Brando VE, Santoleri R, Sammartino M, Kouts M, Uiboupin R, Maljutenko I. 2019. Phytoplankton blooms in the Baltic Sea. In: Copernicus Marine Service Ocean State Report, Issue 3. *J Operat Oceanogr.* 12 (Supp. 1):s26. doi:10.1080/1755876X.2019.163307530.
- Reusch TB, Dierking J, Andersson HC, Bonsdorff E, Carstensen J, Casini M, Czajkowski M, Hasler B, Hinsby K, Hyytiäinen K, et al. 2018. The Baltic Sea as a time machine for the future coastal ocean. *Sci Adv.* 4(5): eaar8195. doi:10.1126/sciadv.aar8195.
- Rolf C, Elfving T. 2015. Increasing nitrogen limitation in the Bothnian Sea, potentially caused by inflow of phosphate-rich water from the Baltic proper. *Ambio.* 44(7):601–611. doi:10.1007/s13280-015-0675-3.
- Saraiva S, Meier HEM, Andersson H, Höglund A, Dieterich C, Gröger M, Hordoir R, Eilola K. 2019. Baltic Sea ecosystem response to various nutrient load scenarios in present and future climates. *Clim Dyn.* 52(5-6):3369–3387. doi:10.1007/s00382-018-4330-0.
- Savchuk OP. 2018. Large-scale nutrient dynamics in the Baltic Sea, 1970–2016. *Front Mar Sci.* 5:95. doi:10.3389/fmars.2018.00095.
- Vahtera E, Conley DJ, Gustafsson BG, Kuosa H, Pitkänen H, Savchuk OP, Tamminen T, Viitasalo M, Voss M, Wasmund N, Wulff F. 2007. Internal ecosystem feedbacks enhance nitrogen-fixing cyanobacteria blooms and complicate management in the Baltic Sea. *Ambio.* 186–194. doi:10.1579/0044-7447(2007)36[186:IEFENC]2.0.CO;2.
- Viktorsson L, Ekeröth N, Nilsson M, Kononets M, Hall POJ. 2013. Phosphorus recycling in sediments of the central Baltic Sea. *Biogeosciences.* 10(6):3901. doi:10.5194/bg-10-3901-2013.
- Wulff F, Sokolov A, Savchuk O. 2013. Nest—a decision support system for management of the Baltic Sea. A User manual. Stockholm: Baltic Nest Institute, Stockholm University, Sweden.
- Section 2.6. Long term changes monitored in two Mediterranean Channels**
- Astraldi M, Balopoulos S, Candela J, Font J, Gačić M, Gasparini GP, Manca B, Theocharis A, Tintoré J. 1999. The role of straits and channels in understanding the characteristics of Mediterranean circulation. *Prog Oceanogr.* 44:65–108.
- Ben Ismail S, Sammari C, Gasparini GP, Béranger K, Mouldi B, Aleya L. 2012. Water masses exchanged through the Channel of Sicily: evidence for the presence of new water masses on the Tunisia-Sicily side of the channel. *Deep Sea Res I.* 63(2012):65–81.
- Ben Ismail S, Schroeder K, Sammari C, Gasparini GP, Borghini M, et al. 2014. Interannual variability of water mass properties in the Tunisia-Sicily channel. *J Mar Syst.* 135:14–28.
- Béthoux JP, Gentili B. 1996. The Mediterranean Sea, coastal and deep-sea signatures of climatic and environmental changes. *J Marine Syst.* 7:383–394.
- Béthoux JP, Gentili B, Tailliez D. 1998. Warming and freshwater budget change in the Mediterranean since the 1940s, their possible relation to the greenhouse effect. *Geophys Res Lett.* 25:1023–1026.
- Collins M, Sutherland M, Bouwer L, Cheong S-M, Frölicher T, Jacot Des Combes H, Koll Roxy M, Losada I, McInnes K, Ratter B, et al. 2019. Extremes, abrupt changes and managing risk. In: H.-O. Pörtner, D.C. Roberts, V. Masson-Delmotte, P. Zhai, M. Tignor, E. Poloczanska, K. Mintenbeck, A. Alegría, M. Nicolai, A. Okem, J. Petzold, B. Rama, N.M. Weyer, editor. IPCC special report on the Ocean and Cryosphere in a changing climate. In press.
- Cook BI, Anchukaitis KJ, Touchan R, Meko DM, Cook ER. 2016. Spatiotemporal drought variability in the Mediterranean over the last 900 years. *J Geophys Res Atmos.* 121:2060–2074. DOI:10.1002/2015JD023929.
- Desbruyères D, McDonagh EL, King BA. 2017. Global and full-depth Ocean temperature trends during the early twenty-first century from Argo and repeat hydrography. *J Clim.* 30:1985–1997. doi:10.1175/JCLI-D-16-0396.1.
- Fuda J-L, Etiope G, Millot C, Faveli C, Calcara M, Smriglio G, Boschi E. 2002. Warming, salting and origin of the Tyrrhenian deep water. *Geophys Res Lett.* 29(18):1886. doi:10.1029/2001gl014072.
- Krahmann G, Schott F. 1998. Long term increases in Western Mediterranean salinities and temperatures: anthropogenic and climatic sources. *Geophys Res Lett.* 25(22):4209–4212.
- Leaman KD, Schott F. 1991. Hydrographic structure of the convection regime in the Gulf of lions: winter 1987. *J Phys Oceanogr.* 21:575–598.
- Meysignac B, Boyer T, Zhao Z, Hakuba MZ, Landerer FW, Stammer D, Köhl A, Kato S, L'Ecuyer T, Ablain M, et al. 2019. Measuring global Ocean heat content to estimate the earth energy imbalance. *Front Mar Sci.* 6:432. doi:10.3389/fmars.2019.00432.
- Millot C, Candela J, Fuda J-L, Tber Y. 2006. Large warming and salinification of the Mediterranean outflow due to changes in its composition. *Deep-Sea Res.* 53:656–666. doi:10.1016/j.dsr.2005.12.017..
- Roether W, Manca BB, Klein B, Bregant D, Gerogopolous D, Beitzel V, Kovacevic V, Luchetta A. 1996. Recent changes in Eastern Mediterranean deep waters. *science.* New Series. 271(5247):333–335.
- Rohling EJ, Bryden H. 1992. Man-induced salinity and temperature increase in the western Mediterranean deep water. *J Geophys Res.* 97:11191–11198.
- Ryabinin V, Barbière J, Haugan P, Kullenberg G, Smith N, McLean C, Troisi A, Fischer A, Aricò S, Aarup T, et al. 2019. The UN decade of Ocean science for sustainable development. *Front Mar Sci.* 6:470. doi:10.3389/fmars.2019.00470.
- Schroeder K, et al. 2016. Abrupt climate shift in the Western Mediterranean Sea. *Sci Rep.* 6:23009. doi:10.1038/srep23009.
- Schroeder K, Chiggiato J, Ben Ismail S, Borghini M, Patti B, Sparnocchia S. 2019. Mediterranean deep and intermediate water mass properties. In: Copernicus Marine service Ocean state report, issue 3. *J Operat Oceanogr.* 12 (Supp. 1):s18–s21. doi:10.1080/1755876X.2019.1633075.
- Schroeder K, Chiggiato J, Josey SA, Borghini M, Aracri S, Sparnocchia S. 2017. Rapid response to climate change in a marginal sea. *Sci Rep.* 7:4065. doi:10.1038/s41598-017-04455-5.
- Schroeder K, Ribotti A, Borghini M, Sorgente R, Perilli A, Gasparini GP. 2008. An extensive western Mediterranean deep water renewal between 2004 and 2006. *Geophys Res Lett.* 35:L18605. doi:10.1029/2008GL035146.

Curriculum vitae

Personal data

Name: Mariliis Kõuts
Date of birth: 29.05.1987
Phone: +372 5181 585
E-mail: mariliis.kouts@taltech.ee

Institutions and positions

01.07.2022–... Tallinn University of Technology, School of Science, Department of Marine Systems, Engineer (1,00)
01.01.2017–30.06.2022 Tallinn University of Technology, School of Science, Department of Marine Systems, Junior Researcher (1,00)
01.01.2016–31.12.2016 Tallinn University of Technology, Institute of Marine Systems at TUT, Junior Researcher (1,00)
2009–31.12.2015 Tallinn University of Technology, Institute of Marine Systems at TUT, engineer (1,00)

Academic degrees

Mariliis Kõuts, Master's Degree, 2013, (sup) Markus Vetemaa; Lauri Saks, Muuga lahel ja Käsmu lahel talvituvate aulide (Clangula hyemalis) toitumisökoloogia: kaaspüügil põhineva andmestiku analüüs (Feeding ecology of wintering long-tailed ducks (Clangula hyemalis) on Muuga and Käsmu Bay: a study based on bycatch data), University of Tartu.

Mariliis Kõuts, Phd student, (sup) Gennadi Lessin; Urmas Raudsepp, Nutrient and detritus dynamics in the Baltic Sea, Tallinn University of Technology School of Science, Department of Marine Systems.

Education

01.09.2015–... Tallinn University of Technology – PhD
2010–2013 Tartu University – MSc
2006–2010 Tartu Ülikool – BSc
1995–2006 Tallinn English College
1994–1995 Kehra Primary School

Completed projects

VA18004 “Copernicus Marine Environment Monitoring Service’s at Baltic Monitoring and Forecasting Centre” (1.01.2018–31.03.2021); Principal Investigator: Urmas Raudsepp; Tallinn University of Technology, School of Science, Department of Marine Systems (partner); Financier: Mercator Océan; Financing: 544 100 EUR.

IUT19-6 “Multi-scale physical processes controlling the biogeochemical signal dynamics in the stratified Baltic Sea” (1.01.2014–31.12.2019); Principal Investigator: Urmas Lips; Tallinn University of Technology, Institute of Marine Systems at TUT, Tallinn University of Technology, School of Science, Department of Marine Systems; Financier: Estonian Research Council; Financing: 1 380 000 EUR.

VEU15017 “Sustainable Shipping and Environment of the Baltic Sea region” (1.04.2015–31.03.2018); Principal Investigator: Urmas Raudsepp; Tallinn University of Technology, Institute of Marine Systems at TUT (partner); Financier: Estonian Research Council; Financing: 149 616 EUR.

VEU676 “Sunken wreck environmental risk assessment (SWERA)” (14.05.2014–30.04.2016); Principal Investigator: Tarmo Kõuts; Tallinn University of Technology (partner), Tallinn University of Technology, Institute of Marine Systems at TUT (partner); Financier: Commission of the European Communities; Financing: 95 228 EUR.

VEU663 “Geopositional early warning system for marine oil spill recognition in the Baltic Sea (GEOILWATCH)” (1.05.2014–30.04.2016); Principal Investigator: Tarmo Kõuts; Tallinn University of Technology (partner), Tallinn University of Technology, Institute of Marine Systems at TUT (partner); Financier: Commission of the European Communities; Financing: 98 760 EUR.

Lep13166 “EIA on Finngulf LNG Balticconnector natural gas pipeline” (21.11.2013–31.05.2015); Principal Investigator: Inga Lips; Tallinn University of Technology (partner), Tallinn University of Technology, Institute of Marine Systems at TUT (partner); Financier: OÜ Entec Eesti; Financing: 62 700 EUR.

Lep14059 “Study cruises for schools in the frame of Gulf of Finland Year 2014” (11.04.2014–30.06.2014); Principal Investigator: Inga Lips; Tallinn University of Technology (partner), Tallinn University of Technology, Institute of Marine Systems at TUT (partner); Financier: Estonian Museum of Natural History; Financing: 10 752 EUR.

Lep 13030 “Maritime spatial planning of sea area in Hiiu county” (1.03.2013–30.05.2014); Principal Investigator: Urmas Lips; Tallinn University of Technology (partner), Tallinn University of Technology, Institute of Marine Systems at TUT (partner); Financier: Artes Terrae LLC; Financing: 37 250 EUR.

SLOMI10134T “Mitigation of negative impact of seals in Estonian fisheries using AHD’s and seal-proof netting material” (1.07.2010–31.12.2013); Principal Investigator: Markus Vetemaa; University of Tartu (partner), University of Tartu, Faculty of Science and Technology (old), Estonian Marine Institute, University of Tartu (partner); Financier: Estonian Agricultural Registers and Information Board; Financing: 213 465 EUR.

Lep11033 “Mustjala vallas Ninase külas asuva Saaremaa sadama detailplaneeringu koostamine ja detailplaneeringuga kavandatava tegevuse keskkonnamõju strateegiline hindamine” (21.04.2011–31.12.2012); Principal Investigator: Urmas Raudsepp; Tallinn University of Technology, Institute of Marine Systems at TUT (partner); Financier: Port of Tallinn; Financing: 18 406 EUR.

Lep11081 “Assessment of environmental impact of construction the 0 quai in Paldiski North Harbour” (15.10.2011–15.11.2012); Principal Investigator: Tarmo Kõuts; Tallinn University of Technology, Institute of Marine Systems at TUT (partner); Financier: Port of Paldiski; Financing: 15 100 EUR.

Lep11097 “Meresõitja METOC veebiportaali loomine” (1.11.2011–10.01.2012); Principal Investigator: Tarmo Kõuts; Tallinn University of Technology, Institute of Marine Systems at TUT (partner); Financier: Estonian Maritime Administration; Financing: 16 840 EUR.

Publications

2021

Kõuts, M.; Maljutenko, I.; Elken, J.; Liu, Y.; Hansson, M.; Viktorsson, L.; Raudsepp, U. (2021). Recent regime of persistent hypoxia in the Baltic Sea. *Environmental Research Communications*, 3 (7). DOI: 10.1088/2515-7620/ac0cc4.

Maljutenko, I.; Hassellöv, I. M.; Eriksson, M.; Ytreberg, E.; Yngsell, D.; Johansson, L.; Jalkanen, J. P.; Kõuts, M.; Kasemets, M. L.; Moldanova, J.; Magnusson, K.; Raudsepp, U. (2021). Modelling spatial dispersion of contaminants from shipping lanes in the Baltic Sea. *Marine Pollution Bulletin*, 173 (A), #112985. DOI: 10.1016/j.marpolbul.2021.112985.

2019

Raudsepp, U.; She, J.; Brando, V. E.; Santoleri, R.; Sammartino, M.; Kõuts, M.; Uiboupin, R.; Maljutenko, I. (2019). Phytoplankton blooms in the Baltic Sea. *Journal of Operational Oceanography*, 12 (sup1), s21–s26. DOI: 10.1080/1755876X.2019.1633075.

Raudsepp, U.; Maljutenko, I.; Kõuts, M. (2019). Cod reproductive volume potential in the Baltic Sea. *Journal of Operational Oceanography*, 12 (sup1), s26–s28. DOI: 10.1080/1755876X.2019.1633075.

Raudsepp, U.; Maljutenko, I.; Kõuts, M.; Granhag, L.; Wilewska-Bien, N.; Hassellöv, I.-M.; Eriksson, K. M.; Johansson, L.; Jalkanen, J.-P.; Karl, M.; Matthias, V.; Moldanova, J. (2019). Shipborne nutrient dynamics and impact on the eutrophication in the Baltic Sea. *The Science of The Total Environment*, 671, 189–207. DOI: 10.1016/j.scitotenv.2019.03.264.

Von Schuckmann, K.; Le Traon, P. Y.; Smith, N.; Pascual, A.; Djavidnia, S.; Gattuso, J. P.; Grégoire, M.; Nolan, G.; Aaboe, S.; Aguiar, E.; et al. (2019). Copernicus Marine Service Ocean State Report, Issue 3. *Journal of Operational Oceanography*, 12 (Sup1), S1–S123. DOI: 10.1080/1755876X.2019.1633075.

2018

von Schuckmann, Karina; Le Traon, Pierre-Yves; Aaboe, Signe; Fanjul, Enrique Alvarez; Autret, Emmanuelle; Axell, Lars; Aznar, Roland; Benincasa, Mario; Bentamy, Abderahim; Boberg, Fredrik; Bourdallé-Badie, Romain; Nardelli, Bruno Buongiorno; Brando, Vittorio E.; Bricaud, Clément; Breivik, Lars-Anders; Brewin, Robert J.W.; Capet, Arthur; Ceschin, Adrien; Ciliberti, Stefania; Cossarini, Gianpiero ... Zacharioudaki, Anna, Zuo, Hao (2018). Copernicus Marine Service Ocean State Report. *Journal of Operational Oceanography*, 11, 1–142. DOI: 10.1080/1755876X.2018.1489208.

2014

Kolesova, N.; Kõuts, M.; Siimon, K.-L.; Raudsepp, U. (2014). Changes in the morphology of *Fucus vesiculosus* L. and abundance of seaweed associated fauna along the coastal sea of Estonia. *Baltic International Symposium (BALTIC), 2014 IEEE/OES*, 1–12. DOI: 10.1109/BALTIC.2014.6887832.

Elulookirjeldus

Isikuandmed

Nimi: Mariliis Kõuts
Sünniaeg: 29.05.1987
Telefon: +372 5181 585
E-post: mariliis.kouts@taltech.ee

Töökohad ja ametid

01.07.2022–...	Tallinna Tehnikaülikool, Loodusteaduskond, Meresüsteemide instituut, Insener (1,00)
01.01.2017–30.06.2022	Tallinna Tehnikaülikool, Loodusteaduskond, Meresüsteemide instituut, Nooremteadur (1,00)
01.01.2016–31.12.2016	Tallinna Tehnikaülikool, TTÜ Meresüsteemide Instituut, Nooremteadur (1,00)
2009–31.12.2015	Tallinna Tehnikaülikool, TTÜ Meresüsteemide Instituut, insener (1,00)

Teaduskraadid

Magistrikraad, 2013, (juh) Markus Vetemaa; Lauri Saks, Muuga lahel ja Käsmu lahel talvituvate aulide (Clangula hyemalis) toitumisökoloogia: kaaspüügil põhineva andmestiku analüüs, Tartu Ülikool

Doktorant, (juh) Gennadi Lessin; Urmas Raudsepp, Nutrient and detritus dynamics in the Baltic Sea (Toitainete ja detriidi dünaamika Läänemeres), Tallinna Tehnikaülikool, Loodusteaduskond, Meresüsteemide instituut.

Haridustee

01.09.2015–...	Tallinna Tehnikaülikool, doktoriõpe
2010–2013	Tartu Ülikool, magistriõpe
2006–2010	Tartu Ülikool, bakalaureuseõpe
1995–2006	Tallinna Inglise Kolledž
1994–1995	Kehra Keskkool

Lõppenud projektid

VA18004 “Copernicus merekeskkonna seireteenused Läänemere seire- ja prognoosikeskuses” (1.01.2018–31.03.2021); Vastutav täitja: Urmas Raudsepp; Tallinna Tehnikaülikool, Loodusteaduskond, Meresüsteemide instituut (partner); Finantseerija: Mercator Océan; Eraldatud summa: 544 100 EUR.

IUT19-6 “Erinevat mastaapi füüsikaliste protsesside mõju biogeokeemilise signaali dünaamikale stratifitseeritud Läänemeres” (1.01.2014–31.12.2019); Vastutav täitja: Urmas Lips; Tallinna Tehnikaülikool, TTÜ Meresüsteemide Instituut, Tallinna Tehnikaülikool, Loodusteaduskond, Meresüsteemide instituut; Finantseerija: Sihtasutus Eesti Teadusagentuur; Eraldatud summa: 1 380 000 EUR.

VEU15017 "Läänemere jätkusuutlik laevandus ja keskkond" (1.04.2015–31.03.2018); Vastutav täitja: Urmas Raudsepp; Tallinna Tehnikaülikool, TTÜ Meresüsteemide Instituut (partner); Finantseerija: Sihtasutus Eesti Teadusagentuur; Eraldatud summa: 149 616 EUR.

VEU676 "Laevavrakkide keskkonnamõju hindamine (SWERA)" (14.05.2014–30.04.2016); Vastutav täitja: Tarmo Kõuts; Tallinna Tehnikaülikool (partner), Tallinna Tehnikaülikool, TTÜ Meresüsteemide Instituut (partner); Finantseerija: Euroopa Komisjon; Eraldatud summa: 95 228 EUR.

VEU663 "Õlireostuse varajase avastamise süsteem Läänemere jaoks (GEOILWATCH)" (1.05.2014–30.04.2016); Vastutav täitja: Tarmo Kõuts; Tallinna Tehnikaülikool (partner), Tallinna Tehnikaülikool, TTÜ Meresüsteemide Instituut (partner); Finantseerija: Euroopa Komisjon; Eraldatud summa: 98 760 EUR.

Lep13166 "Finnigulf LNG Balticconnector: Keskkonnamõju hindamine" (21.11.2013–31.05.2015); Vastutav täitja: Inga Lips; Tallinna Tehnikaülikool (partner), Tallinna Tehnikaülikool, TTÜ Meresüsteemide Instituut (partner); Finantseerija: OÜ Entec Eesti; Eraldatud summa: 62 700 EUR.

Lep14059 "Soome lahe aasta 2014 raames õppereiside korraldamine" (11.04.2014–30.06.2014); Vastutav täitja: Inga Lips; Tallinna Tehnikaülikool (partner), Tallinna Tehnikaülikool, TTÜ Meresüsteemide Instituut (partner); Finantseerija: Eesti Loodusmuuseum; Eraldatud summa: 10 752 EUR.

Lep 13030 "Hiiu maakonna mereala ruumilise planeeringu koostamine" (1.03.2013–30.05.2014); Vastutav täitja: Urmas Lips; Tallinna Tehnikaülikool (partner), Tallinna Tehnikaülikool, TTÜ Meresüsteemide Instituut (partner); Finantseerija: Artes Terrae OÜ; Eraldatud summa: 37 250 EUR.

SLOMI10134T "Hülgekahjude vähendamine püügivahendite hülgekindlamaks ehitamise ja hülgepeletite kasutusele võtmise abil" (1.07.2010–31.12.2013); Vastutav täitja: Markus Vetemaa; Tartu Ülikool (partner), Tartu Ülikool, Loodus- ja tehnoloogiateaduskond, Tartu Ülikooli Eesti Mereinstituut (partner); Finantseerija: Põllumajanduse Registre ja Informatsiooni Amet; Eraldatud summa: 213 465 EUR.

Lep11033 "Mustjala vallas Ninase külas asuva Saaremaa sadama detailplaneeringu koostamine ja detailplaneeringuga kavandatava tegevuse keskkonnamõju strateegiline hindamine" (21.04.2011–31.12.2012); Vastutav täitja: Urmas Raudsepp; Tallinna Tehnikaülikool, TTÜ Meresüsteemide Instituut (partner); Finantseerija: AS Tallinna Sadam; Eraldatud summa: 18 406 EUR.

Lep11081 "Paldiski Põhjasadama 0 kai rajamise keskkonnamõjude hindamine" (15.10.2011–15.11.2012); Vastutav täitja: Tarmo Kõuts; Tallinna Tehnikaülikool, TTÜ Meresüsteemide Instituut (partner); Finantseerija: Paldiski Sadamate AS; Eraldatud summa: 15 100 EUR.

Lep11097 "Meresõitja METOC veebiportaali loomine" (1.11.2011–10.01.2012); Vastutav täitja: Tarmo Kõuts; Tallinna Tehnikaülikool, TTÜ Meresüsteemide Instituut (partner); Finantseerija: Veeteede Amet; Eraldatud summa: 16 840 EUR.

Publikatsioonid

2021

Kõuts, M.; Maljutenko, I.; Elken, J.; Liu, Y.; Hansson, M.; Viktorsson, L.; Raudsepp, U. (2021). Recent regime of persistent hypoxia in the baltic sea. *Environmental Research Communications*, 3 (7). DOI: 10.1088/2515-7620/ac0cc4.

Maljutenko, I.; Hassellöv, I. M.; Eriksson, M.; Ytreberg, E.; Yngsell, D.; Johansson, L.; Jalkanen, J. P.; Kõuts, M.; Kasemets, M. L.; Moldanova, J.; Magnusson, K.; Raudsepp, U. (2021). Modelling spatial dispersion of contaminants from shipping lanes in the Baltic Sea. *Marine Pollution Bulletin*, 173 (A), #112985. DOI: 10.1016/j.marpolbul.2021.112985.

2019

Raudsepp, U.; She, J.; Brando, V. E.; Santoleri, R.; Sammartino, M.; Kõuts, M.; Uiboupin, R.; Maljutenko, I. (2019). Phytoplankton blooms in the Baltic Sea. *Journal of Operational Oceanography*, 12 (sup1), s21–s26. DOI: 10.1080/1755876X.2019.1633075.

Raudsepp, U.; Maljutenko, I.; Kõuts, M. (2019). Cod reproductive volume potential in the Baltic Sea. *Journal of Operational Oceanography*, 12 (sup1), s26–s28. DOI: 10.1080/

Raudsepp, U.; Maljutenko, I.; Kõuts, M.; Granhag, L.; Wilewska-Bien, N.; Hassellöv, I.-M.; Eriksson, K. M.; Johansson, L.; Jalkanen, J.-P.; Karl, M.; Matthias, V.; Moldanova, J. (2019). Shipborne nutrient dynamics and impact on the eutrophication in the Baltic Sea. *The Science of The Total Environment*, 671, 189–207. DOI: 10.1016/j.scitotenv.2019.03.264.

Von Schuckmann, K.; Le Traon, P. Y.; Smith, N.; Pascual, A.; Djavidnia, S.; Gattuso, J. P.; Grégoire, M.; Nolan, G.; Aaboe, S.; Aguiar, E.; et al. (2019). Copernicus Marine Service Ocean State Report, Issue 3. *Journal of Operational Oceanography*, 12 (Sup1), S1–S123. DOI: 10.1080/1755876X.2019.1633075.

2018

von Schuckmann, Karina; Le Traon, Pierre-Yves; Aaboe, Signe; Fanjul, Enrique Alvarez; Autret, Emmanuelle; Axell, Lars; Aznar, Roland; Benincasa, Mario; Bentamy, Abderahim; Boberg, Fredrik; Bourdallé-Badie, Romain; Nardelli, Bruno Buongiorno; Brando, Vittorio E.; Bricaud, Clément; Breivik, Lars-Anders; Brewin, Robert J.W.; Capet, Arthur; Ceschin, Adrien; Ciliberti, Stefania; Cossarini, Gianpiero ... Zacharioudaki, Anna, Zuo, Hao (2018). Copernicus Marine Service Ocean State Report. *Journal of Operational Oceanography*, 11, 1–142. DOI: 10.1080/1755876X.2018.1489208.

2014

Kolesova, N.; Kõuts, M.; Siimon, K.-L.; Raudsepp, U. (2014). Changes in the morphology of *Fucus vesiculosus* L. and abundance of seaweed associated fauna along the coastal sea of Estonia. *Baltic International Symposium (BALTIC)*, 2014 IEEE/OES, 1–12. DOI: 10.1109/BALTIC.2014.6887832.

ISSN 2585-6901 (PDF)
ISBN 978-9949-83-946-9 (PDF)